COPPER COMPLEXES WITH BPA- AND PHEN-BASED LIGANDS AS ARTIFICIAL NUCLEASES

Inaugural-Dissertation
to obtain the academic degree
Doctor rerum naturalium (Dr. rer. nat.)

submitted to the Department of Biology, Chemistry and Pharmacy
of Freie Universität Berlin

by
AIRLANGGA ARYA JANITRA SUDARGA TJAKRAATMADJA
from Bonn

2016

The present work was carried out under the supervision of Prof. Dr. Nora Kulak from January 2012 to February 2016 at the Institute of Chemistry and Biochemistry, Freie Universität Berlin.

First Referee: Prof. Dr. Nora Kulak
Second Referee: Prof. Dr. Christian Müller
Date of Defense: 13th May 2016

ZUSAMMENFASSUNG

Krebs zählt zu den häufigsten Todesursachen weltweit. Die am häufigsten vorkommenden Krebsarten sind bei Frauen Brustkrebs und bei Männern Prostatakrebs. Je nach Krankheitszustand werden verschiedene Therapien wie die chirurgische, Radio-, Chemo- und hormonale Therapie angewendet. Das bekannteste Zytostatikum Cisplatin zeigt nicht nur Aktivitäten gegenüber verschiedene Tumorzellen auf, sondern auch Nachteile, wie z.B. zahlreiche Nebenwirkungen und Resistenzen. Aus diesem Grund sind Verbindungen mit essentiellen Übergangsmetallen wie Kupfer (Cu) und Zink (Zn) als Zytostatika in der Medizinischen Bioanorganischen Chemie von hoher Bedeutung. Hierbei kann die Zytotoxizität u.a. durch DNA-Spaltung in Tumorzellen entstehen. In Verbindung mit aromatischen *N*-Donor-Liganden wurden in dieser Arbeit Cu(II)-Komplexe als künstliche DNA-Spalter oder artifizielle Nukleasen untersucht. Einzelheiten bezüglich der hydrolytischen und oxidativen DNA-Spaltmechanismen sind in **KAPITEL 1** beschrieben.

Es ist bekannt, dass Cu(II)-Komplexe des aromatischen Liganden bpa (Bis(2-picolyl)amin) die DNA auf hydrolytische Weise spalten können. In dieser Arbeit wurden neue Cu(II)-bpa-Derivate mit verschiedenen Seitenketten synthetisiert, charakterisiert und hinsichtlich der hydrolytischen und oxidativen DNA-Spaltung untersucht. Die Wechselwirkung von ausgewählten bpa-Komplexen mit Kalbsthymus-DNA (CT-DNA) wurde mithilfe der Circulardichroismus (CD)-Spektroskopie bestimmt. Weitere Einzelheiten sind in **KAPITEL 2** zu finden.

Das weibliche Sexualhormon Östrogen kann durch die Zellmembran diffundieren und am Östrogenrezeptor (ER) binden, um die Transkription von steroidregulierten Genen zu stimulieren. Natürlich vorkommende Östrogene wurden am bpa-Liganden angeknüpft, um die DNA von ER-positiven Krebszellen gezielt anzugreifen. Cu(II)-Komplexe dieser Östrogen-bpa-Derivate wurden bezüglich der hydrolytischen und oxidativen DNA-Spaltung ausgewertet. Die Zytotoxizität gegenüber Brustkrebszellen wurde mithilfe des MTT-Assays überprüft. Weitere Einzelheiten sind in **KAPITEL 3** zu finden.

Eine der am längsten bekannten, kupferhaltigen artifiziellen Nukleasen enthält den aromatischen Liganden phen (1,10-Phenanthrolin), und kann die DNA oxidativ spalten. In dieser Arbeit wurden phen-Derivate mit langen Alkylketten synthetisiert, um einen amphiphilen Charakter zu gewährleisten. Studien bezüglich

oxidativer DNA-Spaltung, BSA(Rinderserumalbumin)-Spaltung und Zytotoxizität gegenüber Brustkrebszellen wurden mit ausgewählten Cu(II)-Komplexen der alkylierten phen-Derivate durchgeführt. Weitere Einzelheiten sind in **KAPITEL 4** zu finden.

ABSTRACT

Cancer is one of the leading causes of death worldwide. In women, the most common type of cancer is breast cancer and in men, the most common type of cancer is prostate cancer. Depending on the stage of the disease different kinds of therapies are used, comprising surgery, radio-, chemo- and hormonal therapy. The best-known anticancer drug cisplatin not only shows activity in various tumor types, but also disadvantages, e.g. large numbers of side effects and resistances. Therefore, compounds containing essential trace elements such as copper (Cu) and zinc (Zn) acting as cytostatic agents are of great importance in the field of medicinal bioinorganic chemistry. In particular, cytotoxicity can occur through DNA cleavage in tumor cells. In combination with aromatic *N*-donor ligands, Cu(II) complexes performing as synthesized DNA cleavers or artificial nucleases have been studied in this work. Details of the mechanism regarding hydrolytic as well as oxidative DNA cleavage are described in **CHAPTER 1**.

It is known that Cu(II) complexes of the aromatic ligand bpa (bis(2-picolyl)amine) are able to cleave DNA through the hydrolytic pathway. In this work, novel Cu(II) bpa derivatives containing various side chains have been synthesized, characterized and subjected to both hydrolytic and oxidative DNA cleavage studies. Interaction of chosen bpa complexes with calf thymus (CT) DNA has been determined via circular dichroism (CD) spectroscopy. Details can be found in **CHAPTER 2**.

Well-known as female sex hormones, estrogens are able to diffuse across the cell membrane and further bind to estrogen receptors (ER) in order to stimulate the transcription of steroid-regulated genes. Naturally appearing estrogens were linked to the bpa ligand in order to target DNA of ER-positive cancer cells. Cu(II) complexes of the synthesized estrogen bpa derivatives were thus evaluated regarding hydrolytic as well as oxidative DNA cleavage. Cytotoxicity studies towards breast cancer cells were carried out via MTT assay. Details can be found in **CHAPTER 3**.

One of the first known artificial nucleases containing copper comprises the aromatic ligand phen (1,10-phenanthroline), which is able to cleave DNA oxidatively. In this work, phen derivatives with long alkyl chains have been synthesized in order to ensure an amphiphilic feature. Studies regarding oxidative DNA cleavage, proteolytic BSA (bovine serum albumin) cleavage and cytotoxicity towards breast

cancer cells were carried out with chosen Cu(II) complexes of the alkylated phen derivatives. Details can be found in **CHAPTER 4**.

TABLE OF CONTENTS

TABLE OF FIGURES

TABLE OF SCHEMES

ABBREVIATIONS

bpa	Bis(2-picolyl)amine
CD	Circular dichroism
$CHCl_3$	Chloroform
COSY	Correlation spectroscopy
CT	Calf thymus
^{1}D	1-dimensional
^{2}D	2-dimensional
DCC	*N,N'*-Dicyclohexylcarbodiimide
DCM	Dichloromethane
DEPT	Distortionless enhancement by polarization transfer
DIC	*N,N'*-Diisopropylcarbodiimide
DMAP	Dimethylaminopyridine
DMF	Dimethylformamide
DMSO	Dimethylsulfoxide
DNA	Deoxyribonucleic acid
EA	Elemental analysis
EDC	1-Ethyl-3-(3-dimethylaminopropyl)carbodiimide
ESI	Electrospray ionization
EtOH	Ethanol
HMBC	Heteronuclear multiple-bond correlation spectroscopy
HMQC	Heteronuclear multiple-quantum correlation spectroscopy
imda	Iminodiacetic acid
itpy	Imidazole terpyridine
m/z	molecular mass number/charge number of the ion
MALDI	Matrix-assisted laser desorption/ionization
MCF-7	Michigan Cancer Foundation – 7 (breast cancer cell line)
MeOH	Methanol
MS	Mass Spectrometry
MTT	3-(4,5-Dimethylthiazol-2-yl)-2,5-diphenyltetrazolium bromide
NMR	Nuclear magnetic resonance
PBS	Phosphate buffered saline
Pd/C	Palladium on charcoal

phen	1,10-Phenanthroline
PS	Polystyrene
RCS	Reactive chlorine species
RNA	Ribonucleic acid
RNS	Reactive nitrogen species
ROS	Reactive oxygen species
SDS-PAGE	Sodium dodecyl sulfate polyacrylamide gel electrophoresis
SOD	Superoxide dismutase
tacn	1,4,7-Triazacyclononane
tamen	*N,N'*-Tetra(4-antipyrylmethyl)-1,2-diaminoethane
THF	Tetrahydrofurane
TOF	Time-of-flight mass spectrometer
TLC	Thin layer chromatography
TMPyP	5,10,15,20-Tetrakis(1-methyl-4-pyridinio)porphyrintetra(*p*-toluenesulfonate)
TRIS	Tris(hydroxymethyl)aminomethane

CHAPTER 1

INTRODUCTION

1.1   From DNA to cancer

The cell is the smallest structurally visible unit of all known living organisms. The appearance and functionality of cells are defined by their fundamental building blocks: the DNA (deoxyribonucleic acid) and the RNA (ribonucleic acid). The DNA is the carrier of the genetic information in humans and almost all other organisms and many viruses. Nearly every cell in a person's body has the same DNA, which is mostly located in the cell nucleus as nuclear DNA. Herein, the DNA is coiled to form chromosomes. The DNA can also be found in the mitochondria as mitochondrial DNA or mtDNA.[1]

   The fundamental building blocks of the DNA are composed of four nucleobases: adenine (A), guanine (G), cytosine (C) and thymine (T), whereas RNA contains uracil (U) instead of thymine (T) (***Fig. 1.1***). The nucleobases pair up with each other, A with T and C with G, to form units called base pairs.[2]
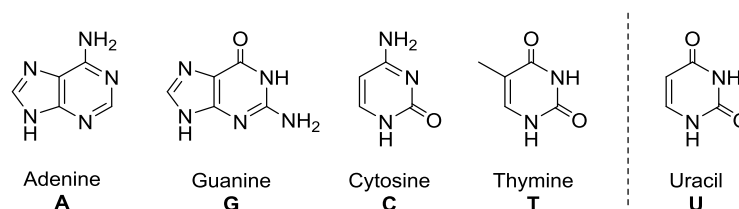
Fig. 1.1 *Structure of the nucleobases adenine (A), guanine (G), cytosine (C), thymine (T) and uracil (U).*

   Each base is also attached to a monosaccharide sugar molecule called deoxyribose and a phosphate molecule. The composition of a nucleobase, a monosaccharide sugar and a phosphate group is called a nucleotide. The nucleotides are connected by covalent bonds between the sugar of one nucleotide and the phosphate of the next, resulting in an alternating sugar-phosphate backbone. Furthermore, the nucleotides are organized as polynucleotides in two long biopolymer strands which are coiled around each other to form a spiral called a

double helix. The double helix is stabilized by hydrogen bonds between nucleotides and base-stacking interaction among aromatic nucleobases (***Fig. 1.2***).[1, 3]
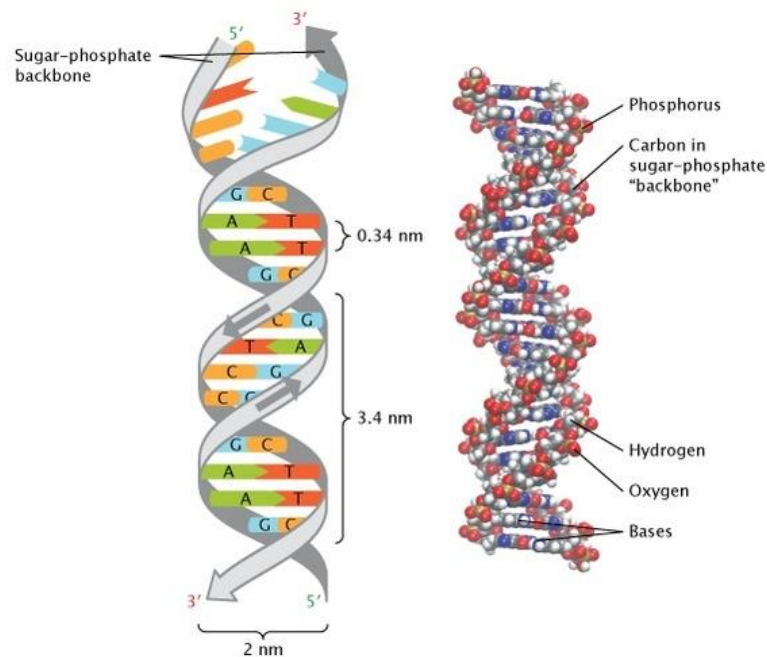
Fig. 1.2 *Left: Simplified illustration of DNA. The grey ribbons, which represent the sugar-phosphate backbone, have arrows that run in opposite directions to indicate that the two strands of the helix are arranged in an anti-parallel manner. The upper end of one strand is labeled five prime (5'), and the lower end of the same strand is labeled three prime (3'). The upper end of the opposite strand is labeled conversely. As a result, the 5' end of one strand matches up with the 3' end of the other strand on each end of the double helix. The two strands are held together by the pairing of complementary nucleotide bases on opposite DNA strands. Right: Molecular model of DNA. Reprinted with permission from L. Pray, Nature Education, **2008**, 1, 100.[3]*

Specific segments of the DNA are called genes. A gene contains a definite order of codons. A group of three bases as a three-base sequence or nucleotide triplet results in the codon, which specifies a single amino acid. The assignment of those amino acids can be determined by the genetic code, which contains information for the production of RNA. Compared to the DNA structure, the RNA structure encloses the sugar ribose instead of deoxyribose. The messenger RNA or mRNA, one of the most important RNA types, contains information for the production of proteins. Proteins are responsible for the biological development of living organisms and for the metabolism in the cell. The process whereby new proteins in cells are generated is called protein biosynthesis. The protein biosynthesis is the key step for the performance of gene expression.[1, 4]

A change of the base sequence of the DNA is called mutation, whereby a DNA error can be caused. Another way to cause DNA errors is the DNA damage, which can occur by endogenous agents like reactive oxygen species (ROS), reactive nitrogen species (RNS) or reactive chlorine species (RCS).[5] Here, the chemical structure of the DNA can be altered due to a missing base from the DNA backbone or a break in a DNA strand. Exogenous agents causing DNA damage are ionizing radiations such as UV light, X-rays and gamma rays, genetically harmful chemicals like ethidium bromide and arsenic acid, or viruses.[6-11] A DNA damage can be repaired by various processes such as base excision repair (BER) or nucleotide excision repair (NER), where enzymes like polymerase and ligase are playing a central role.[12] In contrast, a mutation cannot be recognized by the aforementioned enzymes and thus cannot be repaired, if the base change is present in both strands.

When the ratio between DNA damage and DNA repair remains stable, the DNA will continue participating in the metabolism of the healthy cell. If the rate of DNA damage exceeds the rate of DNA repair, the cell can change into a diseased cell due to early senescence, early apoptosis (programmed cell death) or malignant tumors.[13, 14] Malignant tumors are well known as cancers. In comparison to healthy cells, cancer cells have a higher mutation rate and an uncontrolled cell growth. Cancer is one of the leading causes of death worldwide. In women, the most common type of cancer is breast cancer. In men, the most common type of cancer is prostate cancer.[15] Depending on the stage of the disease different kinds of therapies are used, comprising surgery, radio-, chemo- and hormonal therapy.

1.2 Metal complexes for cancer therapy

In nature, metals are essential elements serving biochemical processes for living organisms. Especially transition metals are endowed with unique properties including redox activity, variable coordination modes and reactivity towards organic substrates and biomolecules. The health status of a cell depends on the amount of the metals and their coordinated ligands. From there transition metal complexes have become promising components in the research of potential anticancer agents.[16, 17]

The breakthrough in the field of medicinal bioinorganic chemistry happened in 1965, when Krigas and Rosenberg discovered that cisplatin can inhibit the cell division of the bacteria *Escherichia coli* (*E. coli*).[18] Until today, cisplatin is used as a chemotherapeutic drug either alone or in combination with other drugs for the treatment of several cancer types including bladder, ovarian, testicular and lung cancer. Unfortunately, systemic toxicity and large number of side effects are outlining a huge disadvantage and resistances against platinum-based drugs are occurring quite often.[19]

As shown in *Scheme 1.1*, cisplatin is administered intravenously, and while it circulates in the blood where the chloride concentration is high (~100 mM), Pt(II) remains coordinated to its chloride ligands. Upon entering the cell where the chloride concentration is low (~4 mM), however, the chloride ligands of cisplatin are replaced presumably by water molecules, generating a positively charged aquated species that can react with nucleophilic sites on intracellular macromolecules to form protein, RNA, and DNA adducts. The reaction with DNA yields monofunctional adducts intrastrand crosslinks and interstrand crosslinks with the platinum atom coordinated to the N7-position of guanine or adenine. Cancer treatment with cisplatin results in inhibition of DNA replication, RNA transcription, arrest at the G2 phase of the cell cycle and/or programmed cell death.[19]

The research of other platinum complexes has been expanded and tested over the past decades, rendering carboplatin, oxaliplatin and satraplatin the most beneficial platinum-based drugs.[20, 21] Although the disadvantages of the cisplatin-based compounds persist, they are used as chemotherapeutic drugs in clinical cancer treatment to this day.[22, 23] Therefore, DNA cleaving agents or drugs containing transition metals which are more compatible with the human body have been widely explored.[24-26]
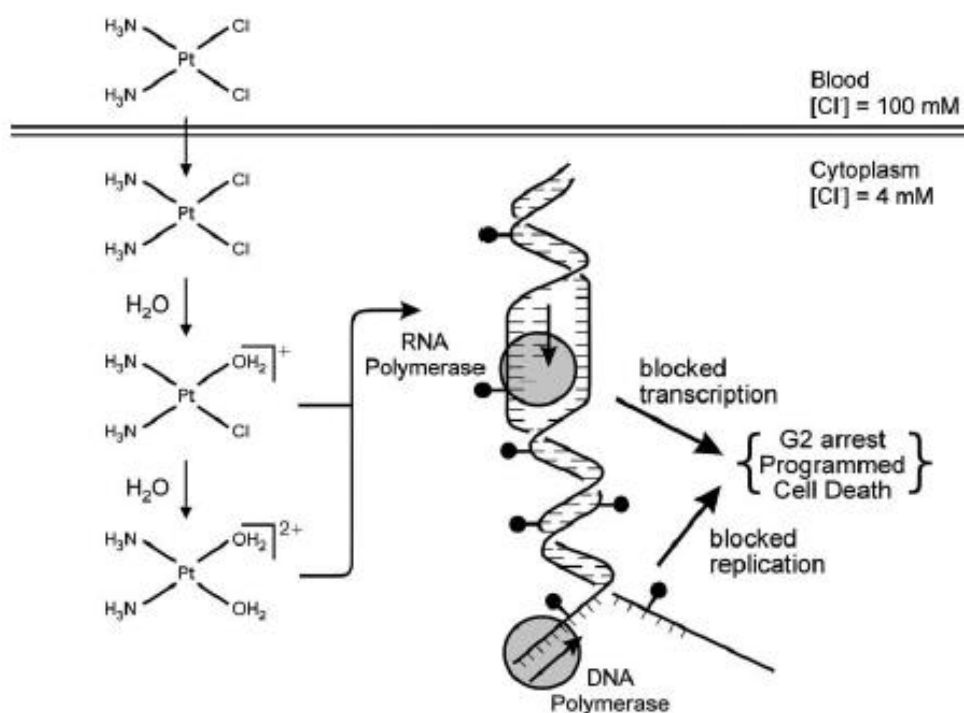
Scheme 1.1 *Mechanistic effect of cisplatin in the cytoplasm. Reprinted with permission from M. Kartalou, J. Essigmann, Mutation Research/Fundamental and Molecular Mechanisms of Mutagenesis, 2001, 478, 23.[19]*

Another approach to cancer therapy is the destruction of DNA in cells with an increased mitotic activity, whereby the DNA cleavage mechanism proceeds either oxidatively or hydrolytically.[26-28] The hydrolytic cleavage mechanism is preferred by redox-inert metals like zinc, magnesium and calcium, whereas the oxidative cleavage mechanism is preferred by redox-active metals such as iron and copper.[29]

In the hydrolytic pathway (**Scheme 1.2**), a hydroxide ion generated by a metal-coordinated water molecule attacks the phosphate ester bond and causes elimination of an alkoxide through an intramolecular S_N2 mechanism.[30] The hydrolytic cleavage mechanism can be naturally initiated by enzymes called nucleases, which are divided into endo- and exonucleases.[31] Well-known nucleases are deoxyribonuclease and ribonuclease. The fundamental and applied research of artificial metallonucleases represents large numbers of beneficial approaches in the field of medicinal chemistry.[26, 32, 33] Metallonucleases such as Co(III)-tamen and Cu(II)-tacn complexes follow the hydrolytic pathway of the DNA cleavage.[34-36]
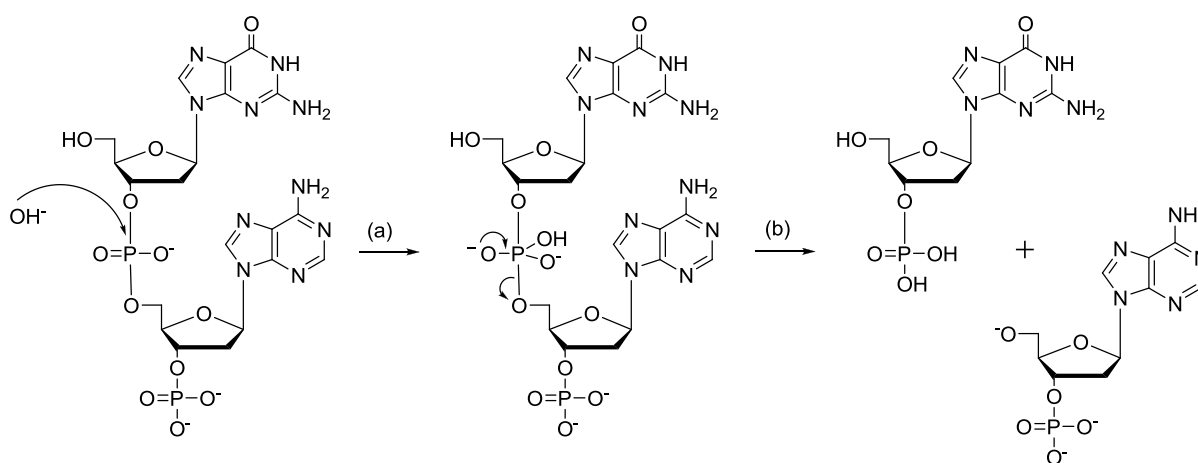
Scheme 1.2 *Hydrolytic DNA cleavage mechanism. A hydroxide ion generated by a metal-coordinated water molecule attacks the phosphate ester bond (left). After formation of a five-membered transition state (middle), an alkoxide is eliminated through an intramolecular S_N2 mechanism (right).*

In the oxidative cleavage mechanism (**Scheme 1.3**), the elimination of a hydrogen atom becomes priority. It is caused by a hydroxyl radical, whereby a water molecule forms (a). For example, the complexes [Mn(TMPyP)](OAc)$_5$ and [Cu(Itpy)$_2$](ClO$_4$)$_2$ serve as suitable medium to cleave the C1'-H.[37, 38] In the next step, a double bond is formed (b) by activated copper-oxo species such as [CuOH]$^{2+}$, as in the case of bis(1,10-phenanthroline)copper(I).[39] The addition of the hydroxyl group leads to the elimination of the phosphate. Then, a carbonyl group is formed by elimination of the nucleobase (c). At the end, a proton and the oligonucleotide-3'-phosphate are eliminated, so that 5-methylene-2-furanone is generated (d).[40]

The discrimination between the two mechanisms is carried out by kinetic, theoretical and spectroscopic studies. Furthermore, the type of the central atom and the ligand are important factors for drawing conclusions about the mechanism. The fact that a compound is able to cleave the DNA in both ways therefore cannot be excluded as it is the case e.g. with [Cu(imda)(phen)(H$_2$O)].[41]
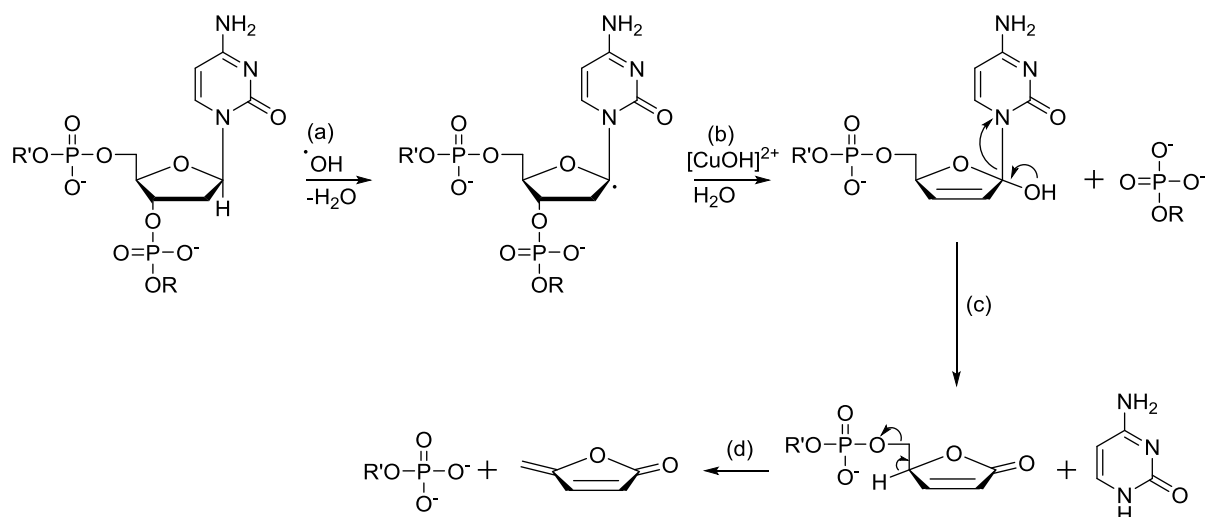
Scheme 1.3 *One possible oxidative DNA cleavage mechanism caused by bis(1,10-phenanthroline)copper(I). The elimination of the nucleobase (here: cytosine) leads to the formation of 5-methylene-2-furanone.[39]*

1.3   Copper complexes and their impact in medicine

Copper is one of the essential transition metals. It exists in the human body in two oxidation states, Cu(I) (Cu$^+$) and Cu(II) (Cu^{2+}). It is responsible for the absorption of iron in the gastrointestinal tract and acts as a component of various enzymes, e.g. cytochrome c oxidase (COX) and superoxide dismutase (SOD).[42, 43] From the viewpoint of the ligand field theory, the reduced form Cu$^+$ has no preference for geometry due to its completely filled d^{10} configuration. As opposed to this, Cu(II) prefers different distorted coordination arrangements caused by the Jahn-Teller effect of the d^9 configuration.[44] Due to their Lewis acidity and redox activity, Cu(II) complexes can cleave the DNA through the hydrolytic as well as the oxidative pathway.[41] This special and flexible feature has been explored intensively, with the result that Cu(II) chelating agents have a huge potential as chemotherapeutic drugs.[44]

Well-known copper chelators are disulfiram (DSF), clioquinol (CQ) and diethyldithiocarbamate (DDTC) (**Fig. 1.3**).[45-48] In the presence of copper, DSF can inhibit the growth of breast cancer cells.[49] Furthermore, copper-bearing components of both CQ and DDTC can decrease the expression of the androgen receptor (AR) and inhibit tumor growth of human prostate cells.[48, 50]

DSF   **CQ**   **DDTC**
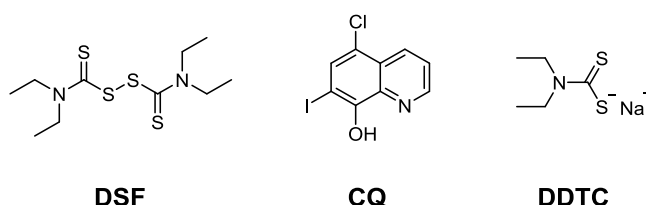
Fig. 1.3 Chemical structure of disulfiram (DSF, left), clioquinol (CQ, middle) and diethyldithiocarbamate (DDTC, right).

The role of copper complexes with aromatic *N*-donor ligands performing as artificial nucleases has been evaluated in diverse variants.[51] Phenanthroline was established as one of the first *N*-donor ligands with strong oxidative Cu(II)-dependent DNA cleavage activity. Besides that, similar systems such as bipyridine (bpy), terpyridine (tpy) and bis(2-picolyl)amine (bpa) metal complexes have been studied.[52-54] The mechanism of dephosphorylation and DNA hydrolysis caused by Cu(II) bpa complexes has been described in the late 90s.[55, 56]

1.4   Aims and objectives

The aim of this thesis is the synthesis of novel Cu(II) complexes with bpa and phen-based *N*-donor ligands. These artificial metallonucleases are designed such that they cause a higher cleavage activity towards DNA and a higher cytotoxicity towards the MCF-7 breast cancer cell line as compared to their precursors.

It has been assumed that Cu(II) complexes of bpa ligands containing an hydroxyalkyl ether can cleave DNA hydrolytically. For a closer examination of this property, the side chain length of the alkyl ether substituent should be modified. Crystal structures of the Cu(II) bpa complexes shall provide useful information regarding the coordination sphere and DNA cleavage mechanism. By tuning the aforementioned ether tethers, an increased DNA cleavage activity is expected compared to the already known Cu(II) bpa complexes.[57, 58]

Furthermore, it is proposed to link an estrogenic moiety to the bpa ligand, since estrogen receptors (ERs) occur in breast cancer cells.[59] Besides that, estrogens can make use of their lipophilicity to increase the cellular uptake of bpa.[60] Here, both the bpa and estrogen moiety should be connected by ester groups via Steglich esterification.[61] The functionalization of the bpa ligand could possibly aggravate the precipitation of its Cu(II) complexes. In this case, analytical studies can be performed *in situ*. Compared to their precursors, the synthesized bpa estrogen derivatives (+ Cu) shall effect an increased DNA affinity and a higher DNA cleavage activity due to probable interaction between the estrogenic moiety and DNA. A higher cytotoxicity towards the ER(+)-breast cancer cell line MCF-7 is thus expected. The application of bpa estrogen derivatives could be of great interest in the field of bioinorganic and medicinal chemistry.

For the synthesis of new Cu(II) phen complexes, the phen ligand should be acylated in 5-position or in 5,6-position resulting in the formation of amphiphilic phen derivatives.[62-65] Since acylation with long alkyl chains may result in an excessive hydrophobicity, the synthesis of amphiphilic Cu(II) phen compounds can be aggravated. In this case, analytical studies can be also performed *in situ*. DNA cleavage studies, protein cleavage studies and cytotoxicity studies with MCF-7 cells shall visualize the acylation effect of the phen derivatives (+ Cu). Overall, the Cu(II) phen derivatives shall have the ability to be formed into micelles and liposomes,

respectively, which are promising applications as drugs that work via passive targeting.[66, 67]

CHAPTER 2

BPA ALKYL ETHER DERIVATIVES

Cu(II)-coordinating bpa ligands with different hydroxyalkyl substituents (***Fig. 2.1***) at the aliphatic amino group and their hydrolytic cleavage activity of bis(2,4-dinitrophenyl)phosphate (BNPP) as a DNA model have been described by Chin *et al.*[57] Metzler-Nolte *et al.* have subsequently presented metal complexes (M(II) = Co, Ni, Zn, Cu) of ligand **1b** (***Scheme 2.2***), which contains an elongated hydroxyalkyl substituent with an ether group (***Fig. 2.1***).
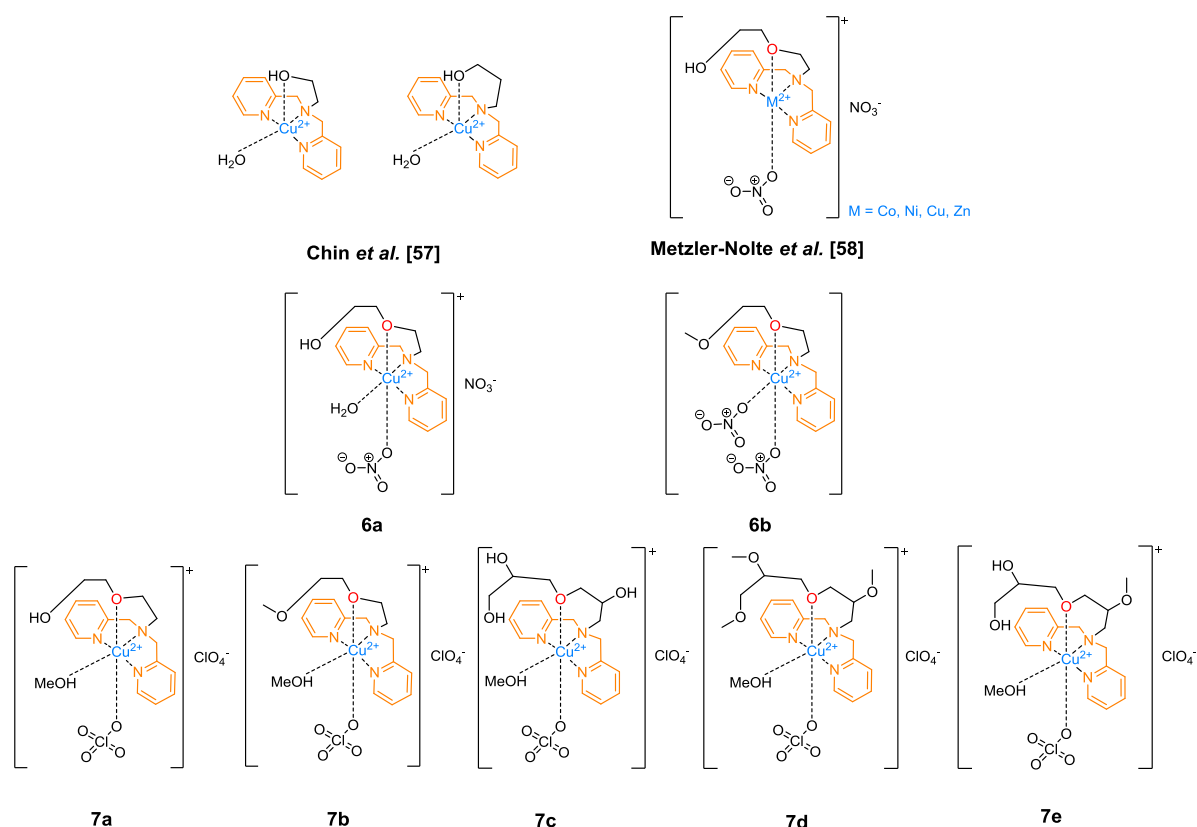
Fig. 2.1 *Overview of literature-known bpa complexes and bpa complexes presented within this work (**7a** carries a methanol solvent molecule as an equatorial ligand as derived from X-ray crystallography analysis[68], whereas elemental analysis pointed to an aqua ligand at this coordination site). **6a** has been reported to carry an aqua ligand[58]. Elemental analysis, however, did not show any water.*

They showed that these bpa complexes are able to cleave the phosphodiester bonds of plasmid DNA with higher efficiency compared to the complexes described by Chin *et al.*, which was confirmed by gel electrophoresis.[58] Among the metals investigated, Cu(II) and Co(II) showed the highest DNA cleavage activity, whereas

Zn(II) and Ni(II) caused only little DNA cleavage. It has been proposed that cleavage occurs hydrolytically based on a crystal structure of complex **6a** ([Cu(**1b**)(ONO$_2$)(OH$_2$)]NO$_3$). The reason for the comparatively high hydrolytic cleavage activity was attributed to the close proximity of the pendant hydroxyl group (proton acceptor) and an aqua ligand. The coordinated water molecule can thus get deprotonated and cleave the phosphodiester bond through an addition-elimination mechanism (**Scheme 2.1**).[58]
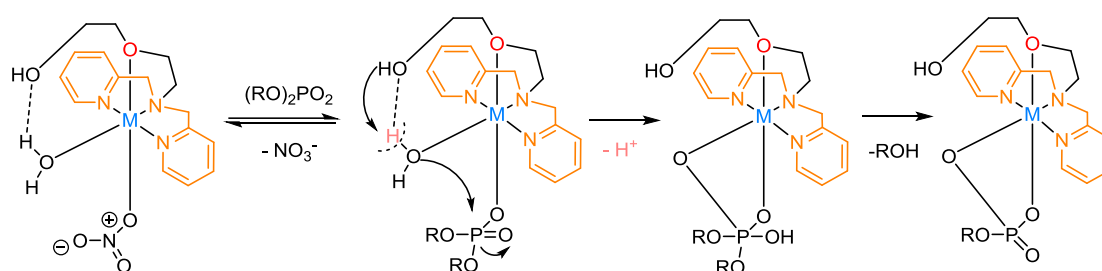
Scheme 2.1 *Hydrolytic DNA cleavage mechanism as proposed by Metzler-Nolte et al.[58]*

In this work, the synthesis and characterization of bpa derivatives with different side chain lengths and functionalities, aiming to optimize the nuclease activity of the respective Cu(II) complexes, is described. In addition, the purpose herein is also to gain a better insight into the aforementioned proposed hydrolytic DNA cleavage mechanism, into a possible oxidative pathway and into the overall interactions of the described complexes with DNA.

2.1   Results and discussion

2.1.1 Synthetic strategies

The synthesis of bpa ligands relies on the mechanism of the reductive amination (***Scheme 2.2***), which proceeds under acidic conditions. Herein, the amino alcohol ether **1a** attacks the aldehyde group of the starting material pyridine-2-aldehyde and forms an intermediate imine after the loss of a water molecule. The intermediate imine is then reduced by the reducing agent NaBH(OAc)$_3$. The repetition of the process leads to the formation of the tertiary amine **1b**.
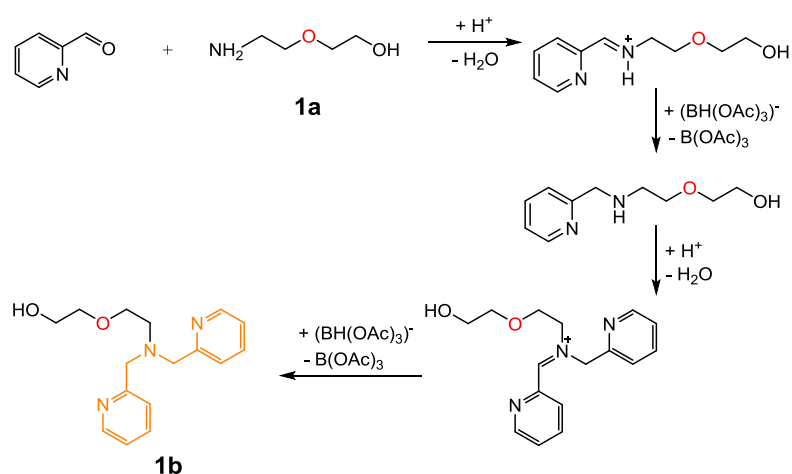
Scheme 2.2 *Reductive amination mechanism for the synthesis of **1b**.*

It is primarily tried to synthesize bpa ligands with different chain lengths (compared to **1b**). Thereupon, elongation of the bpa hydroxyalkyl substituent (starting from the bpa ligands of Chin *et al.*)[57] through vinylation or allylation was not successful (***Scheme 2.3***).[69] Further hydroboration as originally planned could thus not be performed.[70]
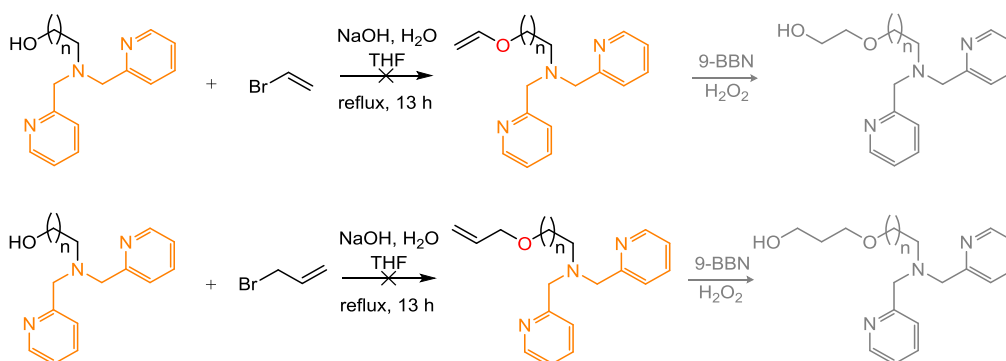
Scheme 2.3 *Elongation of the side chain of the bpa ligand (n = 1,2).*

Due to the unsuccessful elongation strategy the synthesis of amino alcohols, like **1a** with different chain lengths, was tried. As shown in **Scheme 2.4**, protective groups such as benzyl and cbz were applied within this concept, but the coupling reactions led to the formation of undesired by-products through intramolecular reactions, probably due to the high nucleophilicity of the nitrogen atom.[71-73] This issue could neither be solved by the introduction of an azido alcohol instead of an amino alcohol.[74]
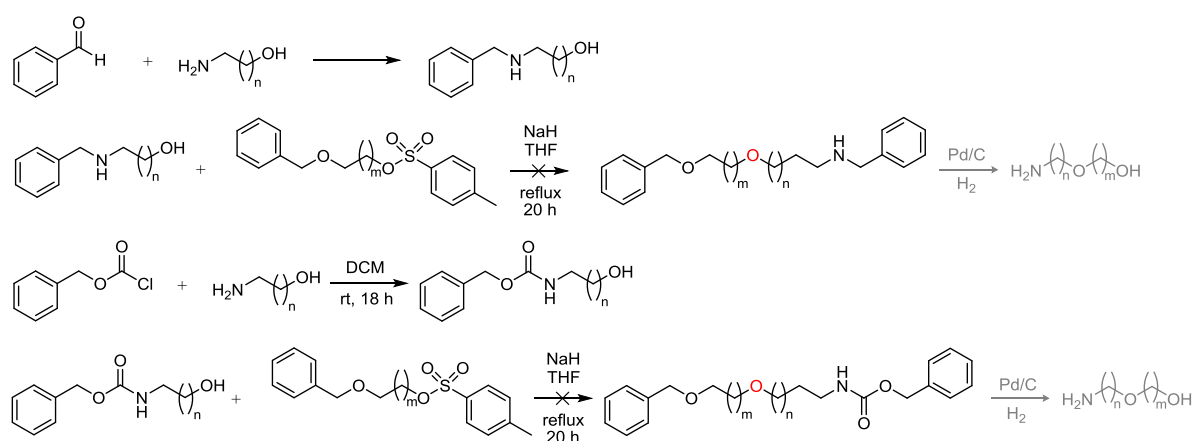
Scheme 2.4 *Synthesis of amino alcohol ethers using benzyl and cbz protecting groups (n = 2,3 ; m = 2,3).*

As shown in **Scheme 2.5**, the monobenzylated ethane and propane diol was connected to an allyl bromide and the amine could be obtained by hydroboration amination (a)[69, 75]. However, it was not possible to isolate the desired, deprotected product. Besides that, the amino alcohol ether obtained from hydroboration of amino propoxy vinyl ether (b)[76] could only be characterized by mass spectrometry, but not by ^{1}H NMR spectroscopy.
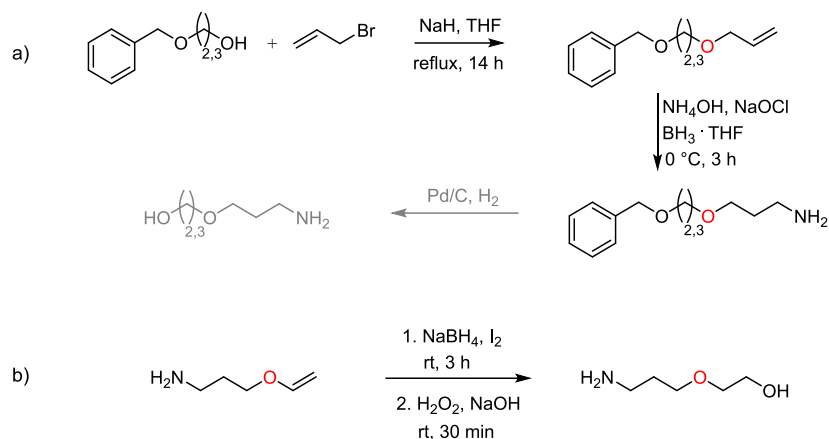
Scheme 2.5 *a) Synthesis of amino alcohol ethers using monobenzylated diols and allyl bromide. The amine is formed via hydroboration amination of the alkene. b) Hydroboration of amino propoxy vinyl ether.*

Because it was not possible to synthesize the aforementioned desired amino ethers with convincing results regarding NMR characterization, we focused on the reports of Inagaki *et al.*[77] and Haag *et al.*[78] Herein, the syntheses of amino ethers **2d**, **3e** and **4b** with additional functionalities such as hydroxyl and methoxy groups were described. Combined with the bpa ligand, effects of the aforementioned amino ether functionalities regarding DNA binding and cleavage can be analyzed in detail. The synthesis of amino ethers **2d**, **3e**, **4b**, the novel amino ether **5c** as well as the corresponding bpa derivatives **1b**, **2e**, **3f**, **4c** and **5d** are presented within this thesis (**Scheme 2.6**).[77-79]
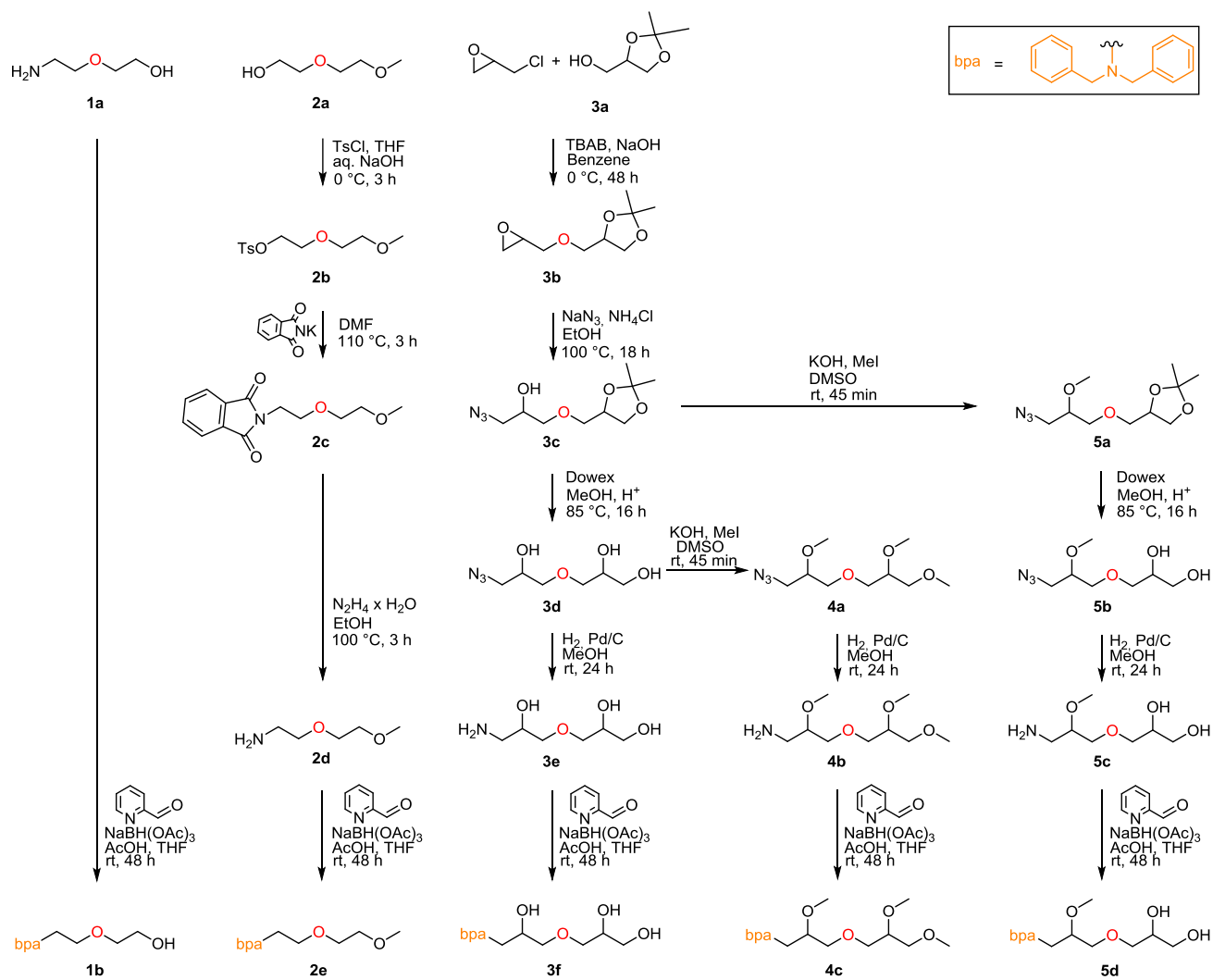
Scheme 2.6 *Synthesis of the bpa derivatives **1b, 2e, 3f, 4c** and **5d** at a glance.*

2.1.2 Synthesis of the linkers

According to the synthetic pathway shown in **Scheme 2.7**, the tosylation of **2a** was carried out as described by Inagaki *et al.*[77] The yield of **2b** (91**%**) is comparable to the literature value (91**%**)[77].
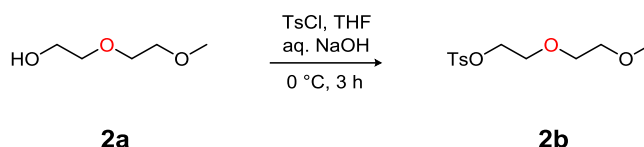
Scheme 2.7 *Synthesis of 2-(2-methoxyethoxy)ethyl tosylate (2b).*

Afterwards, the synthesis of **2c** was performed through substitution of the tosyl group of **2b** with a phthalimide group (**Scheme 2.8**).[77] During the work-up process, it was proven via ^{1}H NMR spectroscopy, that DMF was still present in the crude product. After repeating the work-up it was possible to remove the excess of DMF completely. Compared to the literature value (90**%**)[77], only a moderate yield was thus reached for **2c** (49**%**).
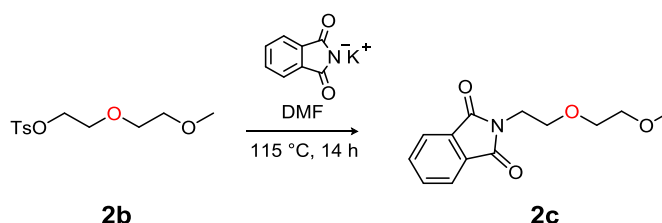
Scheme 2.8 *Synthesis of N-[2-(2-methoxyethoxy)ethyl]phthalimide (2c).*

The phthalimide group of **2c** was cleaved to yield amine **2d** with a moderate amount (62**%** for **2d**, Lit.[77] 91**%**, **Scheme 2.9**). **2d** was successfully analyzed by ^{1}H NMR, ^{13}C NMR spectroscopy and ESI mass spectrometry.
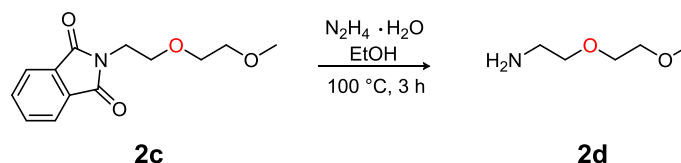
Scheme 2.9 *Synthesis of 2-(2-methoxyethoxy)ethylamine (2d).*

In the synthesis of 1,2-isopropylidene glyceryl glycidyl ether (IGG, **Scheme 2.10**) purification via column chromatography as suggested in the literature

procedure was not necessary.[79] The clean compound **3b** was obtained with a moderate yield (29**%** for **3b**, Lit.[79] 51**%**) and successfully analyzed by ^{1}H NMR spectroscopy.
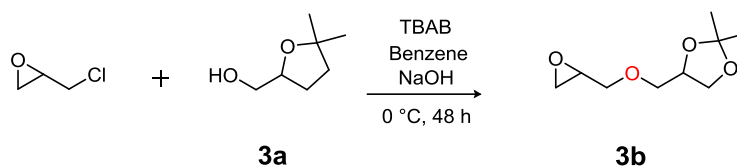
Scheme 2.10 *Synthesis of 1,2-isopropylidene glyceryl glycidyl ether (IGG)).*

Compound **3c** was synthesized according to Haag *et al.* by epoxide opening of **3b** (**Scheme 2.11**) and yielded 85**%** (Lit.[78] 93**%**).
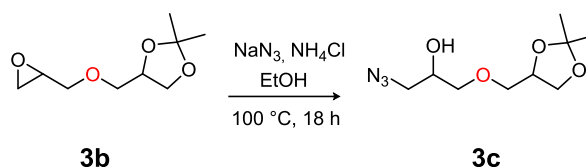
Scheme 2.11 *Synthesis of 1,2-isopropylidene glyceryl (1-azido-2-propanol) ether (**3c**).*

Thereafter, the acetal deprotection of **3c** was carried out with Dowex resin to obtain azide **3d** (**Scheme 2.12**) with a high yield (93**%** for **3d**, Lit.[78] 93**%**).
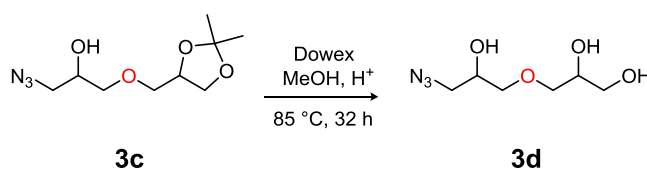
Scheme 2.12 *Synthesis of propylene glycol (1-azido-2-propanol) ether (**3d**).*

The reduction of the azide **3d** was carried out using hydrogen gas with palladium on charcoal as a catalyst[78], since a procedure with lithium aluminum hydride as described in the literature was unsuccessful (**Scheme 2.13**)[80]. During the work-up process, complete separation of the catalyst from the product through a celite pad was challenging and required additional filtration with a double filter to separate the catalyst completely. 97**%** of the desired product **3e** was successfully obtained (Lit.[78] 99**%**).
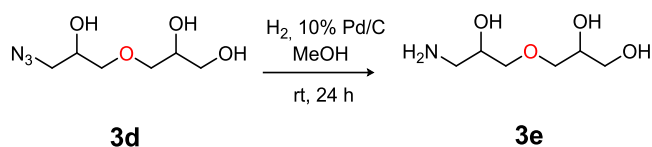
Scheme 2.13 Synthesis of propylene glycol (1-amino-2-propanol) ether (**3e**).

The methylation of **3d** was carried out with methyl iodide (**Scheme 2.14**). It has to be noted that during the work-up iced water is needed in order to simplify the removal of DMSO. **4a** was obtained with a sufficient yield (87**%**, Lit.[78] 82**%**). Afterwards, the reduction of azide **4a** was performed in the same way as described for compound **3e** (**Scheme 2.14**)[78], resulting in a high yield for **4b** (95**%**, Lit.[78] 93**%**).
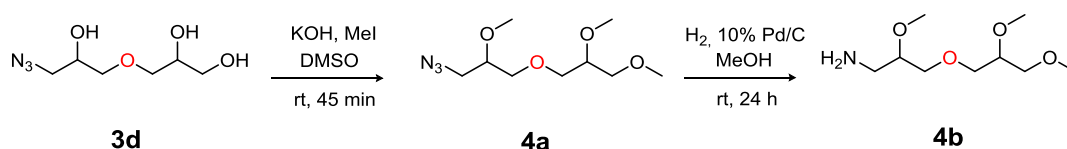
Scheme 2.14 Synthesis of 1,2-methoxy propylidene (1-azido-2-methoxypropanol) ether (**4a**) and 1,2-methoxy propylidene (1-amino-2-methoxypropanol) ether (**4b**).

For the synthesis of **5a**, propylene glycol **3c** was methylated in the same way as described in the synthesis of **4a** (**Scheme 2.15**). The following syntheses are based on the procedure of **3d** and **3e**. The novel literature-unknown compounds **5a-c** could be obtained with high yields (92**%** for **5a**, 87**%** for **5b** and 99**%** for **5c**) and were characterized successfully by ^{1}H NMR spectroscopy, ^{13}C NMR spectroscopy and ESI mass spectrometry.
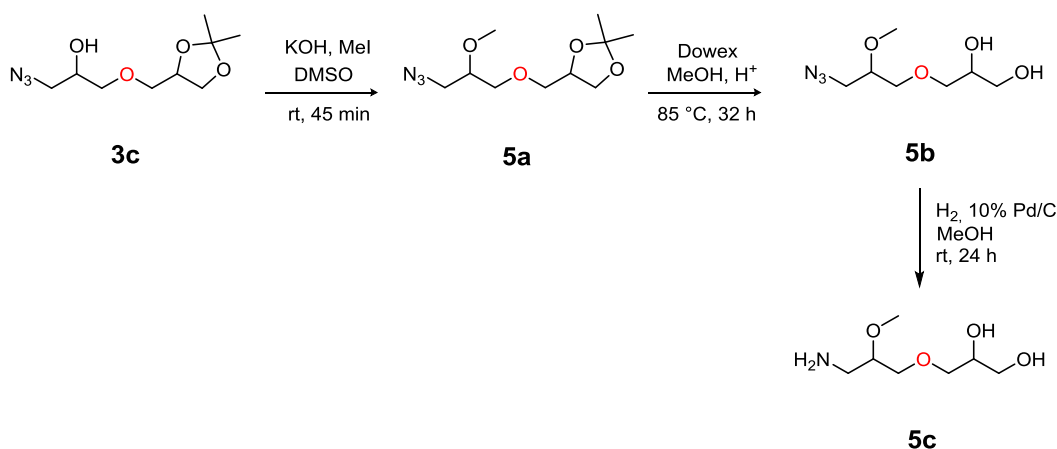
Scheme 2.15 Synthesis of 1,2-isopropylidene glyceryl (1-azido-2-methoxypropanol) ether (**5a**), propylene glycol (1-azido-2-methoxypropanol) ether (**5b**) and propylene glycol (1-amino-2-methoxypropanol) ether (**5c**).

2.1.3 Synthesis of bpa ligands

The synthesis of the bpa ligands was accomplished following a reductive amination mechanism. Both bpa ligands **1b** and the novel compound **2e** were obtained in moderate yields (76**%** for **1b**, Lit.[58] 79**%**; 71**%** for **2e**). The yield for **4c** was surprisingly high (98**%**) (**Scheme 2.16**). Because the compound was already reported in the literature, **1b** was only analyzed by ^{1}H NMR spectroscopy. All other bpa derivatives were characterized by ^{1}H NMR, ^{13}C NMR spectroscopy and ESI mass spectrometry.
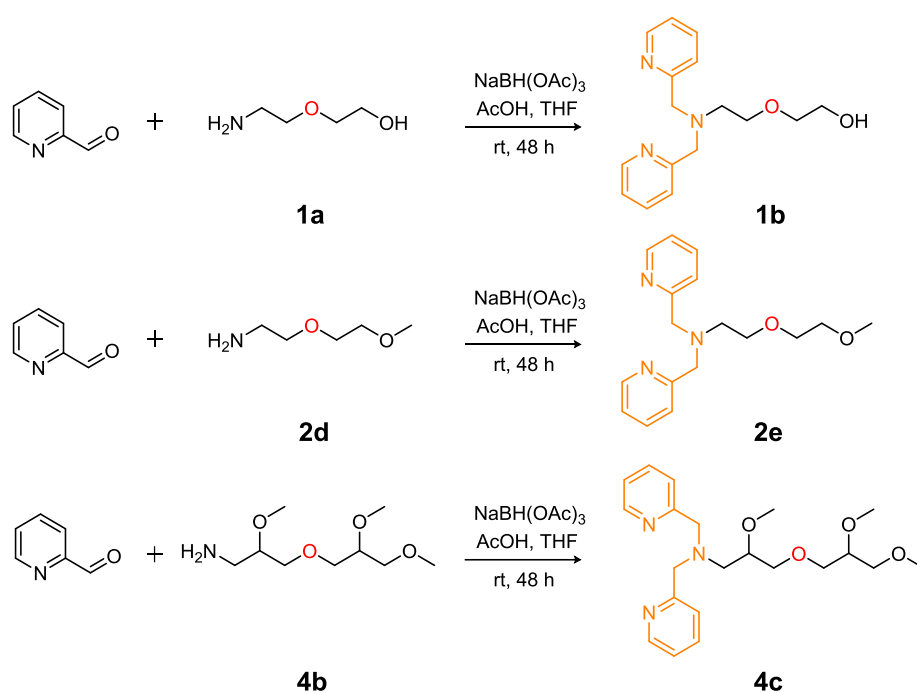
Scheme 2.16 Synthesis of 1b, 2e and 4c.

The synthesis of **3f** was carried out in the same way as described in the synthesis of **1b** and **2e** but due to insolubility of **3e** in THF, methanol was added (**Scheme 2.17**). During the work-up process, the organic phase was washed two times instead of three times, because compound **3f** was expected to be water-soluble due to the solubility of **3e** in water. This feature may be due to the presence of three OH groups in **3e** (and therefore **3f**) which leads to a higher polarity and may result in a higher solubility in polar solvents. It was not possible to obtain the product from the aqueous phase directly. Because of that, the residue (from the evaporated organic phase) was diluted in water and another work-up was carried out as described by Kirin *et al.*[81] Compound **3f** was isolated with a yield of only 4**%**. The synthesis of **5d**

was carried out with the same work-up process as performed for **3f** because **5d** was also expected to be more likely water soluble due to the presence of two OH groups, even though compound **5c** was soluble in THF. The desired product **5d** was obtained with a yield of 16**%**.
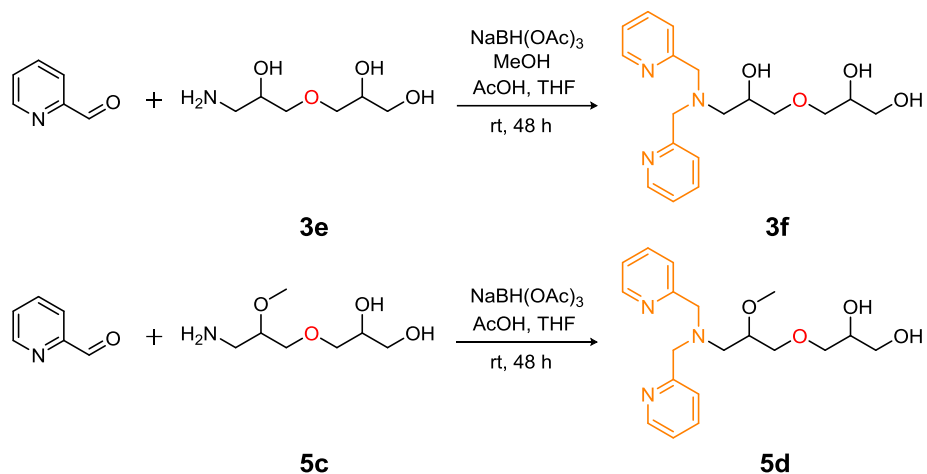
Scheme 2.17 *Synthesis of* **3f** *and* **5d**.

2.1.4 Synthesis of the bpa complexes

2.1.4.1 Nitrate Complexes

The synthesis of bpa complexes was performed with the compounds **1b**, **2e**, **3f**, **4c** and **5d** in ethanol (***Scheme 2.18***).[58] After addition of copper nitrate, the color of the bpa solution changed from light green to light brown (**1b**) to dark green (**2e**). However, it was only possible to isolate a nitrate complex from the bpa ligands **1b** and **2e**.

The compounds **6a** and **6b** were isolated with moderate yields (35% for **6a**, Lit.[58] 45**%**; 30**%** for **6b**) and analyzed successfully by ESI mass spectrometry and elemental analysis.

1b   **6a**

6b
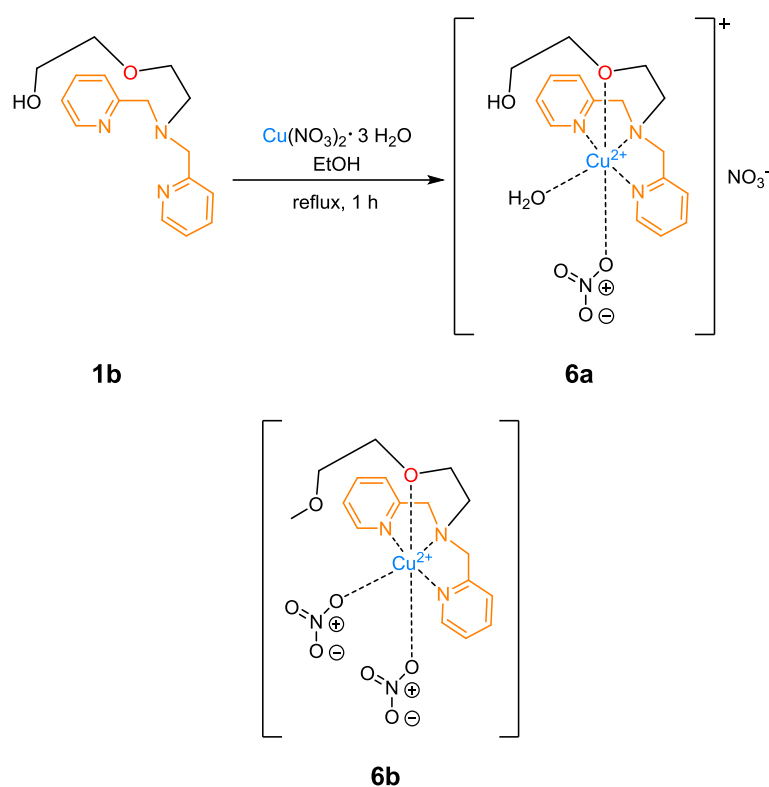
Scheme 2.18 *Synthesis of complex **6a** (**6a** has been reported to carry an aqua ligand[58]. Elemental analysis, however, did not show any water.) and structural formula of **6b**.*

2.1.4.2 Perchlorate complexes

For the synthesis of **7a** the copper complex formation of **1b** was carried out with another anion, here perchlorate (**Scheme 2.19**). The other complexes **7b–e** were formed from the bpa ligands **2e**, **3f**, **4c** and **5d**. The color of the bpa solution changed from light yellow (**1b**) or brown (**2e**, **3f**, **4c** and **5d**) to dark blue (**1b** and **4c**), dark green (**2e**) or dark tourqiuse (**3f** and **5d**). During the synthesis of perchlorate complexes **7a-e** the complex solution was treated with diethyl ether at -40 °C instead of slow ether diffusion (as suggested for the nitrate bpa complex **6a**)[58] at room temperature or at 4 °C (as suggested for bpa perchlorate complex **7a**)[68] because no precipitate could be formed at room temperature and 4 °C, respectively. After treatment at -40 °C, a precipitate occurred and the solid was further dried in vacuo overnight.

All perchlorate complexes could be isolated with moderate yields ranging from 21% to 40%. The synthesized compounds **7a–e** were analyzed successfully by ESI mass spectrometry and elemental analysis. The perchlorate complexes were hygroscopic, and were thus stored under inert atmosphere.
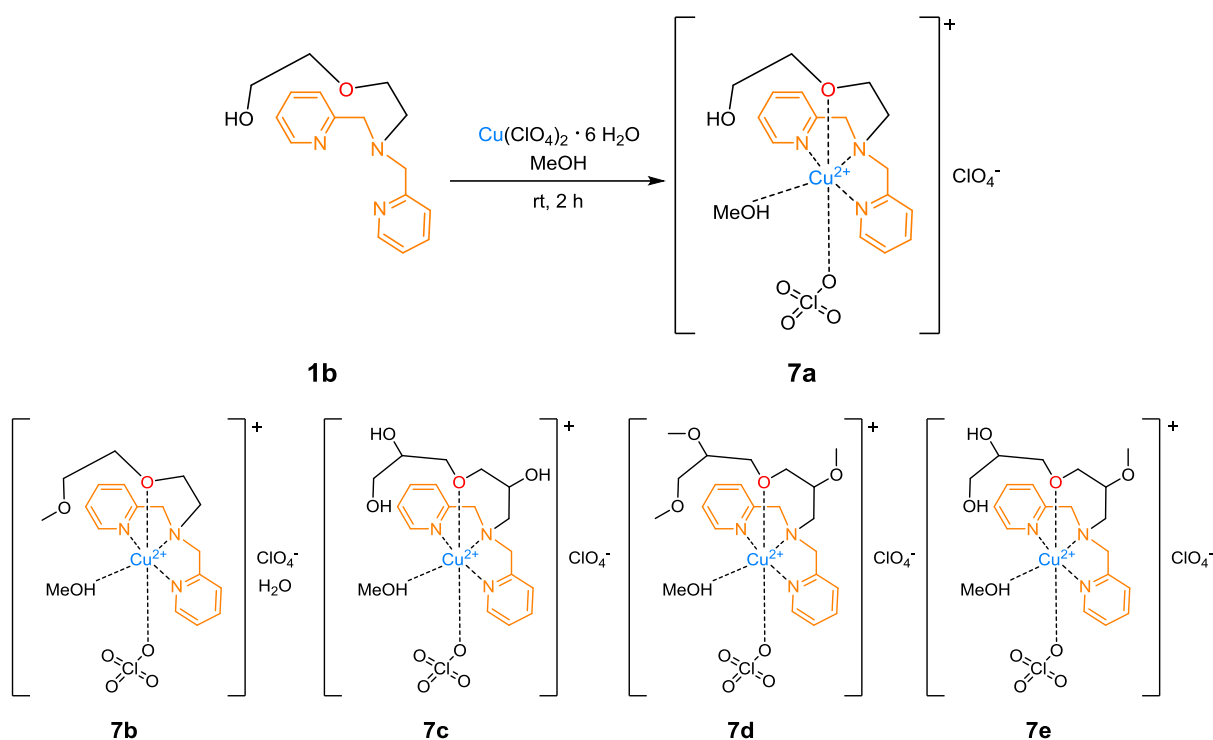
Scheme 2.19 *Synthesis of complex **7a** (**7a** carries a methanol solvent molecule as an equatorial ligand as determined by X-ray crystallography [68], whereas elemental analysis pointed to an aqua ligand at this coordination site) and structural formulae of **7b**, **7c**, **7d** and **7e**.*

2.1.5 Description of crystal structures

X-ray crystal structures of [Cu(**1b**)(H$_2$O)(ONO$_2$)]NO$_3$ **6a** (CCDC 218710)[58] and [Cu(**1b**)(MeOH)(OClO$_3$)]ClO$_4$ **7a** (CCDC612379)[68] have been reported before by Metzler-Nolte *et al.* and Mikata *et al.*, but are included in the following discussion because of their similarity with the complexes presented herein.

Single crystals of copper(II) complexes [Cu(**2e**)(ONO$_2$)$_2$] **6b** (CCDC 1440789) and [Cu(**2e**)(MeOH)(OClO$_3$)]ClO$_4$ **7b** (CCDC 1440791) were obtained by slow diffusion of diethyl ether in a methanolic solution of the complexes. *Table 2.1* summarizes crystal data and structure refinement parameters of **6b** and **7b**.

The structure of **6b** is shown in *Fig. 2.2* and selected bond lengths are shown in *Table 2.2*. The complex crystallized in the monoclinic space group P2$_1$/c (as **6a**[58]) and exhibits a neutral Cu(II) complex without any additional solvent molecule in the asymmetric unit. The Cu(II) centre is surrounded in a distorted octahedral fashion by six donor atoms including three nitrogen and one oxygen atom of **2e**. Two additional coordinated oxygen atoms arise from two nitrato ligands. This is in contrast to complex **6a** that contains the non-methylated ether tether ligand **1b**, where the second oxygen is provided by an aqua ligand, and the second nitrate ion belongs to the outer coordination sphere.

The basal plane in **6b** includes three nitrogen atoms from the bpa ligand and one oxygen atom from a nitrato ligand (in **6a** from an aqua ligand, respectively). Bond lengths in **6b** differ just slightly from each other and range from 1.959 to 2.046 Å. The copper atom lies 0.138 Å above the mean plane, defined by N1, N3, N2 and O1. The maximum deviation is shown by N1 (-0.130 Å) and N3 (+0.137 Å). Both facts indicate a significant deformation in the octahedral arrangement around the copper centre. The axial bonds are elongated with a Cu-O4 distance of 2.367 Å and 2.633 Å for Cu-O7, significantly less than the sum of the van der Waals radii of copper and oxygen (2.92 Å). The numbers for **6a** deviate only slightly from the ones reported above, indicating that despite the methyl group at O8 and an aqua ligand in place of the nitrato ligand, the structures are very similar. Differences are as expected only observed for the angles in the equatorial plane that accommodates the aqua and one nitrato ligand, respectively. Angles differ remarkably from the ideal 90° of an undistorted octahedron (e.g. O1-Cu-N3 171° for **6a**, 163° for **6b**). Intermolecular π-π stacking can be observed between two adjacent pyridine planes for both complexes

(*Fig. 2.3* for **6a** and **6b**). The structure of **6a** is stabilized by two hydrogen bonds (O1-H1a...O8, O1-H1b...O9 (ONO$_2$)) of the aqua ligand, whereas no such hydrogen bonding is possible in the methylated species **6b** because of an additional nitrato ligand occupying this coordination site instead of water.
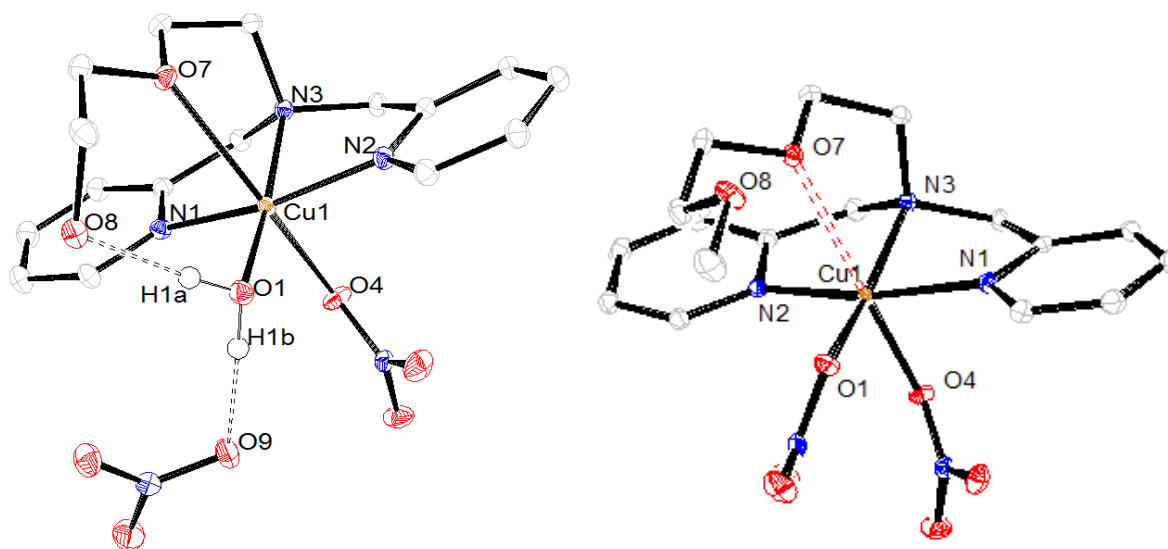
Fig. 2.2 *Comparison of ORTEP-III views of complexes **6a**[58] and **6b** without hydrogen atoms for clarity with 50% ellipsoid probability.*

A   **B**
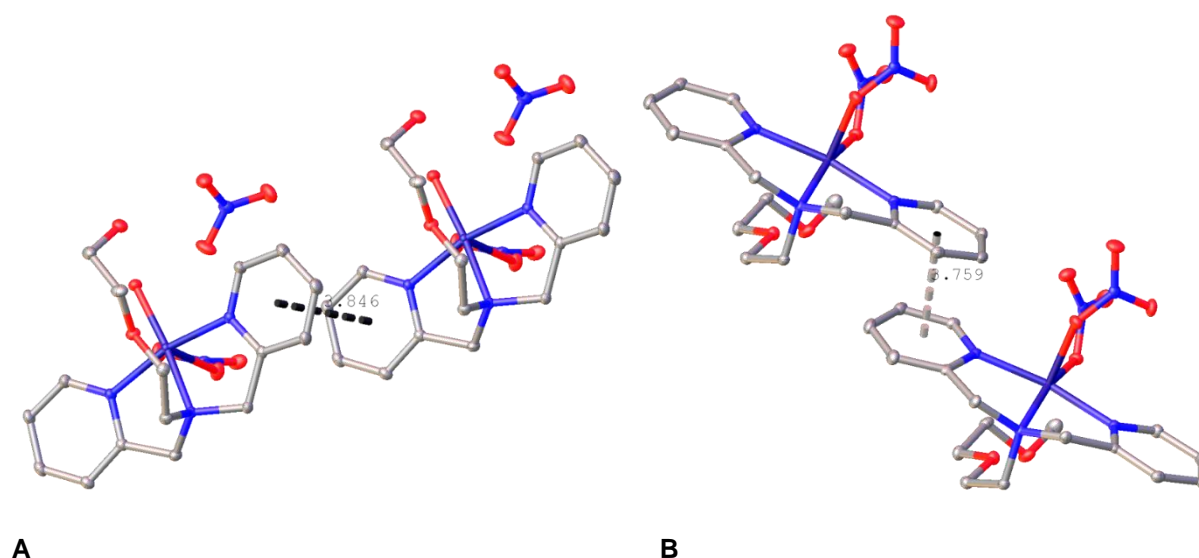
Fig. 2.3 *Olex2 picture of two molecules **6a** (A) and **6b** (B), respectively, with π-π contact between NCCCCC planes.*

The perchlorate complex **7b** crystallizes like its nitrate analogue **6b** in the monoclinic space group P2$_1$/c, whereas **7a** crystallizes in the orthorhombic space group Pbca[68] The structures of **7a** and **7b** are shown in *Fig. 2.4* and selected bond lengths and angles of **7a** and **7b** are shown in *Table 2.2*. Both molecules contain a

cationic species, [Cu(**1b**)(MeOH)(OClO$_3$)]$^+$ (**7a**) [Cu(**2e**)(MeOH)(OClO$_3$)]$^+$ (**7b**) and one perchlorate counter anion. The centre atom is also coordinated by six surrounding atoms in a distorted octahedral fashion but compared to **6b** one anion is exchanged by a solvent molecule (CH$_3$OH). A reason for that could be the steric influence of the perchlorate anion compared to the smaller nitrato ligand, which leads to the smaller methanol occupying the sixth position in the octahedral environment of Cu(II). Regardless of the length and substitution of the ether tether, both complexes, **7a** and **7b** show almost equal binding lengths for the coordinated atoms to Cu(II) (*Table 2.2*). Bond lengths in the basal plane for **7a** and **7b** are in the same range compared to **6b** and axial ligands exhibit a distance of 2.47 Å for the Cu-O4 bond and 2.48 Å for Cu-O2 (**7b**), respectively, and 2.48 Å for Cu-O4 and 2.45 for Cu-O2 (**7a**).
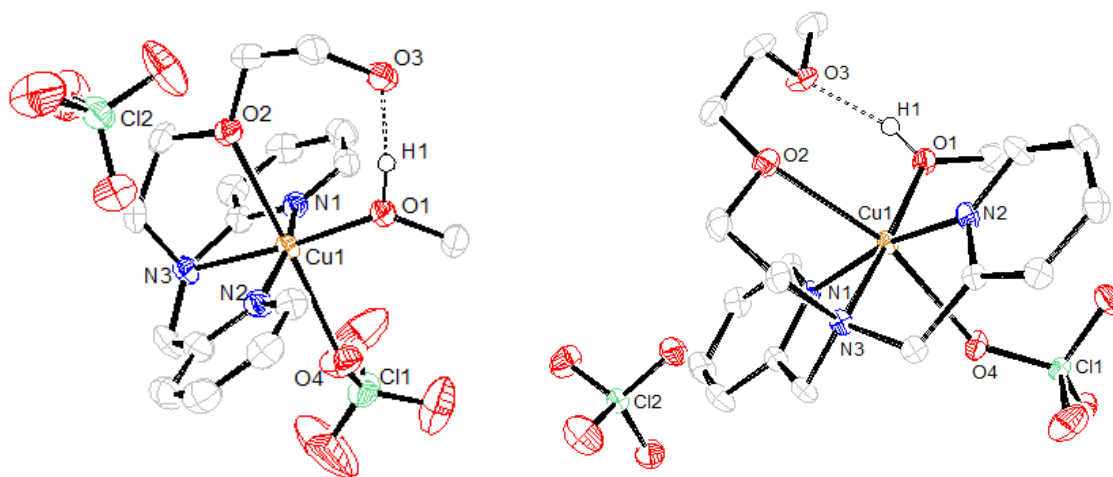
Fig. 2.4 *Comparison of ORTEP-III views of complexes **7a** and **7b** with 50% ellipsoid probability including intramolecular H bonding.*

There is a considerably shorter binding length for the oxygen of the bpa chain to the copper centre (Cu-O2) in the perchlorate complexes **7a** and **7b** when compared to the nitrato complexes **6a** and **6b** (Cu-O7: 2.56 and 2.63 Å, respectively), whereas the nitrato ligand is closer to the copper centre (Cu-O4: 2.34 and 2.37 Å, respectively). Generally, the structures regarding the mean plane and the copper atom related to the basal plane are less distorted compared to **6b** with a maximum deviation for N3 of -0.117 Å in **7a** and -0.103 Å in **7b** concerning the basal plane. The copper atom in both molecules lies just slightly above the square plane with distances of 0.030 (**7a**) and 0.005 Å (**7b**), respectively. Both complexes exhibit an intramolecular hydrogen bond O1-H…O3 between the coordinated methanol and an

oxygen atom of the chain in the bpa ligand (*Table 2.3*). In contrast to **6a** and **6b**, no intermolecular π-π interaction between pyridine moieties is observable.

In conclusion, the crystal system seems to depend on the substitution of the bpa ligand. All complexes are Jahn-Teller distorted as indicated by a value of 9.8 (0.82 for **6a**) for the tetragonality *T*.[82, 83] Furthermore, the molecular structure of the molecule itself is more dependent on the anion resulting from the used copper salt, but the way of coordination of the bpa ligand to the copper centre does not differ significantly. The extent of hydrogen bonding, however, depends on both, the type of bpa ligand and the anion used.

Table 2.1 *Crystal data and structure refinement parameters of complexes* **6b** *and* **7b**.

	6b	7b
CCDC deposition number	1440789	1440791
Empirical formula	$C_{17}H_{23}CuN_5O_8$	$C_{18}H_{27}Cl_2CuN_3O_{11}$
Formula weight	488.94	595.86
Crystal system	monoclinic	monoclinic
Space group	$P2_1/c$	$P2_1/c$
a (Å)	8.1392(8)	8.6944(3)
b (Å)	28.827(3)	26.5046(12)
c (Å)	8.4997(9)	11.3350(5)
α (°)	90	90
β (°)	98.922(3)	110.0202(14)
γ (°)	90	90
V ($Å^3$)	1970.1(4)	2454.21(18)
Z	4	4
Density (g cm^{-3})	1.648	1.613
μ (MoK_α)(mm^{-1})	0.71073	0.71073
F(000)	1012.0	1228.0
T (K)	100.09	100.0
Ө min-max (deg)	2.53-26.40	2.45-26.49
Data set [h, k, l]	$-10 \leq h \leq 8$, $-35 \leq k \leq 36$, $-10 \leq l \leq 10$	$-10 \leq h \leq 10$, $-33 \leq k \leq 33$, $-14 \leq l \leq 14$
Refinement	Least squares	Least squares
R_1 (reflections) [all data]	0.0311 (4038)	0.0412 (5056)
R_1 (reflections) [$I \geq 2\sigma(I)$]	0.0263 (3651)	0.0324 (4403)
wR_2	0.0648	0.0727

	Goodness-of-fit	1.061	1.071
	Largest diff. peak and hole (e Å⁻³)	0.37 and -0.39	0.45 and -0.46

Table 2.2 *Selected bond lengths (Å) and angles (°) of complexes **6a**, **6b**, **7a** and **7b**.*

	6a[58]	6b		7a[68]	7b
Cu-N1	1.996	1.9950(14)	Cu-N1	1.985	1.9756(18)
Cu-N2	1.990	1.9940(14)	Cu-N2	1.981	1.9642(18)
Cu-N3	2.044	2.0460(13)	Cu-N3	2.013	2.0133(18)
Cu-O1	1.981	1.9590(12)	Cu-O1	1.954	1.9603(16)
Cu-O4	2.338	2.3672(12)	Cu-O2	2.452	2.4787(16)
Cu-O7	2.562 (cal.)	2.633 (cal.)	Cu-O4	2.478	2.4716(16)
N1-Cu-N2	165.7	165.06(6)	N1-Cu-N2	165.2	166.62(8)
N1-Cu-N3	83.4	81.41(5)	N1-Cu-N3	83.5	84.81(7)
N2-Cu-N3	82.3	83.69(5)	N2-Cu-N3	82.4	83.45(7)
O1-Cu-N1	98.5	92.47(5)	O1-Cu-N1	98.8	96.66(7)
O1-Cu-N2	95.6	102.21(5)	O1-Cu-N2	95.6	95.60(7)
O1-Cu-N3	171.2	163.80(5)	O1-Cu-N3	172.1	174.70(7)
O4-Cu-O7	163.169 (cal.)	161.269 (cal.)	O2-Cu-O4	176.2	164.66(6)

Table 2.3 *Hydrogen bond (Å) and angle (°) of complexes **7a** and **7b**.*

complex	O-H...O	d (O-H)	d (H...O)	<(OHO)
6a[58]	O1-H1a...O8	0.849	1.818 (cal.)	174.5 (cal.)
6b	O1-H1b...O9 (ONO₂)	0.855	1.876 (cal.)	167.9 (cal.)
7a[68]	O1-H1...O3	0.876(9)	1.676 (cal.)	166.6 (cal.)
7b	O1-H1...O3	0.865(9)	1.746 (cal.)	161.1 (cal.)

2.1.6 Gel electrophoretic studies

*Agarose gel electrophoresis is a useful method to study the DNA cleavage activity of specific organic or inorganic compounds. Using this method, the cleavage of plasmid DNA (e.g. pBR322[84]) can be investigated. The metal complexes might cause random nicks or cuts to one of the DNA strands. Therefore, the supercoiled form (sc, Form I) opens to form an open circular (Form II) after one nick and subsequently linear form (Form III) if two nicks on complementary strands are within a short distance. Finally, the DNA gets decomposed into small pieces of different size which cannot be separated in the assay, but appear as a smear. After ethidium bromide staining and gel visualization under ultraviolet light, the conformational states (Form I, II, III) of the DNA can be assigned to the bands shown in the gel (**Fig. 2.5**).[85]*
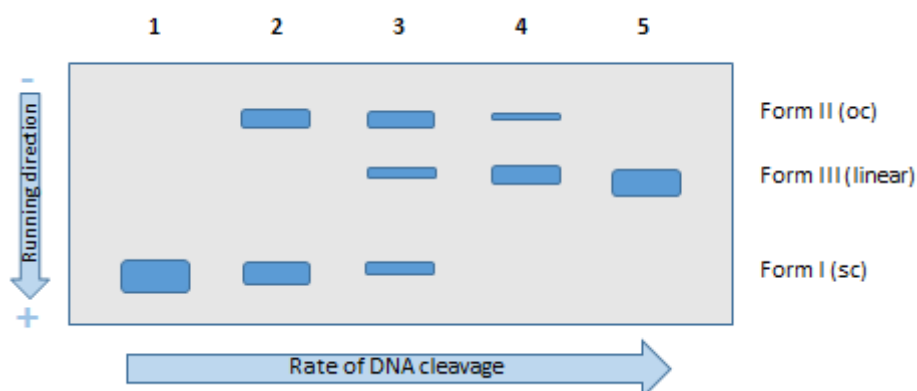
***Fig. 2.5.** Cleavage of Form I to Form II and Form III plasmid DNA by agarose gel electrophoresis.*

2.1.6.1   Hydrolytic cleavage

In order to assess the DNA cleavage ability of the complexes, supercoiled (sc) pBR322 DNA (Form I) was incubated with varying concentrations of **6a–b** and **7a–e** in Tris-HCl buffer (50 mM) at pH 7.4 for 24 h (***Fig. 2.6** and **Fig. 2.7***).
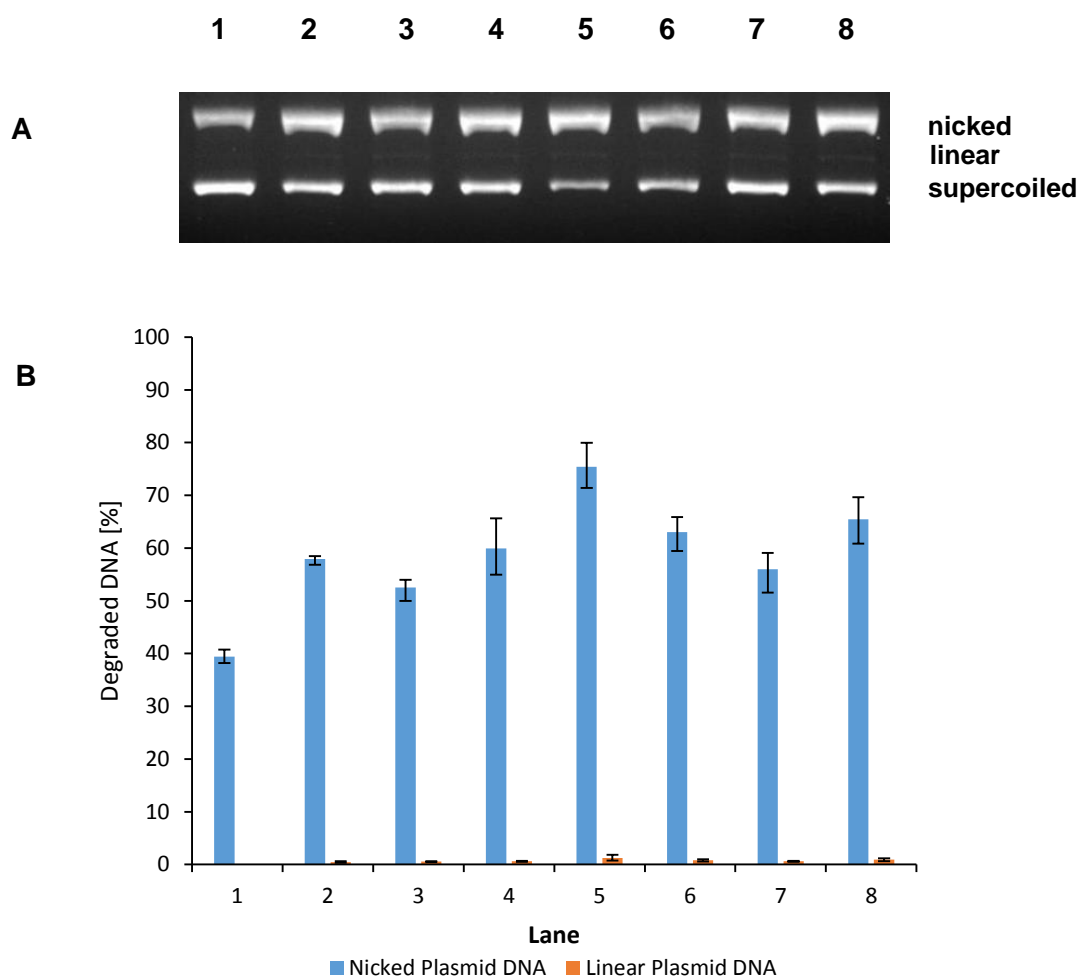
Fig. 2.6 *(A) Cleavage activity of the complexes monitored by **1%** agarose gel electrophoresis after incubation at 37 ℃ for 24 h. Every lane contained 0.2 µg plasmid DNA in 50 mM Tris-HCl buffer (pH 7.4) (representative gel). Lane 1: Reference DNA; lane 2: **6a** (1.25 mM); lane 3: **6b** (1.25 mM); lane 4: **7a** (1.25 mM); lane 5: **7b** (1.25 mM); lane 6: **7c** (1.25 mM); lane 7: **7d** (1.25 mM); lane 8: **7e** (1.25 mM). (B) Percentage of degraded DNA (error bars represent the standard deviations from three independent experiments).*
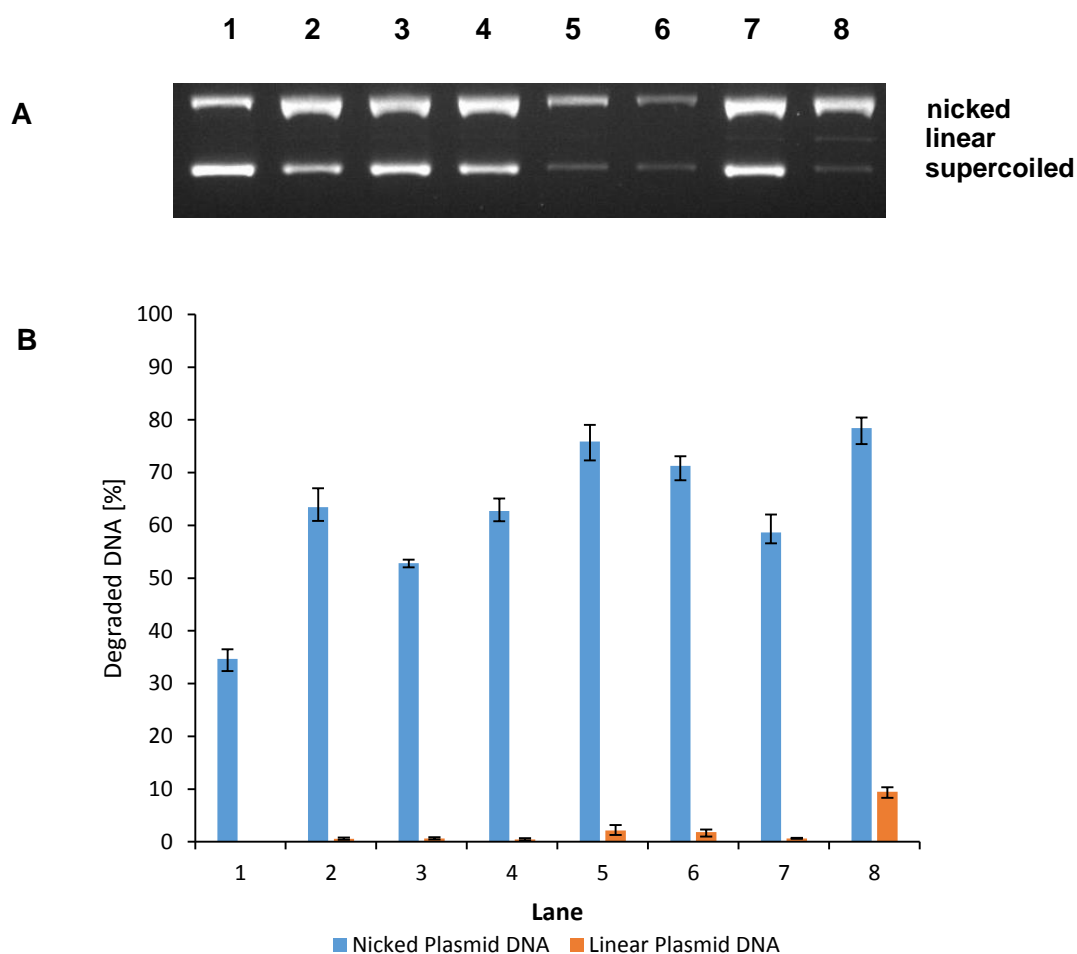
Fig. 2.7 *(A) Cleavage activity of the complexes monitored by 1% agarose gel electrophoresis after incubation at 37 °C for 24 h. Every lane contained 0.2 µg plasmid DNA in 50 mM Tris-HCl buffer (pH 7.4) (representative gel). Lane 1: Reference DNA; lane 2: **6a** (5 mM); lane 3: **6b** (5 mM); lane 4: **7a** (5 mM); lane 5: **7b** (5 mM); lane 6: **7c** (5 mM); lane 7: **7d** (5 mM); lane 8: **7e** (5 mM). (B) Percentage of degraded DNA (error bars represent the standard deviations from three independent experiments).*

As it can be seen in lane 1 of both **Fig. 2.6** and **Fig. 2.7**, even the reference DNA was converted into 35–40**%** of Form II due to the long incubation time of 24 h. At 5 mM concentration, percentages of cleaved plasmid were still higher for the employed complexes (55–80**%** of Form II and 1-10**%** of Form III). At 1.25 mM concentration and under identical conditions, the complexes **6a–b** and **7a–d** (lanes 2–7, **Fig. 2.6**) exhibited similar DNA cleavage activity, but only up to 1% of linear plasmid was obtained. Metzler-Nolte *et al.* reported[58] complex **6a** showing cleavage activity within the same order of magnitude, however, the experimental conditions were slightly different (pUC19 plasmid, 5 mM NaCl, 5 mM Tris HCl buffer).

Although only small differences in cleavage activity are observed for the complexes tested, the study produced high reproducibility with small error bars and

thus allows to some extent to draw conclusions connecting DNA cleavage activity and the structures of the complexes applied. According to the mechanism postulated by Metzler-Nolte *et al.*[58], the hydroxyl group (***Scheme 2.1***) abstracts a proton of a coordinated water molecule. Although in the crystal structure in some cases MeOH occupies this coordination site, it should be uncontroversial that in aqueous solution an aqua ligand can replace MeOH.

Complex **6a** possibly is a more efficient DNA cleaver than **6b** due to the hydrogen bonds that can be formed by the aqua ligand as deduced from the crystal structure (***Fig. 2.2***) and promote hydrolytic DNA cleavage. This situation corroborates the mechanism as reported by Metzler-Nolte *et al.*[58] It can be assumed, however, that the nitrato ligands of **6b** are also exchanged with aqua ligands in aqueous solution, enabling hydrogen bonding also in this case. Additionally, the lower proton acceptor ability of the methylethyl ether in **6b** compared to the free hydroxyl group of **6a** might be a reason for the lower activity of **6b**. Indeed, ethanol (as a simplification of the 2(3)-hydroxyl-ethoxy(propoxy) tether in **6a**, but also in **7a**, **7c** and **7e**) is a better proton acceptor, i.e. Brønsted base (pK_A of the conjugate acid -2.4)[86], in comparison to methylethyl ether (as a simplification of 2(3)-methoxy-ethoxy(propoxy) tethers as in **6b**, but also **7b** and **7d**, pK_A of the conjugate acid -3.8[87]).

When **6a** is compared to its perchlorate equivalent **7a**, as expected, the counter ion does not have any influence and results in similar DNA cleavage activity of the two complexes. However, when **6b** and **7b** are compared, the perchlorate complex is a more efficient DNA cleaver. The structures of complexes **6b** and **7b** are too similar as indicated by characteristic bond lengths and angles (***Table 2.2***) to serve as a basis of discussion for the differences in cleavage activity. In particular, it is to be expected that in aqueous solution they approximate each other structurewise.

Chin *et al.* [57] have shown before that hydroxypropyl substituents at the bpa moiety lead to more efficient cleavers of phosphate ester bonds than ligands with hydroxyethyl tethers. This was justified with the closer proximity of the reactive hydroxyl group to the aqua ligand to be deprotonated and the substrate to be cleaved, respectively, due to the bulkiness of the longer tether. Indeed, at a 5 mM concentration **7e** with a 3-hydroxypropyl-propoxy tether outreaches the complex **6a** known to the literature carrying a 2-hydroxyethyl-ethoxy tether by a factor of 10 with relating to the yield of linear DNA. Also **7b** and **7c** still yield twice as much linear DNA

in comparison to **6a**. The longer alkyl chain analogue **7d** of the methylated complex **7b**, however, is less active, which might be attributed to the additional methoxy group in position 2 of the propoxy linker.

Interestingly, Chin *et al.*[57] have observed two different mechanisms for the two tethers mentioned above. Whereas for the hydroxypropyl tether a fast transesterification process is postulated, the hydroxyethyl tethered complex showed slower hydrolysis of BNPP due to an exchange of the tether by a hydroxide anion. Thus, depending on which mechanism applies to the complexes presented here, also differences in DNA cleavage activity might be observed. On the other hand, as also stated by Metzler-Nolte *et al.*[58] BNPP might not be a realistic model for DNA, and comparisons between BNPP-based and plasmid DNA-based studies might be problematic.

2.1.6.2 Oxidative cleavage

In order to assess the oxidative DNA cleavage ability of the complexes, supercoiled (sc) pBR322 DNA (Form I) was incubated with varying concentrations of **6a–b** and **7a–e** in Tris-HCl buffer (50 mM) at pH 7.4 for 2 h in the presence of a reducing agent, here ascorbate. Concerning the oxidative cleavage (***Fig. 2.8***), the complexes showed similar activity (about 90**%** of Form II and 5–10**%** of Form III) at a concentration of 12.5 µM.

At a concentration of 50 µM, all bpa complexes produce complete cleavage of the supercoiled DNA into ca. 70–75**%** of Form II and 25–30**%** of Form III (***Fig. 2.9***). This is to be expected since oxidative cleavage activity should not depend on the linker type used, but only on the redox activity of the copper center.
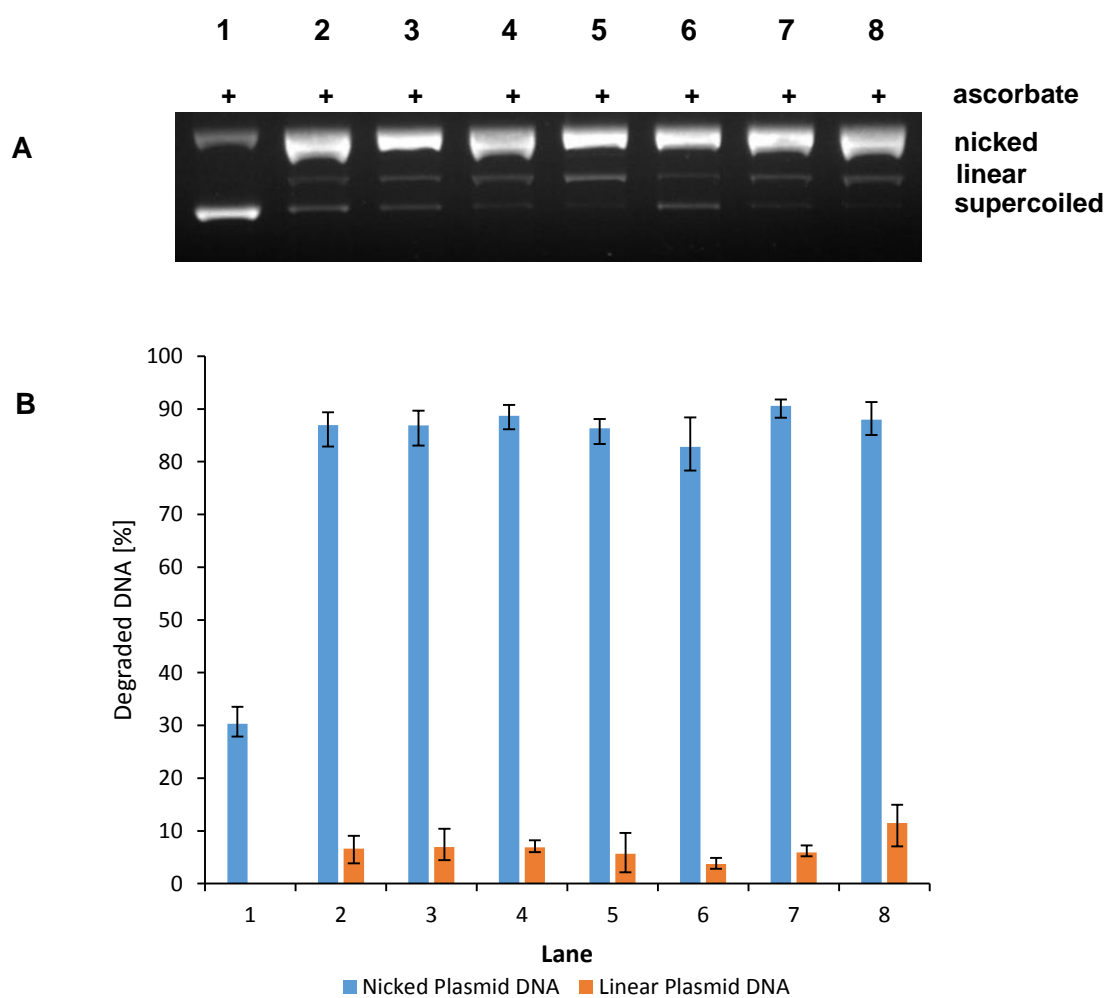
Fig. 2.8 (A) Cleavage activity of the complexes monitored by 1% agarose gel electrophoresis after incubation at 37 °C for 2 h. Every lane contained 0.2 µg plasmid DNA in 50 mM Tris-HCl buffer (pH 7.4) in the presence of ascorbate (1 mM) (representative gel). Lane 1: Reference DNA; lane 2: **6a** (12.5 µM); lane 3: **6b** (12.5 µM); lane 4: **7a** (12.5 µM); lane 5: **7b** (12.5 µM); lane 6: **7c** (12.5 µM); lane 7: **7d** (12.5 µM); lane 8: **7e** (12.5 µM). (B) Percentage of degraded DNA (error bars represent the standard deviations from three independent experiments).
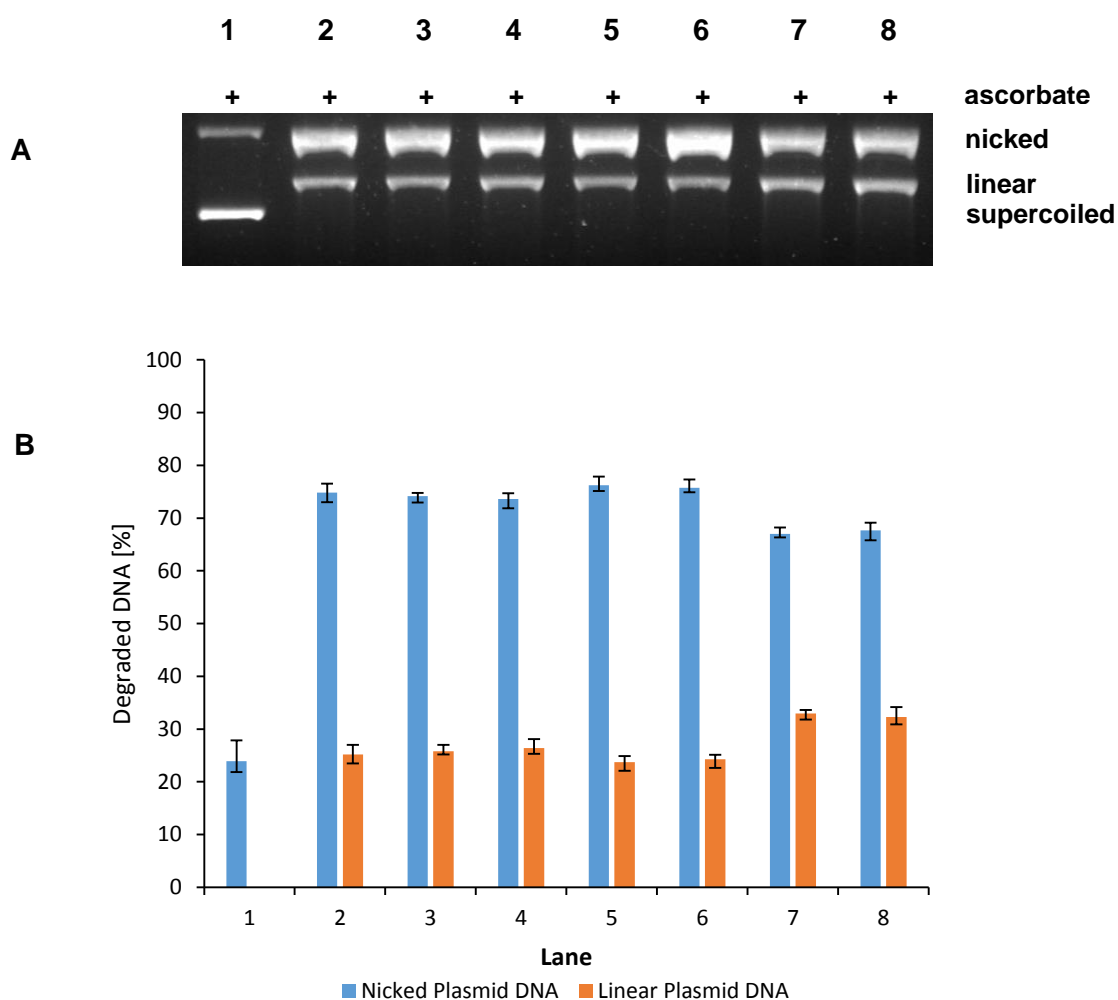
Fig. 2.9 (A) *Cleavage activity of the complexes monitored by 1% agarose gel electrophoresis after incubation at 37 °C for 2 h. Every lane contained 0.2 μg plasmid DNA in 50 mM Tris-HCl buffer (pH 7.4) in the presence of ascorbate (1 mM) (representative gel). Lane 1: Reference DNA; lane 2:* **6a** *(50 μM); lane 3:* **6b** *(50 μM); lane 4:* **7a** *(50 μM); lane 5:* **7b** *(50 μM); lane 6:* **7c** *(50 μM); lane 7:* **7d** *(50 μM); lane 8:* **7e** *(50 μM). (B) Percentage of degraded DNA (error bars represent the standard deviations from three independent experiments).*

A very recent study by Kim *et al*. has shown that the substitution pattern of bpa copper complexes did influence the oxidative cleavage activity. The cleavage efficiencies of complexes of the type [Cu(R-benzyl-bpa)(NO$_3$)$_2$] (R = OMe, CH$_3$, H, F and NO$_2$) were therein compared with the unsubstituted bpa complex. Electron-donating groups like CH$_3$ in the *para*-position of the benzyl substituent led to an enhancement, whereas electron-withdrawing groups lead to a reduction in DNA cleavage activity.[88] Such substitutions might indeed have a direct effect on the redox potential of the copper complexes, whereas the alkyl linkers used in this study should not have such an influence and should thus result in similar cleavage activity for all complexes investigated.

2.1.6.3 ROS studies for oxidative cleavage

*Reactive oxygen species (ROS) are constantly formed in the human body and removed by antioxidant defenses. An antioxidant is a substance that, when present at low concentrations compared to that of an oxidizable substrate, significantly delays or prevents oxidation of that substrate. Antioxidants can act by scavenging biologically important ROS such as $O_2^{-}\cdot$, H_2O_2 and $\cdot OH$ by preventing their formation, or by repairing the damage that they cause. One problem with scavenging-type antioxidants is that secondary radicals derived from them can often themselves cause biological damage like DNA cleavage. In the upcoming studies we use different quenchers to investigate the formed ROS, which are possibly involved in the DNA cleavage. For example, SOD decomposes two $O_2^{-}\cdot$ molecules by catalyzing a dismutation reaction, involving an oxidative reaction to one equivalent oxygen and reduction of another equivalent to hydrogen peroxide (**Scheme 2.20**).[89]*

$$O_2^{-}\cdot \ + \ O_2^{-}\cdot \ + \ 2\,H^+ \ \longrightarrow \ H_2O_2 \ + \ O_2$$
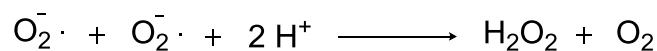
Scheme 2.20 *Effect of SOD on the reactive oxygen species $O_2^{-}\cdot$*

In order to characterize the essential reactive oxygen species responsible for the oxidative DNA cleavage of the complexes, exemplarily **7a**, **7c** and **7d** were investigated and incubated in the presence of DNA and ascorbate with different scavengers for the following species (shown in ***Fig. 2.10*** for **7a** representatively):[90-93]

a) *tert*-Butanol for hydroxyl radicals

b) DMSO for hydroxyl radicals

c) Sodium azide (NaN$_3$) for singlet oxygen

d) Catalase for hydrogen peroxide

e) Superoxide dismutase for superoxide
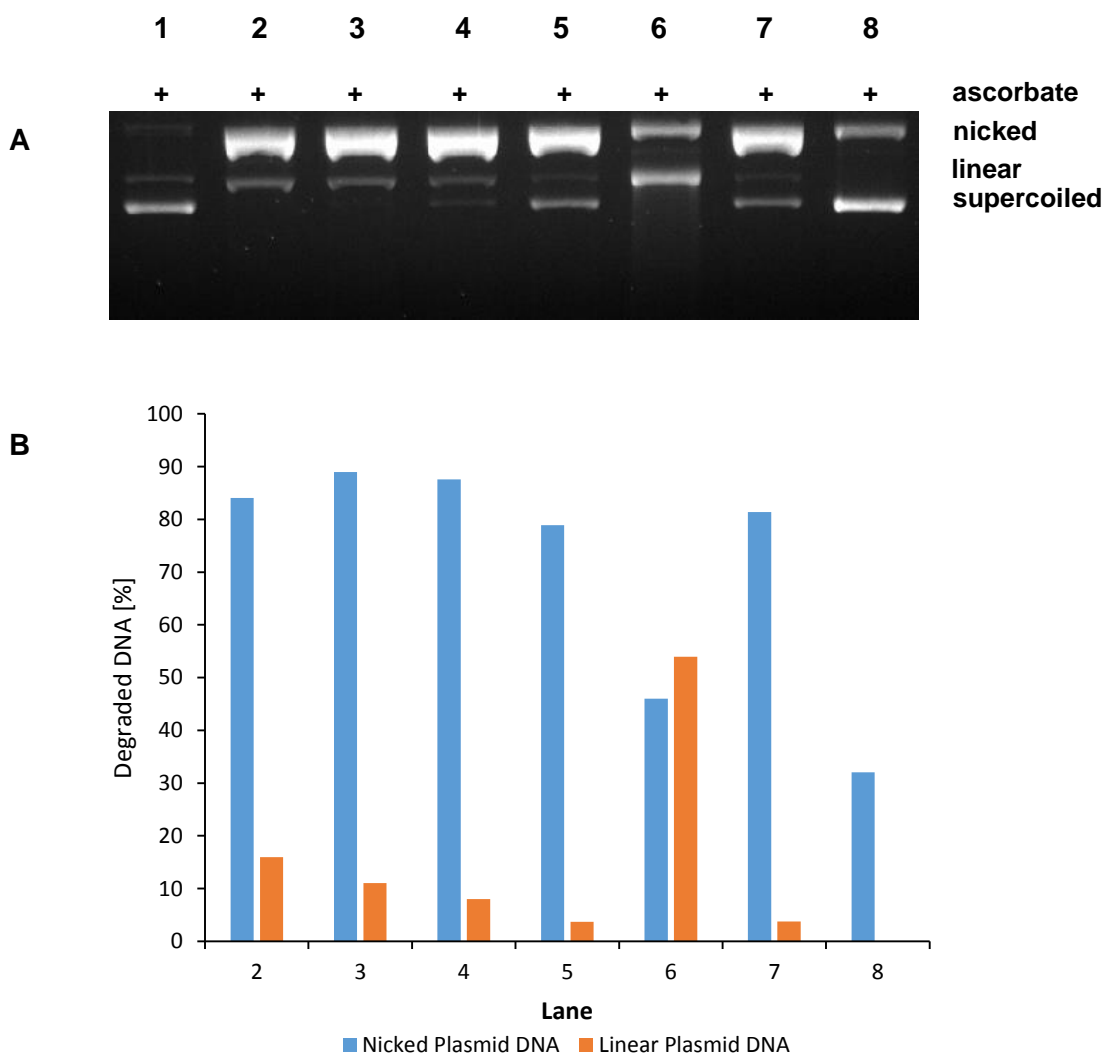
Fig. 2.10 *(A) Quenching effects on DNA cleavage by **7a** monitored by 1% agarose gel electrophoresis after incubation at 37 °C for 2 h. Every lane contained 0.2 µg plasmid DNA in 50 mM Tris-HCl buffer (pH 7.4) and 0.125X PBS in the presence of ascorbate (1 mM) (representative gel). Lane 2-7 contained 50 µM of **7a**. Lane 1: DNA ladder; lane 2: reference; lane 3: 200 mM ᵗBuOH; lane 4: 200 mM DMSO, lane 5: 10 mM NaN₃; lane 6: 2.5 mg/mL catalase; lane 7: 313 U/mL superoxide dismutase; lane 8: reference DNA. (B) Percentage of degraded DNA.*

Compared to lane 2 (***Fig. 2.10***) containing the reference, the DNA cleavage of **7a** was surprisingly increased in the presence of catalase, for which there is no reasonable explanation at the moment. Only a small scavenging effect was observed in the presence of ᵗBuOH and DMSO (lanes 3 and 4). A distinct quenching as indicated by the reappearance of supercoiled DNA happened only in the case of NaN3 and superoxide dismutase (lanes 5 and 7). Most probably, singlet oxygen and superoxide are involved in the DNA cleaving process. These species have recently been identified as the active species also in the oxidative DNA cleavage by the

complexes [Cu(R-benzyl-bpa)(NO$_3$)$_2$], mentioned above. The origin of singlet oxygen is unclear, but it is likely that singlet oxygen is generated from hydrogen peroxide, which might be formed by superoxide radicals.[89, 94] The superoxide radical might be produced by the coordination of O$_2$ to the Cu(I)complex through the following reaction:[88]

$$Cu(II)complex + ascorbate \longrightarrow Cu(I)complex + ascorbate^{-} \cdot + H^{+}$$

$$Cu(I)complex + O_2 \rightleftharpoons \left[Cu(I)\text{-}O_2 \rightleftharpoons Cu(II)\text{-}O_2^{-} \cdot \right] \rightleftharpoons Cu(II)complex + O_2^{-} \cdot$$
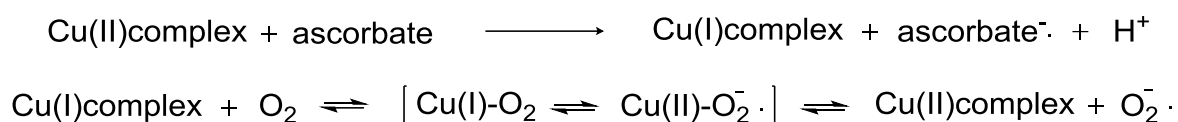
Scheme 2.21 *Generation of superoxide by bpa complexes in the presence of ascorbate.[88]*

Complexes **7c** and **7d** showed a very similar behavior (not shown).

2.1.6.4   Investigation of possible ROS in the absence of ascorbate

Hydrolytic cleavage activity has been proposed for bpa complexes before, regardless of the metal present in the complex (i.e. redoxactive or redoxinactive).[58] There are, however, several literature examples for complexes with redoxactive metals[95, 96] and even redoxinert metals[97], where oxidative cleavage can occur in the absence of reducing agents. The term "self-activating" nucleases was coined for such complexes that carry out DNA cleavage by using their redoxactive ligand systems as redox partners.

In order to find out, if ROS could also be generated in the absence of ascorbate, DNA cleavage studies were carried out with the same complex concentration as used in the hydrolytic cleavage studies and in absence of any reducing agent. For the DNA cleavage of **7a**, **7c** and **7d** the following scavengers were used (shown in **Fig. 2.11** for **7a** representatively):

a) *tert*-Butanol for hydroxyl radicals
b) DMSO for hydroxyl radicals
c) Sodium azide (NaN$_3$) for singlet oxygen

The enzymes catalase and superoxide dismutase were not applied as above (**Fig. 2.10**) due to the long incubation time, which might have resulted in an inactivation/decomposition of the enzymes.

No significant change of DNA cleavage activity occurred for all the complexes **7a**, **7c** and **7d** indicating the absence of hydroxyl radicals and singlet oxygen (**Fig. 2.11**, results of **7c** and **7d** are not shown). Although this experiment did not catch superoxide and H$_2$O$_2$ as potential ROS, it can be assumed that hydrolytic DNA cleavage is the predominant mechanism in the absence of reducing agents.
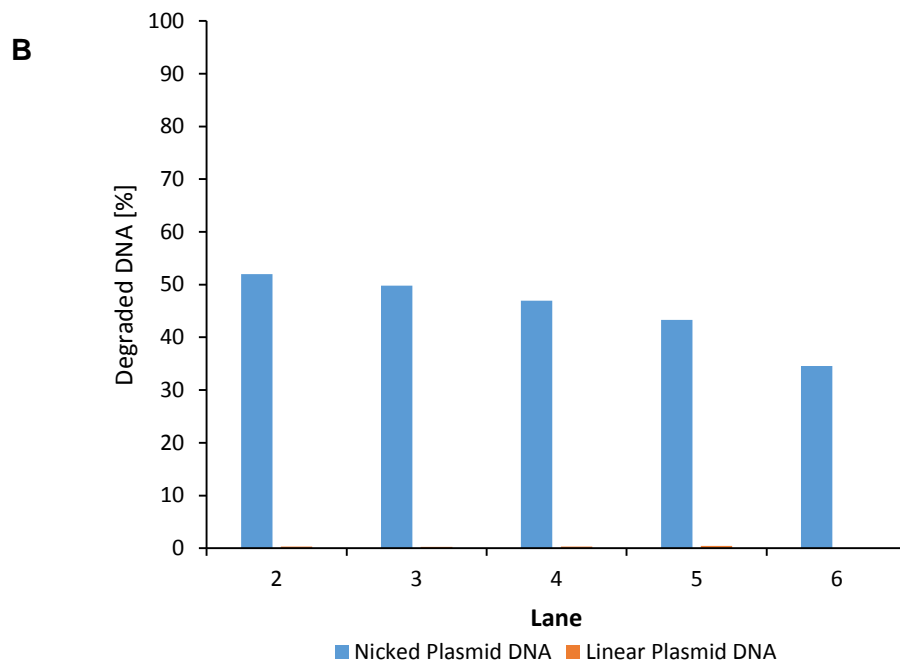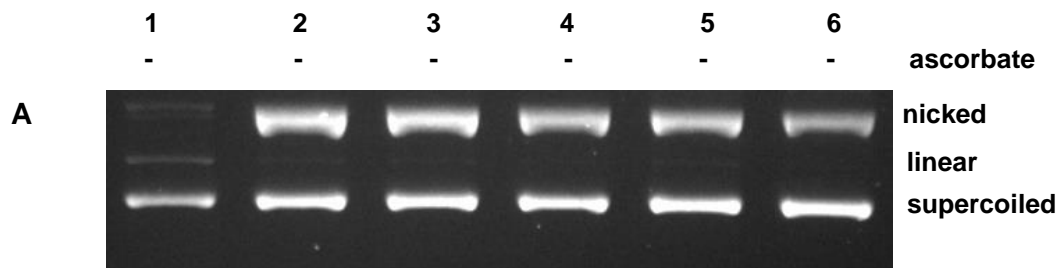
Fig. 2.11 (A) Quenching effects on DNA cleavage by **7a** monitored by 1% agarose gel electrophoresis after incubation at 37 °C for 24 h. Every lane contained 0.2 µg plasmid DNA in 50 mM Tris-HCl buffer (pH 7.4) and 0.125X PBS (representative gel). Lane 2-5 contained 5 mM of **7a**. Lane 1: DNA ladder; lane 2: reference; lane 3: 200 mM tBuOH; lane 4: 200 mM DMSO, lane 5: 10 mM NaN$_3$; lane 6: reference DNA. (B) Percentage of degraded DNA.

2.1.7 CD spectroscopy

*Circular dichroism (CD) is based on dichroism involving left and right circularly polarized light (**Fig. 2.12**). It is a useful spectroscopic method for studying optically active chiral molecules or conformational changes that occur during the folding and unfolding of proteins. In the latter case, the wavelengths and magnitudes of the ellipticity bands of the amide backbones of proteins are dependent on their conformation making them a useful index of protein folding. Proteins with a high degree of order, such as those with a high helical content, have large distinctive CD bands that are not present in unfolded proteins.[98, 99]*
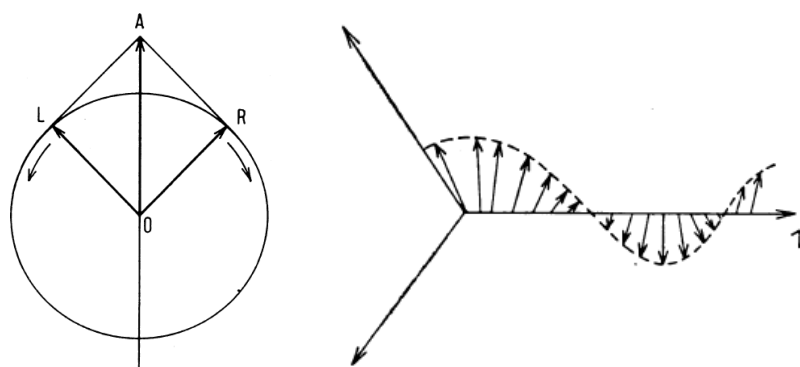
Fig. 2.12 *Resolution of electric vector of plane polarized light into electric vectors of right and left circularly polarized light (left). Electric vector of right circularly polarized light (right). Reprinted with permission from S. Beychok, Science, **1966**, 154, 1288.[99]*

CD spectroscopy was used in order to investigate the interaction between the complexes and CT-DNA. The CD spectrum of CT-DNA consists of a positive band at 277 nm due to base stacking and a negative band at 245 nm due to helicity, which is characteristic of DNA in the right-handed B form. In case of intercalation, the intensities of the bands might be enhanced, which would be attributed to the stabilization of the right-handed B form of CT-DNA. In case of little or no perturbation on the base stacking and helicity bands, the interaction of the complexes with DNA might be affected by means of groove binding or electrostatic interaction mode.[100] Complexes **7a**, **7c** and **7d** were exemplarily chosen to be incubated with CT-DNA at 1/R = [complex]/[DNA] = 0.5 and the CD spectra were recorded at room temperature in Tris–HCl buffer, pH 7.4. Compared to the CD spectrum of CT-DNA only small

changes in both positive and negative bands were identified in the presence of the complexes (*Fig. 2.13*), suggesting that the CT-DNA helicity is not disturbed by the interactions of the bpa complexes and that the binding mode might be non-intercalative.[101]
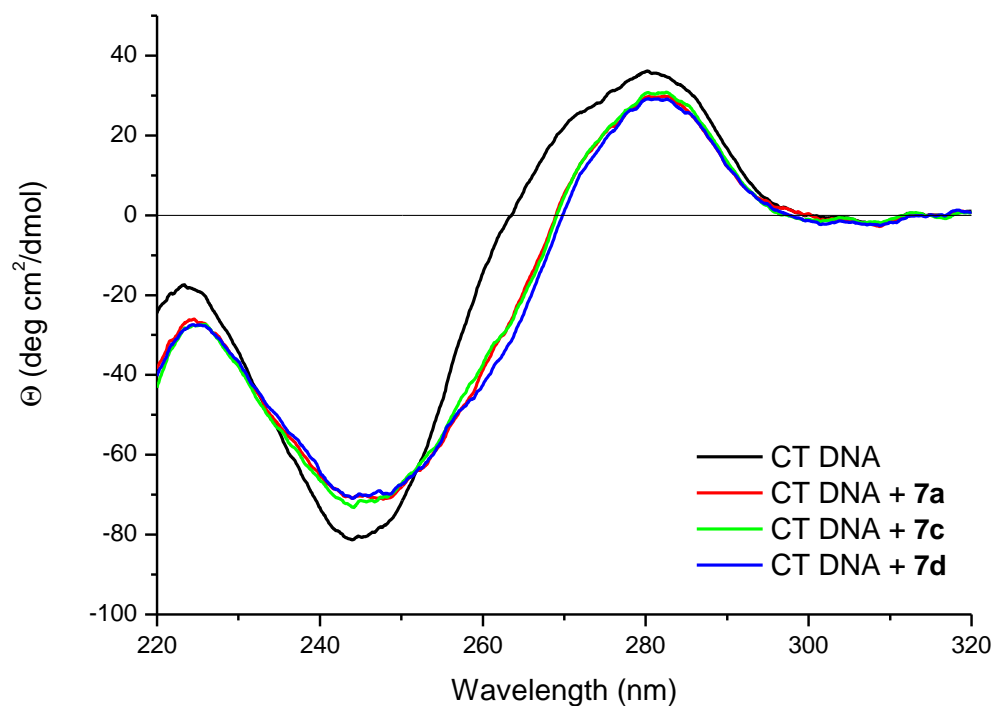
Fig. 2.13 *CD spectra of CT-DNA and its interaction with **7a**, **7c** and **7d** where [complex]/[CT-DNA] = 0.5. All spectra were recorded at room temperature in Tris–HCl buffer, pH 7.4.*

CHAPTER 3

BPA ESTROGEN DERIVATIVES

Sex steroids are steroid hormones classified in three types: androgens, estrogens and progestogens. Androgens are defined as male sex hormones, whereas both estrogens and progestogens as female sex hormones, although all types are present in each sex. The major naturally existing sex steroid in women is estrogen and includes estrone (E1), estradiol (E2) and estriol (E3) (*Fig. 3.1*).[102]

Estrone (E1)   Estradiol (E2)   Estriol (E3)
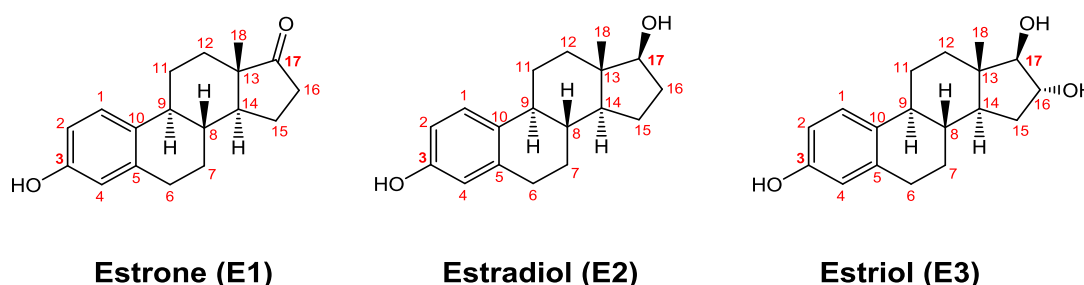
Fig. 3.1 *Chemical structure of estrone (E1, left), estradiol (E2, middle) and estriol (E3, right).*

The best known progestogen is progesterone, which is responsible for the growth of the endometrium.[103] Estrogens as well as progestogens have the ability to diffuse across the cell membrane. Once inside the cell, they bind to and activate estrogen receptors (ERs) or progesterone receptors (PRs), respectively, which in turn modulate the expression of many genes.
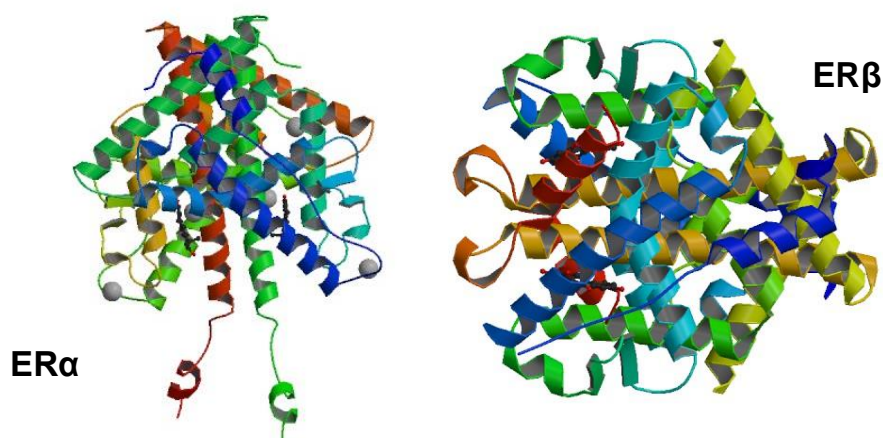
Fig. 3.2 *Left: structure of ERα ligand-binding domain complexed to estradiol (PDB ID: 1A52).[104] Right: Human ERβ ligand-binding domain in complex with partial agonist genistein (PDB ID: 1QKM).[105]*

The two different forms of the ER are called ERα and ERβ (*Fig. 3.2*). Estrogens have different affinities regarding the ERs. For example, estradiol binds equally well to both receptors whereas estrone preferably binds to ERα.[106]

Over the past 30 years, the treatment of breast cancer that test positive for either ERs or PRs has been studied.[107]

Concerning the modeling of estrogen derivatives for specific drug delivery, three important aspects should be taken into account. First, the affinity of the carrier drug complex towards the ER should be efficient. Second, the molecule should have favorable cellular transport properties. Third, an additional functionality such as a metal center that might participate in medical therapy could increase the effect of the drug. Some estradiol linked platinum anticancer agents have been reported previously by Lippard *et al.*[108] The DNA binding and cleavage activities of Cu(II) complexes of estrogen-macrocyclic polyamine conjugates have been described by Yu *et al.*[60] Fang *et al.* reported that through solid-phase synthesis on the carboxyl group of the steroid oleanolic acid, functionalization of the hydroxyl group could be enabled.[109]

Related to the above mentioned properties of MCF-7 cells it was tried to create a suitable drug consisting of an estrogenic, an ester-based and a metallonuclease-based moiety (*Scheme 3.1*).
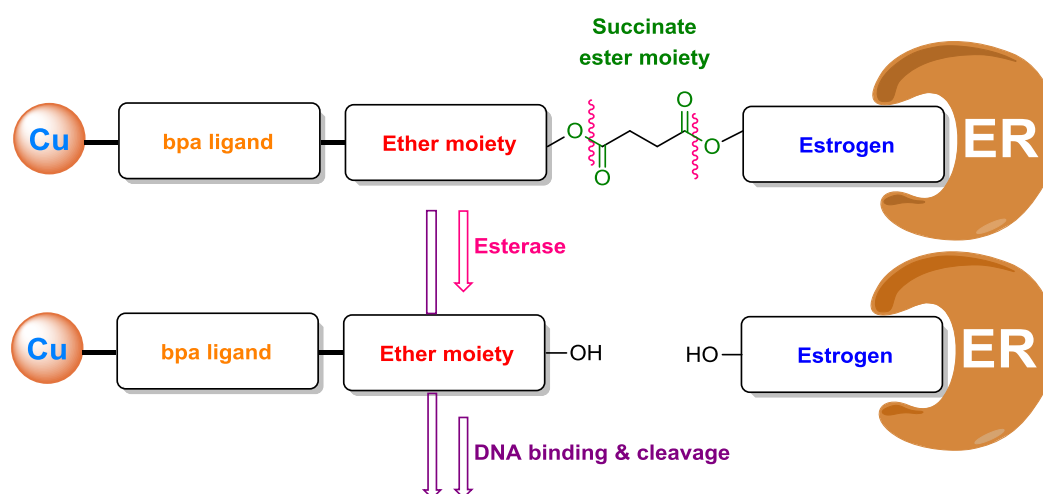
Scheme 3.1 *Estrogenic bpa derivatives as drug models.*

Estrone and estradiol have been chosen as estrogens due to their natural appearances. The bpa ligand[58] has been chosen as a metallonuclease because the ligand can initiate transition metal coordination and perform as a DNA cleaver (cf.

CHAPTER 2). Both abovementioned features shall be connected with ester groups in order to design the upper drug model shown in **Scheme 3.1**. Although this drug model could bind to and cleave DNA already, it is likely that ester cleavage could lead to a faster DNA binding and cleavage process. Regarding this, Finlay *et al*. reported that about 85**%** of total esterase activity was found in the cytoplasmic fraction of MCF-7 cells.[59] The synthesis of the novel bpa estrogen derivatives **8b** and **9b** are presented within this project (***Fig. 3.3***).

8b   **9b**
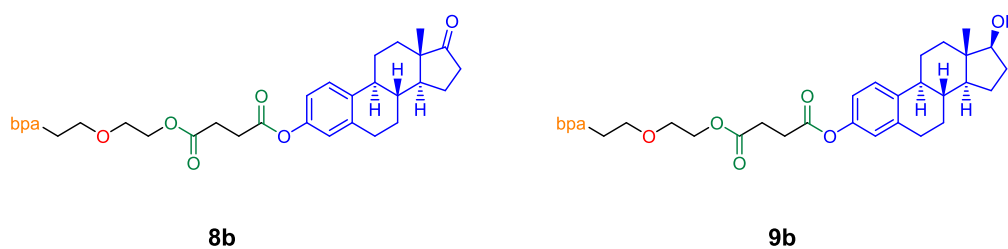
Fig. 3.3 *Left: Estrone derivative* ***8b***. *Right: Estradiol derivative* ***9b***.

3.1 Results and discussion

3.1.1 Synthetic strategies

For the design of estrogen bpa compounds, several syntheses have been performed following the elongation strategies of estradiol and estrone (**Scheme 3.2**). It was tried to elongate the estrogen with succinic anhydride and further couple the novel compound with the bpa ligand.[110]
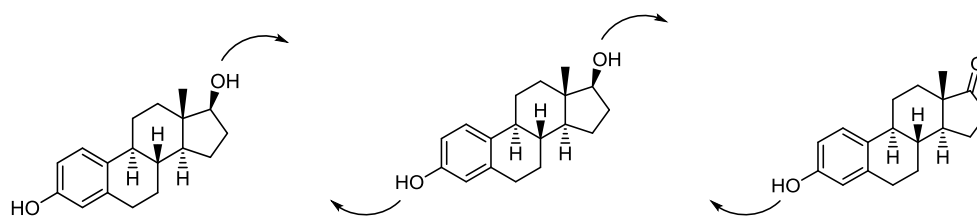
Fig. 3.4 *Elongation strategies of estradiol and estrone*

Within the first steps, an estrogenic succinate compound was synthesized as described by Yellin *et al.* and Peng *et al.* (for estrone, **Scheme 3.2**).[110, 111] The esterification of estrone succinate with the corresponding bpa resulted in a product compound, which was only detectable in the mass spectrum but not in the ^{1}H NMR spectrum. In addition to that, it was not possible to apply this strategy for estradiol succinate due to selectivity issues regarding the two hydroxyl groups of estradiol. Esterification under Steglich's conditions failed.[61]
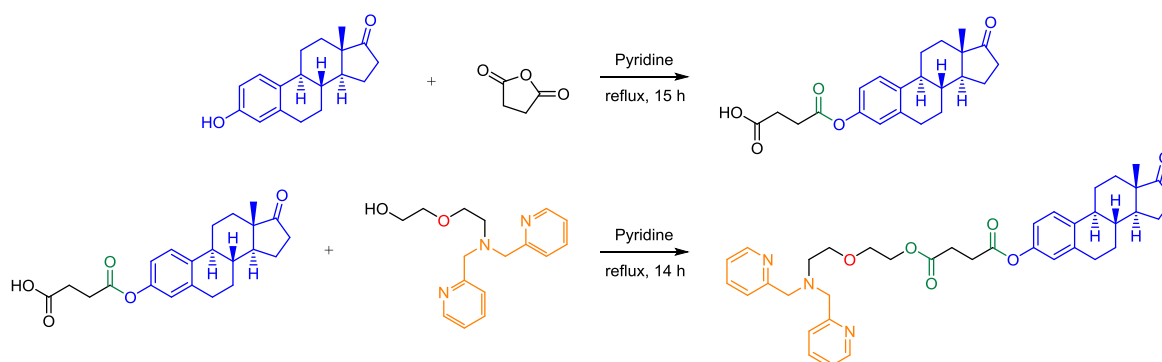
Scheme 3.2 *Synthesis of estrone succinate and esterification of estrone succinate with bpa ligand* **1b**.

Therefore, the introduction of a methyl group (**Scheme 3.3**) as a protecting group was tested. Herein, estrone was functionalized in C3-position.[112, 113] After functionalization the ketone group was reduced to form the hydroxyl group in C17-position. Then, after esterification of the methoxylated estradiol and bpa succinate

the product was only detected in the mass spectrum. The use of an acetoxy group[114] as protecting group was unsuccessful.
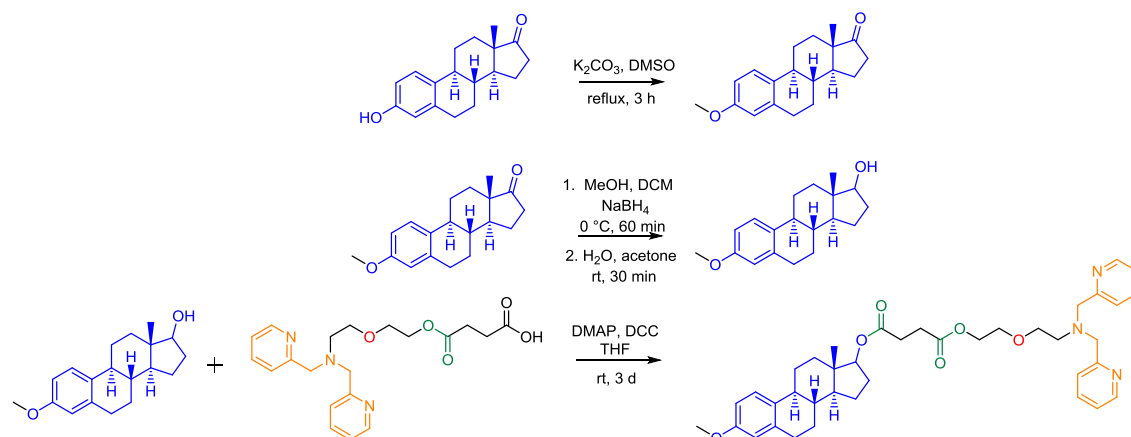
Scheme 3.3 *Synthesis of methylated estrone derivatives.*

Furthermore, it was planned to simplify the coupling process of the estrogen moiety with the bpa moiety using click strategy. The basic components of the Huisgen cycloaddition were synthesized during this project but the final click reaction of the bpa azide with ethinyl estradiol was unsuccessful (**Scheme 3.4**).[115]
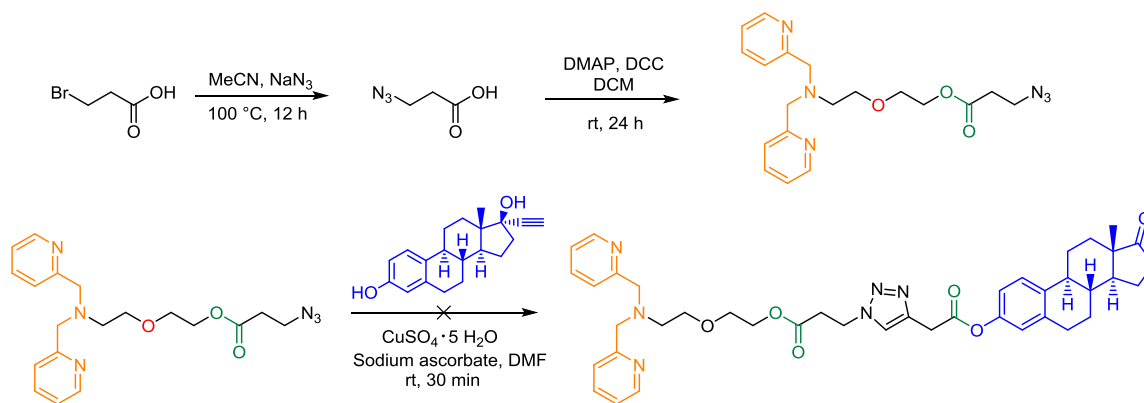
Scheme 3.4 *Click strategy for modeling estrogen bpa derivatives.*

Due to the emergence of some undesired compounds and unsuccessful purification steps, one-step reactions of estrogen with bpa succinate via esterification were deliberated.[61, 116] Besides the reaction at room temperature we focused on the microwave assisted pathway for the esterification in this project.[117-119] The synthetic pathway of the bpa estrogen derivatives is shown in *Scheme 3.5*.
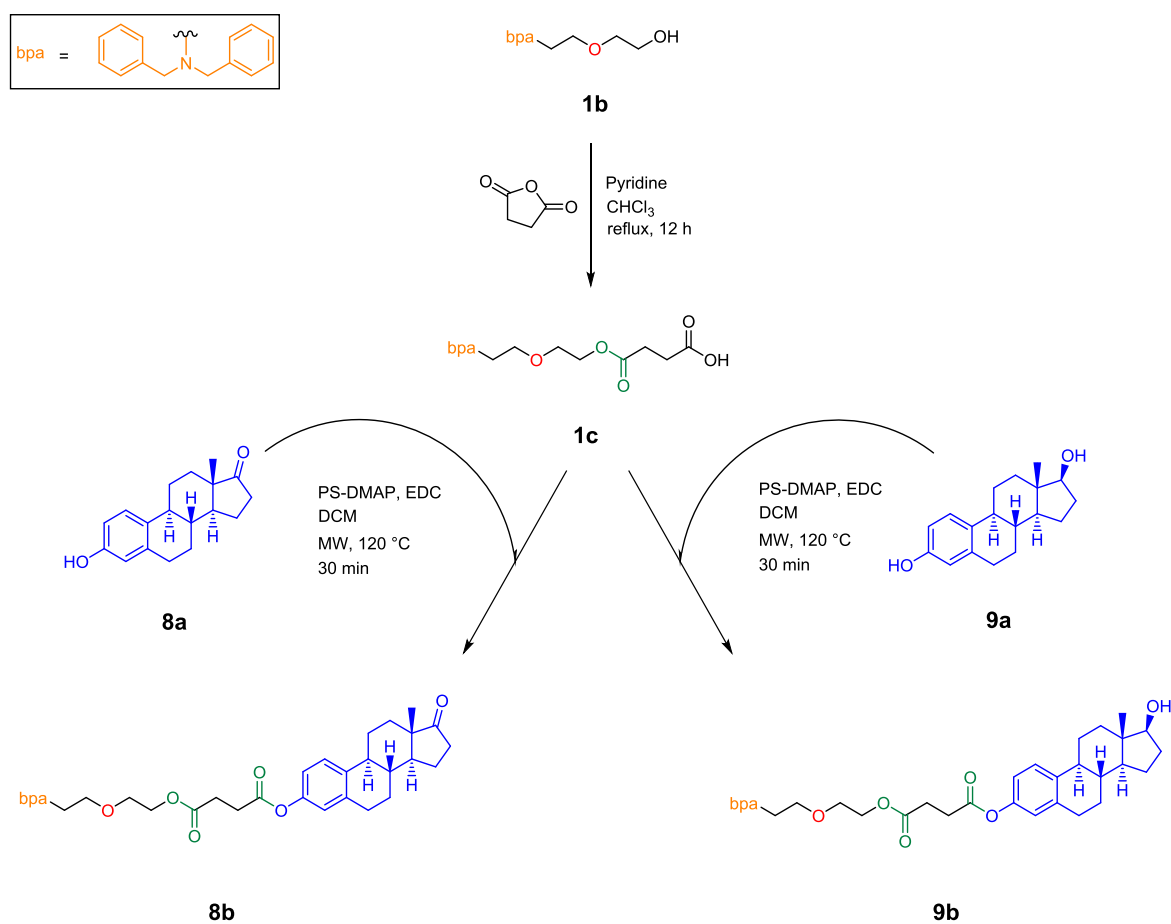
Scheme 3.5 *Synthesized compounds of estrogen derivatives **8b** and **9b** at a glance.*

3.1.2 Synthesis of bpa succinate

1c was synthesized by a base assisted esterification of **1b** (*Scheme 3.6*).[110] Because large amounts of **1c** were needed for the next steps, synthesis of **1b** was repeated in a larger scale.

For the synthesis of **1c**, it has to be taken into account that ester groups are not stable towards acids. This is why complete removal of excessive pyridine was not feasible by treatment with HCl at acidic pH values. Even a weakly acidic pH of 5 led to product loss. Little impurities of pyridine were visible in the ^{1}H NMR spectrum, but no further purification attempts were made, because the following reaction involved the use of pyridine derivatives as a reagent. Nonetheless, quantitative evaluation of the ^{1}H NMR spectrum resulted in a calculated yield of 47**%** for bpa succinate **1c**.
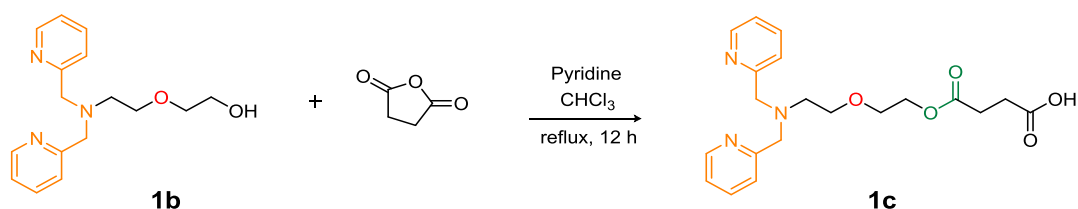
Scheme 3.6 *Synthesis of the bpa succinate **1c**.*

3.1.3 Synthesis of bpa estrogen derivatives

For the synthesis of **8b** and **9b**, it has been proved that pyridine was not a suitable reagent due to its removability exclusively under acidic conditions, which possibly led to undesired cleavage of the present ester groups. Therefore, we tried to perform the classical Steglich esterification with the use of *N,N'*-dicyclohexylcarbodiimide (DCC) as a coupling reagent and 4-dimethylaminopyridine (DMAP) as a catalyst.[61] The advantage of this reaction is that esters of acid sensitive compounds can be obtained, and that the water resulting from the reaction is removed by the DCC in form of dicyclohexylurea (DCU).

As it can be seen in **Scheme 3.7.**, activation of the carboxylic acid is caused by deprotonation with DCC. In the next step the carboxylate binds to the DCC forming a more reactive species than the free acid. Then, the alcohol can attack the intermediate and form the corresponding ester and DCU. Due to its insolubility in water and in most organic solvents, DCU is easily removable by filtration.
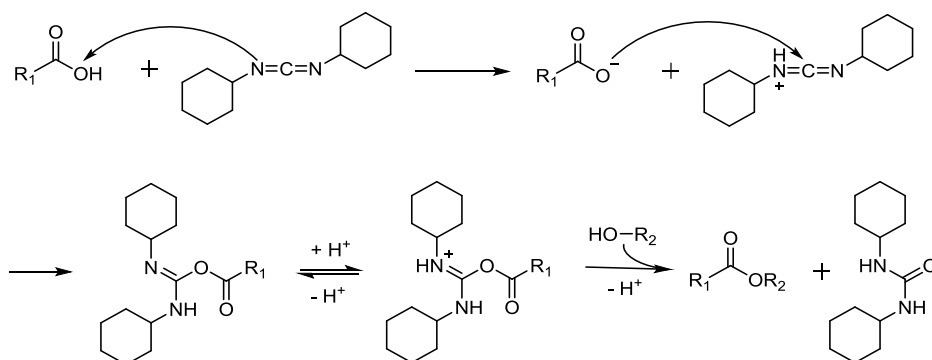
Scheme 3.7 *Steglich esterification reaction mechanism.*

If the esterification is slow, a side reaction in form of a 1,3-rearrangement can occur, which can be suppressed by addition of DMAP (**Scheme 3.8**).
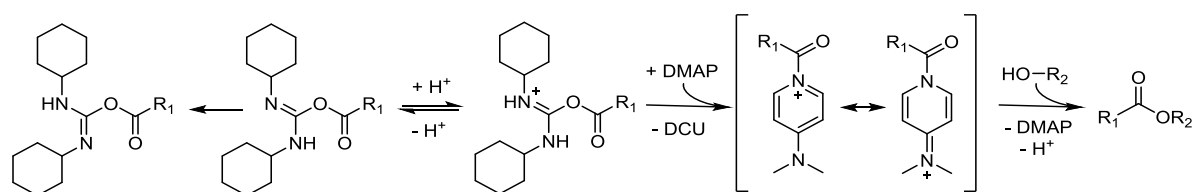
Scheme 3.8 *Possible side reaction and its suppression by DMAP.*

54

In order to avoid by-products, PS-DMAP was used instead of DMAP because the polystyrol can be easily removed by filtration.[116] Besides DCC, we also tested other carbodiimides such as *N,N'*-diisopropylcarbodiimide (DIC) and 1-ethyl-3-(3-dimethylaminopropyl)carbodiimide (EDC).[120] The last mentioned carbodiimide EDC proved to be the most suitable reagent for the synthesis of the bpa estrogen derivatives.

The esterification was performed in the microwave to shorten the reaction time and to increase the efficiency of the reaction. Microwave reactions for the synthesis of estrogenic compounds were reported by Lardy *et al.* and Wähälä *et al.* before.[118, 119] However, due to different conditions regarding the microwave instrument, the reaction time was set to 30 minutes with a temperature of 120 °C.

For standard characterization, the bpa estrogen derivatives were analyzed by ^{1}H NMR, ^{13}C NMR spectroscopy and ESI mass spectrometry. Due to the large number of protons and carbon atoms resulting in complex ^{1}H and ^{13}C NMR spectra the compounds were further analyzed by DEPT (distortionless enhancement by polarization transfer) and by two-dimensional NMR methods such as COSY (correlation spectroscopy), HMBC (heteronuclear multiple-bond correlation spectroscopy) and HMQC (heteronuclear multiple-quantum correlation spectroscopy) to gain deeper insight into the structure. In addition to that, elemental analysis was performed as a final analytical method.

3.1.3.1 Estrone bpa derivative 8b

Scheme 3.9 shows the esterification of **1c** with estrone **8a** to form the estrone bpa derivative **8b**. By using DCC as a reagent, the synthesized and chromatographically purified compound could be detected in the [^1]H NMR spectrum and in the mass spectrum, but analysis by the other NMR spectroscopy methods indicated that the estrogenic starting material **8a** was not removed completely. Further purifications proved to be unsuccessful. After using DIC as carbodiimide, the synthesized compound could be detected in the mass spectra and in both the one- and two-dimensional NMR spectra. Unfortunately, elemental analysis proved that the carbodiimide was not removed completely. A possible reason might be the insolubility of both DCC and DIC in water.

Therefore, esterification has been tried with EDC due to its water solubility. After purification via column chromatography, the selected fractions were washed with water multiple times in order to ensure that excessive EDC is removed completely. It has to be noted that EDC is also easily soluble in organic solvents such as DCM and CHCl$_3$. A better way to remove EDC should be the use of an acidic solution like HCl, which was excluded due to the aforementioned issues. The product could be analyzed successfully by ^{1}H NMR, ^{13}C NMR, DEPT, COSY, HMBC, HSQC spectroscopy and ESI MS. The results of the elemental analysis confirmed that the product contained 2.5 equivalents of water.
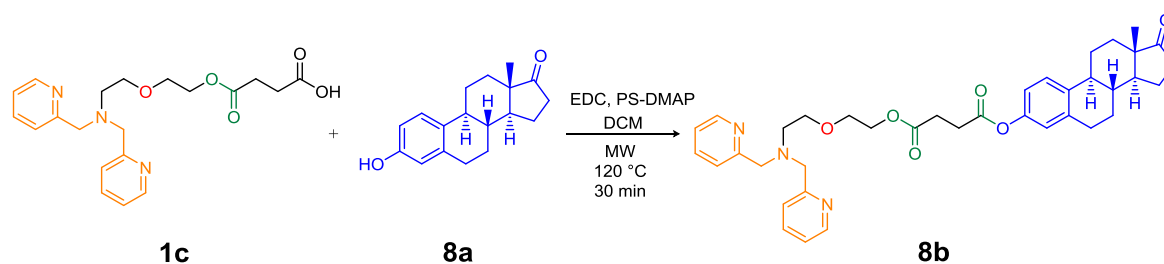
Scheme 3.9 *Microwave-assisted synthesis of estrogen bpa derivative **8b**.*

3.1.3.2   Estradiol bpa derivative 9b

As it can be seen in ***Scheme 3.10***, the synthesis of **9b** has been carried out under the same conditions as in the synthesis of **8b**.[121] Issues due to water insolubility of DCC and DIC also occurred in the case of **9b**.

The use of DCC led to a mixture of the both the monofunctionalized compound **9b** and the bisfunctionalized compound **9b.2**, which was confirmed by one- and two-dimensional NMR spectroscopic and mass spectrometric data.

According to Guo *et al.*, the peak of the $C_{17\alpha}$-H group of estradiol should be visible in the range of 3.48 ppm.[122] It is very likely that the $C_{17\alpha}$-H peak is shifted after functionalization with bpa succinate **1c**. In addition to that, the peak of the aromatic hydroxyl group at C3-position did not appear in the spectra. Therefore, possible formation of compound **9b.1** was excluded (also in the next described reactions). It was not possible to obtain a pure compound after additional chromatographic purifications.

The reaction has been also tried with DIC and compound **9b** could be characterized by the aforementioned one- and twodimensional NMR spectroscopic methods and by ESI MS. Unfortunately, same as in the case of **8b**, elemental analysis proved that the carbodiimide was not removed completely.

Performance of the microwave-assisted esterification with EDC led to the desired estrogen derivative **9b**, which was obtained by chromatographic purification and analyzed successfully by ^{1}H NMR, ^{13}C NMR, DEPT, COSY, HMBC, HSQC spectroscopy and ESI MS. However, elemental analytical data indicated that the product contained 3.5 equivalents of water.
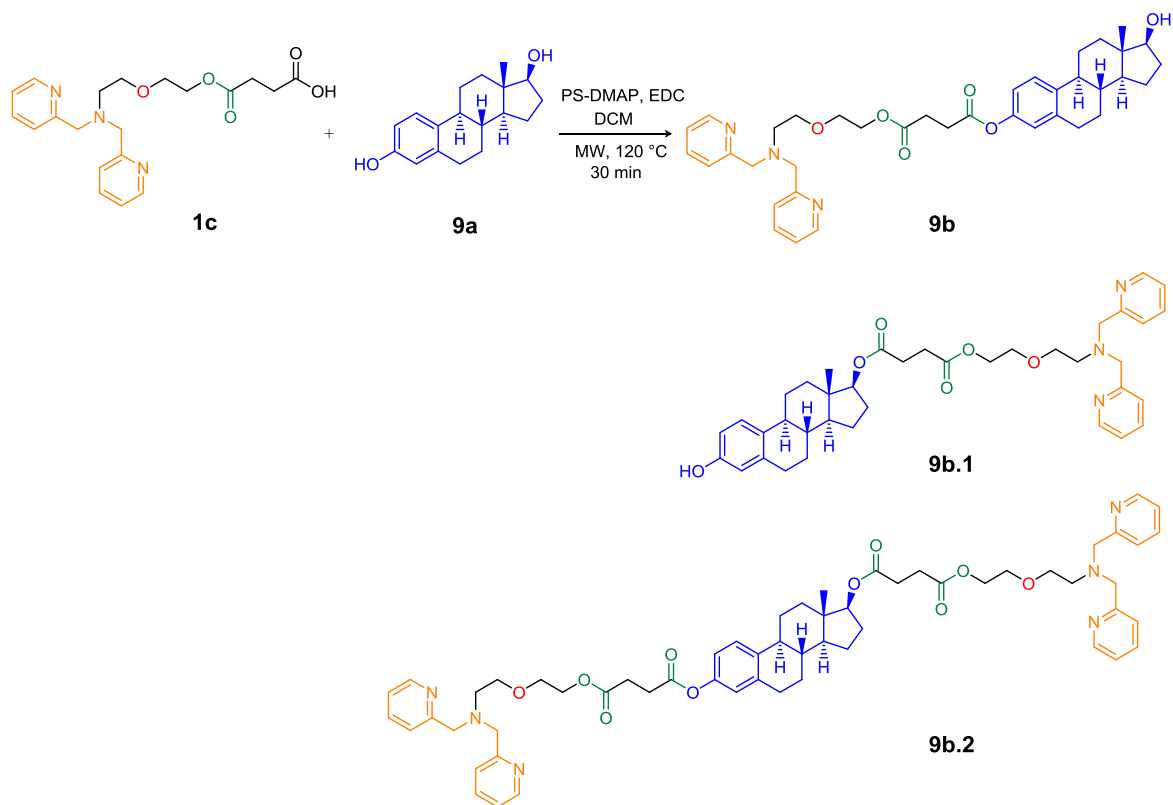
Scheme 3.10 *Microwave-assisted synthesis of estrogen bpa derivative* **9b** *(and its possible by-products* **9b.1** *and* **9b.2***).*

3.1.4   Synthesis of bpa estrogen complexes

The copper complex formation of **8b** and **9b** was carried out with the nitrate and perchlorate anion, respectively, as described in the complex synthesis of the bpa ligands in **2.1.4** (***Scheme 2.18 and 2.19***).[58] The synthesized compounds **8b.C1–2** and **9b.C1–2** were only detected by ESI mass spectrometry but elemental analysis data did not confirm the formation of the complexes. Therefore, Cu(II) complexes were generated *in situ* with a small excess of **8b** and **9b** (0.9 : 1), respectively. For comparison, *in situ* complex synthesis was carried out with **1b** and **1c**.
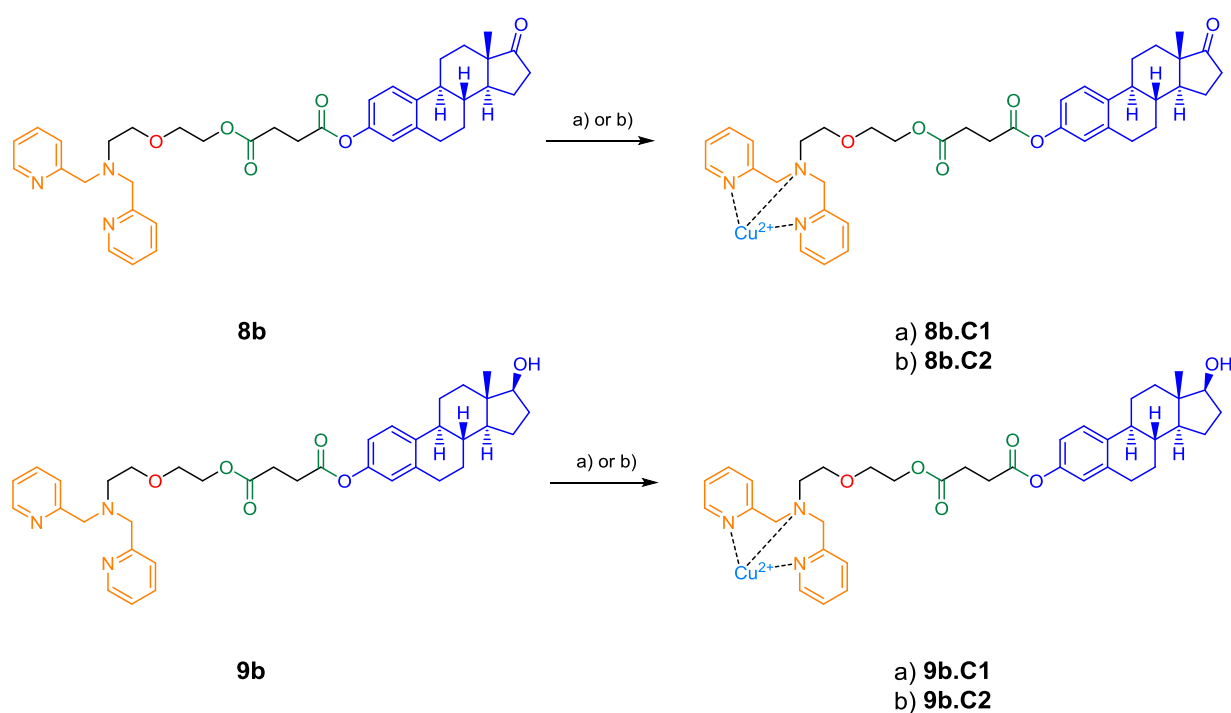
Scheme 3.11 *Synthesis of complexes* ***8b.C1–2*** *and* ***9b.C1–2*** *under the following conditions*
a) Cu(NO₃)₂ · 3 H₂O, EtOH, reflux, 1 h and b) Cu(ClO₄)₂ · 6 H₂O, MeOH, rt, 2 h.

3.1.5 Gel electrophoretic studies

3.1.5.1   Hydrolytic cleavage

To assess the hydrolytic DNA cleavage ability of the estrogen bpa derivatives and their precursors supercoiled (sc) pBR322 DNA (Form I) was incubated with varying concentrations of compounds **6a**, **1b** (**+ Cu**), **1c** (**+ Cu**), **8b** (**+ Cu**) and **9b** (**+ Cu**) in Tris-HCl buffer (50 mM) at pH 7.4 for 24 h. All ligand, complex and *in situ* complex solutions contained 20% DMSO due to the solubility of the bpa estrogen derivatives **8b** and **9b** in 20**%** DMSO at 5 mM concentration. The final DMSO concentration used during the hydrolytic DNA cleavage studies amounted to 5**%** and has also been considered in the reference. The shortfall of the metal salt solution serves to ensure the maximum concentration of formed complex. In order to compare the effect of complex **6a** with its *in situ* variant towards DNA cleavage, the concentration of **6a** was set equally to the concentration of the metal salt solution **1b** + **Cu**.
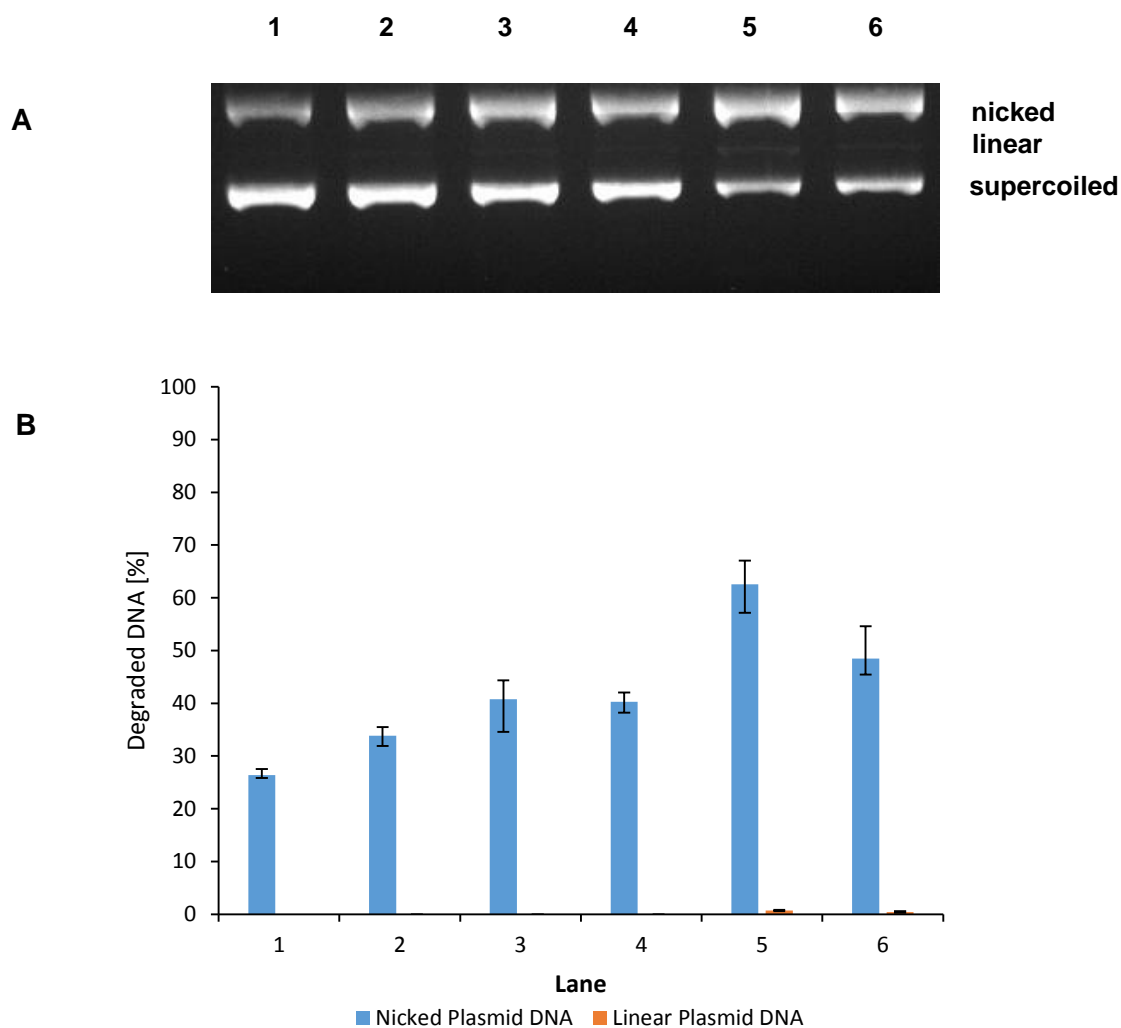
Fig. 3.5 *(A) Cleavage activity of the complexes monitored by 1% agarose gel electrophoresis after incubation at 37 °C for 24 h. Every lane contained 0.2 μg plasmid DNA in 50 mM Tris-HCl buffer (pH 7.4) and 5% DMSO (representative gel). Lane 1: Reference DNA; lane 2:* **6a** *(0.45 mM); lane 3:* **1b** *(0.5 mM) +* **Cu(NO₃)₂** *(0.45 mM); lane 4:* **1c** *(0.5 mM) +* **Cu(NO₃)₂** *(0.45 mM); lane 5:* **8b** *(0.5 mM) +* **Cu(NO₃)₂** *(0.45 mM); lane 6:* **9b** *(0.5 mM) +* **Cu(NO₃)₂** *(0.45 mM). (B) Percentage of degraded DNA (error bars represent the standard deviations from three independent experiments).*

At 0.45 mM concentration of **6a**, **1b + Cu**, **1c + Cu**, **8b + Cu** and **9b + Cu** 30–65% of Form II was obtained (***Fig. 3.5***). No significant difference was observed between **6a** and **1b + Cu** and between **1b + Cu** and **1c + Cu**, which indicates that the *in situ* complex formation and introduction of a succinate moiety did not affect the cleavage activity. Because only the bpa moiety induces the hydrolytic DNA cleavage mechanism, it might not be affected by the estrogenic moiety. However, higher cleavage activities were observed for the bpa estrogen derivatives, whereas **8b + Cu** produced 15% more nicked plasmid DNA than **9b + Cu**. Furthermore, only the bpa estrogen derivatives formed up to 1% of linear plasmid DNA.

Computer modeling results of Wei *et al.* showed that estradiol has the ability to intercalate into DNA. Thus, a possible intercalation of the estrogenic moiety might be responsible for the higher DNA cleavage activity of the bpa estrogen derivatives **8b + Cu** and **9b + Cu**.[123] Regarding the binding mode, estrogenic metabolites like catechol estrogens bind covalently to DNA, whereas the parent hormones estrone and estradiol are not able to form covalent bonds with nucleotide bases.[124]
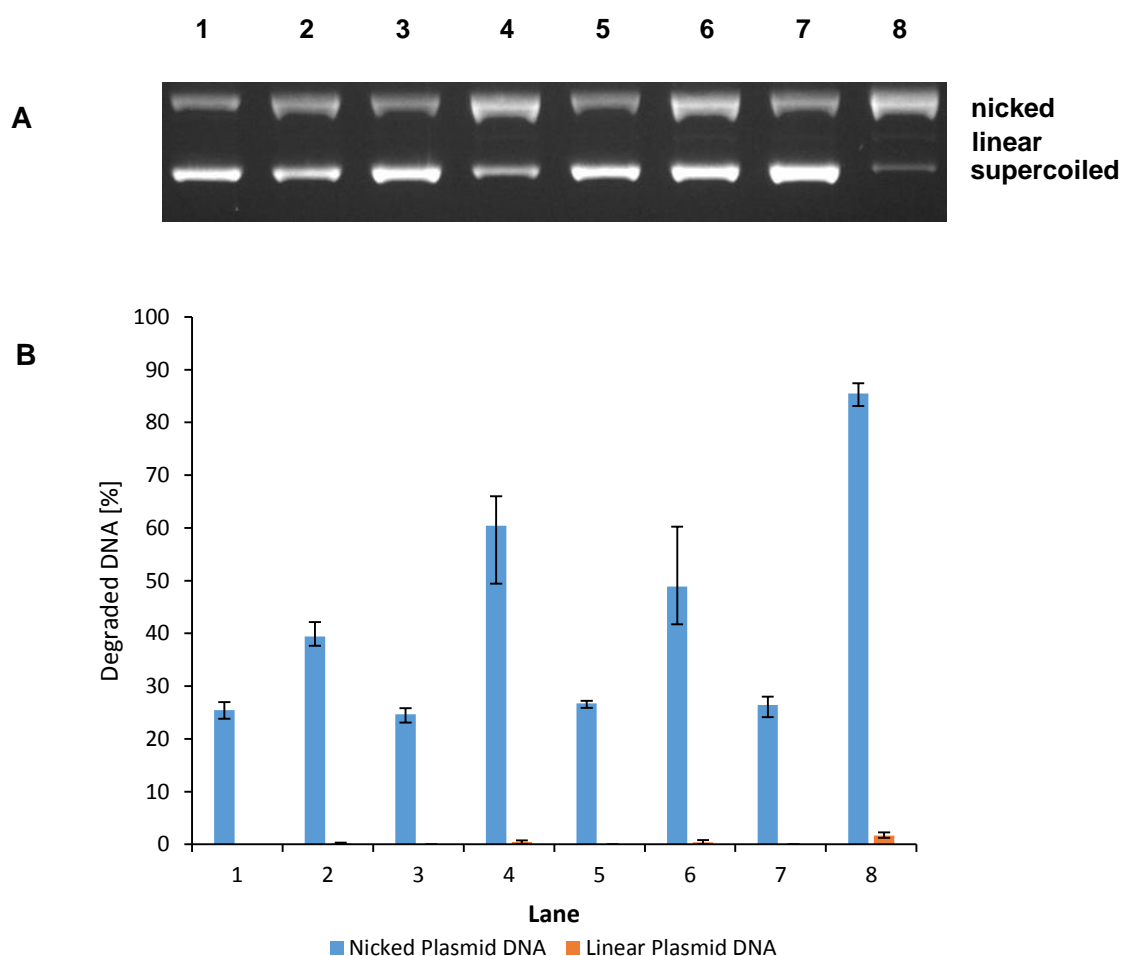
Fig. 3.6 *(A) Cleavage activity of the complexes monitored by 1% agarose gel electrophoresis after incubation at 37 °C for 24 h. Every lane contained 0.2 µg plasmid DNA in 50 mM Tris-HCl buffer (pH 7.4) and 5% DMSO (representative gel). Lane 1: Reference DNA; lane 2: 6a (1.13 mM); lane 3: 1b (1.25 mM); lane 4: 1b (1.25 mM) + Cu(NO₃)₂ (1.13 mM); lane 5: 1c (1.25 mM); lane 6: 1c (1.25 mM) + Cu(NO₃)₂ (1.13 mM); lane 7: 8b (1.25 mM); lane 8: 8b (1.25 mM) + Cu(NO₃)₂ (1.13 mM). (B) Percentage of degraded DNA (error bars represent the standard deviations from three independent experiments).*
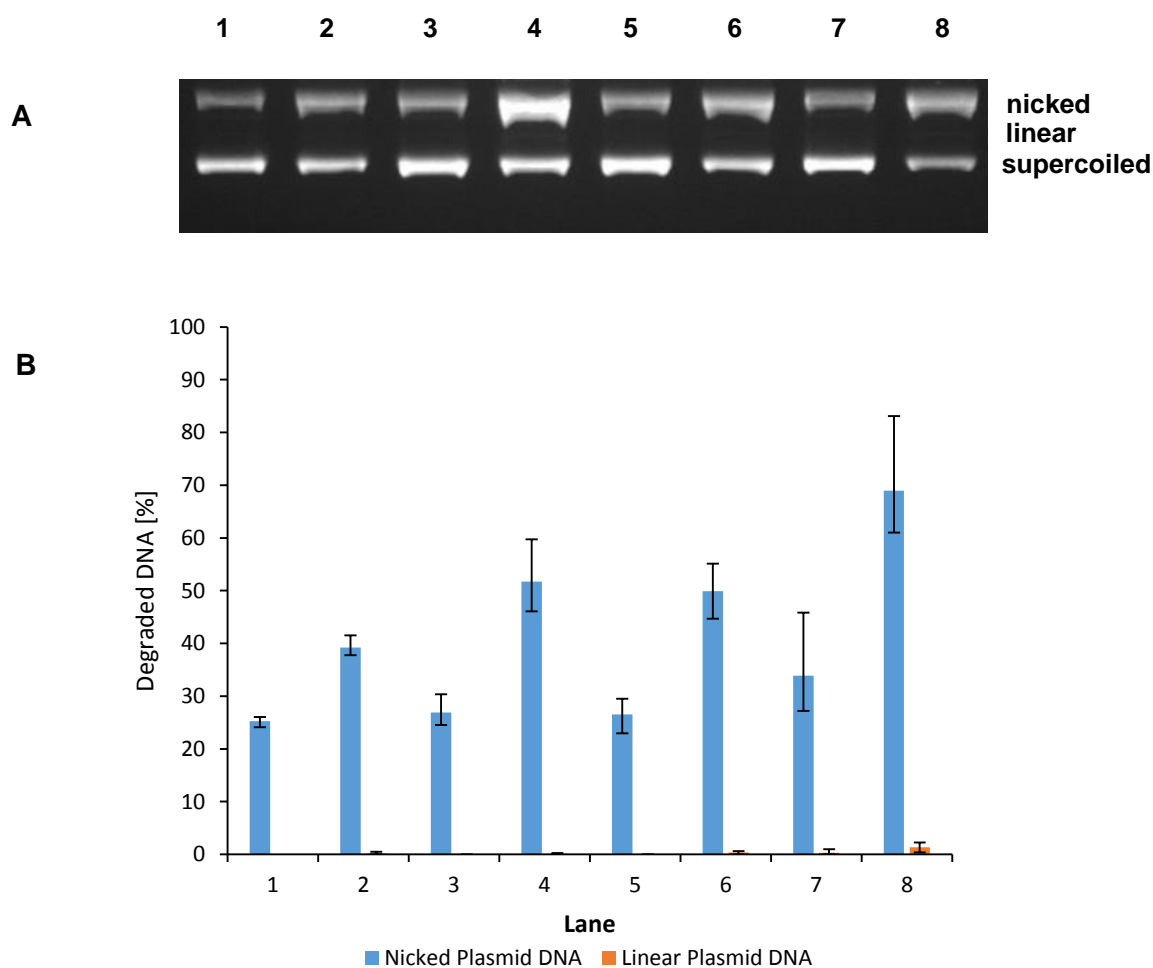
Fig. 3.7 (A) Cleavage activity of the complexes monitored by *1%* agarose gel electrophoresis after incubation at 37 °C for 24 h. Every lane contained 0.2 µg plasmid DNA in 50 mM Tris-HCl buffer (pH 7.4) and *5%* DMSO (representative gel). Lane 1: Reference DNA; lane 2: *6a* (1.13 mM); lane 3: *1b* (1.25 mM); lane 4: *1b* (1.25 mM) + *Cu(NO₃)₂* (1.13 mM); lane 5: *1c* (1.25 mM); lane 6: *1c* (1.25 mM) + *Cu(NO₃)₂* (1.13 mM); lane 7: *9b* (1.25 mM); lane 8: *9b* (1.25 mM) + *Cu(NO₃)₂* (1.13 mM). (B) Percentage of degraded DNA (error bars represent the standard deviations from three independent experiments).

At 1.13 mM Cu(II) concentration and under identical conditions, all complexes showed a higher DNA cleavage activity (40–85**%** of Form II, *Fig. 3.6* and *Fig. 3.7*) than at 0.45 mM concentration. Compared to the reference, cleavage activity of just the ligands **1b**, **1c**, **8b** and **9b** towards DNA did not show any changes in absence of copper and at 1.25 mM concentration (*Fig. 3.6* and *Fig. 3.7*). **1c + Cu** showed similar cleavage activity compared to **1b + Cu**. As opposed to this, both **8b + Cu** and **9b + Cu** showed a higher activity than their precursors and produced up to 2**%** of linear plasmid DNA (Form III). Compared to 0.45 mM concentration, probably more estrogenic moieties intercalate into DNA at higher complex concentrations leading to a higher cleavage activity.

Yu *et al.* have reported on the cleavage activity of Cu(II) complexes of estrogen cyclen (1,4,7,10-tetraazacyclododecane) conjugates towards pUC19 DNA.

Similar to our case, the estrogen cyclen complexes showed a higher DNA cleavage activity (at 1.43 mM concentration) compared to cyclen. Furthermore, the estrone cyclen complex showed a higher cleavage activity towards DNA than the estradiol cyclen complex. The reason might be the lower binding ability of the estradiol cyclen complex ($K_{app} = 0.93 \times 10^4$) compared to the estrone cyclen complex ($K_{app} = 1.53 \times 10^7$). Herein, it was postulated that the functional groups of the steroidal D-ring may play a key role in the cleavage activity.[60] A similar behavior was determined in the case of **8b + Cu** compared to **9b + Cu**, whereby **8b + Cu** produced more form II DNA (ca. 85%) than **9b + Cu** (ca. 60%).

3.1.5.2 Oxidative cleavage

In order to evaluate the oxidative DNA cleavage ability pBR322 DNA (Form I) was incubated with varying concentrations of compounds **6a**, **1b** (**+ Cu**), **1c** (**+ Cu**), **8b** (**+ Cu**) and **9b** (**+ Cu**) in Tris-HCl buffer (50 mM) at pH 7.4 for 2 h and in the presence of ascorbate as reducing agent.

Fig. 3.8 *(A) Cleavage activity of the complexes monitored by 1% agarose gel electrophoresis after incubation at 37 °C for 2 h. Every lane contained 0.2 µg plasmid DNA in 50 mM Tris-HCl buffer (pH 7.4) and 1% DMSO in the presence of ascorbate (1 mM) (representative gel). Lane 1: Reference DNA; lane 2: **6a** (11.3 µM); lane 3: **1b** (12.5 µM) + **Cu(NO₃)₂** (11.3 µM); lane 4: **1c** (12.5 µM) + **Cu(NO₃)₂** (11.3 µM); lane 5: **8b** (12.5 µM) + **Cu(NO₃)₂** (11.3 µM); lane 6: **9b** (12.5 µM) + **Cu(NO₃)₂** (11.3 µM). (B) Percentage of degraded DNA (error bars represent the standard deviations from three independent experiments).*

The ligand, complex and *in situ* complex solutions were diluted with water resulting in a final concentration of **1%** DMSO, which has been considered in the reference DNA.

At 11.3 µM concentration, 45–90**%** of Form II and up to 4**%** of Form III were obtained in the presence of **6a**, **1b + Cu**, **1c + Cu**, **8b + Cu** or **9b + Cu** (***Fig. 3.8***). Complex **1b + Cu** showed a higher cleavage activity than the bpa succinate complex **1c + Cu** and the estrogen bpa complexes **8b + Cu** and **9b + Cu**. In comparison to hydrolytic DNA cleavage conditions only µM concentrations are needed (11.3 µM vs. 1.13 mM).

As seen exemplarily in ***Fig. 3.9*** and at 50 µM concentration, **1b**, **1c** and **8b** (lanes 3, 5 and 7) did not show cleavage activity changes compared to the reference DNA (lane 1). In the presence of Cu(II) and at 45 µM concentration, **6a**, **1b**, and **1c** produced 85% of Form II and 10–15% of Form III (lanes 2, 4 and 6). **8b + Cu** (lane 8) showed a distinctly higher cleavage activity compared to all other lanes, resulting in complete cleavage of Form I DNA to Form II and Form III DNA. The amount of Form III was increased 6–8 fold. The same applied to compound **9b** (not shown).

Fig. 3.9 *(A) Cleavage activity of the complexes monitored by 1% agarose gel electrophoresis after incubation at 37 °C for 2 h. Every lane contained 0.2 µg plasmid DNA in 50 mM Tris-HCl buffer (pH 7.4) and 1% DMSO in the presence of ascorbate (1 mM) (representative gel). Lane 1: Reference DNA; lane 2: **6a** (45 µM); lane 3: **1b** (50 µM); lane 4: **1b** (50 µM) + **Cu(NO₃)₂** (45 µM); lane 5: **1c** (50 µM); lane 6: **1c** (50 µM) + **Cu(NO₃)₂** (45 µM); lane 7: **8b** (50 µM); lane 8: **8b** (50 µM) + **Cu(NO₃)₂** (45 µM). (B) Percentage of degraded DNA (error bars represent the standard deviations from three independent experiments).*

At 45 µM concentration and otherwise identical conditions, all complexes showed a higher DNA cleavage activity (compared to 11.3 µM concentration) and most likely a complete conversion of Form I to Form II and Form III (***Fig. 3.10***). As already expected, **6a** and **1b** + **Cu** exhibit a similar DNA cleavage activity. **1c** + **Cu** showed a higher DNA cleavage activity than at 11.3 µM concentration and a similar DNA cleavage activity compared to both **6a** and **1b** + **Cu**. The three complexes **6a**, **1b** + **Cu** and **1c** + **Cu** produced 85–90% of Form II and 10–15% of Form III (lanes 2-4). Interestingly, as already mentioned in the case of **8b** + **Cu** at 11.3 µM concentration, about 85% of Form III and 15% of Form II were obtained in the

presence of **8b + Cu** and **9b + Cu**, respectively (lanes 5 and 6). This indicates that the estrogenic moiety might significantly influence the redox activity of the Cu(II) center.

Concerning the aforementioned assertions of Yu *et al.*, the functional group of the D-ring seems not to affect the cleavage activity significantly.[60] Also in the case of **8b + Cu** and **9b + Cu** DNA cleavage activity was comparable. However, possible reasons or causes regarding the mechanism were not discussed up to date. The formation of estrogenic radicals is usually favored at the aromatic A-ring.

For example, an *o*-quinone form of estrogen produces free radicals through redox cycling in human breast cancer cells.[125] In the presence of the well-known heme protein cytochrome P450, it is able to subject estrogens to oxidative metabolism. Herein, hydroxylation can also occur at the A-, B- or D-ring.[126] Roy *et al.* reported that E2 can induce mitochondrial (mt) reactive oxygen species as signal-transducing messengers.[127]

As already shown in the aforementioned hydrolytic cleavage studies, the increased oxidative cleavage activity of bpa estrogen derivatives might be caused by the higher DNA affinity compared to their precursors. Another possible reason may be originated from an intramolecular rearrangement, where the metal center approaches the oxygen atom at the C17-position in order to change the coordination sphere (therefore also the redox potential) or to generate radicals of the estrogen (in the presence of ascorbate) (***Scheme 3.12***). ROS studies were carried out and the results were evaluated in the next paragraph.
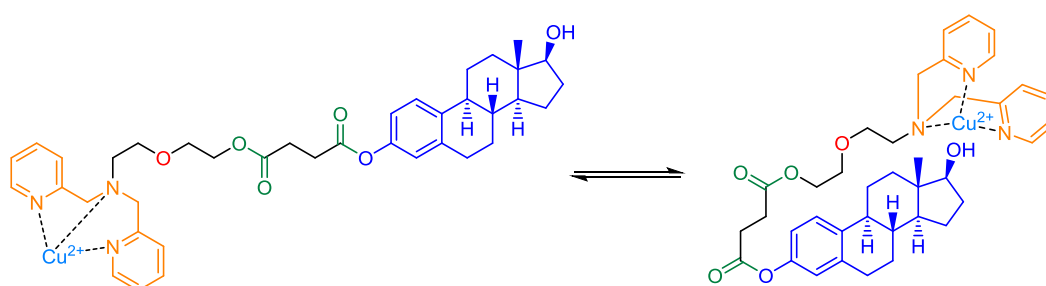
Scheme 3.12 *Proposed intramolecular rearrangement of **9b**.*
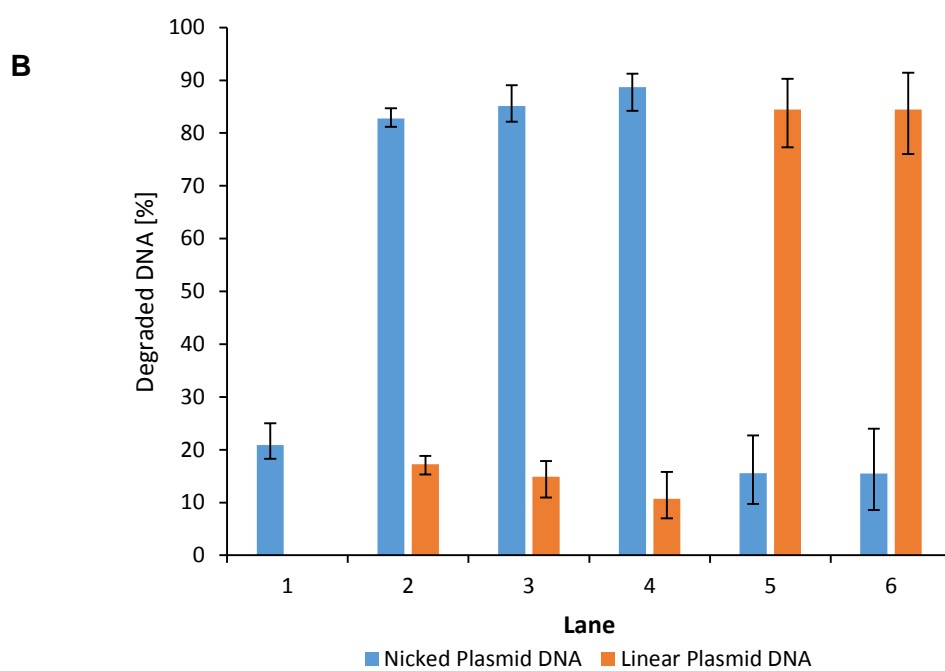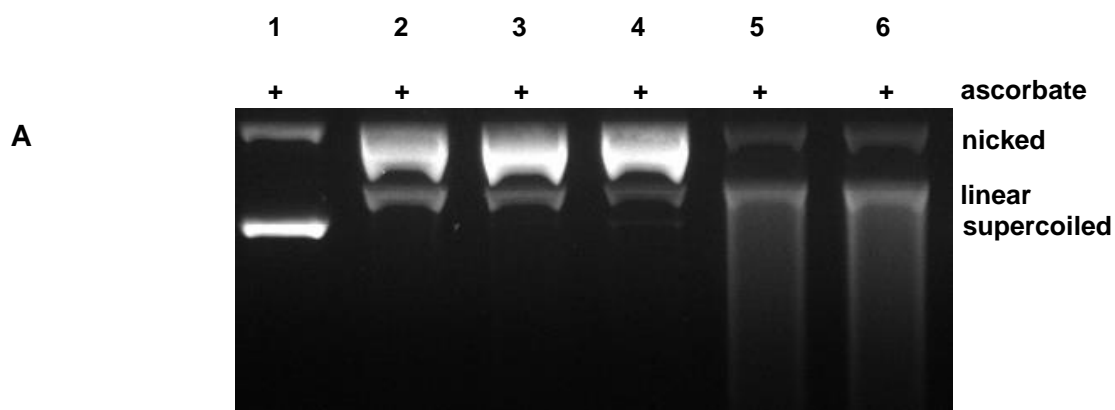
Fig. 3.10 *(A) Cleavage activity of the complexes monitored by 1% agarose gel electrophoresis after incubation at 37 ℃ for 24 h. Every lane contained 0.2 µg plasmid DNA in 50 mM Tris-HCl buffer (pH 7.4) and 1% DMSO in the presence of ascorbate (1 mM) (representative gel). Lane 1: Reference DNA; lane 2: **6a** (45 µM); lane 3: **1b** (50 µM) + **Cu(NO₃)₂** (45 µM); lane 4: **1c** (50 µM) + **Cu(NO₃)₂** (45 µM); lane 5: **8b** (50 µM) + **Cu(NO₃)₂** (45 µM); lane 6: **9b** (50 µM) + **Cu(NO₃)₂** (45 µM). (B) Percentage of degraded DNA (error bars represent the standard deviations from three independent experiments).*

3.1.5.3   ROS studies for oxidative cleavage

In order to characterize the essential reactive oxygen species responsible for the DNA cleavage of **6a**, **1b + Cu**, **1c + Cu**, **8b + Cu** and **9b + Cu** we used different scavengers:

a) *tert*-Butanol for hydroxyl radicals
b) DMSO for hydroxyl radicals
c) Sodium azide (NaN_3) for singlet oxygen
d) Catalase for hydrogen peroxide
e) Superoxide dismutase (SOD) for superoxide

As already shown for the bpa complexes mentioned above (**2.1.6.3**), for **6a** small scavenging effect in the presence of NaN_3 and SOD were observed, indicating that both singlet oxygen and superoxide can be involved in the DNA cleaving process (not shown). **1b + Cu** did not show avenging effects in the presence of NaN_3 and SOD (lanes 5 and 7, *Fig. 3.11*). Despite that, the involvement of NaN_3 and SOD cannot be excluded due to the similarity of **6a** and **1b + Cu**. However, DNA cleavage of **1b + Cu** was increased in the presence of DMSO (probably due to contamination or pipetting errors) and catalase (*Fig. 3.11*).

According to Hansberg *et al.*, catalase can be oxidized by singlet oxygen.[128] In addition to that, catalase can be inactivated in the presence of ascorbate and Cu(II) by free radical attack on the enzyme.[129] It has to be mentioned that differences regarding complex stability and redox activity may occur, because **1b + Cu** was prepared *in situ* compared to **6a**. As it can be seen in *Fig. 3.13*, no remarkable quenching effect was observed, but the cleavage activity of **8b + Cu** was slightly increased in the presence of catalase (lane 6). The same applies to **9b + Cu** (not shown). The oxidation of catalase is probable, but it is not clear, whether singlet oxygen is involved in the oxidative DNA cleavage process of **8b + Cu**. In order to find out, whether oxidative cleavage occurs in absence of a reducing agent, ROS studies were carried out without ascorbate and with a longer incubation time.

Fig. 3.12 shows the quenching effects on DNA cleavage by **1c + Cu**. A distinct quenching was observed in the presence of DMSO, NaN_3 and catalase (lanes 4–6). From this it follows that hydroxyl radicals, singlet oxygen and hydrogen peroxide play

a prominent role in the oxidative DNA cleaving process. Interestingly, the cleavage activity slightly increased in the presence of ᵗBuOH and SOD (lanes 3 and 7), probably due to contamination or pipetting errors. It is also likely that SOD is inactivated by singlet oxygen.[130] As in the case of the estrogen bpa derivatives, compound **1c** + **Cu** could be also rearranged intramolecularly.
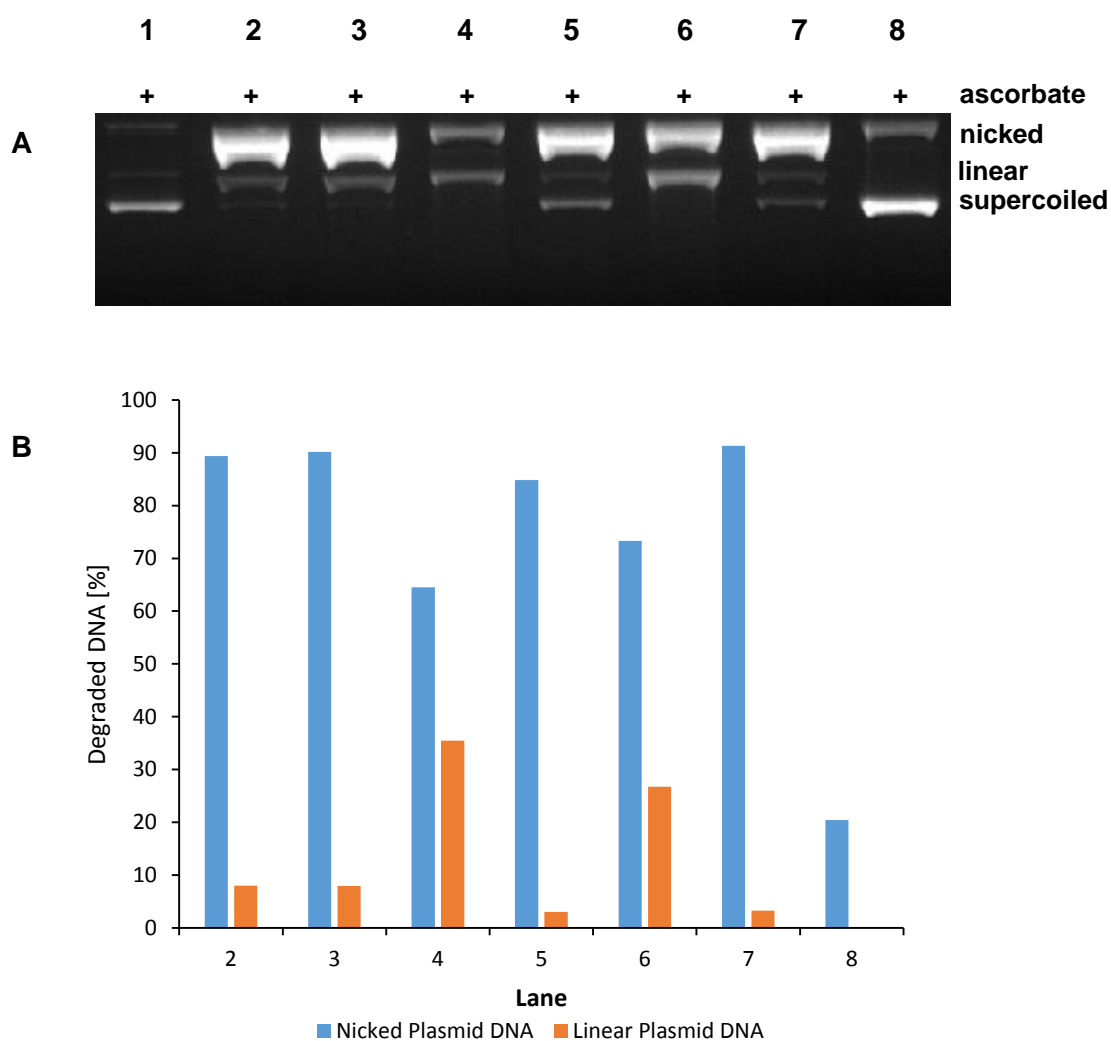
Fig. 3.11 *(A) Quenching effects on DNA cleavage by **1b** + **Cu** monitored by 1% agarose gel electrophoresis after incubation at 37 °C for 2 h. Every lane contained 0.2 µg plasmid DNA in 50 mM Tris-HCl buffer (pH 7.4), 1% DMSO and 0.125X PBS in the presence of ascorbate (1 mM) (representative gel). Lane 2-7 contained 50 µM of **1b** and 45 µM of **Cu(NO₃)₂**. Lane 1: DNA ladder; lane 2: reference; lane 3: 200 mM tBuOH; lane 4: 200 mM DMSO, lane 5: 10 mM NaN₃; lane 6: 2.5 mg/mL catalase; lane 7: 313 U/mL superoxide dismutase; lane 8: reference DNA. (B) Percentage of degraded DNA.*
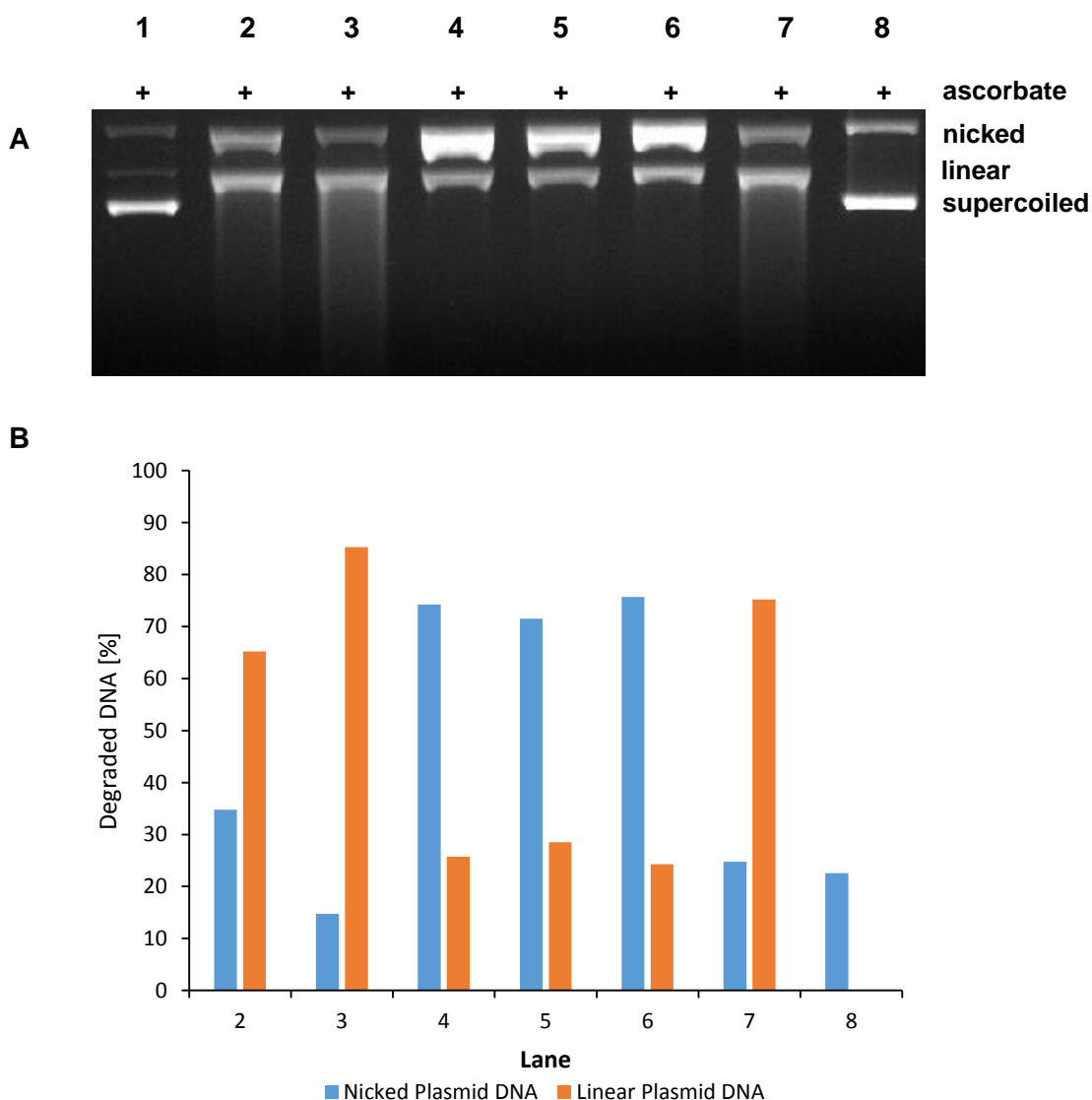
Fig. 3.12 *(A) Quenching effects on DNA cleavage by **1c** + **Cu** monitored by 1% agarose gel electrophoresis after incubation at 37 °C for 2 h. Every lane contained 0.2 µg plasmid DNA in 50 mM Tris-HCl buffer (pH 7.4), 1% DMSO and 0.125X PBS in the presence of ascorbate (1 mM) (representative gel). Lane 2-7 contained 50 µM of **1c** and 45 µM of **Cu(NO₃)₂**. Lane 1: DNA ladder; lane 2: reference; lane 3: 200 mM tBuOH; lane 4: 200 mM DMSO, lane 5: 10 mM NaN₃; lane 6: 2.5 mg/mL catalase; lane 7: 313 U/mL superoxide dismutase; lane 8: reference DNA. (B) Percentage of degraded DNA.*
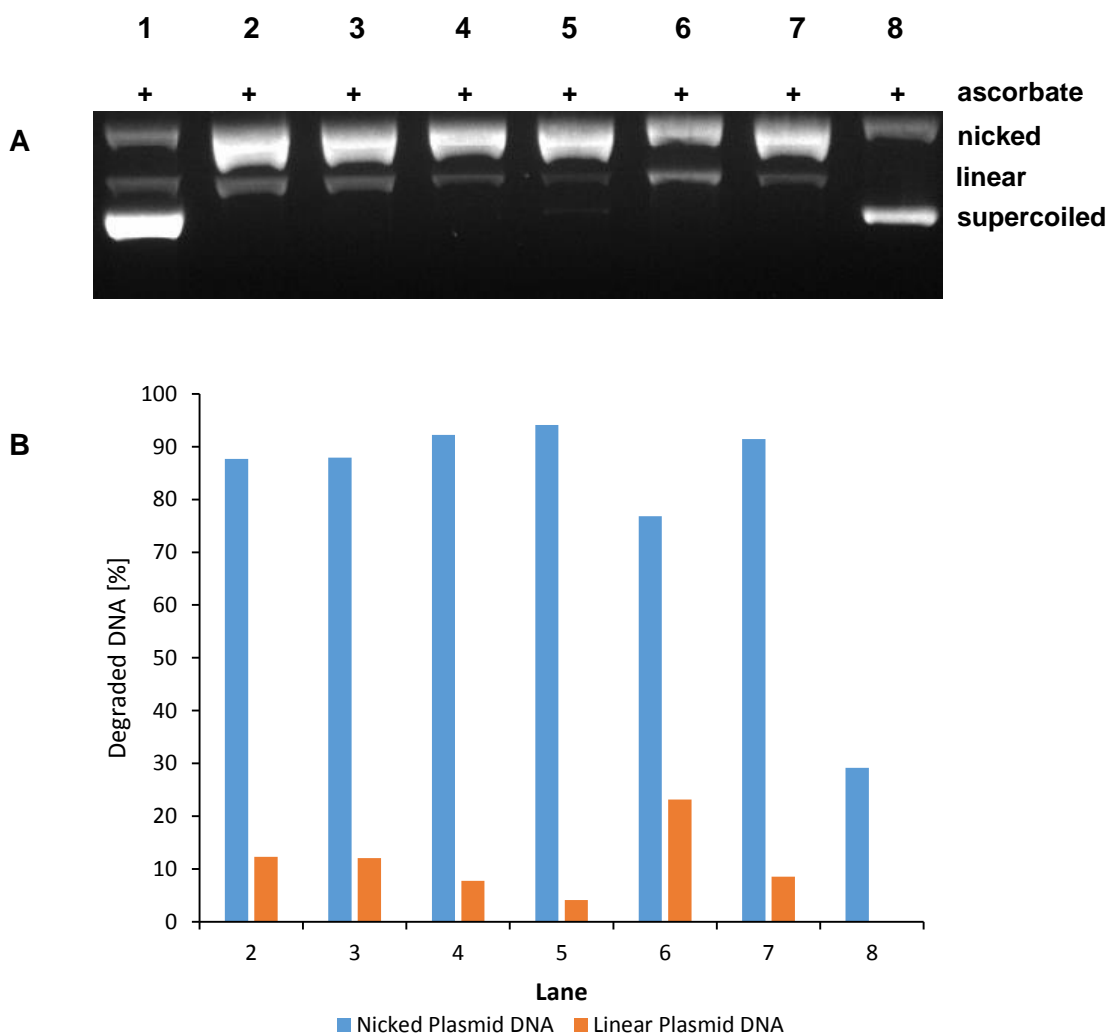
Fig. 3.13 (A) Quenching effects on DNA cleavage by **8b** + **Cu** monitored by 1% agarose gel electrophoresis after incubation at 37 °C for 2 h. Every lane contained 0.2 µg plasmid DNA in 50 mM Tris-HCl buffer (pH 7.4), 1% DMSO and 0.125X PBS in the presence of ascorbate (1 mM) (representative gel). Lane 2-7 contained 50 µM of **8b** and 45 µM of **Cu(NO$_3$)$_2$**. Lane 1: DNA ladder; lane 2: reference; lane 3: 200 mM tBuOH; lane 4: 200 mM DMSO, lane 5: 10 mM NaN$_3$; lane 6: 2.5 mg/mL catalase; lane 7: 313 U/mL superoxide dismutase; lane 8: reference DNA. (B) Percentage of degraded DNA.

3.1.5.4   Investigation of possible ROS in the absence of ascorbate

The motivation of this experiment is described in **2.1.6.4**. In order to find out, if ROS could also be generated in the absence of ascorbate, DNA cleavage studies were carried out with the same complex concentration used in the hydrolytic cleavage studies and in absence of any reducing agent. For the DNA cleavage of **1c + Cu**, **8b + Cu** and **9b + Cu** the following scavengers were used (shown in *Fig. 3.14* for **1c + Cu** and in *Fig. 3.15* for **8b + Cu** representatively):

a) *tert*-Butanol for hydroxyl radicals
b) DMSO for hydroxyl radicals
c) Sodium azide (NaN$_3$) for singlet oxygen

The enzymes catalase and superoxide dismutase were not applied as above (**3.3.4.3**) due to the long incubation time, which might have resulted in an inactivation/decomposition of the enzymes. Significant changes of DNA cleavage activity were observed for **1c + Cu** in the presence of both ^{t}BuOH and NaN$_3$ indicating that oxidative DNA cleavage occurred in absence of ascorbate. However, the DNA cleavage activity of **1c + Cu** was not quenched by DMSO, possibly due to generation of other ROS except hydroxyl radicals.

Compared to **6a**, no quenching effect was expected for **1c + Cu**. Therefore, it is possible that free radicals were generated by intramolecular rearrangement of **1c + Cu**.

In the case of **8b + Cu** (*Fig. 3.15*) and **9b + Cu** (not shown), a distinct quenching effect was observed in the presence of NaN$_3$. This observation is related to the ROS studies shown in *Fig. 3.13*. Therefore, singlet oxygen is at least responsible for the DNA cleaving process. This may explain the aforementioned increased cleavage activity in the presence of catalase (*Fig. 3.13*). Also here, intramolecular rearrangement of **8b + Cu** as described for **9b + Cu** (*Scheme 3.12*) is likely. Overall, DMSO did not show any significant change of DNA cleavage activity indicating that the amount of **5%** DMSO in the hydrolytic DNA cleavage studies are negligible.
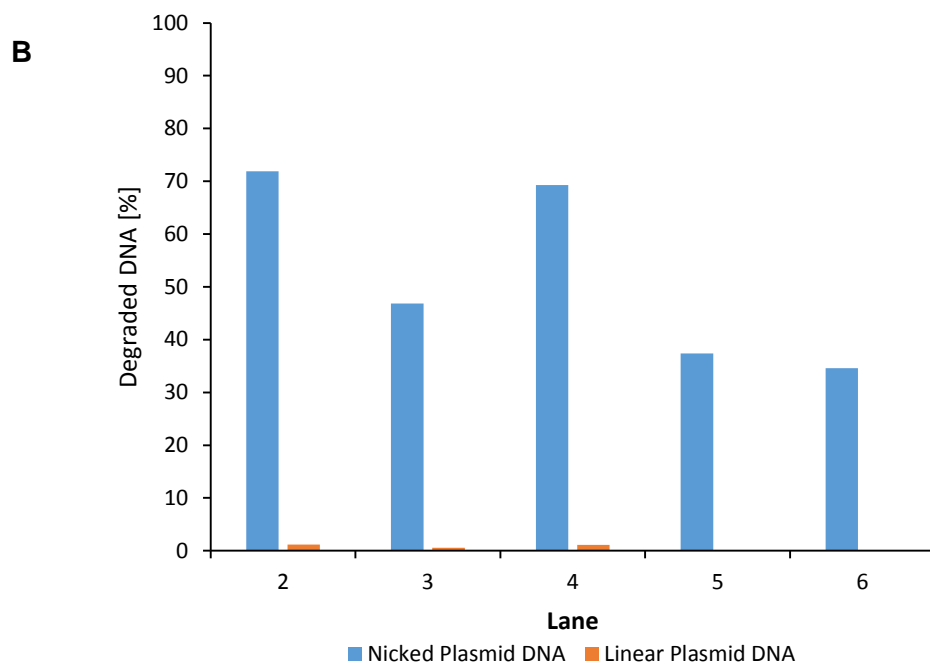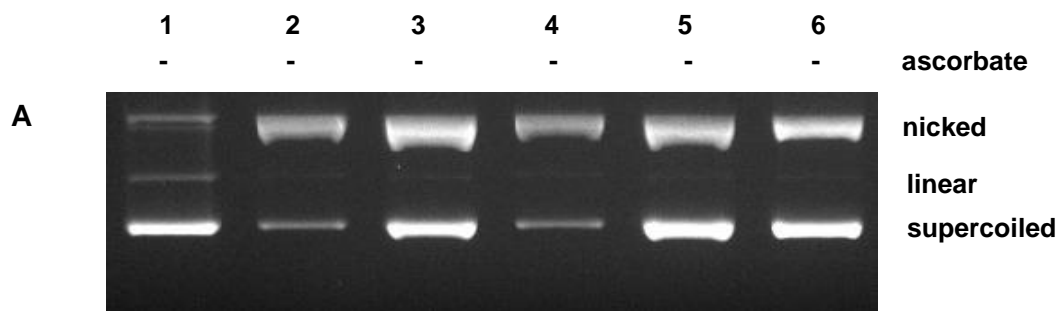
Fig. 3.14 (A) Quenching effects on DNA cleavage by **1c** + **Cu** monitored by **1%** agarose gel electrophoresis after incubation at 37 °C for 24 h. Every lane contained 0.2 μg plasmid DNA in 50 mM Tris-HCl buffer (pH 7.4), **5%** DMSO and 0.125X PBS (representative gel). Lane 2-5 contained 1.25 mM of **1c** and 1.13 mM of **Cu(NO$_3$)$_2$**. Lane 1: DNA ladder; lane 2: reference; lane 3: 200 mM tBuOH; lane 4: 200 mM DMSO, lane 5: 10 mM NaN$_3$; lane 6: reference DNA. (B) Percentage of degraded DNA.
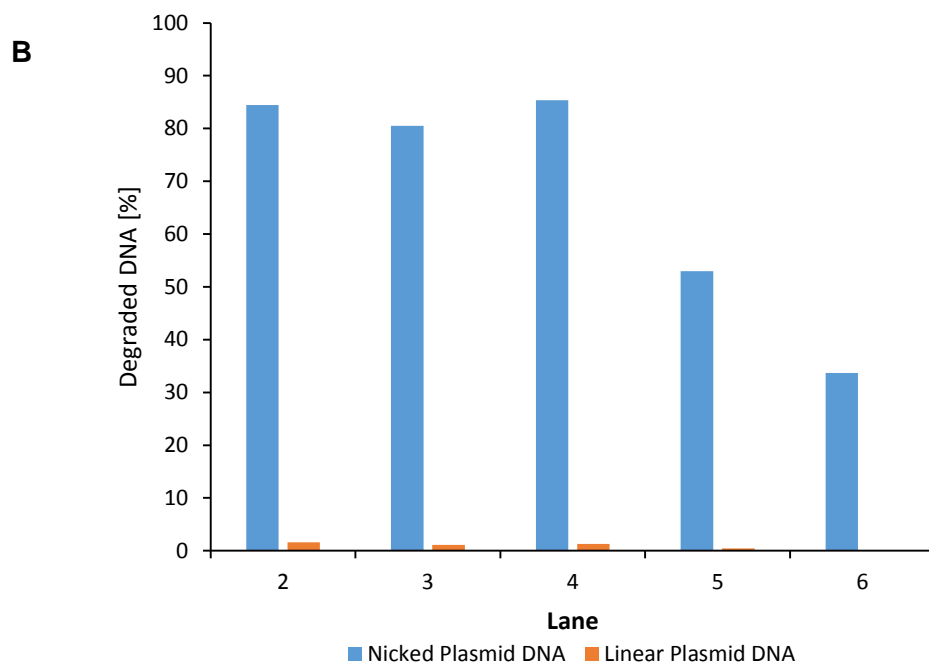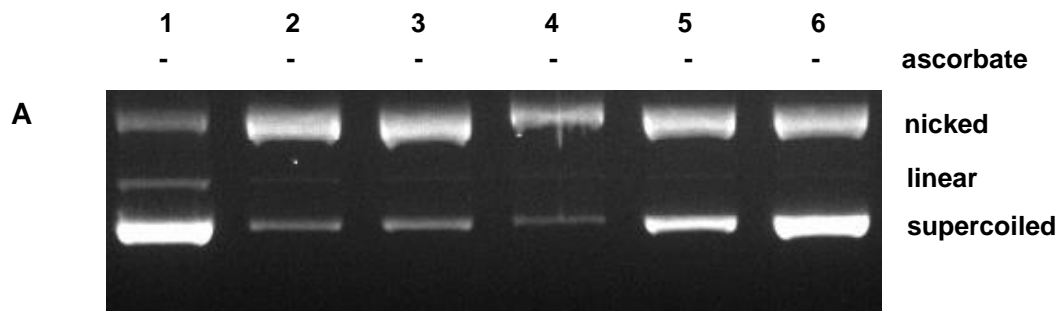
Fig. 3.15 (A) Quenching effects on DNA cleavage by **8b + Cu** monitored by **1%** agarose gel electrophoresis after incubation at 37 °C for 24 h. Every lane contained 0.2 μg plasmid DNA in 50 mM Tris-HCl buffer (pH 7.4), **5%** DMSO and 0.125X PBS (representative gel). Lane 2-5 contained 1.25 mM of **8b** and 1.13 mM of **Cu(NO$_3$)$_2$**. Lane 1: DNA ladder; lane 2: reference; lane 3: 200 mM tBuOH; lane 4: 200 mM DMSO, lane 5: 10 mM NaN$_3$; lane 6: reference DNA. (B) Percentage of degraded DNA.

3.1.6   Cytotoxicity

3.1.6.1   MTT assay

At present colorimetric assays using MTT (methyl-thiazolyl-tetrazolium)[131] are widely used for evaluating the cytotoxicity and cell viability in cell biology. This method was chosen due to the simplicity of the homogeneous protocol, which includes adding two reagents to the wells, but does not require extra steps such as removing liquid or washing the cells that were necessary for e.g. radioisotope incorporation assays. MTT gives a yellowish aqueous solution which, on reduction by dehydrogenases and reducing agents present in metabolically active cells, yields a water insoluble violet-blue formazan (Scheme 3.12). The formazan may be extracted with organic solvents and estimated quantitatively by spectrophotometry. It is currently widely thought that the amount of formazan is directly proportional to the number of living cells. However, such conclusions have been seriously questioned.[132] Nevertheless, the MTT assay was applied because it is commonly used in the literature.

MTT
3-(4,5-dimethylthiazol-2-yl)-2,5-diphenyltetrazolium bromide

Formazan
(*E,Z*)-5-(4,5-dimethylthiazol-2-yl)-1,3-diphenylformazan
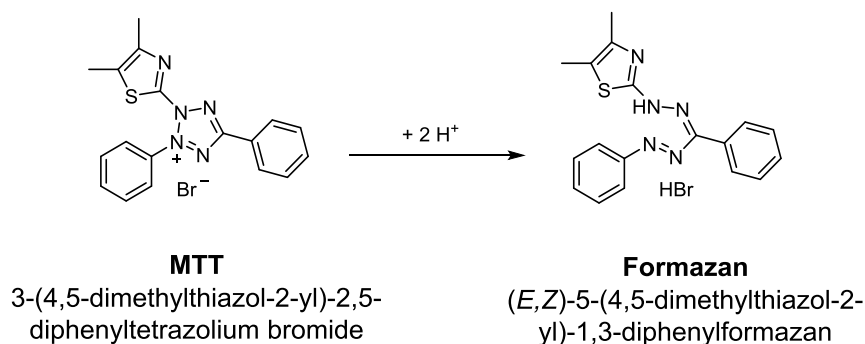
Scheme 3.13 *Reduction of MTT to Formazan.*

The cytotoxicity of estrone (E1), estradiol (E2), **1b**, **1c**, **8b** and **9b** towards MCF-7 breast cancer cells was tested both in absence and in presence of Cu(II). MCF-7 was chosen, because it contains a large number of estrogen receptors. All compounds and *in situ* complexes were firstly prepared and subsequently incubated for 48 h before adding to the cells. Samples with 1 mM concentration were prepared in a 20% DMSO solution. Experiments have also been performed with 20% DMSO only to evaluate the effect of this solvent on the viability of the cells (not shown).

Visualized in *Fig. 3.16*, the presence of Cu(II) did not affect the cytotoxicity of both the estrogens E1 and E2. At 100 µM concentration (*Fig. 3.17*), ligands **1b**, **1c**, **8b** and **9b** showed a higher cytotoxicity in the presence of Cu(II) compared to the results without Cu(II). This effect is not that obvious at 10 µM or lower concentrations. This indicates that the esterification of **1b** does not influence cytotoxicity towards MCF-7 cells. In contrast, a distinctly increased cytotoxic effect was caused by **8b + Cu** and **9b + Cu**. From this it follows that the introduction of estrogenic compounds might play a central role regarding cytotoxicity. Control experiments for Cu(II) alone were carried out but no influence was determined at 10 µM concentration (not shown). This statement implies that the formation of *in situ* complexes of **1b**, **1c**, **8b** and **9b** occurred very likely.
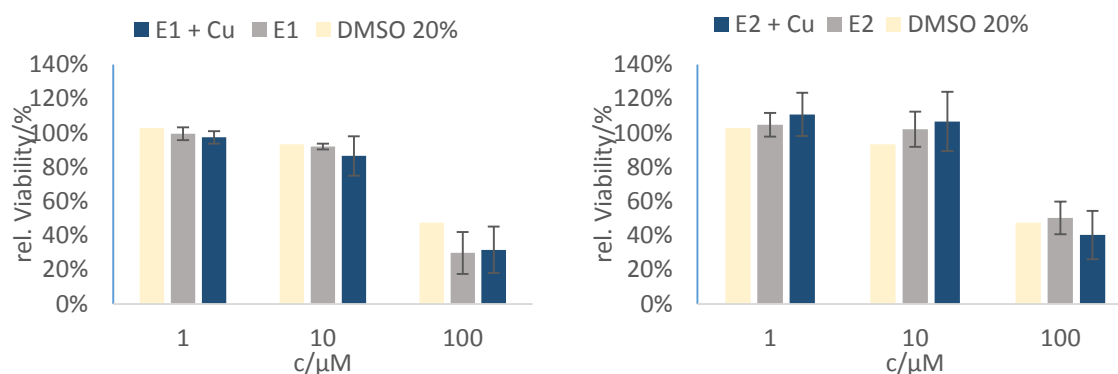
Fig. 3.16 *MTT assay results: Cytotoxicity of* **E1**, **E1 + Cu**, **E2**, **E2 + Cu** *at 1, 10 and 100 µM concentrations with 20% DMSO as positive control. Error bars are +/- SEM.*
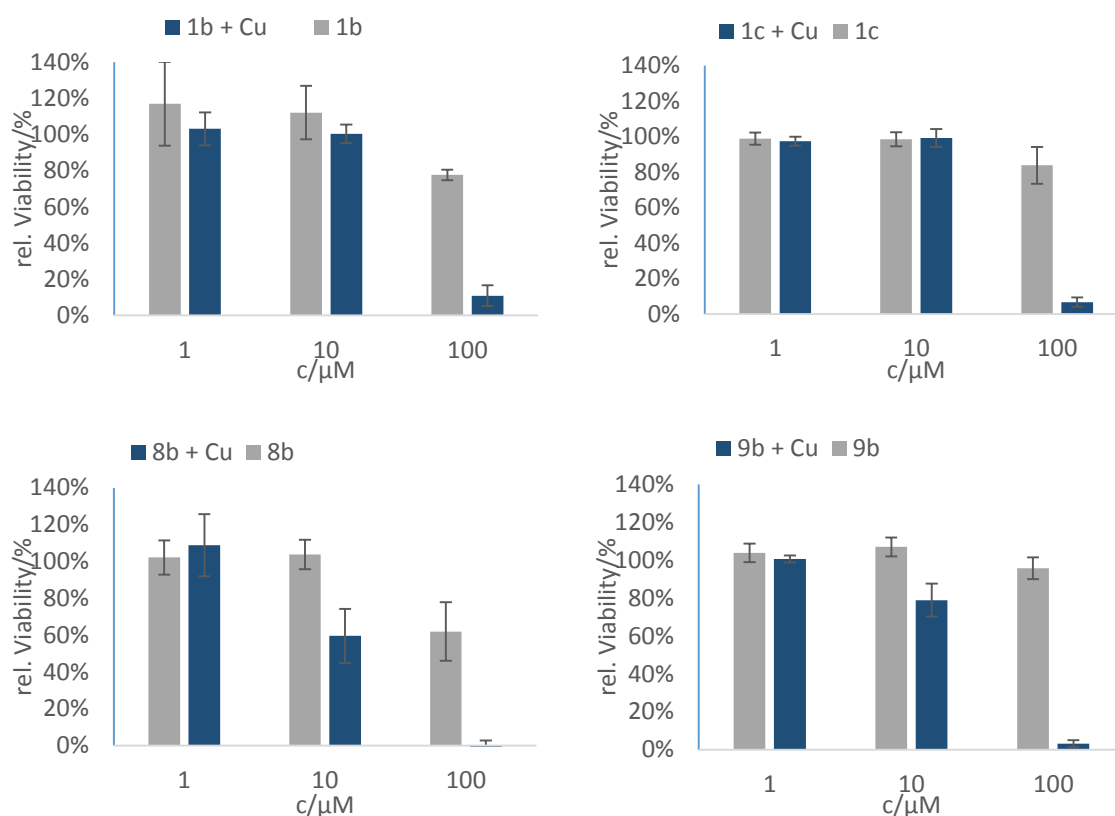
Fig. 3.17 *MTT assay results: Cytotoxicity of* **1b**, **1b + Cu**, **1c**, **1c + Cu**, **8b**, **1b + Cu**, **9b**, **9b + Cu** *at 1, 10 and 100 µM concentrations. Error bars are +/- SEM.*

As it can be seen in **Table 3.1**, calculated IC_{50} values are 11.2 µM for **8b + Cu** and 19.4 µM for **9b + Cu**. At these concentrations, DMSO did not show significant cytotoxic potential (corresponds to 0.2% and 0.4% DMSO), wherefore any influence of DMSO can be neglected for the determination of IC_{50} values of both **8b + Cu** and **9b + Cu**. The IC_{50} values are comparable to that of the currently used chemotherapeutic drug cisplatin (IC_{50}: 26.2 ± 1.1 in MCF-7 cells under the same conditions).[133]

About one decade ago, Lippard *et al*. evaluated the cytotoxicity of estrogen-tethered platinum(IV) complexes towards MCF-7 cells. The complexes comprise a 1:2 metal-ligand ratio and were incubated for 96 h instead of 48 h as in our case. Due to the aforementioned reasons IC_{50} values of the estrogen-tethered Pt(IV) complexes, which are in the range of 2.1–5.5 µM, are not comparable to the values of **8b + Cu** and **9b + Cu**, respectively.[108] Nevertheless, the essential metal copper might ensure a higher compatibility towards the human body.

It can be assumed that the coordination of Cu(II) with **8b** and **9b** occurred and that the estrogenic moiety might influence the cytotoxicity towards the ER(+)-MCF-7 cancer cell line. It is highly probable that the estrogen receptor (ER) is responsible for the preferred cellular uptake of estrogenic derivatives.[108] Investigations regarding the effect of the bpa estrogen derivatives towards ER(-)-MDA-MB-231 breast cancer cell lines, inspired by Hanson *et al.*, are underway.[134]

Table 3.1 *IC$_{50}$ values for **8b + Cu, 9b + Cu** and cisplatin in MCF-7 cells.*

	48 h (in µM)
8b + Cu	11.2 ± 1.0
9b + Cu	19.4 ± 4.9
Cisplatin[133]	26.2 ± 1.1

CHAPTER 4

AMPHIPHILIC PHENANTHROLINE DERIVATIVES

1,10-Phenanthroline (phen) is a well-known *N*-donor ligand and acts as an inhibitor of zinc metallopeptidase and *E. coli* DNA polymerase I.[135-137] Metal complexes of phen and its derivatives possess a high DNA binding affinity and cleavage activity.[138]

The Cu(II) complex of phen was the first known artificial nuclease described by Sigman *et al.* in 1979.[139] They found out that an oligonucleotide could be cleaved and that the cleavage products then inhibited the enzyme E. coli DNA polymerase I. It has been proved that the cleavage of DNA is oxygen-dependent in the presence of reducing agents.[139, 140] In addition to that, proteolytic acitivity of the phen-based complex [Cu(tdp)(tmp)]ClO$_4$ towards bovine serum albumin (BSA) was reported by Palaniandavar *et al.*[133]

Several functionalizations of phen have been studied intensively within the last decades.[51, 141, 142] Long alkyl chains on phen represent the character of a so-called amphiphile, which is composed of both a hydrophilic head and a hydrophobic tail (***Scheme 4.1***). The synthesis of amphiphilic imidazole phen derivatives were reported by Wang *et al.*[143] Furthermore, Mandler *et al.* described the complexation of Cu(II) by alkylated phen derivatives as Langmuir films (***Fig. 4.1***).[144]
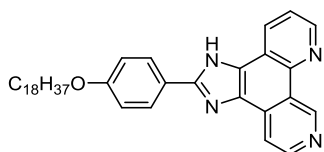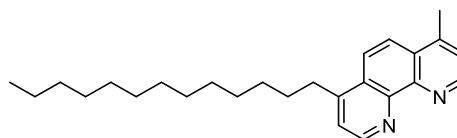
Wang et al. [143]   **Mandler et al. [144]**

Fig. 4.1 *Amphiphilic phen derivatives by Wang et al.[143] and Mandler et al.[144]*

Amphiphilic molecules are able to self-aggregate into particles called micelles, but also into layers or vesicles. Here, the hydrophilic shell of the micelle interacts with water and encloses the hydrophobic moiety (***Scheme 4.1***). This state is reached from the critical micelle concentration (cmc). Micelles can be both potent drugs and drug carriers due to their higher water solubility and cell permeability compared to many

other drugs.[145, 146] Metalliferous micelles (or metallomicelles) have the ability to catalyze the hydrolysis of phosphate esters and carboxyl acid esters.[147, 148]
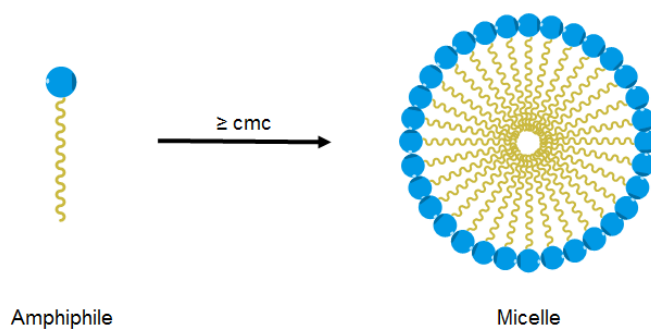
Scheme 4.1 *Formation of a micelle of concentrations above the critical micelle concentration (cmc).*

For the synthesis of amphiphilic phenanthroline dervatives, phen ligands are acylated in 5-position to build a monofunctionalized (single-chain) derivative. Furthermore, the acylation in 5,6-position shall lead to the formation of a bisfunctionalized (double-chain) phen derivative. Both derivatives can act as amphiphiles. Synthetic pathways used in this project are shown in **Scheme 4.2**.
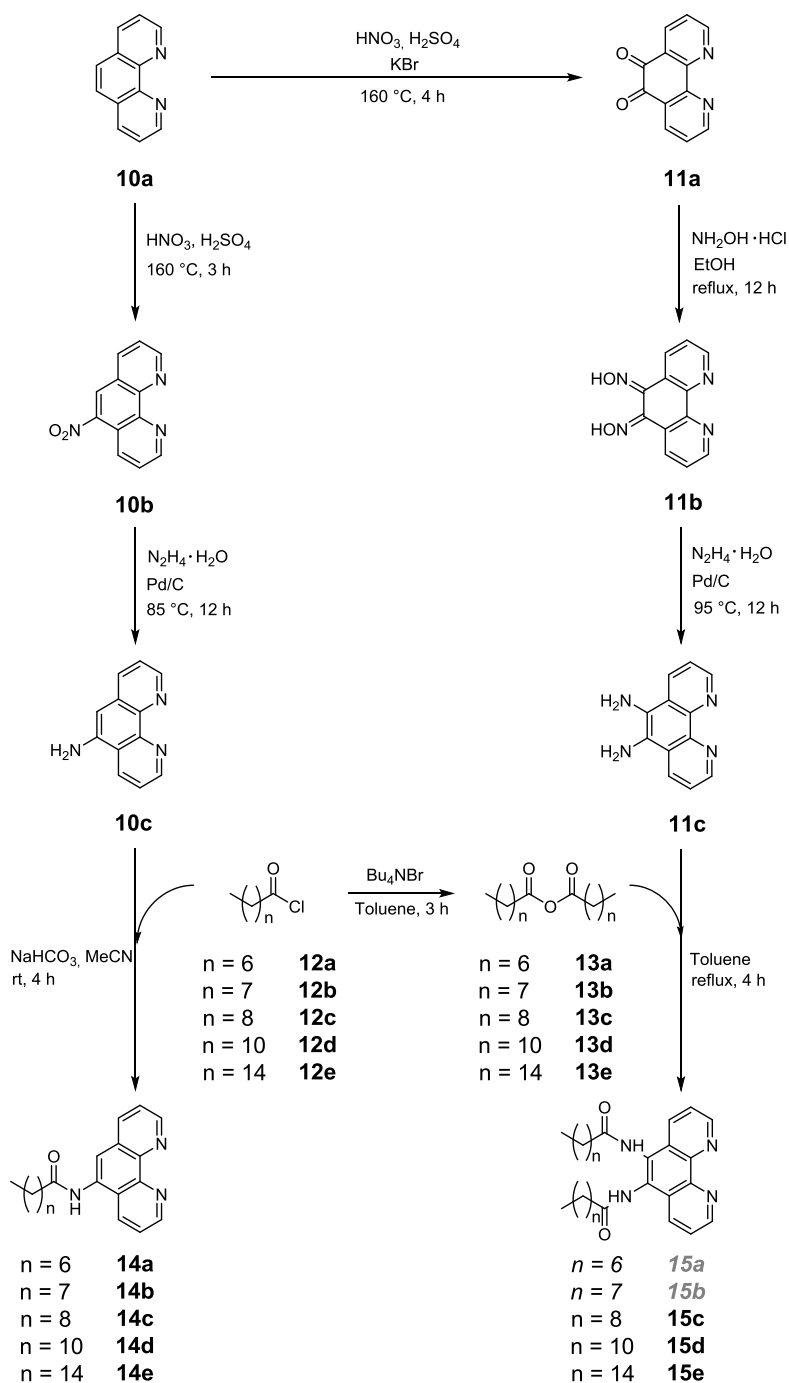
Scheme 4.2 *Synthesis of amphiphilic phenanthroline derivatives at a glance.*

4.1   Results and discussion

4.1.1   Synthesis of phenanthroline ligands

The synthetic pathway of a single-functionalized phenanthroline ligand started with the nitration of compound **10a**. Afterwards, the amine **10c** was synthesized by reduction of the nitro group of **10b** (**Scheme 4.3**).[62] The mixture was filtered over celite to avoid contamination by the catalyst. Furthermore, the residue was cooled quickly with liquid nitrogen to avoid an abrupt exothermic process. The resulting compound was acquired in a moderate yield (29**%** for **10c**, Lit.[62] 46**%**).
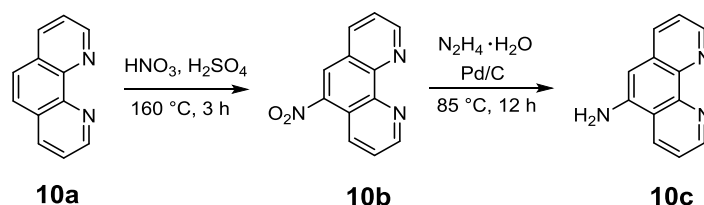
Scheme 4.3 Synthesis of 5-nitro-1,10-phenanthroline (**10b**) and 5-amino-1,10-phenanthroline (**10c**).

For the synthesis of a doubly functionalized phenanthroline ligand, 1,10-phenanthroline-5,6-dione (**11a**) was synthesized according to Neumann *et al.*[63] Then, the synthesis of **11b** was performed without characterization of the compound due to its insolubility in any solvent. **11c** was generated by reduction of the dioxime to the diamine (**Scheme 4.4**).[64] The resulting compound was acquired successfully (84**%** for **11c**, Lit.[64] 83**%**).
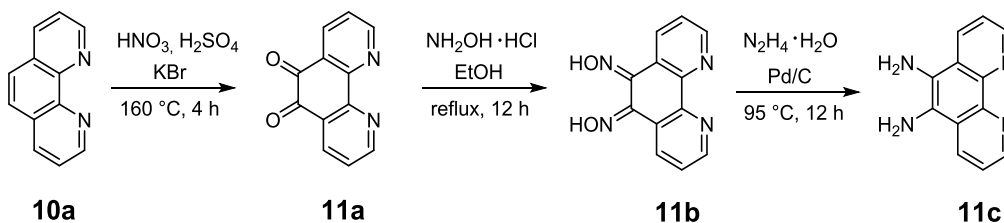
Scheme 4.4 Synthesis of 1,10-phenanthroline-5,6-diamine (**11c**).

4.1.2 Synthesis of mono- and bisfunctionalized phenanthroline

According to Peng *et al.*, the condensation reactions of the monoalkylated and phenanthroline derivatives were carried out with acyl chlorides **12a–e** (*Scheme 4.5*).[65] All compounds **14a–e** were successfully characterized by ^{1}H NMR spectroscopy.

n = 6   **12a**   n = 6   **14a**
n = 7   **12b**   n = 7   **14b**
n = 8   **12c**   n = 8   **14c**
n = 10   **12d**   n = 10   **14d**
n = 14   **12e**   n = 14   **14e**
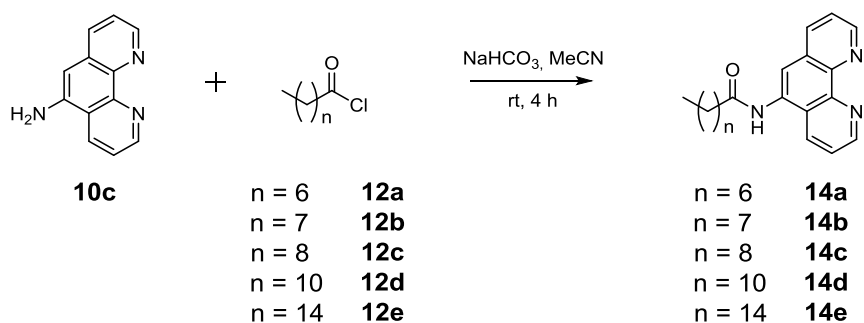
Scheme 4.5 *Synthesis of amphiphilic phenanthroline derivatives **14a–e**.*

Under the same conditions, the synthesis of doubly functionalized phenanthroline derivatives **15a–e** was unsuccessful. Therefore, another reaction was tried according to the synthetic procedure of diamides reported by Vidal-Ferran *et al.*[149] In order to obtain reactive amidation reagents, the syntheses of octanoyl (capryloyl) anhydride (**13a**), nonanoyl (pelargonyl) anhydride (**13b**), decanoyl (capric acid) anhydride (**13c**), dodecanoyl (lauroyl) anhydride (**13d**) and hexadecanoyl (palmitoyl) anhydride (**13e**) were carried out (***Scheme 5.6***).[150] All anhydrides **13a–e** could be synthesized with high yields (84–99%) and analyzed by ^{1}H NMR spectroscopy. Only **13c–e** were detectable in the ESI mass spectra. The melting points are are 40 °C for **13d** and 62 °C for **13e**. Due to their liquid appearance at low temperatures (4 °C), melting points of **13a–c** could not be determined.

n = 6   **12a**   n = 6   **13a**
n = 7   **12b**   n = 7   **13b**
n = 8   **12c**   n = 8   **13c**
n = 10   **12d**   n = 10   **13d**
n = 14   **12e**   n = 14   **13e**
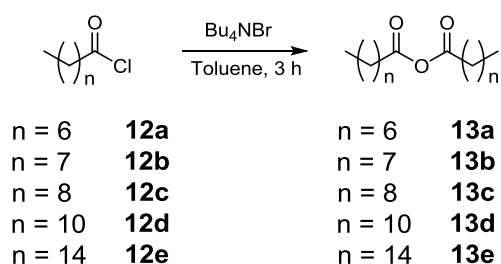
Scheme 4.6 *Synthesis of the anhydrides **13a–e**.*

Finally, the synthesis of **15a–e** were performed by the application of anhydrides **13a–e** (**Scheme 4.7**). Only **15c–e** were characterized successfully by ^{1}H NMR spectroscopy and ESI mass spectrometry.

11c	n = 6	**13a**	n = 6	15a
	n = 7	**13b**	n = 7	15b
	n = 8	**13c**	n = 8	**15c**
	n = 10	**13d**	n = 10	**15d**
	n = 14	**13e**	n = 14	**15e**
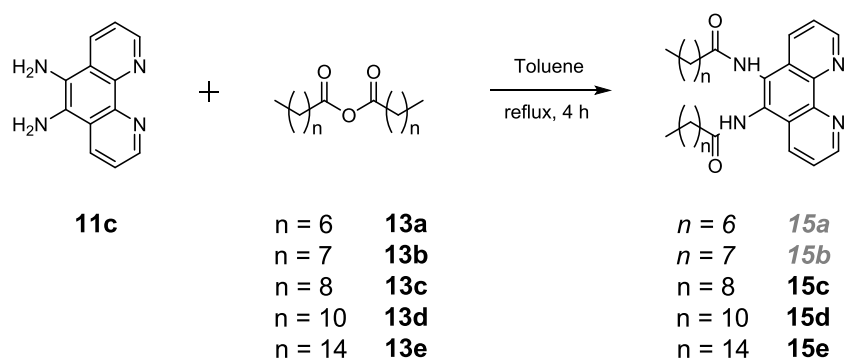
Scheme 4.7 *Synthesis of amphiphilic phenanthroline derivatives* **15a–e**.

4.1.3 Synthesis of phenanthroline complexes

Because only compounds **14a–b** were completely soluble in DMSO, complexations of **14a–b** were carried out with several types of copper salts in different solutions (**Scheme 4.8**). A precipitate was obtained and was characterized by ESI MS spectrometry. After evaluation of the elemental analysis results, however, it was not possible to determine any concrete composition for this precipitate. For that reason, DNA cleavage studies and other analytical investigations were carried out with *in situ* formed Cu(II) complexes, which were generated with an excess of **14a** and **14b**, respectively, to be able to exclude effects from free metal ions.
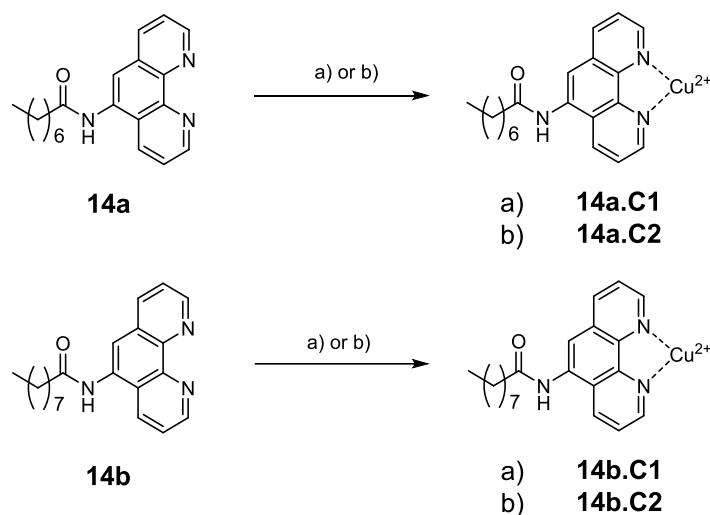
Scheme 4.8 *Synthesis of complexes **14a.C1–2** and **14b.C1–2** under the following conditions a) Cu(NO₃)₂ · 3 H₂O, EtOH, reflux, 1 h and b) Cu(ClO₄)₂ · 6 H₂O, MeOH, rt, 2 h.*

4.1.4 Critical micelle concentration (cmc)

The amphiphilic feature of the alkylated phen derivatives was exploited in order to determine possible micellar formation at a certain concentration. Herein, the "pyrene 1:3 method" according to Ruiz *et al.* was applied.[151] Fluorescence titration of high-concentrated DMSO solutions of compounds **14a** (+ **Cu**) and **14b** (+ **Cu**) was carried out. Although DMSO was considered in the reference, solubility issues occurred. Because of that, determination of the cmc of the alkylated phen derivatives was not possible.

4.1.5　　　DNA cleavage studies

4.1.5.1　　　Oxidative cleavage

In order to evaluate the oxidative DNA cleavage ability, pBR322 DNA (Form I) was incubated with varying concentrations of compounds **14a** (**+ Cu**) and **14b** (**+ Cu**) in Tris-HCl buffer (50 mM) at pH 7.4 for 2 h and in the presence of the reducing agent ascorbate. The corresponding non-alkylated phen **10c** (**+ Cu**) was chosen as a comparison to the alkylated phen derivatives. The ligand and *in situ* complex solutions (in DMSO) were diluted in water resulting in a final concentration of 1**%** DMSO, which has been considered in the reference DNA.
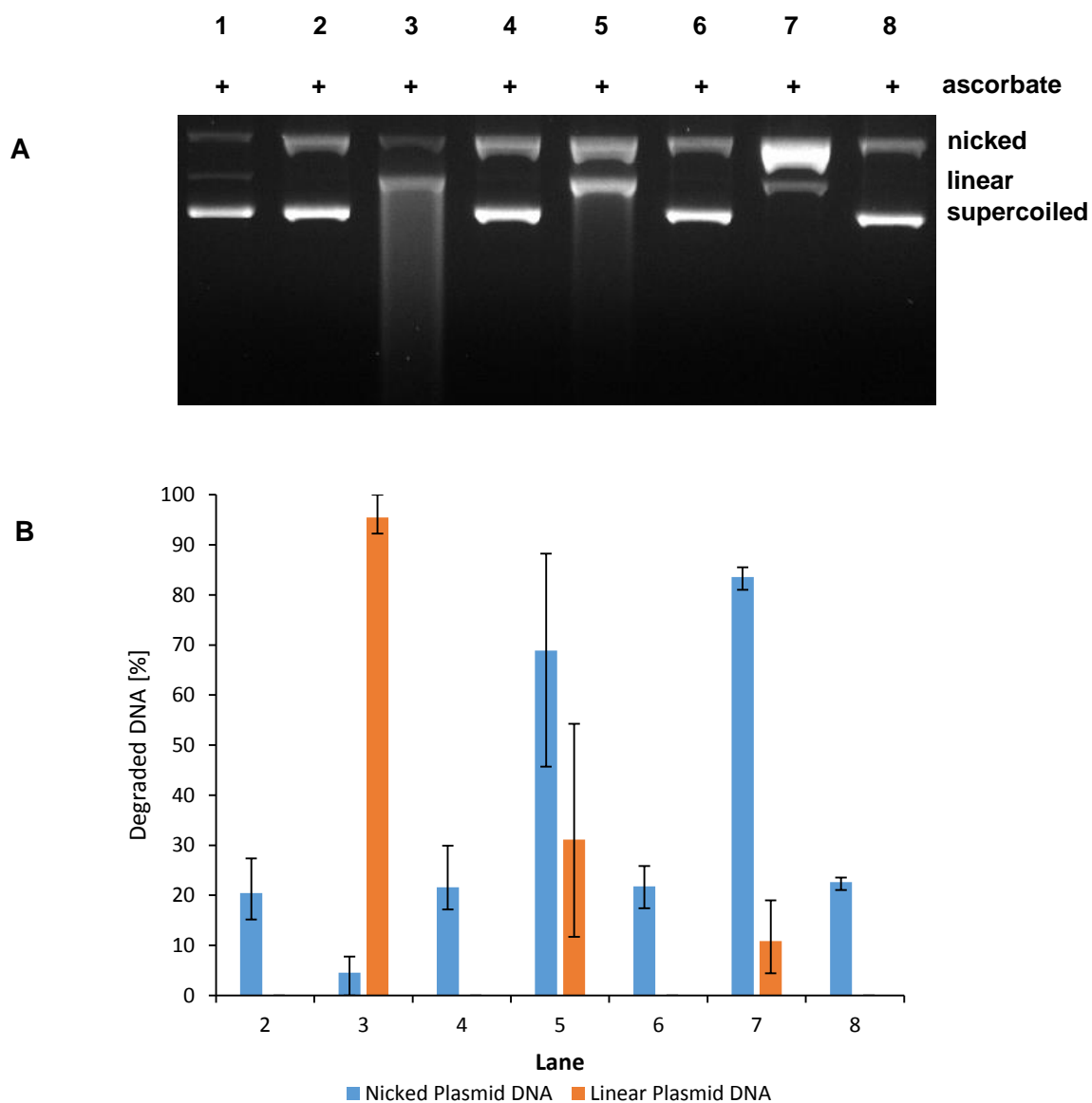
Fig. 4.2 *(A) Cleavage activity of the complexes monitored by 1% agarose gel electrophoresis after incubation at 37 °C for 2 h. Every lane contained 0.2 µg plasmid DNA in 50 mM Tris-HCl buffer (pH 7.4) and 1% DMSO in the presence of ascorbate (1 mM) (representative gel). Lane 1: DNA ladder; lane 2: **10c** (20 µM); lane 3: **10c** (20 µM) + **Cu(NO₃)₂** (18 µM); lane 4: **14a** (20 µM); lane 5: **14a** (20 µM) + **Cu(NO₃)₂** (18 µM); lane 6: **14b** (20 µM); lane 7: **14b** (20 µM) + **Cu(NO₃)₂** (18 µM); lane 8: Reference DNA. (B) Percentage of degraded DNA (error bars represent the standard deviations from three independent experiments).*
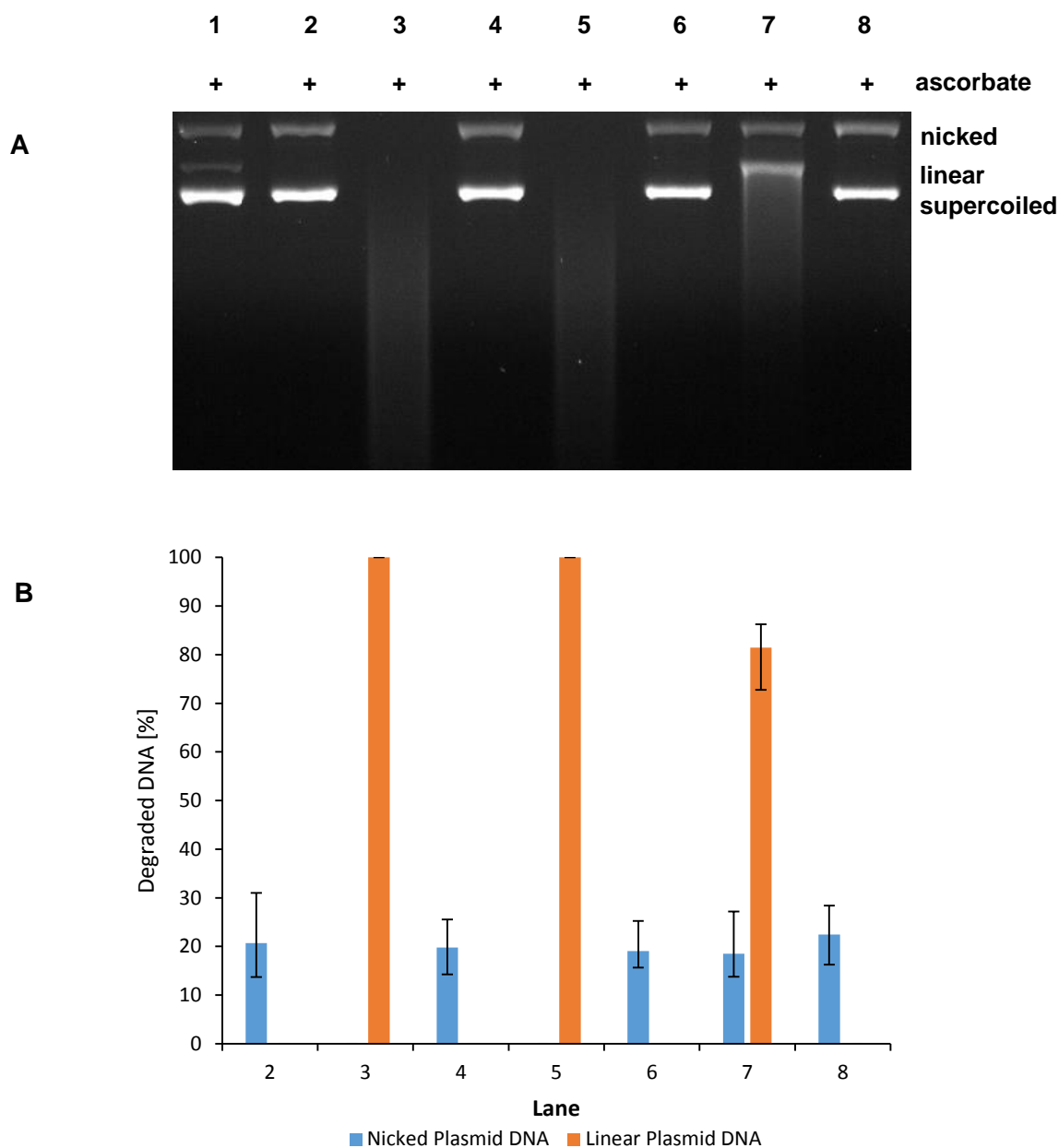
Fig. 4.3 *(A) Cleavage activity of the complexes monitored by 1% agarose gel electrophoresis after incubation at 37 °C for 2 h. Every lane contained 0.2 µg plasmid DNA in 50 mM Tris-HCl buffer (pH 7.4) and 1% DMSO in the presence of ascorbate (1 mM) (representative gel). Lane 1: DNA ladder; lane 2: **10c** (50 µM); lane 3: **10c** (50 µM) + **Cu(NO3)2** (45 µM); lane 4: **14a** (50 µM); lane 5: **14a** (50 µM) + **Cu(NO3)2** (45 µM); lane 6: **14b** (50 µM); lane 7: **14b** (50 µM) + **Cu(NO3)2** (45 µM); lane 8: Reference DNA. (B) Percentage of degraded DNA (error bars represent the standard deviations from three independent experiments).*

At 18 µM complex concentration (***Fig. 4.2***), **10c + Cu** produced approximately 5% of Form II and 95% of Form III (lane 3) and therefore showed the highest cleavage activity compared to **14a + Cu** (50–85% of Form II and 15–50% of Form III, lane 5) and **14b + Cu** (80–85% of Form II and 5–15% of Form III, lane 7). In the absence of copper and at concentrations of both 20 µM and 50 µM (***Fig. 4.2*** and ***Fig.***

4.3), no significant difference (of **10c**, **14a–b**) was observed compared to the reference (lanes 2, 4 and 6).

At 45 µM concentration and under identical conditions, all complexes showed a higher DNA cleavage activity compared to 18 µM concentration and complete cleavage of Form I (***Fig. 4.3***). While **10c + Cu** and **14a + Cu** produced only Form III and fragmented DNA, about 15–25**%** of Form II and 75–85**%** of Form III were obtained in the presence of **14b + Cu**.

The order of DNA cleavage activity is as follows **14b + Cu** < **14a + Cu** < **10c + Cu** and thus proportional to the hydrophilicity of the phen derivatives, whereas phen itself is assumed to be the hydrophilic part of the amphiphile. In order to find out, which oxygen species are inducing the oxidative cleavage, ROS studies were carried out and the results were evaluated in the next paragraph.

When thinking of cell experiments an increase of the hydrophobicity might facilitate the transport of the complexes through the cell membrane on the one hand, but also decrease the DNA binding affinity due to a weaker intercalation on the other hand. According to Palaniandavar *et al.*, substitutions of phen in 5-position eliminates intercalative interaction to CT-DNA.[152] Binding mode studies shall be carried out by CD spectroscopy.

4.1.5.2   ROS studies for oxidative cleavage

In order to characterize the essential reactive oxygen species responsible for the DNA cleavage of **10c + Cu**, **14a + Cu** and **14b + Cu** we used different scavengers:

a) *tert*-Butanol for hydroxyl radicals

b) DMSO for hydroxyl radicals

c) Sodium azide (NaN_3) for singlet oxygen

d) Catalase for hydrogen peroxide

e) Superoxide dismutase for superoxide
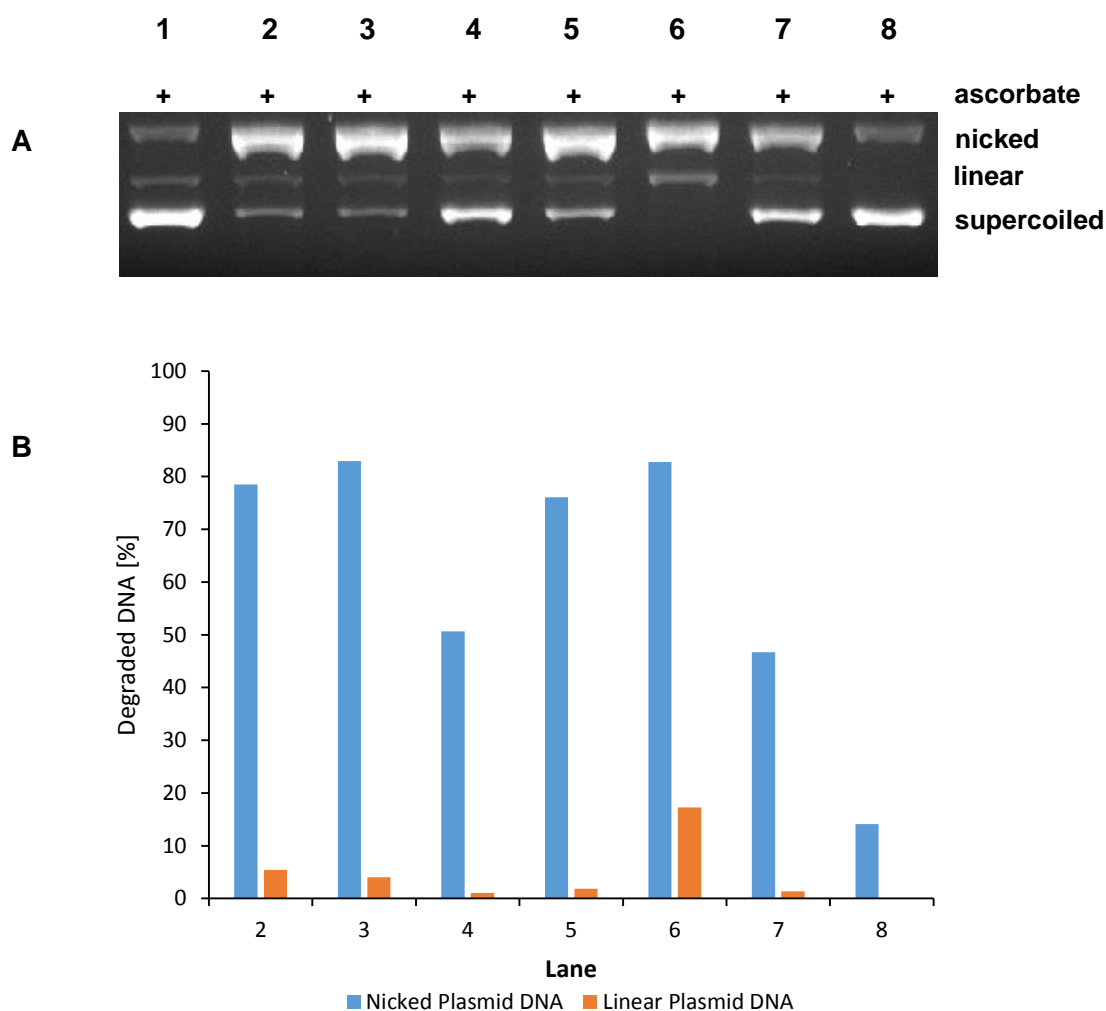
Fig. 4.4 *(A) Quenching effects on DNA cleavage by **10c + Cu** monitored by 1% agarose gel electrophoresis after incubation at 37 °C for 2 h. Every lane contained 0.2 µg plasmid DNA in 50 mM Tris-HCl buffer (pH 7.4), 1% DMSO and 0.125X PBS in the presence of ascorbate (1 mM) (representative gel). Lane 2-7 contained 10 µM of **10c** and 9 µM of **Cu(NO₃)₂**. Lane 1: DNA ladder; lane 2: reference; lane 3: 200 mM tBuOH; lane 4: 200 mM DMSO, lane 5: 10 mM NaN₃; lane 6: 2.5 mg/mL catalase; lane 7: 313 U/mL superoxide dismutase; lane 8: reference DNA. (B) Percentage of degraded DNA.*

In the presence of reducing agents and oxygen, it is known that $[Cu(phen)_2]^{2+}$ can form radicals, which are responsible for the oxidative DNA cleavage (**Scheme 4.9**).[39] According to Sigman *et al.*, the copper bound oxidants Cu^+OH, $Cu^{2+}OH$ or $Cu^{3+}O$ are acting as active species. These active species can generate hydroxyl radicals or superoxides.[140]
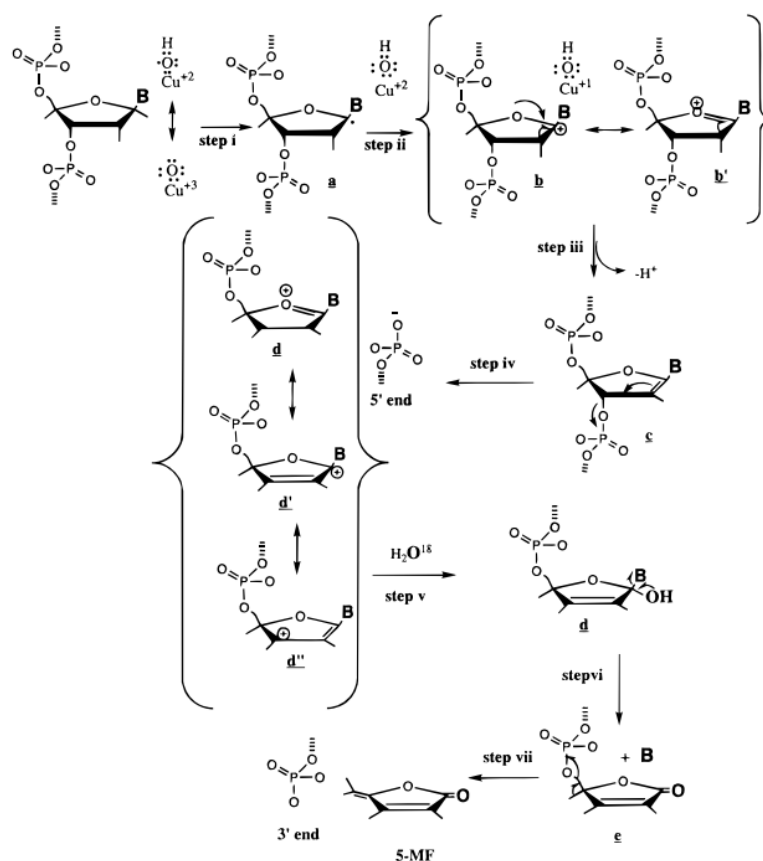
Scheme 4.9 *Generation of 5-methylene furanone (5-MF) in the presence of $[Cu(phen)_2]^{2+}$ Reprinted with permission from M. Meijler, O. Zelenko and D. Sigman, J. Am. Chem. Soc., 1997, 119, 1135.*

Due to the fact that at 20 μM concentration **10c + Cu** caused complete cleavage of Form I plasmid DNA, ROS studies were performed at 10 μM concentration. **10c + Cu** observed slight scavenging effects in the presence of DMSO, NaN_3 and SOD (lanes 4, 5 and 7, **Fig. 4.4**). This indicates that hydroxyl radicals, superoxide and singlet oxygen are possibly involved in the DNA cleaving process. The result is in agreement with $[Cu(phen)_2]^{2+}$, where hydroxyl radicals and superoxide takes part in the oxidative DNA cleavage. According to Palaniandavar *et al.*, hydroxyl radicals are also involved in the oxidative DNA cleavage of the mixed ligand Cu(II) phen complexes.[153]

However, a distinct increase of the DNA cleavage was caused by **10c + Cu** in the presence of catalase (lane 6). As in the case of **8b + Cu** (**3.1.5.3** and **3.1.5.4**), it is likely that catalase might be oxidized by singlet oxygen. Chemiluminescent studies of Qin *et al.* revealed that singlet oxygen is involved in DNA base damage, induced by a Cu(II) phen/ascorbate/H_2O_2 system.[154] In addition to that, it is presumable that the phen ligand coordinates to iron ($K = 10^{21}$), which is present in catalase. It seems unlikely that any iron porphyrin, such as catalase, would be an early victim of ligand competition. In relation to this, it is expected that heme would have a stability constant at least as high as o-phenanthroline and therefore would not be among the less stable iron chelates.[155] According to Mellor *et al.* and in a 1:1 ratio, iron-coordinated phen complexes (*log* K_1 = 5.8) are less stable than copper coordinated phen complexes (*log* K_1 = 9.0). In the case of 3:1 complexes, the order changes making iron phen complexes (*log* K_3 = 10.0) more stable than copper phen complexes (*log* K_3 = 5.0).[156] This statement reveals that iron might be coordinated to **10c** in a ratio unlike 1:1 and cleave DNA without any influence of the quencher catalase. It is also likely that iron bounds to excessive phen ligands, since the concentration of the phen ligand is slightly higher than the copper salt. In order to examine this in more detail, DNA cleavage studies shall be performed with Fe(II) generated *in situ* complexes of **10c**. In addition to that, binding affinities of Fe(II)-**10c** towards catalase and phen shall be compared.

In the case of **14a + Cu**, no distinct quenching was observed (***Fig. 4.5***). DNA cleavage of **14b + Cu** was slightly quenched only in the presence of NaN_3 (***Fig. 4.6***). This indicates that singlet oxygen might be involved in the DNA cleaving process.
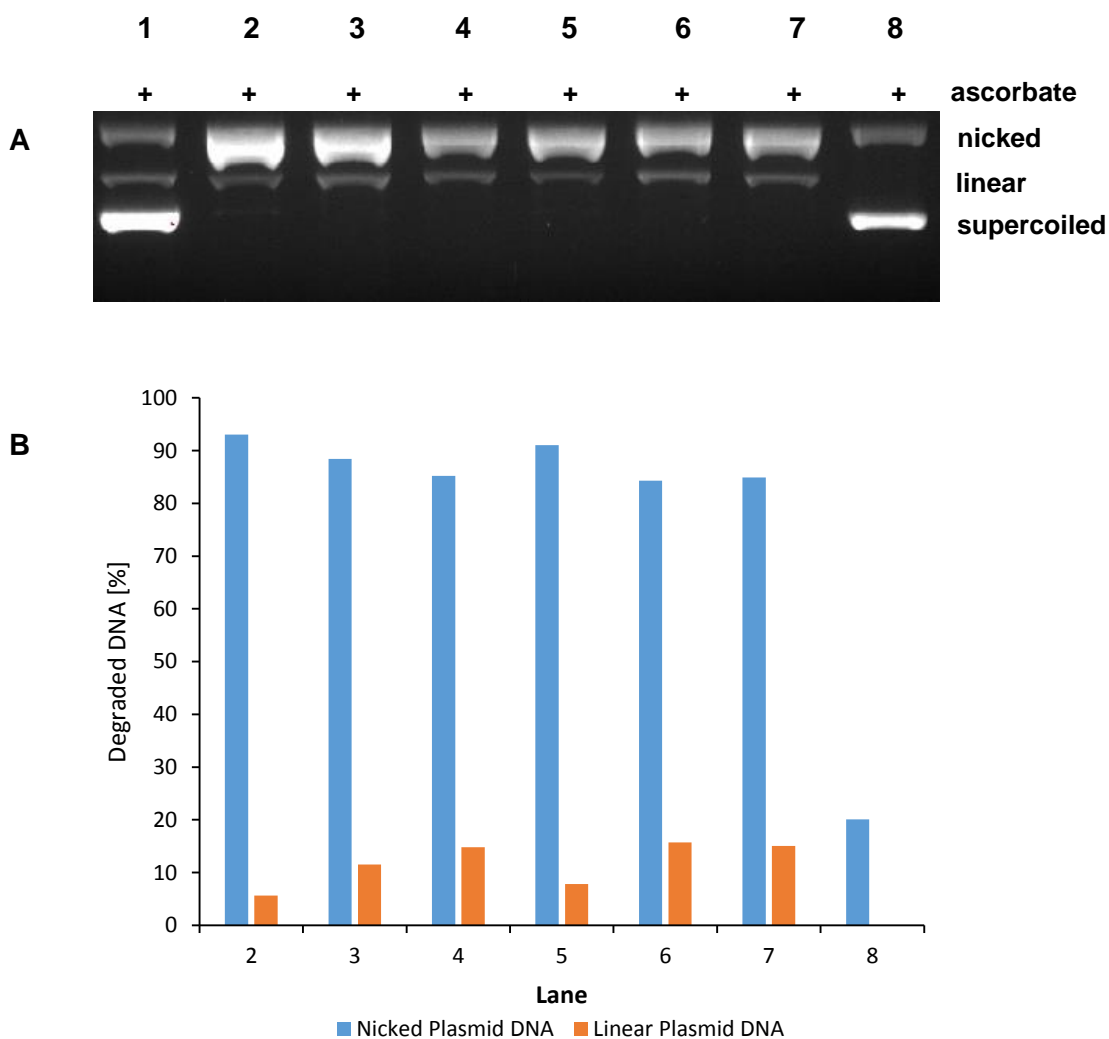
Fig. 4.5 (A) Quenching effects on DNA cleavage by **14a** + **Cu** monitored by 1% agarose gel electrophoresis after incubation at 37 °C for 2 h. Every lane contained 0.2 µg plasmid DNA in 50 mM Tris-HCl buffer (pH 7.4), 1% DMSO and 0.125X PBS in the presence of ascorbate (1 mM) (representative gel). Lane 2-7 contained 20 µM of **14a** and 18 µM of **Cu(NO₃)₂**. Lane 1: DNA ladder; lane 2: reference; lane 3: 200 mM tBuOH; lane 4: 200 mM DMSO, lane 5: 10 mM NaN₃; lane 6: 2.5 mg/mL catalase; lane 7: 313 U/mL superoxide dismutase; lane 8: reference DNA. (B) Percentage of degraded DNA.
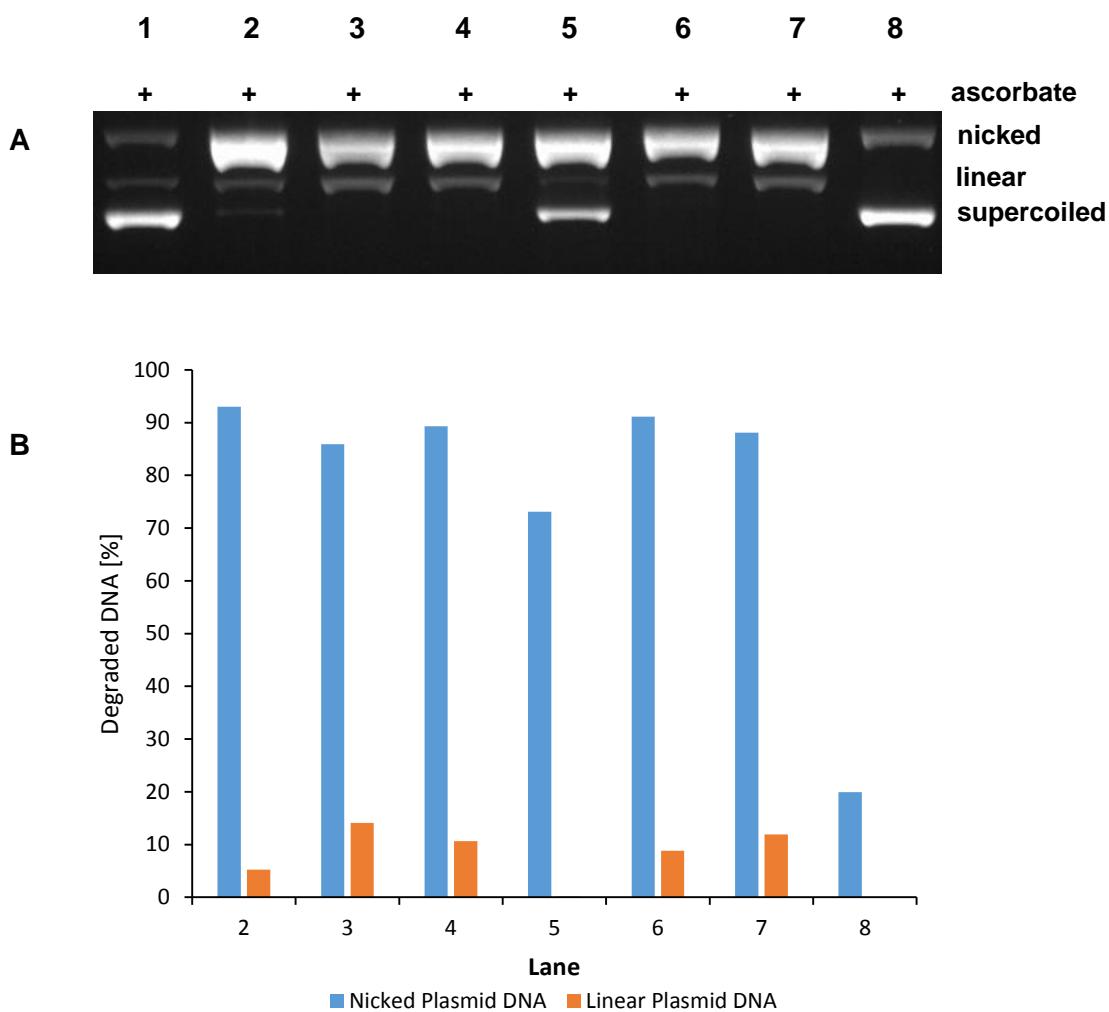
Fig. 4.6 (A) Quenching effects on DNA cleavage by **14b** + **Cu** monitored by 1% agarose gel electrophoresis after incubation at 37 ℃ for 2 h. Every lane contained 0.2 µg plasmid DNA in 50 mM Tris-HCl buffer (pH 7.4), 1% DMSO and 0.125X PBS in the presence of ascorbate (1 mM) (representative gel). Lane 2-7 contained 20 µM of **14b** and 18 µM of **Cu(NO₃)₂**. Lane 1: DNA ladder; lane 2: reference; lane 3: 200 mM tBuOH; lane 4: 200 mM DMSO, lane 5: 10 mM NaN₃; lane 6: 2.5 mg/mL catalase; lane 7: 313 U/mL superoxide dismutase; lane 8: reference DNA. (B) Percentage of degraded DNA.

4.1.5.3 Investigation of possible ROS in the absence of ascorbate

The motivation of this experiment is described in **2.1.6.4**. In order to find out, if ROS could also be generated in the absence of ascorbate, DNA cleavage studies were carried out with the same complex concentration used in the oxidative cleavage studies as described in **4.1.5.1.2** and in absence of any reducing agent (shown in *Fig. 4.7* for **14a + Cu** representatively):
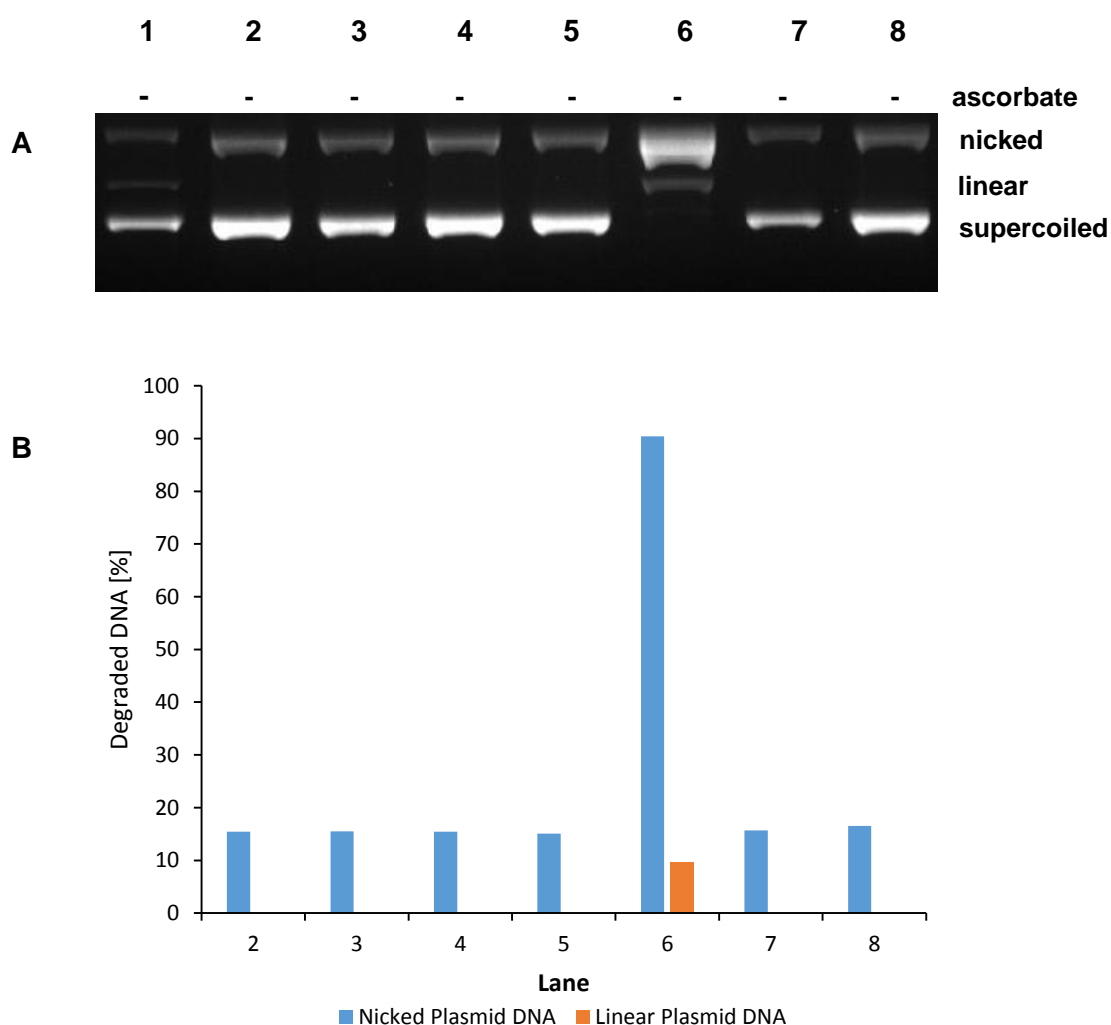
Fig. 4.7 (A) Quenching effects on DNA cleavage by **14a + Cu** monitored by 1% agarose gel electrophoresis after incubation at 37 °C for 2 h. Every lane contained 0.2 µg plasmid DNA in 50 mM Tris-HCl buffer (pH 7.4), 1% DMSO and 0.125X PBS (representative gel). Lane 2-7 contained 20 µM of **14a** and 18 µM of **Cu(NO₃)₂**. Lane 1: DNA ladder; lane 2: reference; lane 3: 200 mM tBuOH; lane 4: 200 mM DMSO, lane 5: 10 mM NaN₃; lane 6: 2.5 mg/mL catalase; lane 7: 313 U/mL superoxide dismutase; lane 8: reference DNA. (B) Percentage of degraded DNA.

Significant changes of DNA cleavage activity were observed for **14a + Cu** in lane 6, where catalase caused a distinctly higher DNA cleavage activity in spite of the absence of ascorbate (*Fig. 4.7*). The same observation was made for the case of **14b + Cu** (not shown). The difference between the DNA cleavage activities in the presence of catalase compared to the other lanes is not as remarkable as in the results shown in *Fig. 4.4*, *Fig. 4.5* and *Fig. 4.6*, where a reducing agent was applied.

As in the case of **10c + Cu** in *Fig. 4.4*, it is very likely that **14a** coordinates to iron ions of catalase, since inhibition of catalase by ascorbate is excluded in this experiment.[129] Also here, iron is probably coordinated to **14a** in a ratio unlike 1:1 and the DNA may be cleaved without any influence of the quencher catalase.[156] Taking into account that one BSA molecule contains 2 hemes, it is likely that about 10-25 hemes might be present in lane 6 (*Fig. 4.7*).[157] The resulting iron content might be enough to bind to **14a** and to decrease the activation of catalase.

As already mentioned above, studies regarding DNA cleavage, DNA binding affinity and catalase activity shall be carried out with Fe(II) generated *in situ* complexes of the phen derivatives.

Studies regarding oxidative DNA cleavage by phen derivatives and in absence of reducing agents were described recently by Palaniandavar *et al.* They found out that Cu(II) phen derivatives with mixed ligands (phen and tridentate Schiff base) could cleave pUC19 DNA completely at 100 µM concentration.[153] In contrast, **14a + Cu** did not show significant changes of DNA cleavage activity at 18 µM concentration (*Fig. 4.7*, lane 2).

4.1.6   Protein cleavage studies

4.1.6.1   SDS-PAGE

The sodium dodecyl sulfate polyacrylamide gel electrophoresis (SDS-PAGE) is a useful method to study the cleavage of proteins (e.g. bovine serum albumin, BSA) into proteins and peptides in the range of 1–500 kDa. The anionic detergent imparts a homogenous negative charge to the protein proportional to its relative molecular mass. The samples are loaded onto a porous gel made from polyacrylamide and bisacrylamide (the latter one can form cross-links between two acrylamide molecules). The gel is placed in a buffer solution and an electrical field is applied.

*Depending on the protein size, small molecules migrate faster to the anode (**Fig. 4.8**). The gels were activated (UV-light-induced reaction of compounds within the gels with tryptophan residues of the protein) to generate fluorescence. After comparison of the bands to a molecular weight size marker, the cleavage products can be assigned to the bands shown in the gel. The cleavage of a single protein can be monitored by intensity loss of the chosen protein band compared to a reference sample of the uncleaved protein of the same concentration.*
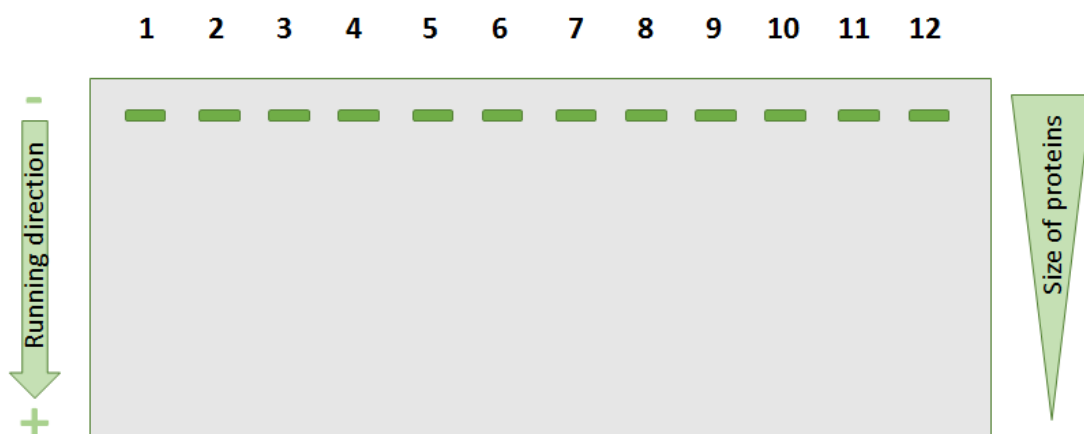
***Fig. 4.8** Schematic construction of a SDS-PAGE.*

In order to investigate the proteolytic activity of the Cu(II) phen complexes, BSA was incubated with certain concentrations of **10c + Cu**, **14a + Cu** and **14b + Cu**. Because conditions of the method regarding alkylated phen derivatives was not known before, experiments were firstly carried out without any reducing agent. Results are shown in **Fig. 4.9**.
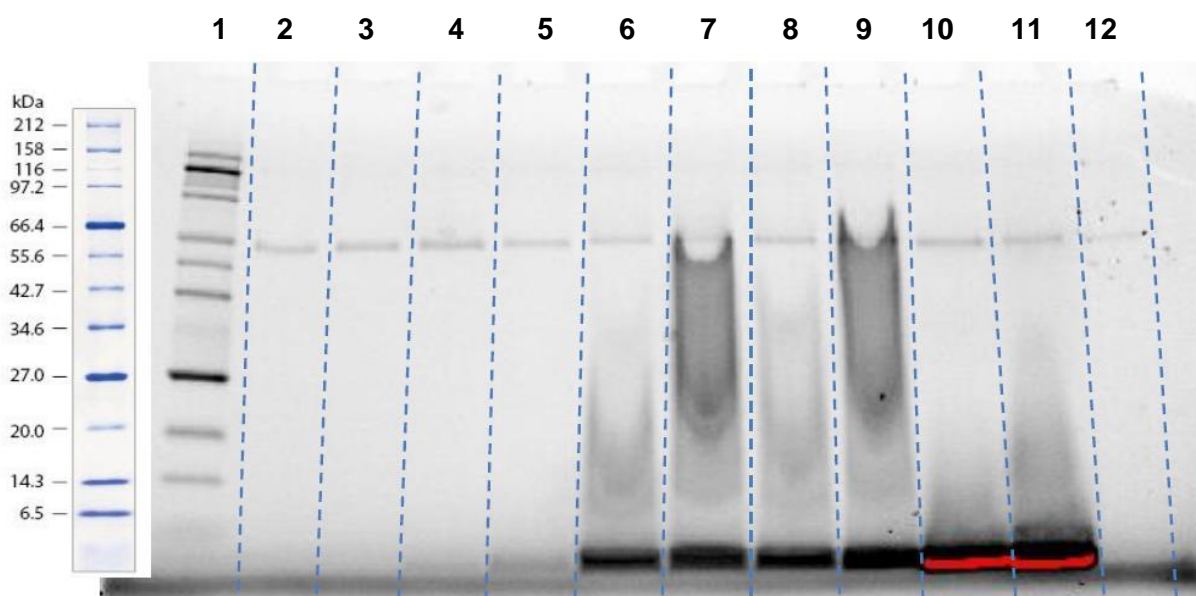
Fig. 4.9 *SDS-PAGE of concentration-dependent BSA degradation by in situ complexes **10c + Cu**, **14a + Cu** and **14b + Cu** after incubation in a Tris-HCl buffer (pH 7.4) at 37 °C for 4 h (representative gel). Lanes 2–11 contained 0.75 µM BSA. Lane 1: Marker; lane 2: reference BSA; lane 3: 0.01 mM **14a + Cu**; lane 4: 0.05 mM **14a + Cu**; lane 5: 0.1 mM **14a + Cu**; lane 6: 0.5 mM **14a + Cu**; lane 7: 1 mM **14a + Cu**; lane 8: 0.5 mM **14b + Cu**; lane 9: 1 mM **14b + Cu**; lane 10: 0.5 mM **10c + Cu**; lane 11: 1 mM **10c + Cu**; lane 12: reference BSA.*

As it can be seen in the range of 66.4 kDa, lanes 3–7 indicate that the increase of the concentration of **14a + Cu** did not lead to significant intensity loss of the BSA band. The same applies for **14b + Cu** and **10c + Cu** at 0.5 and 1 mM concentrations, respectively. Overall, from a concentration of 0.5 mM, **14a + Cu**, **14b + Cu** and **10c + Cu** produce protein fragments with a molecular weight below 6.5 kDa. At 1 mM concentration, only **14a + Cu** and **14b + Cu** (lanes 7 and 9) interestingly showed undeterminable protein fragments.

Interactions of the alkyl chain to hydrophobic domains of the target protein is likely. According to Chang *et al.*, silica-coated magnetic nanoparticles with alkyl groups as hydrophobic pockets are able to interact with BSA.[158] BSA itself exhibits a hydrophobic region, subdomain IIa.[159] Palaniandavar *et al.* have found out that Cu(II) complexes comprising a tetradentate ligand tdp (2-[(2-(2-hydroxyethylamino)-

ethylimino)methyl]-phenol) and a phen-based ligand tmp (3,4,7,8-tetramethyl-1,10-phenanthroline) produce 5 kDa protein fragments from BSA through the hydrolytic pathway. Besides that, proteolytic cleavage studies has been carried out with lysozyme (14.3 kDa), whereas the [Cu(tdp)(tmp)]$^+$ complex produced 4 kDa protein fragments.[160] Investigations with lysozyme can be also applied for **14a + Cu**, **14b + Cu** and **10c + Cu**. The separation of smaller proteins and peptides < 30 kDa shall be carried out with Tricine protein gels.[161] Investigations with myoglobin might be of great interest, since the heme group of myoglobin can act as a hydrophobic pocket for hydrophobic interaction with long alkyl chains.[162]

In order to find out, whether proteolytic activity can be initiated by ROS, oxidative protein cleavage studies shall be performed in the presence of a reducing agent. Furthermore, both BSA and its resulting protein cleavage products shall be detected qualitatively via MALDI-TOF.

4.1.7 Cytotoxicity

4.1.7.1 MTT assay

Determination of cytotoxicity towards MCF-7 breast cancer cell lines was performed with **10c**, **14a** and **14b** both in the absence and presence of Cu(II). Samples with 1 mM concentration were prepared in DMSO. Experiments have also been performed with DMSO only to evaluate the effect of this solvent on the viability of the cells (not shown).

As it can be seen in **Fig. 4.10** and at 1 µM concentration, **14a** and **14b** showed a higher cytotoxicity compared to **10c** in both the presence and absence of Cu(II). The calculated IC_{50} values of phen derivatives **10c**, **14a** and **14b** are in a range of 2–3 µM (**Table 4.1**). In contrast, IC_{50} values of the *in situ* Cu(II) phen complexes **10c + Cu**, **14a + Cu** and **14b + Cu** are in a range of 1–2 µM, making them slightly more cytotoxic than the corresponding ligands **10c**, **14a** and **14b**. Therefore, acylation of phen seems to be hardly critical for the cytotoxicity towards MCF-7 cells. According to Mellor *et al.*, it is likely that the Cu(II) phen complex might contain more than one ligand, because it is possible to coordinate up to three ligands to the metal center.[156] Due to the increased hydrophobicity of **14a** (**+ Cu**) and **14b** (**+ Cu**), multiple ligand coordination might be more likely in the case of **10c** (**+ Cu**). In contrast, the resulting amphiphilic feature of **14a** (**+ Cu**) or **14b** (**+ Cu**) might facilitate the transport of the complexes through the membrane, resulting in higher cellular uptake and therefore higher cytotoxic effects compared to **10c** (**+ Cu**).[133, 163]

Similar binding affinities towards DNA are expected for all compounds, since functionalization did not occur at a position close to the coordination center. Furthermore, it is probable that the intercalation of phen into DNA might play an important part concerning cytotoxicity.

At the aforementioned concentrations, effects of both Cu(II) and DMSO alone were neglected because no distinct cytotoxic effect occurred.

The steeper viability curves of **14a + Cu** and **14b + Cu** compared to **10c + Cu** indicate that the IC_{50} values of both **14a + Cu** and **14b + Cu** might be lower than the one of **10c + Cu** (**Fig. 4.11**). For a closer investigation, multiple measurements shall be performed in the range between 10^0 and 10^1 µM.

Recently, cytotoxicity of Cu(II) complexes of 2,9-dimethyl-1,10-phenanthroline (neocuproine) towards the MCF-7 breast cancer cell line was studied by Palaniandavar *et al.*[133] The presented complexes are composed of an additional tridentate ligand such as bpa. Kumar *et al.* reported that the amphiphilic Co(III) phen complex [Co(phen)$_2$(tetradecylamine)]Cl$_2$ · 3 H$_2$O can reduce the energy status in tumors and to alter hypoxia status in the microenvironment of ME-180 human cervical cancer cells.[163] Cytotoxicity studies of the same complex towards MCF-7 cells was reported recently by Akbarsha *et al.*[164] Compared to Kumar's complex (IC$_{50}$: 8 µM), Palaniandavar's complexes (IC$_{50}$: 11–17 µM), [Cu(phen)$_2$]Cl$_2$ (IC$_{50}$: 14 µM) and to the drug cisplatin (IC$_{50}$: 26.2 µM), cytotoxicity of the *in situ* Cu(II) phen complexes **10c + Cu** (IC$_{50}$: 1.7 µM), **14a + Cu** (IC$_{50}$: 1.5 µM) and **14b + Cu** (IC$_{50}$: 2.2 µM) is increased by one order of magnitude (***Table 4.1***).[133, 165] At these concentrations (corresponds to 0.2% for **10c + Cu**, **14a + Cu** and **14b + Cu**), DMSO did not show significant cytotoxic potential, wherefore any influence of DMSO can be neglected for the determination of IC$_{50}$ values of the Cu(II) phen derivatives. Interestingly, cisplatin requires twice as much time (96 h) in order to induce comparable cytotoxicity towards MCF-7 (IC$_{50}$: 2 µM).[165]
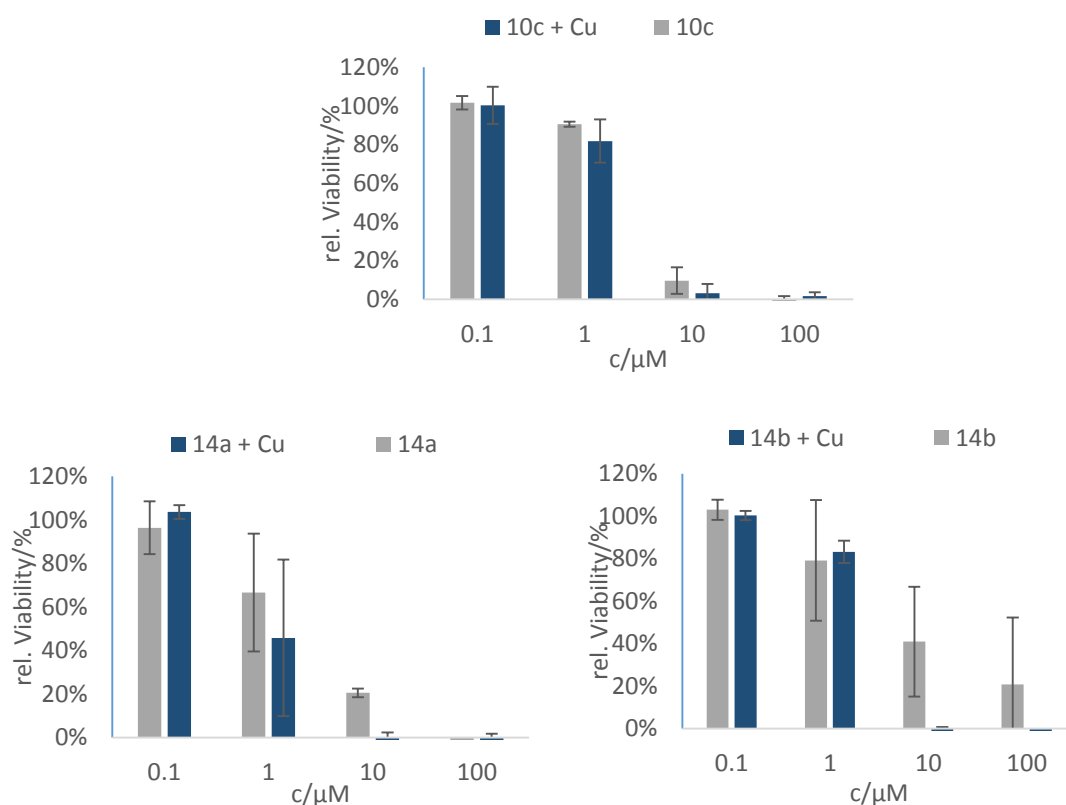
Fig. 4.10 *MTT assay results: Cytotoxicity of **10c**, **10c + Cu**, **14a**, **14a + Cu**, **14b**, **14b + Cu** at 0.1, 1, 10 and 100 µM concentrations for MCF-7 breast cancer cells. Error bars are +/- SEM.*
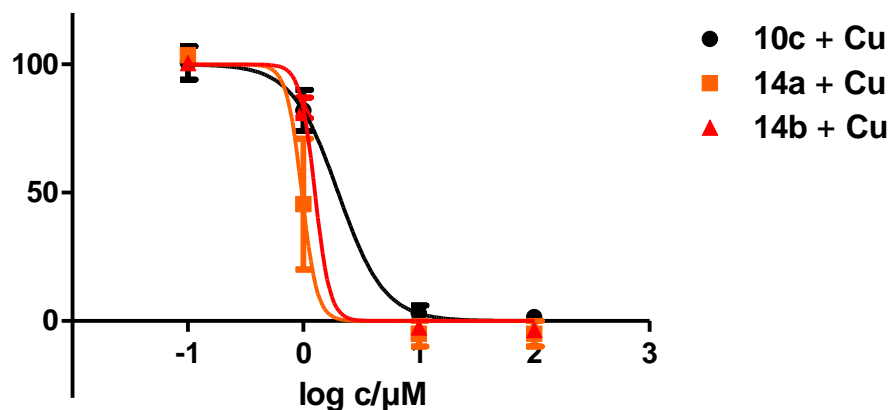
Fig. 4.11 *Cytotoxicity profiles of the complexes **10c** + **Cu**, **14a** + **Cu** and **14b** + **Cu** as determined via MTT assay on ER(+)-MCF-7 breast cancer cells. Error bars are +/- SEM.*

Table 4.1 *IC$_{50}$ values for **10c**, **10c** + **Cu**, **14a**, **14a** + **Cu**, **14b**, **14b** + **Cu** and cisplatin in MCF-7 cells.*

	48 h (in µM)	48 h (in µM)
	without **Cu**	with **Cu**
10c	2.9 ± 1.6	1.7 ± 0.3
14a	1.9 ± 0.6	1.5 ± 0.2
14b	2.7 ± 0.2	2.2 ± 0.2
[Cu(phen)$_2$]Cl$_2$[165]	-	14
[Co(trien)(tetradecylamine)Cl](ClO$_4$)$_2$[164]	8.0 ± 2.0	-
Cisplatin[133]	26.2 ± 1.1	-

CHAPTER 5

CONCLUSION AND FUTURE DIRECTIONS

In this work, the known bpa ligand **1b**[58], four novel derivatives thereof **2e**, **3f**, **4c**, **5d** and their corresponding Cu(II) nitrate complexes **6a-b** and perchlorate complexes **7a–e** have been synthesized. All complexes were incubated with plasmid DNA to evaluate their ability to cleave DNA hydrolytically in the absence of a reducing agent and oxidatively in the presence of a reducing agent. The oxidative DNA cleavage activity was similar for all complexes, indicating that changes in the ligand moiety did not influence the Cu(II/I) redox potential. The hydrolytic cleavage activity, which was investigated at two different concentrations, showed dependences concerning presence or absence of a methyl group at the terminal hydroxyl group, length of the tether, and substitution pattern of the propoxy tether. Regarding hydrolytic DNA cleavage activity, among the complexes **7e** with a hydroxypropyl-propoxy tether distinctly stood out. Despite of the planar aromatic ligands, none of the complexes intercalated into DNA as deduced from CD spectroscopic data.

Two novel estrogenic bpa derivatives **8b** and **9b** have been synthesized and characterized by NMR spectroscopy, mass spectrometry and elemental analysis. The corresponding *in situ* Cu(II) nitrate complexes **8b + Cu** and **9b + Cu** and their precursors **1b + Cu** and **1c + Cu** were subjected to both hydrolytic and oxidative DNA cleavage studies. Hydrolytic DNA cleavage studies revealed that the estrogenic bpa complexes produced small amounts of Form III DNA. Compared to the bpa precursors, the estrogenic bpa complexes **8b + Cu** and **9b + Cu** showed higher oxidative DNA cleavage activity, whereas complete cleavage of Form I DNA to both Form II and Form III was observed. This indicates that the estrogenic moiety might influence the Cu(II/I) redox potential. MTT assay results show that the introduction of an estrogenic moiety to the bpa system significantly increase the cytotoxicity towards ER(+)-MCF-7 breast cancer cell lines. Compared to the drug cisplatin, IC_{50} values of both **8b + Cu** and **9b + Cu** are smaller and therefore might be applicable in the treatment of breast cancer. In order to investigate interactions with estrogen receptors, cytotoxicity studies shall be performed also with ER(-)-MDA-MB-231 breast cancer cell lines as a negative control.[134]

Amphiphilic phen-based derivatives **14a–e** and **15c–e** have been synthesized from 5-amino or 5,6-diamino phen (**10–11c**) and their corresponding acyl chlorides (**12a–e**) or anhydrides (**13c–e**), respectively. Cu(II) complexes of **14a–b** were generated *in situ* (**14a + Cu** and **14b + Cu**) and compared with the precursor **10c + Cu** in the implemented experiments. A micellar formation of the amphiphiles was proposed, but cmc determination via the "pyrene 1:3 method" failed due to solubility issues.[151] Oxidative DNA cleavage studies of the chosen *in situ* complexes reveal that the cleavage activity is as follows **14b + Cu** < **14a + Cu** < **10c + Cu** and thereby proportional to the hydrophilicity of the phen derivatives. MTT assay results and resultant IC_{50} values reveal that the cytotoxicity of both the phen derivatives and their complexes towards the MCF-7 breast cancer cell line is increased by an order of magnitude compared to the drug cisplatin. These results indicate that the amphiphilic phen derivatives might be applicable as cytotoxic agents against breast cancer. Distinct proteolytic activities towards BSA were shown at concentrations between 0.5 and 1 mM, whereas it is not yet clarified, which protein fragments were formed. For a closer investigation regarding the type of protein cleavage, oxidative protein cleavage studies can be performed in the presence of a reducing agent. Furthermore, both BSA and its resulting protein cleavage products can be analyzed by MALDI-TOF.

CHAPTER 6

EXPERIMENTAL SECTION

6.1 Materials and methods

6.1.1 Chemicals

The chemicals and solvents were obtained from commercial sources without further purification.

6.1.2 Chromatography

Thin layer chromatography (TLC) analysis was performed with silica gel 60 F254 coated TLC plates from *Macherey-Nagel*. Column chromatography was performed with silica gel 60 (230 – 400 mesh, pore size 0.040 – 0.063 mm) from *Merck*.

6.1.3 NMR spectroscopy

For the characterization of the synthesized compounds ^{1}H NMR and ^{13}C NMR measurements were recorded on a *JEOL* ECX400, *JEOL* JNM-LA 400 FT-NMR, *JEOL* ECP500, *Bruker* AVANCE500 or *Bruker* AVANCEIII700 spectrometer in solutions of CDCl$_3$, MeOH-d$_4$ or DMSO-d$_6$ with the solvent signal as standard. Other NMR methods such as DEPT, COSY, HMBC and HMQC were performed with the *Bruker* AVANCEIII700 in a CDCl$_3$, MeOH-d$_4$ or DMSO-d$_6$ solution with the solvent signal as standard.

6.1.4 Mass spectrometry

Mass spectral data were measured with the device Agilent 6210 (ESI-TOF, 4 kV), from *Agilent Technologies*, Santa Clara, CA, USA. The flow rate was 4 µL/min and the spray voltage was 4 kV. The desolvation gas was set to 1 bar. All other parameters were optimized for a maximal abundance of the respective [M+H]$^+$.

6.1.5 Elemental analysis

Elemental analysis (EA) was carried out on a *Elementar* vario EL CHNS elemental analyzer (C, H, N) by Rita Friese from Freie Universität Berlin.

6.1.6 X-ray crystallographic data collection and refinement

Single crystals suitable for X-ray analysis were measured on a *Bruker* APEX-II CCD diffractometer by Manuela Weber from Freie Universität Berlin. The crystals were kept at 100.09 K during data collection. The X-ray data were solved by Carsten Lüdtke from Freie Universität Berlin. For data correction SADBS (*Bruker*, 2014) and SAINT (*Bruker*, 2013) were used. Using Olex2[166], the structures were solved with the ShelXS[167] structure solution program using Direct Methods and refined with the ShelXL[168] refinement package using Least Squares minimization.

6.1.7 CD spectroscopy

The circular dichroism (CD) spectra were measured on a *Jasco* J-810 Spectropolarimeter with a continuous flow of nitrogen at room temperature with 1 cm pathway cells. The CD spectra were run from 320 to 220 nm at 100 nm min^{-1} and the buffer background was subtracted automatically. Data were recorded at 0.1 nm intervals. The CD spectrum of calf thymus DNA (100 µM) alone was recorded as the control experiment. 50 µM of complex concentration was used for recording the CD spectra.

6.1.8 DNA cleavage experiments

Plasmid DNA pBR322 was purchased from *Carl Roth GmbH*. DNA cleavage experiments were performed with 0.2 µg DNA. Incubation of samples was performed in 50 mM Tris-HCl buffer (pH 7.4, *Fisher Scientific*) at 37 °C for 24 h in case of hydrolytic cleavage reactions. The oxidative cleavage was examined by DNA incubation for 2 h in the presence of the reducing agent ascorbate (1 mM, *Acros Organics*).

For the performance of ROS studies, DNA was incubated for 2 h in the presence of ascorbate (1 mM) and either 200 mM *tert*-butanol, 200 mM DMSO, 10 mM NaN$_3$, 2.5 mg/mL catalase (from bovine liver, 2-5 units/µL, *Sigma-Aldrich*) or 5 units/µL of superoxide dismutase from bovine erythrocytes (*Sigma-Aldrich*). Addition of 2X phosphate buffered saline (PBS, *Fisher Scientific*) to all samples (except for the reference) was necessary because superoxide dismutase was kept in 10X PBS and catalase had to be pre-incubated at 37 °C in 1X PBS for 30 min. The resulting PBS concentration in every incubation mixture amounts 0.125X altogether.

All cleavage experiments except for the quenching reactions were carried out three times, the error bars result from the standard deviation.

After incubation, DNA samples were run on horizontal agarose gels from *Lonza* (**1%**) containing ethidium bromide (0.2 µg/mL, *Fisher Scientific*) in 0.5x TBE buffer (*Fisher Scientific*) for 2 h at 40 V. The bands of supercoiled (Form I), open circular (Form II) and linear (Form III) DNA were visualized by fluorescence imaging of ethidium bromide on a *Bio-Rad* GelDoc EZ Imager. Data analysis was performed with *Bio-Rad*'s Image Lab Software (Version 3.0). The intensity of the bands was measured using the supercoiled control DNA as standard. Taking into account that the supercoiled Form I of plasmid DNA has a smaller affinity to bind ethidium bromide, its intensity was multiplied with a correction factor of 1.22.[169]

6.1.9 Protein cleavage experiments

In a typical experiment, to Tris-HCl buffer (50 mM final concentration, pH 7.4, in deionized water) the protein of interest was added from a stock solution (75 µM for BSA). The final protein concentration was 0.75 µM. The metal complexes were added in the respective concentrations from an *in situ* formed stock solution.

The samples were incubated for 4 h at 37 °C. After incubation 10 µL of the 500 µL incubation solution were added to 3.3 µL of reducing loading buffer (Rotiload 1, Carl Roth) and incubated for 5 minutes at 85 °C. 10 µL of this solution were loaded onto the gel (Any kD™ Mini-PROTEAN® TGX Stain-Free™ Gels, Bio-Rad). Electrophoresis was carried out at 150 V for 30 min in SDS buffer (Laemmli Buffer, Carl Roth; Rotiphorese® 10x SDS-PAGE, Carl Roth) using a vertical electrophoresis unit (Mini-PROTEAN Tetra cell, Bio-Rad). The gels were activated (UV-light-induced

reaction of compounds within the gels with tryptophan residues of the protein) to generate fluorescence and recorded with a Bio-Rad Gel Doc™ EZ system.

6.1.10 MTT assay

MTT assays were prepared and evaluated by Dr. Stephanie Wedepohl from Freie Universität Berlin. MCF-7 cells (*DSMZ* - German Collection of Microorganisms and Cell Cultures, No. ACC 115) were routinely maintained in RPMI medium without phenol red (*Life Technologies*/*Thermo Fisher Scientific* #11835-105) supplemented with 10**%** FBS (*FBS Superior*, #S0615, Biochrom AG), 1**%** penicillin/streptomycin (*Life Technologies* #15140) and 1% MEM non-essential amino acids (PAA, #M11-003) at 3 °C and 5% CO_2 and passaged twice a week. For MTT assay, 1 x 10^5 cells/mL were seeded into 96-well cell culture plates at 100 µL/well and grown over night. The next day, culture medium was removed and replaced with 50 µL/well fresh medium and 50 µL of 2-fold concentrated serial dilutions of the test compounds. Compounds were incubated for 48 h at 37 °C and 5**%** CO_2 on the cells. Afterwards, the cell culture supernatants were discarded and replaced with 100 µL/well fresh medium and 10 µL/well MTT (Thiazolyl Blue Tetrazolium Bromide, *Sigma-Aldrich* #M5655-1G, 5 mg/mL stock solution in PBS) and incubated for another 4 h at 37 °C. Then, medium was discarded and formazan crystals were dissolved by addition of 100 µL/well isopropanol with 0.04 M HCl. Absorbance was read at 570 nm in a *Tecan* Infinite M200 Pro microplate reader.

All compounds were tested as tenfold serial dilutions in duplicates and the assays were repeated 3 times independently to calculate errors. Relative viabilities were calculated as average absorbance values of the treated wells divided by the average absorbance values of the well with untreated cells. IC_{50} values were calculated by fitting a non-linear dose-response curve (log(inhibitor) vs. response – variable slope) using GraphPad Prism software.

6.1.11 Microwave

Microwave synthesis has been carried out in an *Anton Paar* Monowave 300 at 9 bar and 20 W.

6.2 Synthesis of bpa alkyl ether derivatives

6.2.1 Synthesis of amino ethers

6.2.1.1 Synthesis of 2-(2-methoxyethoxy)ethyl tosylate (2b)

2a

$C_5H_{12}O_3$
120.15

2b

$C_{12}H_{18}O_5S$
274.33
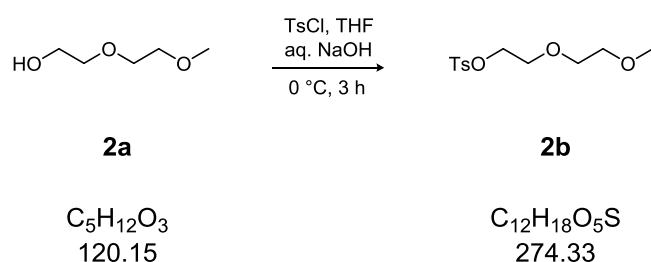
Reagents	15.3 g (127 mmol)	2-(2-Methoxyethoxy)ethanol (**2a**)
	25.5 g (134 mmol)	Tosyl chloride
	30 mL	NaOH (24**%**)
	45 mL	THF

Preparation

To a solution of 2-(2-methoxyethoxy)ethanol (**2a**) in THF (10 mL) a 24**%** NaOH aqueous solution was slowly added at 0 °C, and the mixture was stirred for 5 min. Then, a solution of tosyl chloride in THF (35 mL) was added dropwise. After stirring at 0 °C for 3 h, the reaction mixture was poured into ice-cold water (100 mL) and then stirred until the ice melted. The aqueous layer was extracted with $CHCl_3$. The collected organic phase was dried over Na_2SO_4, filtered and evaporated under reduced pressure.

Yield	31.07 g (113 mmol) 91**%**	**Lit.**[77] 91**%**

Appearance   colorless oil

^{1}H NMR   (CDCl$_3$, 400 MHz): δ(ppm) = 2.40 (s, 3 H, H$_{16}$), 3.30 (s, 3 H, H$_8$), 3.41–3.46 (m, 2 H, H$_5$), 3.51–3.55 (m, 2 H, H$_4$), 3.62–3.67 (m, 2 H, H$_2$), 4.08–4.18 (m, 2 H, H$_1$), 7.30 (d, J = 8.4 Hz, 2 H, H$_{Ar}$), 7.75 (d, J = 8.3 Hz, 2 H, H$_{Ar}$). *(Assignments according to [77], measured in CDCl$_3$)*

114

6.2.1.2   Synthesis of *N*-[2-(2-methoxyethoxy)ethyl]phthalimide (2c)

2b   **2c**

C$_8$H$_4$KNO$_2$ C$_{12}$H$_{18}$O$_5$S   C$_{13}$H$_{15}$NO$_4$
185.22   274.33   249.27
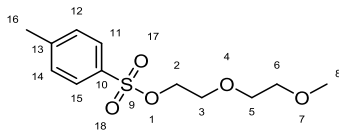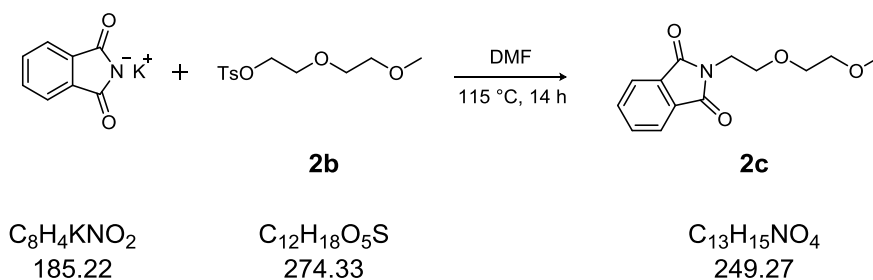
Reagents	15.0 g (54.7 mmol)	2-(2-Methoxyethoxy)ethyl tosylate (**2b**)
	10.1 g (54.7 mmol)	Potassium phthalimide
	45 mL	DMF

Preparation

2-(2-Methoxyethoxy)ethyl tosylate (**2b**) and potassium phthalimide were dissolved in DMF and the reaction mixture was refluxed at 115 °C for 14 h. After cooling down to room temperature the mixture was diluted with water and extracted with ethyl acetate. The organic phase was dried over Na$_2$SO$_4$, filtered and evaporated under reduced pressure. The residue was diluted with CHCl$_3$ and washed with brine (3 x 50 mL) until DMF was removed completely as verified through ^{1}H NMR. The organic layer was dried over Na$_2$SO$_4$, and the solvents were removed under reduced pressure at 40 °C.

Yield	6.64 g (26.6 mmol) 49**%**	**Lit.**[77] 90**%**

Appearance	yellow oil

^{1}H NMR	(CDCl$_3$, 400 MHz): δ(ppm) = 3.29 (s, 3 H, H$_8$), 3.43–3.51 (m, 2 H), 3.60–3.66 (m, 2 H), 3.73 (t, *J* = 5.9 Hz, 2 H), 3.89 (t, *J* = 5.9 Hz, 2 H), 7.69 (dd, *J* = 5.5, 3.0 Hz, 2 H, H$_{Ar}$), 7.82 (dd, *J* = 5.4, 3.1 Hz, 2 H, H$_{Ar}$). *(Assignments according to [77], measured in CDCl$_3$)*

HR MS-ESI	*m/z* [**2c** + H]$^+$ Calc. 250.1073, Found 250.1098
	m/z [**2c** + Na]$^+$ Calc. 272.0892, Found 272.0961

6.2.1.3   Synthesis of 2-(2-methoxyethoxy)ethylamine (2d)

2c

C$_{13}$H$_{15}$NO$_4$
249.27

2d

C$_5$H$_{13}$NO$_2$
119.16
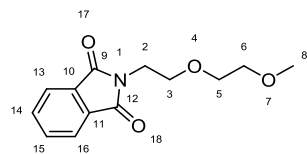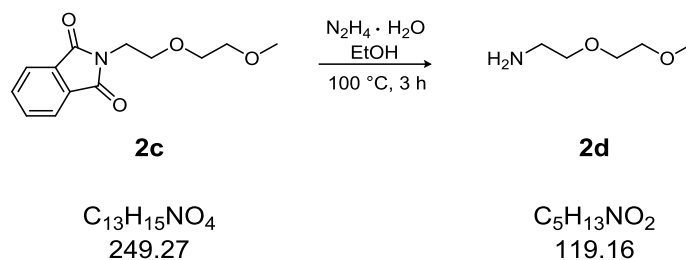
Reagents	6.64 g (26.6 mmol)	*N*-[2-(2-Methoxyethoxy)ethyl]phthalimide (**2c**)
	2.13 g (42.6 mmol)	Hydrazine monohydrate
	30 mL	EtOH

Preparation

A mixture of *N*-[2-(2-methoxyethoxy)ethyl]phthalimide (**2c**) and hydrazine monohydrate in EtOH was refluxed at 100 °C for 3 h. After cooling down to room temperature, the mixture was filtered and the filtrate was evaporated. Acetone (50 mL) was added to the residue and the precipitate was filtered. Subsequently, the filtrate was concentrated under reduced pressure.

Yield	1.98 g (16.6 mmol) 62**%**	**Lit.**[77] 91**%**

Appearance	orange oil

^{1}H NMR (CDCl$_3$, 500 MHz): δ(ppm) = 1.83 (s, 1 H), 2.00 (s, 1 H), 2.15 (s, 1 H), 2.87 (t, *J* = 5.3 Hz, 1 H), 3.35–3.39 (m, 2 H), 3.41 (t, *J* = 6.4 Hz, 1 H), 3.50 (t, *J* = 5.3 Hz, 1 H), 3.52–3.55 (m, 2 H), 3.60 (dd, *J* = 5.7, 3.3 Hz, 1 H), 3.64 (dd, *J* = 5.6, 3.8 Hz, 1 H), 3.73 (t, *J* = 6.5 Hz, 1 H).

HR MS-ESI *m/z* [**2d** + H]$^+$ Calc. 120.0973, Found 120.1047

6.2.1.4 Synthesis of 1,2-isopropylidene glyceryl glycidyl ether, IGG (3b)

3a **3b**

C_3H_5ClO $C_6H_{12}O_3$ $C_9H_{16}O_4$
92.52   132.16   188.22
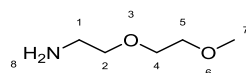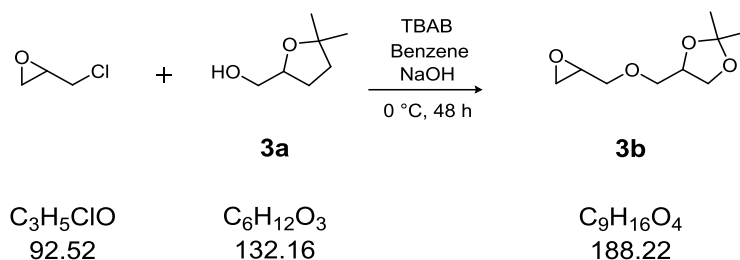
Reagents   13.0 g (98.4 mmol)   Solketal (**3a**)

18.4 g (198 mmol)   Epichlorohydrine

3.22 g (9.99 mmol)   Tetrabutylammonium bromide (TBAB)

20 mL   NaOH (50%)

20 mL   Benzene

Preparation

A mixture of solketal **3a**, epichlorohydrine, benzene, 50% NaOH and tetra-*n*-butylammonium bromide was cooled down to 0 °C and then stirred for 48 h. The reaction mixture was diluted with diethyl ether and washed with water (3 x 75 mL), saturated NaHCO₃ solution (3 x 75 mL) and brine (3 x 75 mL). The collected organic phase was dried over Na_2SO_4, filtered and evaporated under reduced pressure. Afterwards, the product was distilled at 165 °C and 1.2 mbar (b.p. 90 °C).

Yield   5.28 g (28.1 mmol) 29%   **Lit.**[79] 51%

Appearance   colorless liquid

¹H NMR   (CDCl₃, 400 MHz): δ(ppm) = 1.34 (m, 3 H, H₁₂,₁₃), 1.40 (m, 3 H, H₁₂,₁₃), 2.58 (ddd, *J* = 5.0, 3.9, 2.7 Hz, 1 H, H₇), 2.73–2.82 (m, 1 H, H₇), 3.08–3.18 (m, 1 H), 3.40 (ddd, *J* = 17.6, 11.7, 6.0 Hz, 1 H), 3.46–3.64 (m, 2 H), 3.71 (td, *J* = 8,3, 6.4 Hz, 1 H), 3.80 (ddd, *J* = 13.4, 11.7, 2.9 Hz, 1 H), 4.04 (ddd, *J* = 8.0, 6.4, 1.5 Hz, 1 H), 4.27 (dq, *J* = 11.6, 5.8, 5.3 Hz, 1 H, H₁). (*Assignments according to [79], measured in CDCl₃*)
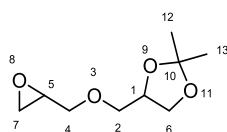
6.2.1.5 Synthesis of 1,2-isopropylidene glyceryl (1-azido-2-propanol) ether (3c)

3b

$C_9H_{16}O_4$
188.22

3c

$C_9H_{17}N_3O_4$
231.25
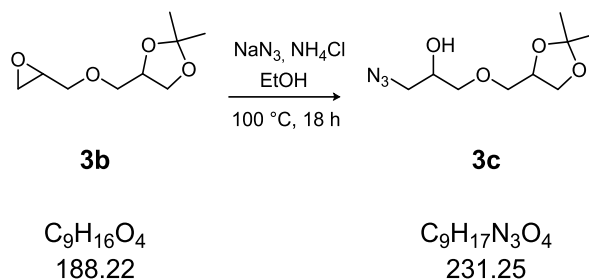
Reagents	5.42 g (28.8 mmol)	IGG (**3b**)
	9.35 g (144 mmol)	Sodium azide
	3.54 g (66.2 mmol)	Ammonium chloride
	150 mL	EtOH (80%)

Preparation

A mixture of **3b**, sodium azide and ammonium chloride in 80% EtOH was refluxed at 100 °C for 18 h. The reaction mixture was poured into ice-cold water. The solution was extracted with DCM and washed with water (3 x 50 mL) and brine (3 x 50 mL). The organic phase was dried over Na_2SO_4, filtered and evaporated under reduced pressure.

Yield	5.65 g (24.4 mmol) 85%	**Lit.**[78] 93%

Appearance	light yellow oil

^{1}H NMR (CDCl₃, 500 MHz): δ(ppm) = 1.33 (m, 3 H, $H_{13,14}$), 1.40 (m, 3 H, $H_{13,14}$), 2.92 (dd, J = 7.8, 4.9 Hz, 1 H), 3.26–3.40 (m, 2 H), 3.47–3.61 (m, 4 H), 3.69 (ddd, J = 8.3, 6.4, 2.9 Hz, 1 H), 3.88–3.97 (m, 1 H), 3.99–4.06 (m, 1 H), 4.21–4.31 (m, 1 H, H_1). (*Assignments according to [79], measured in CDCl₃*)

^{13}C NMR (CDCl₃, 126 MHz): δ(ppm) = 25.4 ($C_{13,14}$), 26.8 ($C_{13,14}$), 53.4 (2x), 66.4 (2x), 69.7 (2x), 72.6 (2x), 73.0 (2x), 74.8 (2x), 109.7. (*Assignments according to [79], measured in CDCl₃*)

6.2.1.6   Synthesis of propylene glycol (1-azido-2-propanol) ether (3d)

3c

$C_9H_{17}N_3O_4$
231.25

3d

$C_6H_{13}N_3O_4$
191.19
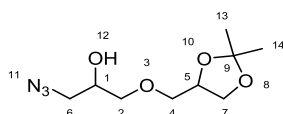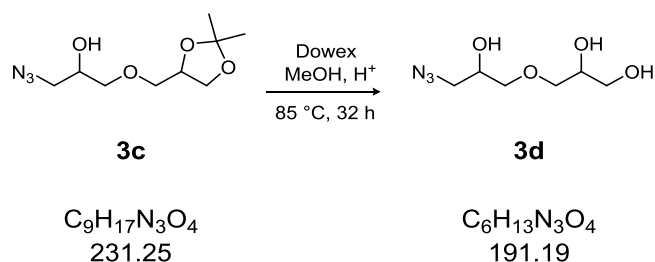
Reagents	5.65 g (24.4 mmol)	1,2-Isopropylidene glyceryl (1-azido-2-propanol) ether (**3c**)
	25.0 g	Dowex W50X8
	300 mL	MeOH (80**%**)

Preparation

3c was stirred with Dowex (15 g) in MeOH (150 mL) and refluxed at 85 °C for 16 h. After the mixture was cooled down to room temperature the ionic exchange material was filtered and the filtrate was concentrated. Then, the residue was treated again with Dowex (10 g) in MeOH (150 mL) and the reaction was repeated.

Yield   4.32 g (22.6 mmol) 93**%**   **Lit.**[78] 93**%**

Appearance   dark yellow oil

¹H NMR   (CDCl₃, 500 MHz): δ(ppm) = 3.35 (dd, J = 5.9, 2.5 Hz, 2 H), 3.48–3.65 (m, 8 H), 3.69 (dd, J = 11.7, 3.6 Hz, 1 H), 3.90 (dq, J = 6.3, 3.0, 2.6 Hz, 1 H), 3.96 (ddt, J = 9.4, 6.1, 3.4 Hz, 1 H).

HR MS-ESI   Calc. *m/z* [**3d** + H]⁺ 192.0973, Found 192.0982
Calc. *m/z* [**3d** + NH₄]⁺ 209.1238, Found 209.1250
Calc. *m/z* [**3d** + Na]⁺ 214.0792, Found 214.0807
Calc. *m/z* [**3d** + K]⁺ 230.0532, Found 230.0552

6.2.1.7   Synthesis of propylene glycol (1-amino-2-propanol) ether (3e)

3d

$C_6H_{13}N_3O_4$
191.19

3e

$C_6H_{15}NO_4$
165.19
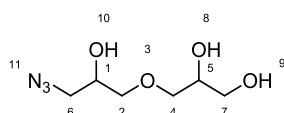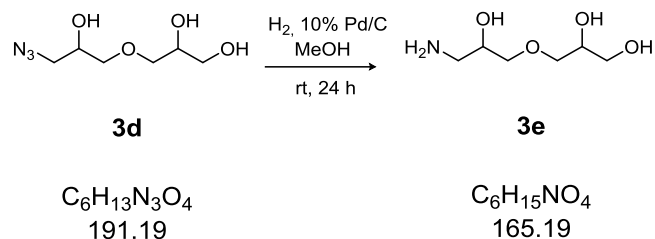
Reagents	1.19 g (5.72 mmol)	Propylene glycol (1-azido-2-propanol) ether (**3d**)
	0.12 g	10% Pd/C
	24 mL	MeOH

Preparation

10% Pd/C was added to a solution of **3d** in MeOH. The reaction mixture was stirred under hydrogen atmosphere for 24 h. After the catalyst was removed completely via repeated filtration through Celite and standard filters, the filtrate was evaporated under reduced pressure.

Yield	0.99 g (5.99 mmol) 97%	**Lit.**[78] 99%

Appearance	light yellow oil

¹H NMR   (MeOH-d₄, 500 MHz): δ(ppm) = 2.63 (ddd, J = 13.1, 7.4, 1.0 Hz, 1 H), 2.74 (dd, J = 13.1, 4.3 Hz, 1 H), 3.42–3.51 (m, 3 H), 3.51–3.60 (m, 3 H), 3.69–3.79 (m, 2 H).

¹³C NMR   (MeOH-d₄, 126 MHz): δ(ppm) = 44.0 (C₆), 48.5, 63.0, 70.9 (2x), 72.5, 73.5.

HR MS-ESI m/z [**3e** + H]⁺ Calc. 166.1073, Found 166.1211
m/z [**3e** + Na]⁺ Calc. 188.0892, Found 188.0918
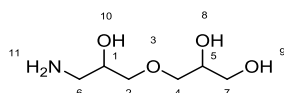
6.2.1.8 Synthesis of 1,2-methoxy propylidene (1-azido-2-methoxy-propanol) ether (4a)

	3d	4a
	$C_6H_{13}N_3O_4$	$C_9H_{19}N_3O_4$
	191.09	233.27
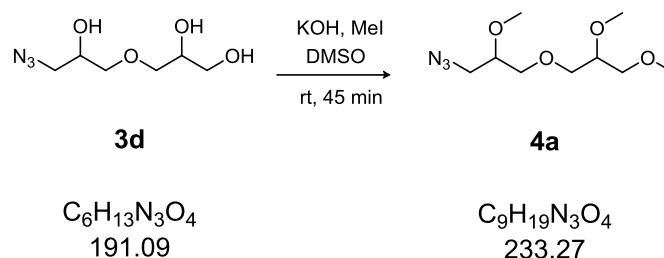
Reagents 2.01 g (10.5 mmol) Propylene glycol (1-azido-2-propanol) ether (**3d**)

7.09 g (126 mmol) KOH

8.97 g (63.2 mmol) Iodomethane

30 mL Dry DMSO

Preparation

A solution of **3d** and KOH in DMSO was stirred for 10 min under argon atmosphere. Iodomethane was added to the solution and the reaction mixture was stirred for additional 45 min. The reaction was quenched by addition of ice-cold water and further extraction with DCM. The combined organic layers were washed with water and dried over Na_2SO_4, filtered and evaporated. Subsequently the residue was filtered through a silica gel layer (MeOH/DCM 1:4) and the filtrate was concentrated under reduced pressure.

Yield 2.15 g (9.20 mmol) 87% **Lit.**[78] 82%

Appearance light yellow liquid

¹H NMR (CDCl₃, 500 MHz): δ(ppm) = 3.26–3.35 (m, 1 H), 3.36 (s, 3 H, H₁₂,₁₃,₁₄), 3.37–3.44 (m, 2 H), 3.45 (s, 3 H, H₁₂,₁₃,₁₄), 3.46 (s, 3 H, H₁₂,₁₃,₁₄), 3.46–3.60 (m, 8 H).

HR MS-ESI *m/z* [**4a** + Na]⁺ Calc. 256.1292, Found 256.1293
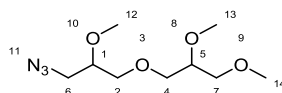
6.2.1.9 Synthesis of 1,2-methoxy propylidene (1-amino-2-methoxy-propanol) ether (4b)

4a

$C_9H_{19}N_3O_4$
233.27

4b

$C_9H_{21}NO_4$
207.27
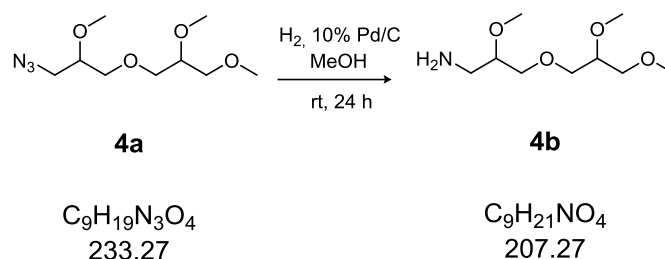
Reagents	1.27 g (5.42 mmol)	1,2-Methoxy propylidene (1-azido-2-methoxypropanol) ether (**4a**)
	0.13 g	10% Pd/C
	24 mL	MeOH

Preparation

10% Pd/C was added to a solution of **4a** in MeOH. The reaction mixture was stirred under hydrogen atmosphere for 24 h. After filtration of the catalyst, the filtrate was concentrated under reduced pressure.

Yield   1.07 g (5.15 mmol) 95%   **Lit.**[78] 93%

Appearance   light yellow oil

^{1}H NMR   (CDCl$_3$, 500 MHz): δ(ppm) = 2.72 (dd, J = 13.3, 6.5 Hz, 1 H), 2.84 (dd, J = 13.3, 4.1 Hz, 1 H), 3.26–3.33 (m, 1 H), 3.34 (s, 3 H, H$_{12,13,14}$), 3.34–3.41 (m, 2 H), 3.42 (s, 3 H, H$_{12,13,14}$), 3.43 (s, 3 H, H$_{12,13,14}$), 3.43–3.59 (m, 8 H).

^{13}C NMR   (CDCl$_3$, 126 MHz): δ(ppm) = 43.1 (C$_6$), 57.9 (2x), 58.1 (2x), 59.4, 71.0, 71.1, 71.6 (2x), 72.3, 79.3 (2x), 81.5.

HR MS-ESI m/z [**4b** + H]$^+$ Calc. 208.1573, Found 208.1597
                   m/z [**4b** + Na]$^+$ Calc. 230.1392, Found 230.1405
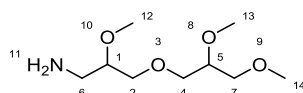
6.2.1.10   Synthesis of 1,2-isopropylidene glyceryl (1-azido-2-methoxy-propanol) ether (5a)


3c

$C_6H_{13}N_3O_4$
191.09

5a

$C_{10}H_{19}N_3O_4$
245.28
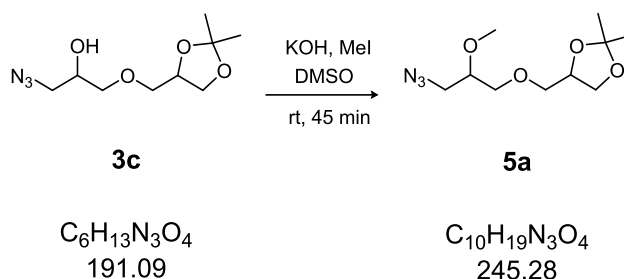
| Reagents	5.76 g (24.9 mmol)	1,2-Isopropylidene glyceryl (1-azido-2-propanol) ether (**3c**)
	16.8 g (298 mmol)	KOH
	21.2 g (149 mmol)	Iodomethane
	75 mL	Dry DMSO

Preparation

A solution of **3c** and KOH in DMSO was stirred under argon atmosphere for 10 min. Iodomethane was added to the solution and the reaction mixture was stirred for additional 45 min. The reaction was quenched by addition of ice-cold water and further extraction with DCM. The combined organic layers were washed with water and dried over Na_2SO_4, filtered and evaporated. Subsequently the residue was filtered through a silica gel layer (MeOH/DCM 1:4) and the filtrate was concentrated under reduced pressure.

| Yield	5.60 g (22.8 mmol) 92**%**
Appearance	light yellow liquid

¹H NMR   (CDCl$_3$, 500 MHz): δ(ppm) = 1.37 (s, 3 H, H$_{13,14}$), 1.43 (s, 3 H, H$_{13,14}$), 3.35 (dd, J = 12.8, 6.0 Hz, 1 H), 3.38–3.44 (m, 1 H), 3.48 (d, J = 1.9 Hz, 3 H, H$_{14}$), 3.49–3.65 (m, 4 H), 3.74 (ddd, J = 8.3, 7.5, 6.3 Hz, 1 H), 4.06 (ddd, J = 8.2, 6.4, 0.9 Hz, 1 H), 4.23–4.31 (m, 1 H, H$_5$). (*Assignments according to [79], measured in CDCl$_3$*)

¹³C NMR   (CDCl$_3$, 126 MHz): δ(ppm) = 24.68 (C$_{13,14}$), 26.05 (C$_{13,14}$), 50.72 (C$_6$), 57.26, 65.93 (2x), 69.93 (2x), 71.86 (2x), 73.92 (2x), 78.50 (2x), 108.75.

HR MS-ESI   *m/z* [**5a** + Na]$^+$ Calc. 268.1292, Found 268.1323

6.2.1.11 Synthesis of propylene glycol (1-azido-2-methoxypropanol) ether (5b)

5a

$C_{10}H_{19}N_3O_4$
245.18

5b

$C_7H_{15}N_3O_4$
205.21
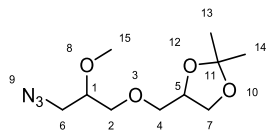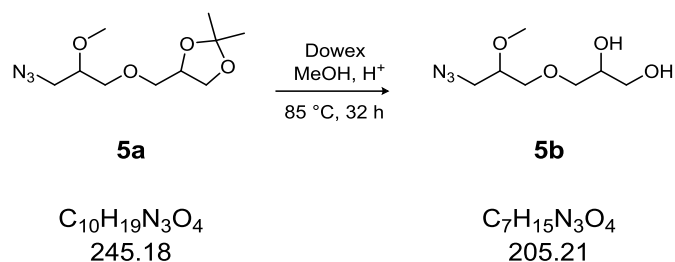
Reagents	5.60 g (22.6 mmol)	1,2-Isopropylidene glyceryl (1-azido-2-methoxypropanol) ether **(5a)**
	30.0 g	Dowex W50X8
	300 mL	MeOH (80**%**)

Preparation

5a was stirred with Dowex (20 g) in MeOH (150 mL) and refluxed at 85 °C for 16 h. After the mixture had cooled down to room temperature, the ionic exchange material was filtered and the filtrate was concentrated. Then, the residue was treated again with Dowex (10 g) in MeOH (150 mL) and the reaction was repeated.

Yield	4.00 g (19.7 mmol) 87**%**
Appearance	dark orange oil
¹H NMR	(CDCl₃, 500 MHz): δ(ppm) = 2.39 (s, 2 H), 3.36 (d, J = 5.9 Hz, 1 H), 3.40 (ddd, J = 12.9, 4.3, 2.1 Hz, 1 H), 3.46 (d, J = 0.9 Hz, 3 H, H₁₂), 3.50 (q, J = 4.8 Hz, 1 H), 3.52–3.64 (m, 5 H), 3.70 (ddd, J = 11.4, 3.9, 2.3 Hz, 1 H), 3.85–3.90 (m, 1 H).
¹³C NMR	(CDCl₃, 126 MHz): δ(ppm) = 51.3 (C₆), 58.0 (2x), 36.9, 70.6 (2x), 70.7, 73.3, 79.3 (2x).
HR MS-ESI	*m/z* [**5b** + Na]⁺ Calc. 228.0992, Found 228.0968

6.2.1.12   Synthesis of propylene glycol (1-amino-2-methoxypropanol) ether (5c)

5b

$C_7H_{15}N_3O_4$
205.21

5c

$C_7H_{17}NO_4$
179.22
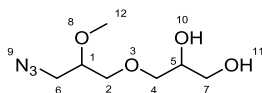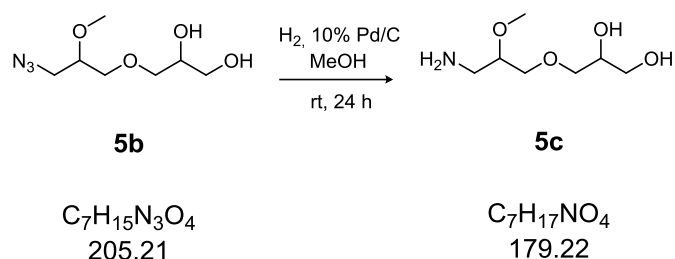
Reagents	4.00 g (19.5 mmol)	Propylene glycol (1-azido-2-methoxypropanol) ether (**5b**)
	0.40 g	10% Pd/C
	50 mL	MeOH

Preparation

10% Pd/C was added to a solution of **5b** in MeOH. The reaction mixture was stirred under hydrogen atmosphere for 24 h. After double-filtration of the catalyst, the filtrate was concentrated under reduced pressure.

Yield	3.50 g (19.5 mmol) 99%
Appearance	light yellow oil
^{1}H NMR	(CDCl$_3$, 500 MHz): δ(ppm) = 2.56 (s, 4 H), 2.80 (ddd, J = 13.1, 5.6, 2.4 Hz, 1 H), 2.89 (dd, J = 4.5, 2.5 Hz, 1 H), 3.33 (t, J = 5.1 Hz, 1 H), 3.41 (s, 3 H, H$_{12}$), 3.48–3.66 (m, 6 H), 3.81–3.87 (m, 1 H).
^{13}C NMR	(CDCl$_3$, 126 MHz): δ(ppm) = 42.3 (C$_6$), 57.7 (2x), 63.8, 70.6 (2x), 70.8, 70.9 (2x), 80.6 (2x).
HR MS-ESI	m/z [**5c** + H]$^+$ Calc. 180.2272, Found 180.1415 m/z [**5c** + Na]$^+$ Calc. 202.2092, Found 202.1084
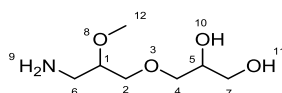
6.2.2 General procedure for the synthesis of bpa ligands

Pyridine-2-aldehyde and acetic acid were added to a solution of dry THF/MeOH and the respective amino ether (**1a**, **2d**, **3e**, **4b**, **5c**) under argon atmosphere. Subsequently sodium triacetoxy borohydride was added to the mixture. The reaction mixture was stirred at room temperature for 48 h. The solvent was removed under reduced pressure. The residue was dissolved in DCM and washed with a saturated aqueous $NaHCO_3$ solution (2 x 100 mL). The organic phase was dried over Na_2SO_4, filtered and evaporated under reduced pressure.

6.2.2.1   Synthesis of 1b

1a

C$_6$H$_5$NO   C$_4$H$_{11}$NO$_2$ C$_{16}$H$_{21}$N$_3$O$_2$
107.11   105.14   287.36
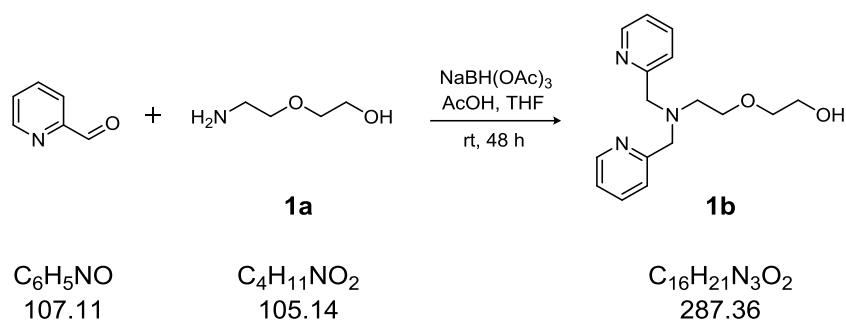
Reagents   4.50 g (42.1 mmol)   Pyridine-2-aldehyde

2.21 g (21.0 mmol)   2-(2-Aminoethoxy)ethanol (**1a**)

11.9 g (56.0 mmol)   Sodium triacetoxyborohydride

2.53 g (42.1 mmol)   Acetic acid

100 mL   dry THF

Preparation

Pyridine-2-aldehyde, **1a**, sodium triacetoxy borohydride, acetic acid and 100 mL THF
were used for the synthetic procedure of **1b**.

Yield   4.60 g (16.0 mmol) 76**%**   **Lit.**[58] 79**%**

Appearance   dark yellow oil

¹H NMR   (CDCl$_3$, 500 MHz): δ(ppm) = 2.84 (t, J = 5.0 Hz, 2 H, H$_2$), 3.53
                 (dd, J = 5.0, 3.8 Hz, 2 H, H$_5$), 3.64–3.68 (m, 2 H, H$_6$), 3.71 (dd, J
                 = 5.0, 3.8 Hz, 2 H, H$_3$), 3.96 (s, 4 H, H$_{9,11}$), 7.17 (ddd, J = 7.4,
                 4.9, 1.1 Hz, 2 H, H$_{15,20}$), 7.56 (d, J = 7.8 Hz, 2 H, H$_{13,22}$), 7.67 (td,
                 J = 7.7, 1.8 Hz, 2 H, H$_{14,21}$), 8.53 (ddd, J = 4.9, 1.7, 0.9 Hz, 2 H,
                 H$_{16,19}$). (*Assignments according to [58], measured in DMSO-d$_6$*)

6.2.2.2   Synthesis of 2e

2d

C$_6$H$_5$NO   C$_5$H$_{13}$NO$_2$
107.11   119.16

C$_{17}$H$_{23}$N$_3$O$_2$
301.39
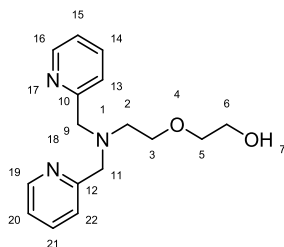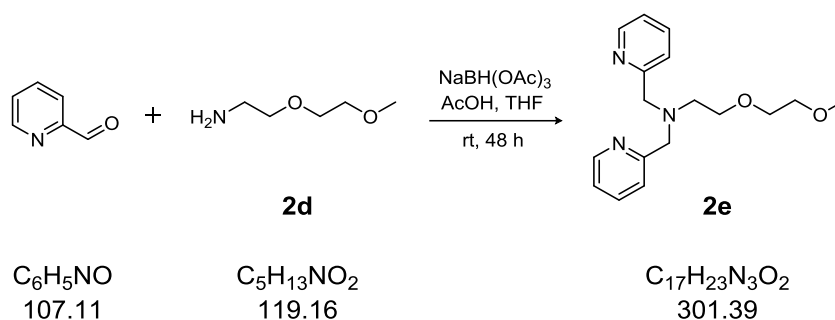
Reagents	1.80 g (16.8 mmol)	2-Pyridinecarboxaldehyde
	1.00 g (8.39 mmol)	2-(2-Methoxyethoxy)ethylamine (**2d**)
	4.73 g (22.3 mmol)	Sodium triacetoxyborohydride
	1.00 g (16.8 mmol)	Acetic acid
	25 mL	dry THF

Preparation

Pyridine-2-aldehyde, **2d**, sodium triacetoxy borohydride, acetic acid and 25 mL THF were used for the synthetic procedure of **2e**.

Yield	1.81 g (6.0 mmol) 71**%**
Appearance	dark brown oil
^{1}H NMR	(CDCl$_3$, 500 MHz): δ(ppm) = 2.86 (t, J = 6.1 Hz, 2 H, H$_2$), 3.37 (s, 3 H, H$_8$), 3.50–3.54 (m, 2 H), 3.55–3.58 (m, 2 H), 3.65 (t, J = 6.1 Hz, 2 H), 3.92 (s, 4 H, H$_{9,11}$), 7.12–7.18 (m, 2 H, H$_{15,20}$), 7.58 (d, J = 7.8 Hz, 2 H, H$_{13,22}$), 7.65 (td, J = 7.6, 1.8 Hz, 2 H, H$_{14,21}$), 8.53 (d, J = 5.8 Hz, 2 H, H$_{16,19}$). (*Assignments according to **1b** in [58], measured in DMSO-d$_6$*)
^{13}C NMR	(CDCl$_3$, 126 MHz): δ(ppm) = 53.6, 59.1, 61.0, 69.6, 70.3, 72.0, 121.9 (C$_{13,22}$), 122.9 (C$_{15,20}$), 136.4 (C$_{14,21}$), 149.0 (C$_{16,19}$), 159.9 (C$_{10,12}$). (*Assignments according to **1b** in [58], measured in DMSO-d$_6$*)
HR MS-ESI	*m/z* [**2e** + H]$^+$ Calc. 302.1873, Found 302.1880

6.2.2.3   Synthesis of 3f

3e

C$_6$H$_5$NO
107.11

C$_6$H$_{15}$NO$_4$
165.19

3f

C$_{18}$H$_{25}$N$_3$O$_4$
347.41
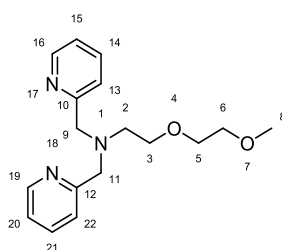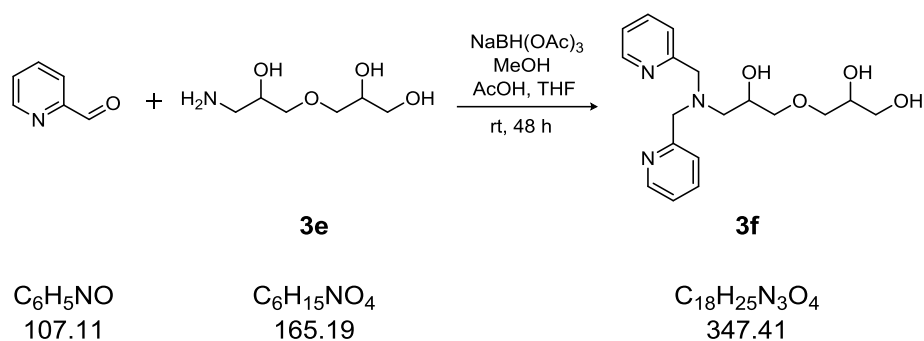
| **Reagents**	6.30 g (58.9 mmol)	2-Pyridinecarboxaldehyde
	4.86 g (29.4 mmol)	Propylene glycol (1-amino-2-propanol) ether (**3e**)
	16.6 g (78.3 mmol)	Sodium triacetoxyborohydride
	3.53 g (58.9 mmol)	Acetic acid
	10 mL	MeOH
	100 mL	Dry THF

Preparation

Pyridine-2-aldehyde, **3e**, sodium triacetoxy borohydride, acetic acid, MeOH and 100 mL THF were used for the synthetic procedure of **3f.** The residue was dissolved in water and a pH of 3 was adjusted with 2 M HCl. After extraction with DCM (5 x 100 mL), the aqueous phase was neutralized with 2 M NaOH until a pH of 7 was reached. The solution was evaporated under reduced pressure. The residue was dissolved in 2-propanol and NaCl was removed by filtration. After removal of the solvent, the residue was dried under reduced pressure overnight.

Yield	0.40 g (1.16 mmol) **4%**

Appearance	dark brown oil

¹H NMR	(CDCl$_3$, 500 MHz): δ(ppm) = 3.23–3.31 (m, 1 H), 3.36 (d, *J* = 5.6 Hz, 2 H), 3.37–3.43 (m, 1 H), 3.56 (dtd, *J* = 17.2, 5.9, 2.1 Hz, 3 H), 3.64 (td, *J* = 11.4, 10.4, 4.1 Hz, 3 H), 3.67–3.78 (m, 2 H), 3.84–3.91 (m, 1 H), 4.46–4.75 (m, 4 H), 7.27 (dd, *J* = 7.5, 5.0 Hz, 2 H, H$_{15,20}$), 7.58–7.64 (m, 2 H, H$_{13,22}$), 7.74 (td, *J* = 7.6, 1.6 Hz, 2 H, H$_{14,21}$), 8.58 (dt, *J* = 5.1, 2.6 Hz, 2 H, H$_{16,19}$). (*Assignments according to **1b** in [58], measured in DMSO-d$_6$*)

¹³C NMR   (CDCl₃, 176 MHz): δ(ppm) = 55.6 (2x), 57.4, 59.0, 59.1, 63.6 (2x), 70.3, 70.5, 70.7 (2x), 73.2, 73.6, 76.0, 123.7 (2x), 124.6 (2x), 137.9, 148.9 (2x).

HR MS-ESI   *m/z* [**3f** + H]⁺ Calc. 348.1872, Found 348.2016
                         m/z [**3f** + Na]⁺ Calc. 370.1692, Found 370.1837

6.2.2.4 Synthesis of 4c

4b   **4c**

C$_6$H$_5$NO   C$_9$H$_{21}$NO$_4$ C$_{21}$H$_{31}$N$_3$O$_4$
107.11   207.27   389.50
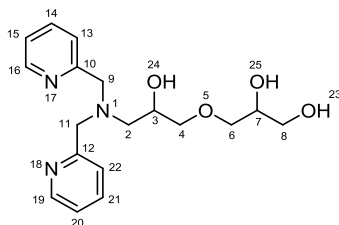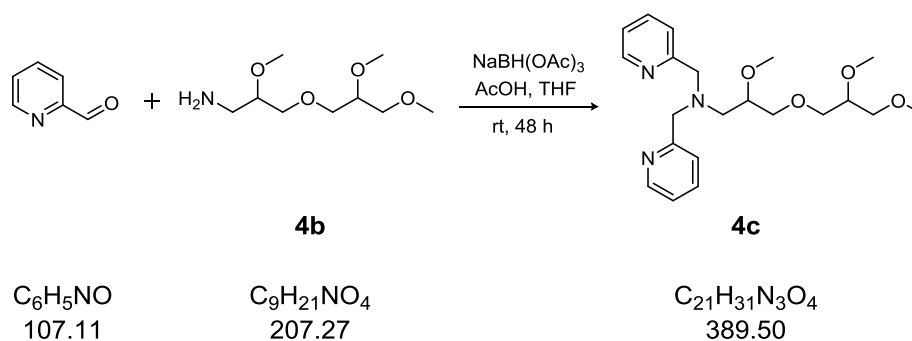
Reagents   0.53 g (4.96 mmol)   2-Pyridinecarboxaldehyde

0.51 g (2.48 mmol)   1,2-Methoxy propylidene (1-amino-2-
methoxypropanol) ether (**4b**)

1.40 g (6.60 mmol)   Sodium triacetoxyborohydride

0.30 g (4.96 mmol)   Acetic acid

15 mL   Dry THF

Preparation

Pyridine-2-aldehyde, **4b**, sodium triacetoxy borohydride, acetic acid and 15 mL THF
were used for the synthetic procedure of **4c**.

**Yield**   0.94 g (2.42 mmol) 98**%**

Appearance   dark yellow oil

¹H NMR   (CDCl$_3$, 500 MHz): δ(ppm) = 3.29 (d, J = 3.7 Hz, 3 H), 3.32 (d, J
= 5.6 Hz, 2 H), 3.36 (s, 3 H, H$_{Me}$), 3.37 (s, 3 H, H$_{Me}$), 3.38–3.52
(m, 8 H), 3.84 (d, J = 2.6 Hz, 4 H), 7.10 (ddd, J = 7.4, 4.9, 1.1 Hz,
2 H, H$_{15,20}$), 7.49 (d, J = 7.7 Hz, 2 H, H$_{13,22}$), 7.61 (td, J = 7.7, 1.8
Hz, 2 H, H$_{14,21}$), 8.47 (dd, J = 5.8, 1.7 Hz, 2 H, H$_{16,19}$).
(*Assignments according to **1b** in [58], measured in DMSO-d$_6$*)

¹³C NMR   (CDCl$_3$, 126 MHz): δ(ppm) = 55.2, 57.8 (2x), 58.0 (2x), 59.3,
61.3, 71.0, 72.4, 79.2, 121.8, 122.0, 123.0, 127.9, 136.4, 137.1,
149.0, 150.3, 159.8.

HR MS-ESI   *m/z* [**4c** + H]⁺ Calc. 390.2373, Found 390.2940
m/z [**4c** + Na]⁺ Calc. 412.2192, Found 412.2334

6.2.2.5 Synthesis of 5d

C6H5NO	C7H17NO4	C19H27N3O4
107.11	179.22	361.44

C_6H_5NO — 107.11

$C_7H_{17}NO_4$ — 179.22

$C_{19}H_{27}N_3O_4$ — 361.44

Reagents

4.19 g (39.1 mmol)	2-Pyridinecarboxaldehyde
3.51 g (19.6 mmol)	Propylene glycol (1-amino-2-methoxy propanol) ether (**5c**)
11.0 g (52.1 mmol)	Sodium triacetoxyborohydride
2.35 g (39.1 mmol)	Acetic acid
100 mL	Dry THF

Preparation

Pyridine-2-aldehyde, **5c**, sodium triacetoxy borohydride, acetic acid and 100 mL THF were used for the synthetic procedure of **5d.** Additional work-up of the residue was performed as described in the synthesis of **3f**.

Yield 1.14 g (3.15 mmol) 16**%**

Appearance dark brown oil

^{1}H NMR (CDCl$_3$, 500 MHz): δ(ppm) = 3.23–3.31 (m, 1 H), 3.36 (d, J = 5.6 Hz, 3 H, H$_{26}$), 3.37–3.43 (m, 1 H), 3.56 (dtd, J = 17.2, 5.9, 2.1 Hz, 4 H), 3.64 (td, J = 11.4, 10.4, 4.1 Hz, 3 H), 3.67–3.78 (m, 2 H), 3.84–3.91 (m, 1 H), 4.46–4.75 (m, 4 H), 7.27 (dd, J = 7.5, 5.0 Hz, 2 H, H$_{15,20}$), 7.58–7.64 (m, 2 H, H$_{13,22}$), 7.74 (td, J = 7.6, 1.6 Hz, 2 H, H$_{14,21}$), 8.58 (dt, J = 5.1, 2.6 Hz, 2 H, H$_{16,19}$). (*Assignments according to 1b in [58], measured in DMSO-d$_6$*)

^{13}C NMR (CDCl$_3$, 176 MHz): δ(ppm) = 55.6 (2x), 57.5, 59.1 (2x), 63.6 (2x), 70.4, 70.6, 70.7 (2x), 73.3, 73.6, 76.1, 123.7 (2x), 124.7 (2x), 137.9, 148.9 (2x).

HR MS-ESI *m/z* [**5d** + H]$^+$ Calc. 362.2073, Found 362.2257
m/z [**5d** + Na]$^+$ Calc. 384.1892, Found 384.2049

6.2.3 General procedure for the synthesis of bpa copper(II) complexes

6a–b: $Cu(NO_3)_2 \cdot 3\ H_2O$ was added to a solution of the bpa ligand (**1b,2e**) in EtOH and the reaction mixture was refluxed for 1 h. Upon addition of the metal salt, the solution turned deep blue. The reaction mixture was filtered into a vial and allowed to cool to room temperature. The vial was placed in a screw-capped container (100 mL), filled with diethyl ether (10 mL) and closed. After standing overnight at room temperature the precipitated product was washed with hexane and diethyl ether and dried under reduced pressure.

7a–e: A solution of $Cu(ClO_4)_2 \cdot 6\ H_2O$ in MeOH was added to a solution of the bpa ligand (**1b**, **2e**, **3f**, **4c**, **5d**) in MeOH and the reaction mixture was stirred for 2 h at room temperature. Upon addition of the metal salt, the solution turned deep blue. Diethyl ether was added to the mixture and the flask was cooled at -40 °C for 5 hours. After removal of the clear solution the residue was dried under reduced pressure.

6.2.3.1   Complex 6a

1b
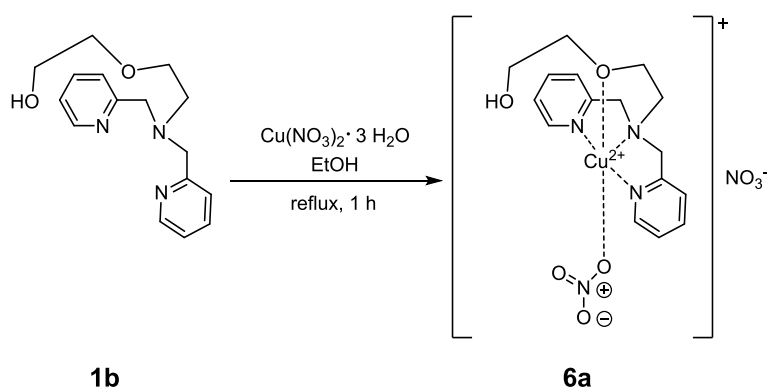
C₁₆H₂₁N₃O₂
287.16

$C_{16}H_{21}N_3O_2$
287.16

6a

$C_{16}H_{21}CuN_5O_8$
474.92

Reagents	0.42 g (1.47 mmol)	**1b**
	0.35 g (1.47 mmol)	$Cu(NO_3)_2 \cdot 3\ H_2O$
	10 mL	EtOH

Yield   0.24 g (0.51 mmol) 35**%**   **Lit.**[58] 45**%**

Appearance   blue solid

HR MS-ESI   *m/z* [[Cu(**1b**)] - H]⁺ Calc. 349.0857, Found 349.0903

m/z $[[Cu(\mathbf{1b})] - H]^+$ Calc. 349.0857, Found 349.0903

EA (%)   for **6a** $C_{16}H_{21}CuN_5O_8$
Calc. C   40.47   H   4.46   N   14.75
Found C   40.20   H   4.49   N   14.73

6.2.3.2   Complex 6b

2e

C$_{17}$H$_{23}$N$_3$O$_2$
301.39

6b
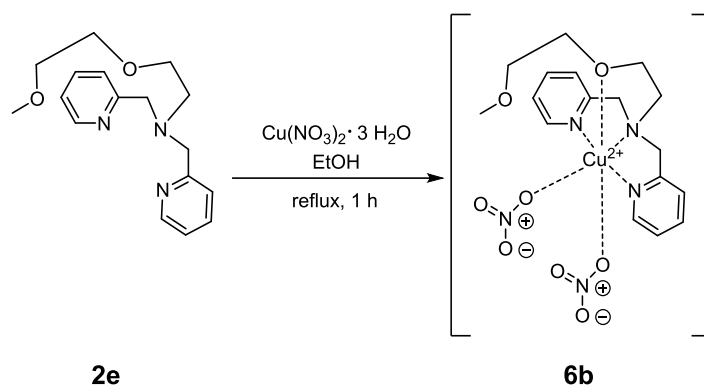
C$_{17}$H$_{23}$CuN$_5$O$_8$
488.94

Reagents	0.54 g (1.79 mmol)	**2e**
	0.43 g (1.79 mmol)	Cu(NO$_3$)$_2$ • 3 H$_2$O
	10 mL	EtOH

Yield   0.26 g (0.54 mmol) 30**%**

Appearance   blue solid

HR MS-ESI   *m/z* [[Cu(**2e**)]]$^+$ Calc. 364.1086, Found 364.1138

EA (%)   for **6b** C$_{17}$H$_{23}$CuN$_5$O$_8$
Calc. C 41.76   H 4.74   N 14.32
Found C 41.76   H 4.85   N 14.02

6.2.3.3   Complex 7a

1b

C$_{16}$H$_{21}$N$_3$O$_2$
287.16

7a

C$_{16}$H$_{23}$Cl$_2$CuN$_3$O$_{11}$
567.82
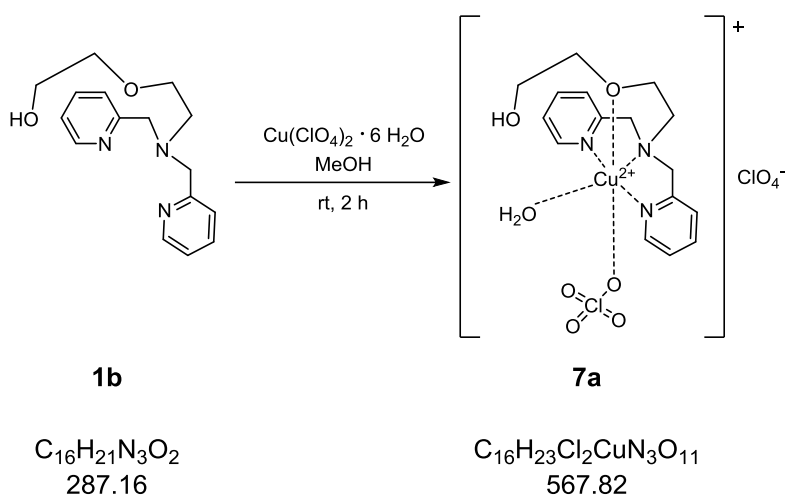
Reagents   0.10 g (0.35 mmol)   **1b**

0.13 g (0.35 mmol)   Cu(ClO$_4$)$_2$ • 6 H$_2$O

3 mL   MeOH

Yield   67.6 mg (0.12 mmol) 34**%**

Appearance   blue solid

HR MS-ESI   *m/z* [[Cu(**1b**)] - H]$^+$ Calc. 349.0857, Found 349.0846

EA (%)   for **7a** C$_{16}$H$_{23}$Cl$_2$CuN$_3$O$_{11}$
Calc. C   33.84   H   4.08   N   7.40
Found C   34.07   H   3.76   N   7.35

6.2.3.4   Complex 7b

2e

$C_{17}H_{23}N_3O_2$
301.39

7b

$C_{18}H_{29}Cl_2CuN_3O_{12}$
613.89
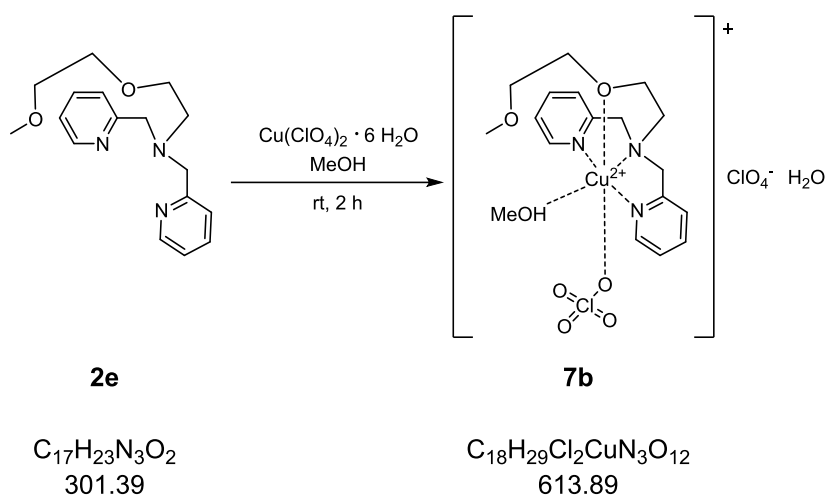
Reagents   0.08 g (0.28 mmol)   **2e**

0.10 g (0.28 mmol) $Cu(ClO_4)_2 \cdot 6\ H_2O$

3 mL   MeOH

Yield   36.1 mg (0.06 mmol) 21**%**

Appearance   dark green solid

HR MS-ESI   *m/z* [[Cu(**2e**)]]$^+$ Calc. 364.1086, Found 364.1094

EA (%)   for **7b** $C_{18}H_{29}Cl_2CuN_3O_{12}$

	C		H		N	
Calc.	C	35.22	H	4.76	N	6.84
Found	C	35.55	H	4.47	N	6.76

6.2.3.5   Complex 7c

3f	**7c**
$C_{18}H_{25}N_3O_4$	$C_{19}H_{29}Cl_2CuN_3O_{13}$
347.41	641.90
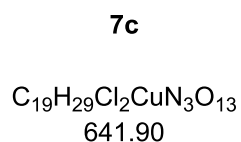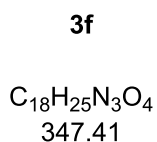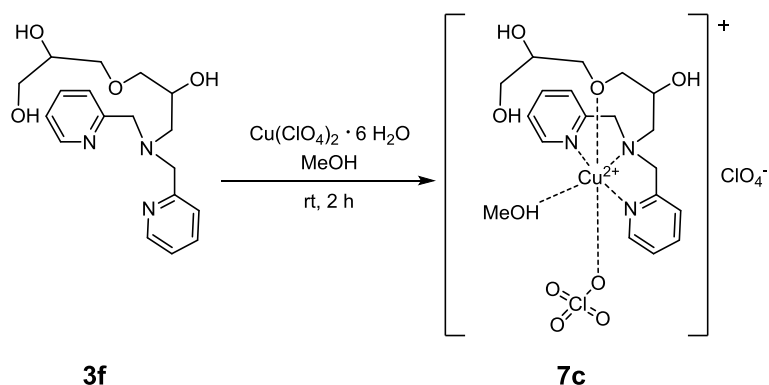
Reagents   0.08 g (0.23 mmol)   **3f**

0.09 g (0.23 mmol) $Cu(ClO_4)_2 \cdot 6\ H_2O$

3 mL   MeOH

Yield   56.1 mg (0.09 mmol) 40**%**

Appearance   dark blue-green solid

HR MS-ESI   *m/z* [[Cu(**3f**)] - H]$^+$ Calc. 409.1068, Found 409.1111

EA (%)   for **7c** $C_{19}H_{29}Cl_2CuN_3O_{13}$
                      Calc. C 35.55   H 4.55   N 6.55
                      Found C 35.69   H 4.28   N 6.69

6.2.3.6   Complex 7d
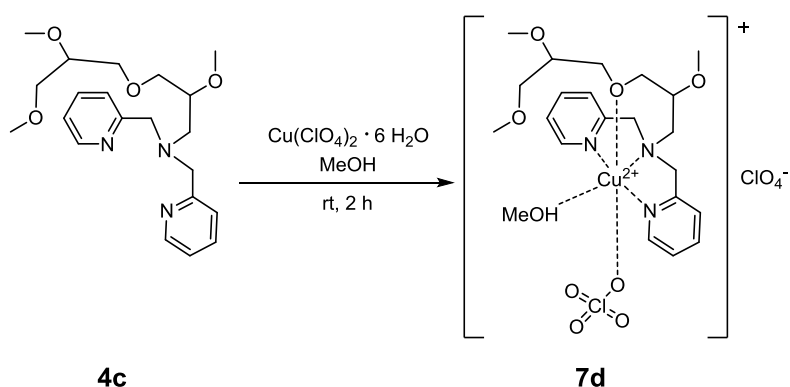
4c	7d
C$_{21}$H$_{31}$N$_3$O$_4$	C$_{22}$H$_{35}$Cl$_2$CuN$_3$O$_{13}$
389.50	683.98

Reagents   0.13 g (0.33 mmol)   **4c**

0.12 g (0.33 mmol)   Cu(ClO$_4$)$_2$ • 6 H$_2$O

3 mL   MeOH

Yield   84.5 mg (0.12 mmol) 38**%**

Appearance   dark blue-green solid

HR MS-ESI   *m/z* [[Cu(**4c**)]]$^+$ Calc. 452.1611, Found 452.1727

EA (%)   for **7d** C$_{22}$H$_{35}$Cl$_2$CuN$_3$O$_{13}$
Calc. C   38.63   H   5.16   N   6.14
Found C   38.57   H   5.43   N   6.26

6.2.3.7 Complex 7e
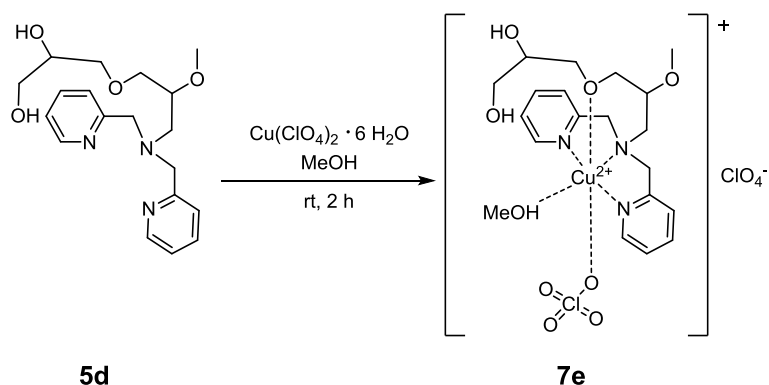
5d

C$_{19}$H$_{27}$N$_3$O$_4$
361.44

7e

C$_{20}$H$_{31}$Cl$_2$CuN$_3$O$_{13}$
655.92

Reagents	0.08 g (0.27 mmol)	**5d**
	0.10 g (0.27 mmol)	Cu(ClO$_4$)$_2$ • 6 H$_2$O
	3 mL	MeOH

Yield   68.4 mg (0.10 mmol) 39**%**

Appearance   dark blue-green solid

HR MS-ESI   *m/z* [[Cu(**5d**)] - H]$^+$ Calc. 423.1225, Found 423.1287

EA (%)   for **7e** C$_{20}$H$_{31}$Cl$_2$CuN$_3$O$_{13}$
Calc.   C   36.62   H   4.76   N   6.41
Found C   36.76   H   4.83   N   6.36

6.3 Synthesis of bpa estrogen derivatives

6.3.1 Synthesis of 1c

1b

$C_{16}H_{21}N_3O_2$
287.36

1c

$C_{20}H_{25}N_3O_5$
387.44
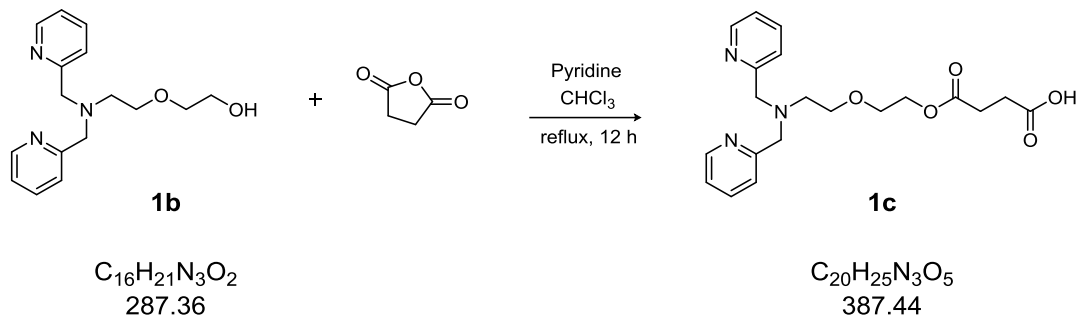
Reagents	8.68 g (30.2 mmol)	**1b**
	15.1 g (151 mmol)	Succinic anhydride
	25 mL	$CHCl_3$
	5 mL	Pyridine

Preparation

1b and succinic anhydride were dissolved in $CHCl_3$. After addition of pyridine, the mixture was stirred under reflux overnight. The solvent was removed under reduced pressure. The residue was dissolved in water and washed with ether. Afterwards, the aqueous phase was extracted with $CHCl_3$. The collected organic phase was dried over Na_2SO_4, filtered and evaporated under reduced pressure.

Yield	5.47 g (14.1 mmol) 47**%**
Appearance	dark green oil
^{1}H NMR	(CDCl$_3$, 500 MHz): δ(ppm) = 2.64–2.57 (m, 4 H), 2.89 (t, J = 5.4 Hz, 2 H, H$_2$), 3.61–3.68 (m, 4 H, H$_{3,6}$), 4.00 (s, 4 H, H$_{9,11}$), 4.26 (m, 2 H), 7.20 (ddd, J = 7.4, 5.1, 1.0 Hz, 2 H, H$_{15,20}$), 7.56 (d, J = 7.8 Hz, 2 H, H$_{13,22}$), 7.70 (td, J = 7.7, 1.8 Hz, 2 H, H$_{14,21}$), 8.54 (ddd, J = 5.0, 1.7, 0.8 Hz, 2 H, H$_{16,19}$), 12.17 (s, 1 H, H$_{28}$). (*Assignments according to **1b** in [58], measured in DMSO-d$_6$*)
HR MS-ESI	*m/z* [**1c** + H]$^+$ Calc. 388.1873, Found 388.2153 *m/z* [**1c** + Na]$^+$ Calc. 410.1692, Found 410.1871
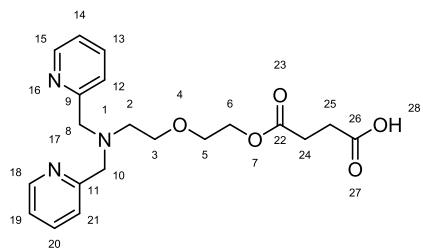
6.3.2   Synthesis of estrone-3-succinate-bpa (8b)

1c	**8a**	**8b**
$C_{20}H_{25}N_3O_5$	$C_{18}H_{22}O_2$	$C_{38}H_{45}N_3O_6$
387.43	270.37	639.79
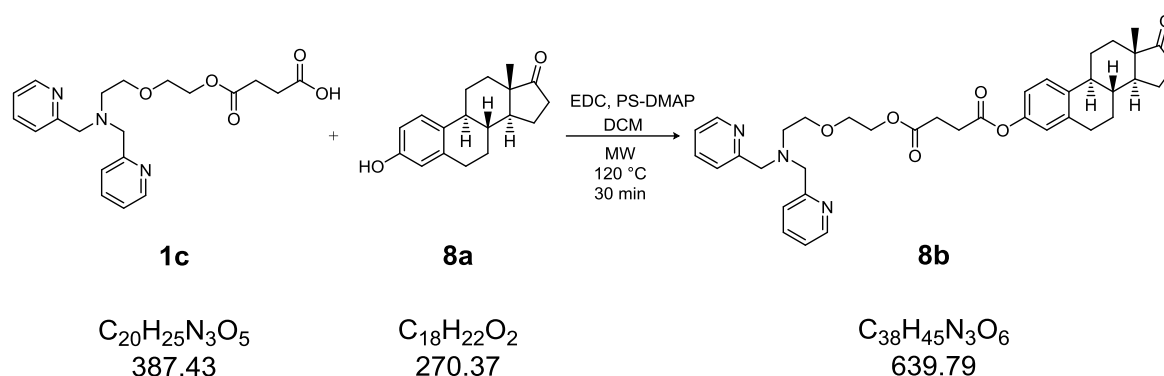
Reagents

0.414 g (1.07 mmol)	**1c**
0.289 g (1.07 mmol)	Estrone (**8a**)
0.401 g (2.14 mmol)	EDC
0.178 g (0.53 mmol)	PS-DMAP
10 mL	Dry DCM

Preparation

Estrone (**8a**), **1c**, PS-DMAP and EDC were suspended in DCM in a 30 mL glass vial equipped with a small magnetic stirring bar. The vial was tightly sealed with a teflon-coated silicone crimp top. The mixture was microwave heated for 30 minutes at 120 °C. After cooling the mixture, the resin was removed by filtration and washed with $CHCl_3$. The filtrate was washed with brine (3 x 100 mL). The combined organic phase was dried over Na_2SO_4, filtered and evaporated under reduced pressure. The pure product was obtained by column chromatography (SiO_2, 30:1:0.3 $CHCl_3$/MeOH/isopropylamine).

Yield	66.5 mg (0.10 mmol) 10**%**

Appearance	brown oil

HR MS-ESI m/z [**8b** + H]$^+$ Calc. 640.3373, Found 640.3425
                         m/z [**8b** + Na]$^+$ Calc. 662.3192, Found 662.3274

EA (%)   for **8b** $C_{38}H_{45}N_3O_6 \cdot 2.5\ H_2O$

Calc.	C	66.65	H	7.36	N	6.14
Found	C	66.67	H	7.40	N	6.28

148
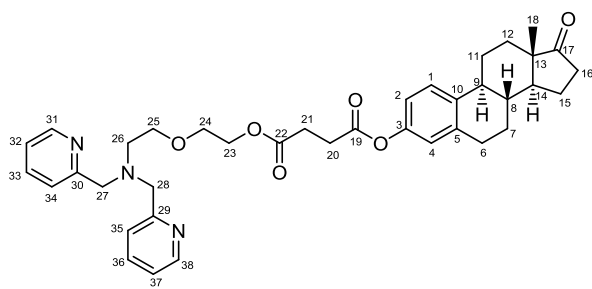
Table 6.1: *Chemical shifts of **8b**.*

Position	δH	δC	DEPT	COSY	HMBC	HMQC
1	7.25 s	126.4	126.4 (CH)	2		1
2	6.83 – 6.87 m	118.8	118.8 (CH)	1	2, 4	2
3	-	148.6	C$_q$		2, 4	
4	6.81 d, *J* = 7.4 Hz	121.6	121.6 (CH)		2, 4	4
5	-	138.1	C$_q$		1	
6α	2.72 t, *J* = 6.9 Hz	29.5	29.5 (CH$_2$)	26	6α, 6β	6α, 6β
6β	2.72 t, *J* = 6.9 Hz			26		
7α	1.94 – 2.08 m	26.5	26.5 (CH$_2$)			7α, 7β
7β	1.94 – 2.08 m					
8	1.40 – 1.66 m	38.1	38.1 (CH)			8
9	2.23 – 2.31 m	44.3	44.3 (CH)		1	9
10	-	137.6	C$_q$		2,4	
11α	2.34 – 2.43 m	25.9	25.9 (CH$_2$)			11α, 11β
11β	1.40 – 1.66 m					
12α	1.40 – 1.66 m	31.7	31.7 (CH$_2$)		18	12α, 12β
12β	1.94 – 2.08 m					
13	-	48.1	C$_q$		11β, 12α, 14, 18	
14	1.40 – 1.66 m	50.6	50.6 (CH)		16α, 18	14
15α	1.40 – 1.66 m	21.7	21.7 (CH$_2$)		12β, 16α, 16β, 18	15α, 15β
15β	1.40 – 1.66 m					
16α	2.50 dd, *J* = 19.3, 8.5	36.0	36.0 (CH$_2$)			16α, 16β
16β	2.14 dt, *J* = 18.9, 9.0					
17	-	220.9	C$_q$			
18	0.90 s	14.0	14.0 (CH$_3$)		11β, 12α, 14	18
19	-	172.3	C$_q$		6α, 6β, 20/21, 23, 26	
20	2.80 – 2.92 m	29.4	29.4 (CH$_2$)			20
21	2.80 – 2.92 m	29.2	29.2 (CH$_2$)			21
22	-	171.3	C$_q$		6α, 6β, 20/21, 26	
23	4.22 s	64.1	64.1 (CH$_2$)	24/25	23, 24/25	23
24	3.60 dt, *J* = 16.4, 5.3	69.8	69.8 (CH$_2$)	23, 26	24/25, 26	24
25	3.60 dt, *J* = 16.4, 5.3	68.9	68.9 (CH$_2$)	23, 26	23, 24/25	25
26	2.80 – 2.92 m	53.7	53.7 (CH$_2$)	6α, 6β	24/25, 27/28	26
27/28	3.90 s	61.0	61.0 (CH$_2$)		26, 27/28	27/28
29/30	-	159.8	C$_q$		27/28	
31/38	8.51 d, *J* = 5.6 Hz	149.1	149.1 (CH)	32/37	31/38, 32/37	31/38
32/37	7.13 dd, *J* = 7.4, 6.1 Hz	122.1	122.1 (CH)	31/38, 33/36	31/38, 32/37, 34/35	32/37
33/36	7.64 td, *J* = 7.7, 1.8	136.6	136.6 (CH)	32/37,	31/38, 33/36, 34/35	33/36
34/35	7.52 d, *J* = 7.7 Hz	123.1	123.1 (CH)	33/36	32/37, 33/36, 34/35	34/35

¹H NMR	(CDCl₃, 700 MHz) δ(ppm) = 0.90 (s, 3 H), 1.40–1.66 (m, 6 H), 1.94–2.08 (m, 3 H), 2.14 (dt, *J* = 18.9, 9.0 Hz, 1 H), 2.23–2.31 (m, 1 H), 2.34–2.43 (m, 1 H), 2.50 (dd, *J* = 19.3, 8.5 Hz, 1 H), 2.72 (t, *J* = 6.9 Hz, 2 H), 2.80–2.92 (m, 6 H), 3.60 (dt, *J* = 16.4, 5.3 Hz, 4 H), 3.90 (s, 4 H), 4.22 (s, 2 H), 6.81 (d, *J* = 7.4 Hz, 1 H), 6.83–6.87 (m, 1 H), 7.13 (dd, *J* = 7.4, 6.1 Hz, 2 H), 7.25 (s, 1 H), 7.55 (d, *J* = 7.7 Hz, 2 H), 7.64 (td, *J* = 7.7, 1.8 Hz, 2 H), 8.51 (d, *J* = 5.6 Hz, 2 H).
¹³C NMR	(CDCl₃, 176 MHz) δ(ppm) = 13.96, 21.72, 25.89, 26.46, 29.18, 29.39, 29.51, 31.68, 35.99, 38.13, 44.28, 48.08, 50.57, 53.67, 60.97, 64.08, 68.85, 69.75, 118.79, 121.61, 122.11, 123.12, 126.51, 136.59, 137.56, 138.14, 148.63, 149.07, 159.84, 171.26, 172.26, 220.92.

6.3.3 Synthesis of estradiol-3-succinate-bpa (9b)

1c	9a	9b
$C_{20}H_{25}N_3O_5$	$C_{18}H_{24}O_2$	$C_{38}H_{47}N_3O_6$
387.43	272.18	641.35
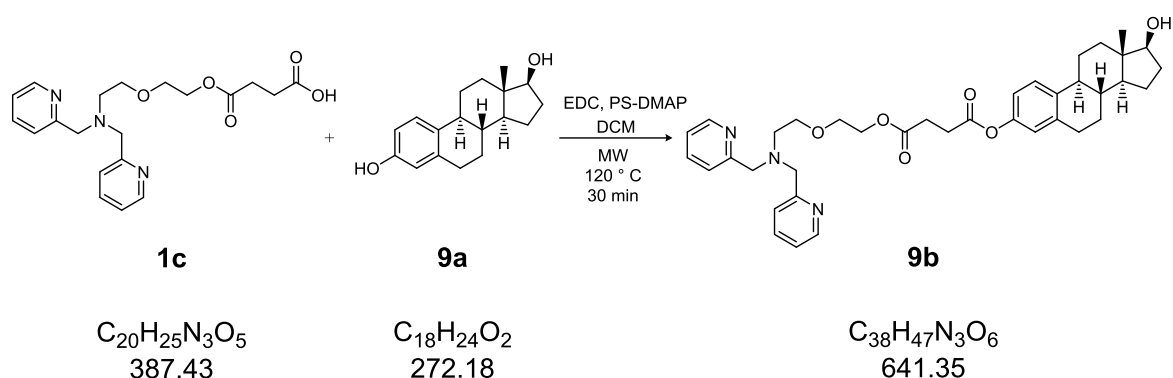
Reagents

0.814 g (2.10 mmol)	**1c**
0.186 g (1.03 mmol)	Estradiol (**9a**)
0.652 g (4.20 mmol)	EDC
0.343 g (1.03 mmol)	PS-DMAP
10 mL	Dry DCM

Preparation

Estradiol (**9a**), **1c**, PS-DMAP and EDC were suspended in DCM in a 30 mL glass vial equipped with a small magnetic stirring bar. The vial was tightly sealed with a teflon-coated silicone crimp top. The mixture was microwave heated for 30 minutes at 120 °C. After cooling the mixture, the resin was removed by filtration and washed with $CHCl_3$. The filtrate was washed with brine (3 x 100 mL). The combined organic phase was dried over Na_2SO_4, filtered and evaporated under reduced pressure. The pure product was obtained by column chromatography (SiO_2, 30:1:0.3 $CHCl_3$/MeOH/isopropylamine).

Yield   64.3 mg (0.10 mmol) 10**%**

Appearance   dark yellow oil

HR MS-ESI   *m/z* [**9b** + H]$^+$ Calc. 642.3573, Found 642.3571
m/z [**9b** + Na]$^+$ Calc. 664.3392, Found 664.3390

EA (%)

for **9b** $C_{38}H_{47}N_3O_6 \cdot 3.5\ H_2O$

	C	H	N
Calc.	64.75	7.72	5.96
Found	64.88	7.87	5.58
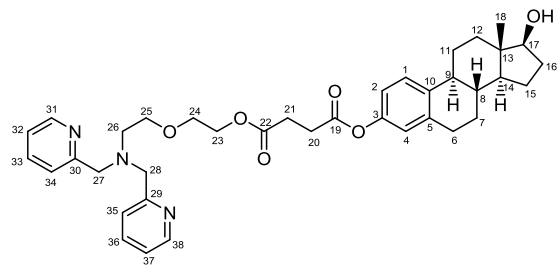
Table 6.2: *Chemical shifts of **9b**.*

Position	δH	δC	DEPT	COSY	HMBC	HMQC
1	7.27 s	126.5	126.4 (CH)	2		1
2	6.84 d, *J* =	118.6	118.6 (CH)	1	2, 4	2
3	-	148.5	C$_q$		2, 4	
4	6.78 – 6.80 m	121.5	121.5 (CH)		2, 4	4
5	-	138.4	C$_q$		1	
6α	2.57 – 2.90 m	30.7	30.7 (CH$_2$)	26		6α, 6β
6β	2.57 – 2.90 m			26		
7α	1.29 – 1.40 m	27.2	27.2 (CH$_2$)			7α, 7β
7β	1.84 – 1.90 m					
8	1.42 – 1.55 m	38.6	38.6 (CH)			8
9	2.18 – 2.24 m	44.3	44.3 (CH)		1	9
10	-	138.1	C$_q$		2,4	
11α	2.29 – 2.34 m	26.3	26.3 (CH$_2$)			11α, 11β
11β	1.42 – 1.55 m					
12α	1.29 – 1.40 m	36.8	36.8 (CH$_2$)		18	12α, 12β
12β	1.92 – 1.97 m					
13	-	43.3	C$_q$		18	
14	1.29 – 1.40 m	50.2	50.2 (CH)		18	14
15α	1.66 – 1.73 m	23.3	23.3 (CH$_2$)			15α, 15β
15β	1.66 – 1.73 m					
16α	2.57 – 2.90 m	29.6	29.6 (CH$_2$)			16α, 16β
16β	2.57 – 2.90 m					
17α		82.0	82.0 (CH)			17α
17β						
18	0.77 s	11.2	11.2 (CH$_3$)		18	18
19	-	172.3	C$_q$		6α, 6β, 16α, 16β, 20/21, 23, 26	
20	2.57 – 2.90 m	29.5	29.5 (CH$_2$)			20
21	2.57 – 2.90 m	29.4	29.4 (CH$_2$)			21
22	-	171.7	C$_q$		6α, 6β, 16α, 16β,	
23	4.10 – 4.26 m	64.1	64.1 (CH$_2$)	24/25	23, 24/25	23
24	3.55 – 3.64 m	69.8	69.8 (CH$_2$)	23, 26		24
25	3.55 – 3.64 m	68.9	68.9 (CH$_2$)	23, 26	23, 24/25	25
26	2.80 – 2.90 m	53.7	53.7 (CH$_2$)	6α, 6β	27/28	26
27/28	3.88 – 3.94 m	61.0	61.0 (CH$_2$)		27/28	27/28
29/30	-	159.9	C$_q$			
31/38	8.51 d, *J* = 1.7 Hz	149.1	149.1 (CH)	32/37	31/38	31/38
32/37	7.11 – 7.17 m	122.1	122.0 (CH)	31/38, 33/36	31/38, 32/37, 34/35	32/37
33/36	7.61 – 7.68 m	136.6	136.6 (CH)	32/37,	31/38, 33/36,	33/36
34/35	7.55 d, *J* =	123.1	123.0 (CH)	33/36	32/37, 33/36,	34/35

¹H NMR (CDCl₃, 700 MHz) δ(ppm) = 0.77 (s, 3 H), 1.29–1.40 (m, 3 H), 1.42–1.55 (m, 4 H), 1.66–1.73 (m, 2 H), 1.84–1.90 (m, 1 H), 1.92–1.97 (m, 1 H), 2.18–2.24 (m, 1 H), 2.29–2.34 (m, 1 H), 2.57–2.74 (m, 5 H), 2.80–2.90 (m, 5 H), 3.55–3.64 (m, 4 H), 3.72 (t, *J* = 8.6 Hz, 1 H), 3.88–3.94 (m, 3 H), 4.10–4.26 (m, 3 H), 6.78–6.80 (m, 1 H), 6.84 (d, *J* = 2.7 Hz, 1 H), 7.11–7.17 (m, 2 H), 7.27 (s, 1 H), 7.55 (d, *J* = 8.1 Hz, 2 H), 7.61–7.68 (m, 2 H), 8.51 (d, *J* = 1.7 Hz, 2 H).

¹³C NMR (CDCl₃, 176 MHz) δ(ppm) = 11.17, 23.26, 26.28, 27.16, 29.35, 29.49, 29.54, 29.65, 30.72, 32.28, 36.81, 38.61, 43.34, 44.27, 50.21, 53.65, 60.96, 64.08, 68.85, 69.77, 76.98, 77.16, 77.34, 81.99, 118.60, 121.53, 122.08, 123.09, 126.50, 136.55, 138.14, 138.16, 138.38, 148.49, 149.11, 159.91, 171.75, 172.26.

6.3.4 *In situ* complex formation of bpa derivatives

For the cleavage activity and cytotoxicity studies complexes of **1b**, **1c**, **8b** and **9b** were generated *in situ* in 20**%** DMSO solution. $Cu(NO_3)_2 \bullet 3\,H_2O$ was applied as metal salt for the formation of the corresponding complexes **1b + Cu**, **1c + Cu**, **8b + Cu** and **9b + Cu**. *In situ* complex solutions were prepared according to the ratio of 0.9:1 (metal salt solution : ligand solution) to ensure that effects regarding both DNA cleavage and cytotoxicity which possibly originate from free metal ions can be excluded.

6.4 Synthesis of phenanthroline derivatives

6.4.1 Synthesis of phenanthroine ligands

6.4.1.1 Synthesis of 5-nitro-1,10-phenanthroline (10b)

10a

$C_{12}H_8N_2$
180.21

10b

$C_{12}H_7N_3O_2$
225.20
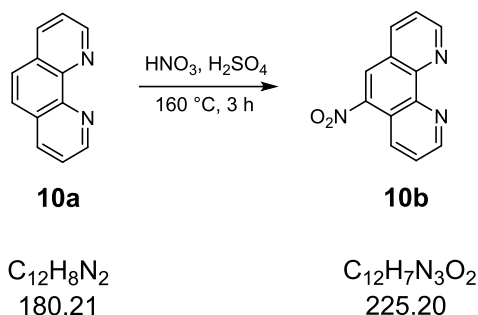
| **Reagents**	3.50 g (19.42 mmol)	1,10-Phenanthroline (**10a**)
	38.1 g (388.5 mmol)	Sulfuric acid
	15.9 g (232.5 mmol)	Nitric acid

Preparation

To a stirred solution of 1,10-phenanthroline (**10a**) in concentrated sulfuric acid, fuming nitric acid was added dropwise at 160 °C. The reaction mixture was kept at 160 °C for 3 h, and subsequently poured into ice-cold water. Then saturated aqueous NaOH was added to this solution to adjust the pH to 3, and a yellow solid precipitated. The precipitate was filtered off, washed with water and dried under reduced pressure.

Yield	3.3 g (14.7 mmol) 76**%**	**Lit.**[62] 99**%**

Appearance	yellow solid

^{1}H NMR (CDCl$_3$, 400 MHz): δ(ppm) = 7.76 (ddd, J = 15.3, 8.4, 4.3 Hz, 2 H, H$_{9,12}$), 8.38 (dd, J = 8.1, 1.8 Hz, 1 H, H$_{10}$), 8.63 (s, 1 H, H$_1$), 8.97 (dd, J = 8.6, 1.6 Hz, 1 H, H$_{11}$), 9.27 (ddd, J = 21.2, 4.3, 1.7 Hz, 2 H, H$_{8,13}$). (*Assignments according to SDBS No. 5094HSP-45-189, measured in CDCl$_3$*)

^{13}C NMR (CDCl$_3$, 101 MHz): δ(ppm) = 121.1 (C$_3$), 124.4, 124.5 (C$_{1,9}$), 125.5, 125.6 (C$_{6,12}$), 132.6 (C$_{11}$), 137.9 (C$_{10}$), 144.3 (C$_2$), 146.3 (C$_4$), 147.7 (C$_3$), 151.6 (C$_{13}$), 153.7 (C$_8$). (*Assignments according to SDBS No. 5094CDS-11-196, measured in CDCl$_3$*)
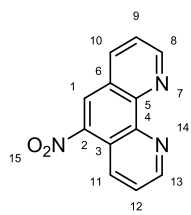
6.4.1.2 Synthesis of 5-amino-1,10-phenanthroline (10c)

10b

C$_{12}$H$_7$N$_3$O$_2$
225.20

10c

C$_{12}$H$_9$N$_3$
195.22
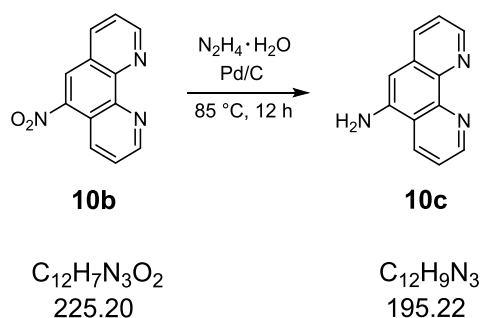
Reagents	2.5 g (11.09 mmol)	5-Nitro-1,10-phenanthroline (**10b**)
	6.7 g (133.6 mmol)	N$_2$H$_4$ • H$_2$O
	1.0 g (cat.)	**5%** Pd/C
	60 mL	EtOH

Preparation

5-Nitro-1,10-phenanthroline (**10b**) was dissolved in EtOH, then Pd/C was added. Hydrazine monohydrate was added dropwise over a period of 30 minutes. After the addition was complete, the mixture was stirred at 85 °C for 12 h. At the end of the reaction, the mixture was filtered over celite and the filtrate was concentrated under reduced pressure. After that, the residue was cooled quickly with liquid nitrogen. Cold EtOH was added to the residue and the mixture was kept overnight at 4 °C. The precipitate was then filtered and dried under reduced pressure.

**Yield**   0.62 g (3.17 mmol) 29**%**   **Lit.**[62] 46**%**

Appearance   dark yellow solid

^{1}H NMR   (DMSO-d$_6$, 400 MHz): δ(ppm) = 6.11 (s, 2 H, H$_{15}$), 6.81 (s, 1 H, H$_1$), 7.46 (ddd, J = 8.1, 4.2, 1.1 Hz, 1 H, H$_{9,12}$), 7.69 (ddd, J = 8.3, 4.2, 1.0 Hz, 1 H, H$_{9,12}$), 8.00 (dt, J = 8.1, 1.4 Hz, 1 H), 8.56–8.74 (m, 2 H), 9.01 (dt, J = 4.2, 1.3 Hz, 1 H). (*Assignments according to [62], measured in DMSO-d$_6$*)

6.4.1.3   Synthesis of 1,10-phenanthroline-5,6-dione (11a)

10a

$C_{12}H_8N_2$
180.21

11a

$C_{12}H_6N_2O_2$
210.19
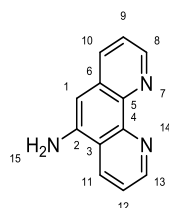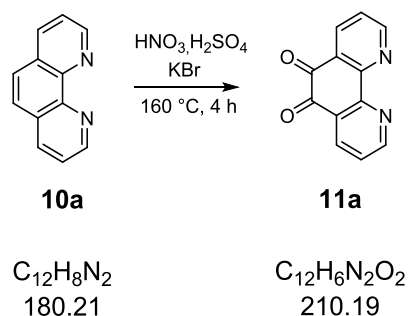
Reagents	5.00 g (27.75 mmol)	1,10-Phenanthroline (**10a**)
	92.5 g (943.4 mmol)	Sulfuric acid
	38.5 g (610.4 mmol)	Nitric acid
	4.95 g (41.62 mmol)	Potassium bromide

Preparation

An icecold mixture of sulfuric acid and nitric acid was added to a mixture of 1,10-phenanthroline (**10a**) and potassium bromide. The reaction mixture was heated up and kept at 160 °C for 4 h, then subsequently poured into 500 mL ice water. Saturated aqueous NaOH was added to this solution to adjust the pH 6 to 7. After washing with CHCl$_3$, the organic layer was dried over Na$_2$SO$_4$, filtered and evaporated under reduced pressure.

Yield   5.8 g (27.6 mmol) 99**%**   **Lit.**[64] 85**%**

Appearance   dark yellow solid

^{1}H NMR   (CDCl$_3$, 400 MHz): δ(ppm) = 7.56 (dd, J = 7.8, 4.7 Hz, 2 H, H$_{9,12}$), 8.47 (dd, J = 7.9, 1.8 Hz, 2 H, H$_{10,11}$), 9.08 (dd, J = 4.7, 1.9 Hz, 2 H, H$_{8,13}$). (*Assignments according to [63], measured in CDCl$_3$*)

6.4.1.4   Synthesis of 1,10-phenanthroline-5,6-dioxime (11b)

11a

$C_{12}H_6N_2O_2$
210.19

11b

$C_{12}H_8N_4O_2$
240.22
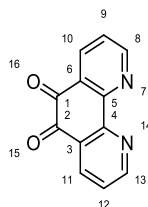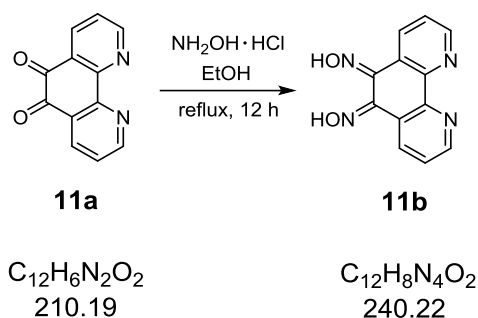
Reagents   5.40 g (25.96 mmol)   1,10-Phenanthroline-5,6-dione (**11a**)

6.31 g (90.84 mmol) $NH_2OH \bullet HCl$

7.68 g (38.93 mmol) $BaCO_3$

120 mL   EtOH

Preparation

A mixture of **11a**, $NH_2OH \bullet HCl$ and $BaCO_3$ in EtOH was stirred and refluxed for 12 h. After removal of the solvent, the residue was treated with 0.2 M HCl, stirred for 30 min and filtered. The light yellow solid was washed successively with water, EtOH and diethyl ether and dried under reduced pressure at 80 °C.

Yield   3.0 g (12.5 mmol) 48%   **Lit.**[64] 95%

Appearance   light yellow solid

No characterization was carried out.

6.4.1.5 Synthesis of 5,6-diamino-1,10-phenanthroline (11c)

11b

$C_{12}H_8N_4O_2$
240.22

11c

$C_{12}H_{10}N_4$
210.23
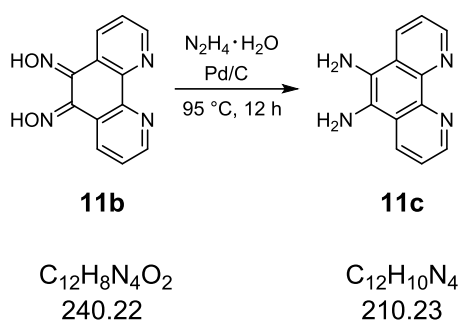
Reagents   0.5 g (2.086 mmol)   1,10-Phenanthroline-5,6-dioxime (**11b**)

4.5 g (90.04 mmol) $N_2H_4 \cdot H_2O$

0.5 g (cat.)   10**%** Pd/C

70 mL   EtOH

Preparation

1,10-Phenanthroline-5,6-dioxime (**11b**) was dissolved in EtOH, then Pd/C was added. Hydrazine monohydrate was added dropwise over a period of 30 minutes. After the addition was complete, the mixture was stirred at 95 °C for 12 h. At the end of the reaction, the hot mixture was filtered over celite. The celite pad was washed 4 times with 20 mL hot EtOH. Then the filtrate was concentrated under reduced pressure. After that, cold water was added to the residue and the mixture was kept overnight at 4 °C. The precipitate was then filtered, washed with cold water and dried under reduced pressure.

Yield   0.37 g (1.74 mmol) 84**%**   **Lit.**[64] 83**%**

Appearance   dark brown solid

^{1}H NMR   (DMSO-d_6, 400 MHz): δ(ppm) = 5.19 (s, 4 H, H$_{15,16}$), 7.56 (dd, J = 8.4, 4.2 Hz, 2 H, H$_{9,12}$), 8.44 (d, J = 8.0 Hz, 2 H, H$_{10,11}$), 8.73 (d, J = 3.8 Hz, 2 H, H$_{8,13}$). (*Assignments according to* **11b** *in [63], measured in CDCl$_3$*)

^{13}C NMR   (DMSO-d_6, 101 MHz): δ(ppm) = 122.5, 122.6, 123.2, 129.0, 141.4, 145.5.
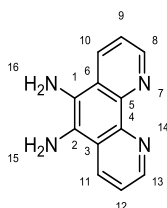
6.4.2 General procedure for anhydride synthesis

13a–b: A 20**%** NaOH solution was added to a mixture of tetrabutylammonium bromide and 10 mL toluene. After the solution cooled to 0 °C, a solution of an acyl chloride (**12a–b**) in 60 mL toluene was added and then stirred for 3 h. The organic layer phase was washed with a 10**%** sodium bicarbonate aqueous solution and water, then dried over Na_2SO_4, filtered and evaporated under reduced pressure.

13c–e: A 20**%** NaOH solution was added to a mixture of tetrabutylammonium bromide and 20 mL toluene. After the solution cooled to 0 °C, a solution of an acyl chloride (**12c–e**) in 120 mL toluene was added and then stirred for 3 h. The organic layer phase was washed with a 10**%** sodium bicarbonate aqueous solution and water, then dried over Na_2SO_4, filtered and evaporated under reduced pressure.

6.4.2.1 Synthesis of octanoyl anhydride (13a)

12a

CH$_{15}$ClO
162.66

13a

C$_{16}$H$_{30}$O$_3$
270.41
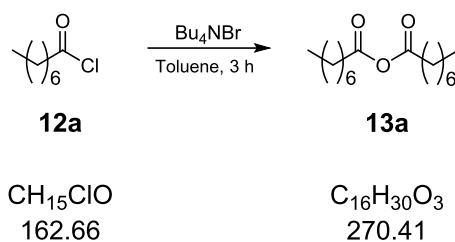
Reagents	6.51 g (40.0 mmol)	Octanoyl chloride (**12a**)
	1.29 g (4.0 mmol)	Tetrabutylammonium bromide
	70 mL	Toluene
	12 mL	20**%** NaOH solution

Yield 4.54 g (16.78 mmol) 84**%**

Appearance colorless liquid

¹H NMR (CDCl$_3$, 400 MHz): δ(ppm) = 0.82–0.93 (m, 6 H), 1.31 (ddd, J = 19.4, 11.4, 4.8 Hz, 16 H), 1.64 (p, J = 7.4 Hz, 4 H), 2.43 (t, J = 7.5 Hz, 4 H).
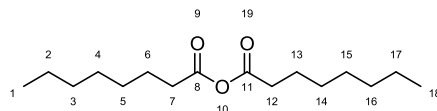
6.4.2.2   Synthesis of nonanoyl anhydride (13b)
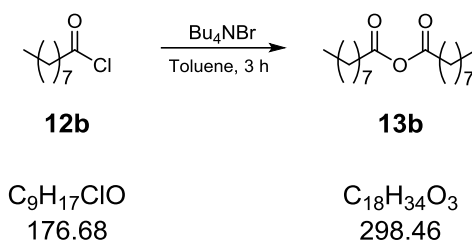

12b

C₉H₁₇ClO
176.68

13b

C₁₈H₃₄O₃
298.46

Reagents	7.07 g (40.0 mmol)	Nonanoyl chloride (**12b**)
	1.29 g (4.0 mmol)	Tetrabutylammonium bromide
	70 mL	Toluene
	12 mL	20**%** NaOH solution

Yield   5.73 g (19.2 mmol) 96**%**

Appearance   colorless liquid

¹H NMR   (CDCl₃, 400 MHz): δ(ppm) = 0.86 (t, *J* = 6.9 Hz, 6 H), 1.30 (dd, *J* = 25.1, 11.5 Hz, 20 H), 1.64 (p, *J* = 7.4 Hz, 4 H), 2.42 (t, *J* = 7.4 Hz, 4 H).

6.4.2.2   Synthesis of nonanoyl anhydride (13b)

12b

$C_9H_{17}ClO$
176.68

13b

$C_{18}H_{34}O_3$
298.46

Reagents	7.07 g (40.0 mmol)	Nonanoyl chloride (**12b**)
	1.29 g (4.0 mmol)	Tetrabutylammonium bromide
	70 mL	Toluene
	12 mL	20**%** NaOH solution

Yield   5.73 g (19.2 mmol) 96**%**

Appearance   colorless liquid

¹H NMR   (CDCl₃, 400 MHz): δ(ppm) = 0.86 (t, *J* = 6.9 Hz, 6 H), 1.30 (dd, *J* = 25.1, 11.5 Hz, 20 H), 1.64 (p, *J* = 7.4 Hz, 4 H), 2.42 (t, *J* = 7.4 Hz, 4 H).
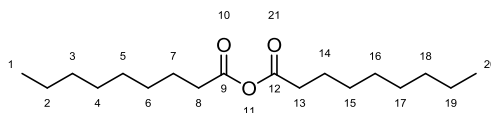
6.4.2.3   Synthesis of decanoyl anhydride (13c)

12c

C$_{10}$H$_{19}$ClO
190.71

13c

C$_{20}$H$_{38}$O$_3$
326.51
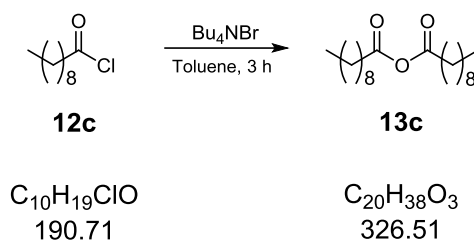
Reagents	12.4 g (64.9 mmol)	Decanoyl chloride (**12c**)
	2.10 g (6.5 mmol)	Tetrabutylammonium bromide
	140 mL	Toluene
	20 mL	20**%** NaOH solution

Yield	10.48 g (32.1 mmol) 99**%**
Appearance	colorless liquid
¹H NMR	(CDCl$_3$, 400 MHz): δ(ppm) = 0.87 (t, J = 8.0 Hz, 6 H, H$_{1,22}$), 1.26 (s, 24 H, H$_{2-6,17-21}$), 1.66 (tt, J = 7.5, 14.9 Hz, 4 H, H$_{7,16}$), 2.42 (t, J = 7.5 Hz, 3 H), 2.86 (t, J = 7.3 Hz, 1 H).
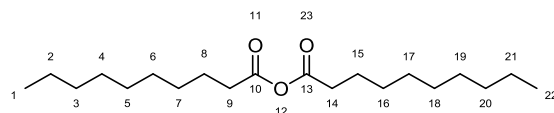
6.4.2.4 Synthesis of dodecanoyl anhydride (13d)

12d

$C_{12}H_{23}ClO$
218.76

13d

$C_{24}H_{46}O_3$
382.62
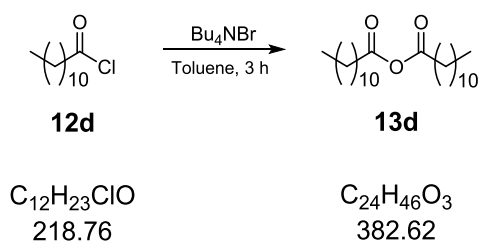
|		
Reagents	14.2 g (64.9 mmol)	Dodecanoyl chloride (**12d**)
	2.10 g (6.5 mmol)	Tetrabutylammonium bromide
	140 mL	Toluene
	20 mL	20**%** NaOH solution

Yield   12.3 g (32.1 mmol) 99**%**

Appearance   colorless liquid

^{1}H NMR   (CDCl$_3$, 400 MHz): δ(ppm) = 0.87 (t, J = 8.0 Hz, 6 H, H$_{1,25}$), 1.24 (s, 32 H, H$_{2-8,18-24}$), 1.58–1.75 (m, 4 H, H$_{9,17}$), 2.43 (t, J = 7.5 Hz, 3 H), 2.87 (t, J = 7.3 Hz, 1 H).
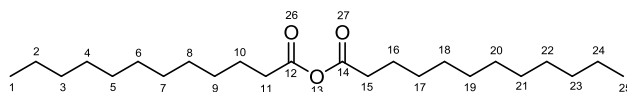
6.4.2.5 Synthesis of hexadecanoyl anhydride (13e)

12e

$C_{16}H_{31}ClO$
274.87

13e

$C_{32}H_{62}O_3$
494.83
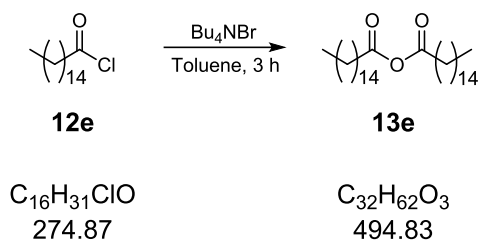
Reagents	17.8 g (64.9 mmol)	Hexadecanoyl chloride (**12e**)
	2.10 g (6.5 mmol)	Tetrabutylammonium bromide
	140 mL	Toluene
	20 mL	20**%** NaOH solution

Yield   15.9 g (32.1 mmol) 99**%**   **Lit.**[150] 90**%**

Appearance   colorless liquid

¹H NMR   (CDCl₃, 400 MHz): δ(ppm) = 0.87 (t, J = 8.0 Hz, 6 H, H₃₄,₃₅), 1.24 (s, 48 H, H₁₋₆,₁₉₋₂₆,₂₈₋₃₀), 1.58–1.77 (m, 4 H, H₇,₁₈), 2.43 (t, J = 7.5 Hz, 3 H), 2.87 (t, J = 7.3 Hz, 1 H).
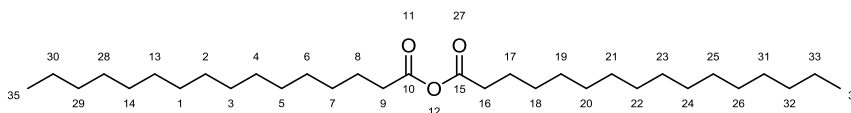
6.4.3 General procedure for the synthesis of monofunctionalized phen derivatives

A mixture of **10c** and NaHCO$_3$ was stirred in acetonitrile. After the solution cooled to 0 °C, a solution of an acyl chloride (**12a–e**) in acetonitrile was added and the mixture was stirred for 4 h at room temperature. The solid was filtered and then washed with acetonitrile, saturated NaHCO$_3$ solution and cold water. The solid was kept at room temperature overnight and subsequently dried under reduced pressure.

6.4.3.1 Synthesis of 14a

10c	**12a**	**14a**
C$_{12}$H$_9$N$_3$	C$_8$H$_{15}$ClO	C$_{20}$H$_{23}$N$_3$O
195.23	162.66	321.42
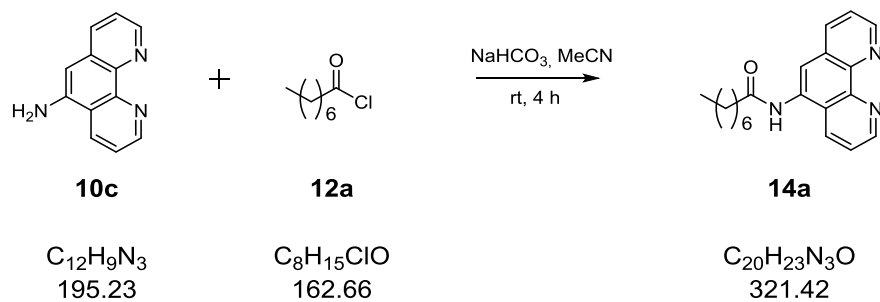
Reagents 97.0 mg (0.50 mmol)   5-Amino-1,10-phenanthroline (**10c**)

134 mg (0.99 mmol)   Octanoyl chloride (**12a**)

56.3 mg (0.67 mmol)   NaHCO$_3$

12 mL   Acetonitrile

Yield   92 mg (0.29 mmol) 58**%**

Appearance   yellow solid

^{1}H NMR   (CDCl$_3$, 400 MHz): δ(ppm) = 0.89 (dd, J = 5.9, 3.1 Hz, 3 H, H$_{24}$), 1.22–1.54 (m, 6 H), 1.84 (d, J = 7.9 Hz, 2 H), 2.00 (s, 2 H), 2.60 (d, J = 8.5 Hz, 2 H), 7.56–7.74 (m, 2 H), 7.98 (s, 1 H), 8.19–8.44 (m, 2 H), 9.02–9.29 (m, 2 H).

6.4.3.2   Synthesis of 14b

	10c	12b	14b
	C$_{12}$H$_9$N$_3$	C$_9$H$_{17}$ClO	C$_{21}$H$_{25}$N$_3$O
	195.23	176.68	335.45
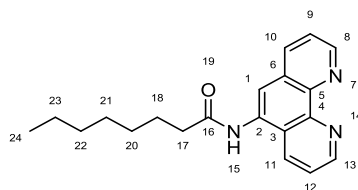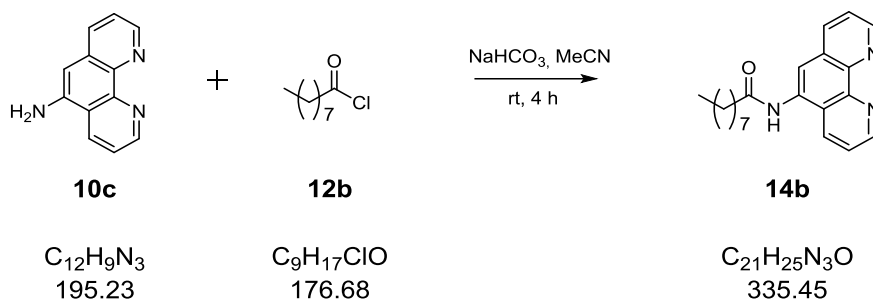
Reagents   97.0 mg (0.50 mmol)   5-Amino-1,10-phenanthroline (**10c**)

148 mg (0.99 mmol)   Nonanoyl chloride (**12b**)

56.3 mg (0.67 mmol)   NaHCO$_3$

12 mL   Acetonitrile

Yield   52 mg (0.15 mmol) 29**%**

Appearance   ocre solid

^{1}H NMR   (CDCl$_3$, 400 MHz): δ(ppm) = 0.89 (s, 3 H, H$_{25}$), 1.11–1.66 (m, 12 H), 1.85 (s, 1 H), 2.57 (s, 1 H), 7.46–7.79 (m, 3 H), 8.11–8.43 (m, 2 H), 9.18 (d, J = 33.5 Hz, 2 H).

6.4.2.3　Synthesis of 14c

| **10c**	**12c**		**14c**
$C_{12}H_9N_3$	$C_{10}H_{19}ClO$		$C_{22}H_{27}N_3O$
195.23	190.71		349.48
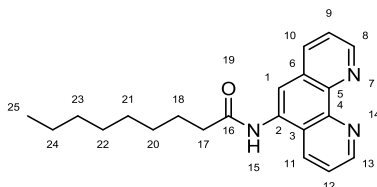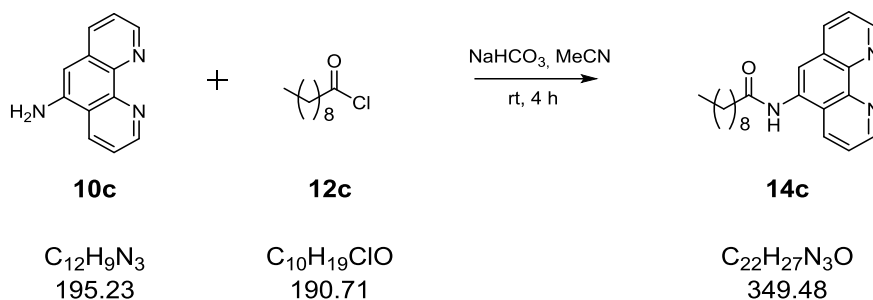
Reagents　0.25 g (1.28 mmol)　　5-Amino-1,10-phenanthroline (**10c**)

0.49 g (2.56 mmol)　　Decanoyl chloride (**12c**)

0.15 g (1.78 mmol)　　NaHCO$_3$

25 mL　　　　　　　　Acetonitrile

Yield　　　　0.33 g (0.95 mmol) 74**%**

Appearance　beige solid

^{1}H NMR　　(CDCl$_3$, 400 MHz): δ(ppm) = 0.88 (t, J = 6.6 Hz, 3 H, H$_{26}$), 1.15–1.52 (m, 14 H), 2.63 (t, J = 7.5 Hz, 2 H), 7.57 (s, 1 H), 7.69 (dd, J = 8.1, 4.5 Hz, 1 H), 8.23 (s, 1 H), 8.26–8.32 (m, 1 H), 8.40 (d, J = 8.6 Hz, 2 H), 8.98–9.01 (m, 1 H), 9.17 (d, J = 4.5 Hz, 1 H).

HR MS-ESI　　m/z [**14c** + H]$^+$ Calc. 350.2227, Found 350.2244
m/z [**14c** + Na]$^+$ Calc. 372.2046, Found 372.2081
m/z [**14c** + K]$^+$ Calc. 388.1785, Found 388.1797

6.4.2.4 Synthesis of 14d

10c	**12d**	**14d**
$C_{12}H_9N_3$	$C_{12}H_{23}ClO$	$C_{24}H_{31}N_3O$
195.23	218.76	377.53
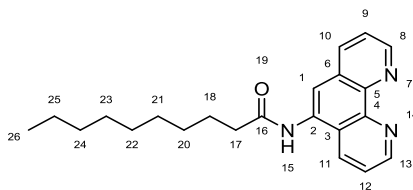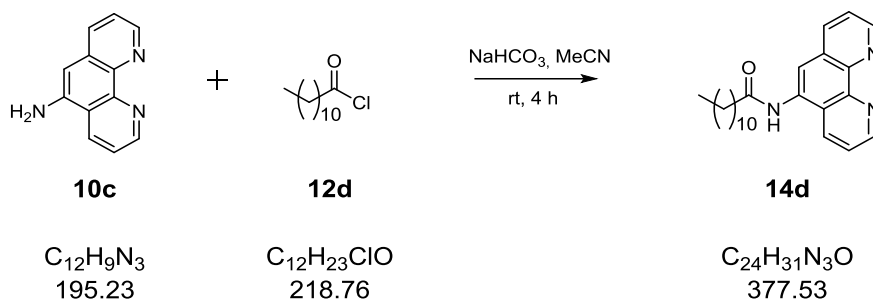
Reagents	0.25 g (1.28 mmol)	5-Amino-1,10-phenanthroline (**10c**)
	0.53 g (2.56 mmol)	Dodecanoyl chloride (**12d**)
	0.15 g (1.78 mmol)	$NaHCO_3$
	25 mL	Acetonitrile

Yield	0.36 g (0.96 mmol) 75**%**	**Lit.**[65] 72**%**

Appearance	orange solid

¹H NMR	(CDCl₃, 400 MHz): δ(ppm) = 0.85–0.90 (m, 3 H, H_{28}), 1.19–1.52 (m, 16 H), 1.81 (p, 2 H), 2.61 (t, J = 14.8 Hz, 2 H), 7.55 (s, 1 H), 7.63 (dd, J = 8.1, 4.4 Hz, 1 H), 8.20 (dd, J = 7.9, 1.8 Hz, 2 H), 8.29 (s, 1 H), 8.38 (d, J = 7.7 Hz, 2 H), 9.00 (d, J = 3.7 Hz, 1 H), 9.11 (d, J = 3.8 Hz, 1 H).

HR MS-ESI	m/z [**14d** + H]⁺ Calc. 378.2540, Found 378.2898 m/z [**14d** + Na]⁺ Calc. 400.2359, Found 400.2381 m/z [**14d** + K]⁺ Calc. 416.2099, Found 416.2105

6.4.2.5   Synthesis of 14e

10c	12e	14e
$C_{12}H_9N_3$	$C_{16}H_{31}ClO$	$C_{28}H_{39}N_3O$
195.23	274.87	433.64
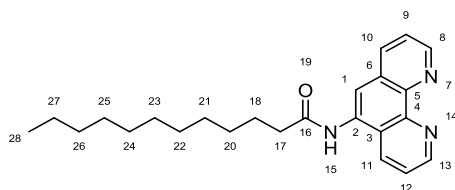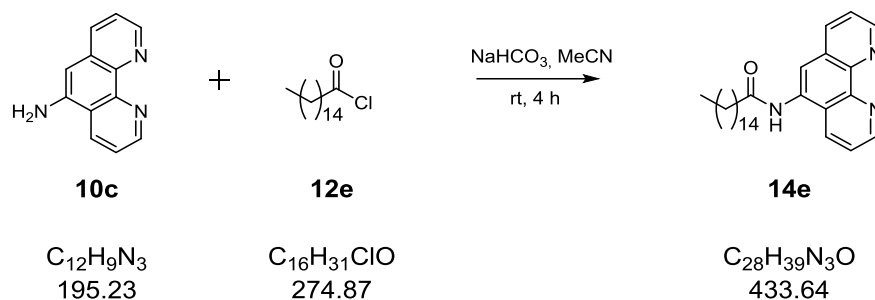
Reagents	0.25 g (1.28 mmol)	5-Amino-1,10-phenanthroline (**10c**)
	0.70 g (2.56 mmol)	Hexadecanoyl chloride (**12e**)
	0.15 g (1.78 mmol)	NaHCO₃
	25 mL	Acetonitrile

Yield   0.67 g (raw yield)

Appearance   beige solid

¹H NMR   (CDCl₃, 400 MHz): δ(ppm) = 0.87 (t, 3 H, H32), 1.20–1.36 (m, 24 H), 1.85 (p, 2 H), 2.56 (d, J = 7.4 Hz, 2 H), 7.60–7.71 (m, 3 H), 8.16–8.33 (m, 3 H), 9.16 (dd, J = 29.6, 4.0 Hz, 2 H).

HR MS-ESI m/z [**14e** + H]⁺ Calc. 434.3199, Found 434.3166
                   m/z [**14e** + Na]⁺ Calc.456.3191, Found 456.2985
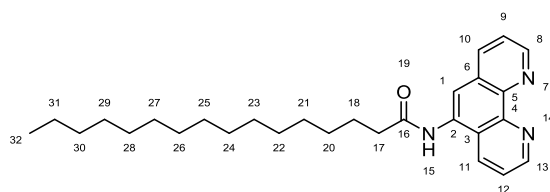
6.4.4 General procedure for the synthesis of bisfunctionalized phen derivatives

A mixture of **11c** and anhydride (**13c–e**) was stirred in toluene and refluxed for 4 h. After the solution cooled to room temperature, the solid was filtered and washed with cold toluene and ether. The solid was kept at room temperature overnight and subsequently dried under reduced pressure.

6.4.4.1   Synthesis of 15c

	11c	13c	15c
	$C_{12}H_{10}N_4$	$C_{20}H_{38}O_3$	$C_{32}H_{46}N_4O_2$
	210.23	326.51	518.75
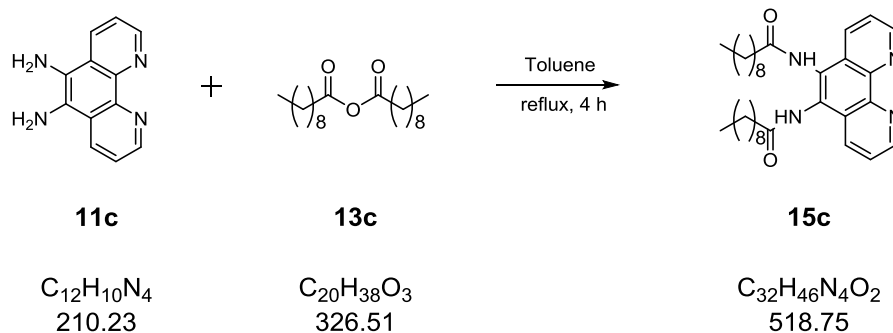
Reagents   0.16 g (0.76 mmol)   5,6-Diamino-1,10-phenanthroline (**11c**)

3.12 g (9.55 mmol)   Decanoyl anhydride (**13c**)

10 mL   Toluene

Yield   100 mg (0.19 mmol) 26**%**

Appearance   dark brown solid

¹H NMR   (CDCl₃, 400 MHz): δ(ppm) = 0.81–1.00 (m, 6 H, H₃₇,₃₈), 1.16–1.33 (m, 28 H), 2.13–2.23 (m, 4 H), 7.52 (s, 2 H), 7.92 (dd, J = 8.1, 4.4 Hz, 2 H), 9.38 (dd, J = 4.4, 1.8 Hz, 2 H), 9.85 (dd, J = 8.1, 1.8 Hz, 2 H).

HR MS-ESI m/z [**15c** + H]⁺ Calc. 519.3673, Found 519.3713

6.4.4.2 Synthesis of 15d

11c	**13d**	**15d**
$C_{12}H_{10}N_4$	$C_{24}H_{46}O_3$	$C_{36}H_{54}N_4O_2$
210.23	382.62	574.85
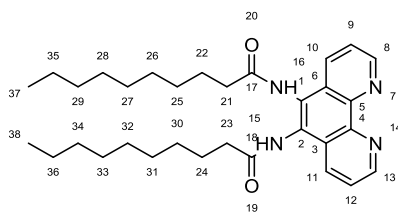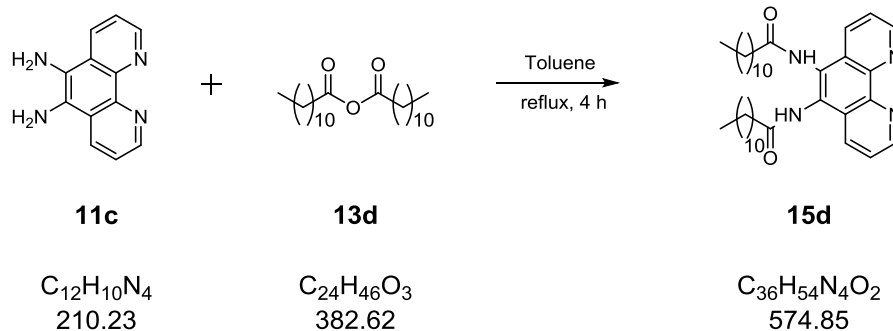
Reagents 0.15 g (0.71 mmol) 5,6-Diamino-1,10-phenanthroline (**11c**)

3.50 g (9.15 mmol) Dodecanoyl anhydride (**13d**)

10 mL Toluene

Yield 77 mg (0.14 mmol) 20**%**

Appearance dark brown solid

^{1}H NMR (CDCl$_3$, 400 MHz): δ(ppm) = 0.89 (t, 6 H, H$_{40,42}$), 1.20–1.34 (m, 40 H), 7.28 (s, 2 H), 7.92 (dd, J = 8.1, 3.9 Hz, 2 H), 9.37 (dd, J = 4.4, 1.8 Hz, 2 H), 9.83 (dd, J = 8.2, 1.6 Hz, 2 H).

HR MS-ESI *m/z* [**15d** + H]$^+$ Calc. 575.4320, Found 575.4355

6.4.4.3   Synthesis of 15e

| **11c**	**13e**	**15e**
$C_{12}H_{10}N_4$	$C_{32}H_{62}O_3$	$C_{44}H_{70}N_4O_2$
210.23	494.83	687.07
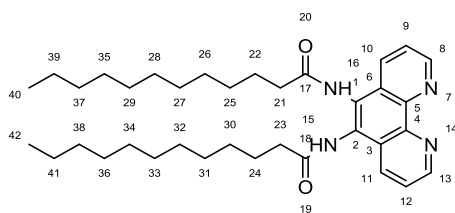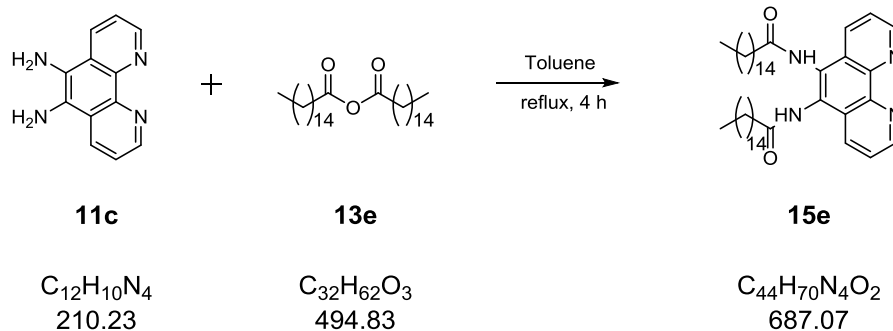
Reagents   0.16 g (0.76 mmol)   5,6-Diamino-1,10-phenanthroline (**11c**)

4.5 g (9.09 mmol)   Hexadecanoyl anhydride (**13e**)

10 mL   Toluene

Yield   0.66 g (raw yield)

Appearance   light brown solid

^{1}H NMR   (DMSO-d6, 400 MHz): δ(ppm) = 0.84 (t, 6 H, $H_{46,50}$), 1.18–1.28 (m, 48 H), 1.47 (p, J = 7.1 Hz, 4 H), 2.18 (t, J = 7.4 Hz, 4 H), 7.16 (s, 2 H), 7.29 (s, 2 H), 9.30 (dd, J = 4.5, 1.7 Hz, 2 H), 9.89 (dd, J = 8.0, 1.7 Hz, 2 H).

HR MS-ESI m/z [**15e** + H]$^+$ Calc. 687.5572, Found 687.5713
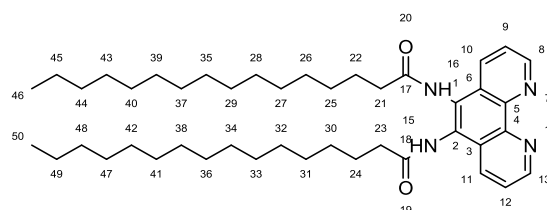
6.4.5 *In situ* complex formation of phen derivatives

For the cmc determination, cleavage activity studies and cytotoxicity studies complexes of **10c**, **14a** and **14b** were generated *in situ* in 20**%** DMSO solution. $Cu(NO_3)_2 \cdot 3\ H_2O$ was applied as metal salt for the formation of the corresponding complexes **10c + Cu**, **14a + Cu** and **14b + Cu**. *In situ* complex solutions were prepared according to the ratio of 0.9:1 (metal salt solution : ligand solution) to ensure that effects regarding both DNA cleavage and cytotoxicity which possibly originate from free metal ions can be excluded.

LIST OF PUBLICATIONS

"Mononuclear Cu(II) and Zn(II) complexes with a simple diamine ligand: synthesis, structure, phosphodiester binding and DNA cleavage studies"
P. Sureshbabu, A. A. J. Sudarga Tjakraatmadja, C. Hanmandlu, K. Elavarasan, N. Kulak and S. Sabiah, *RSC Adv.* **2015**, *5*, 22405-22418.

"Tuning the DNA binding and cleavage of bpa copper complexes by ether tethers with hydroxyl and methoxy groups"
A. A. J. Sudarga Tjakraatmadja, C. Lüdtke, N. Kulak, *Inorg. Chim. Acta* **2016**, accepted.
(Special Issue: "Metal-Nucleic Acid Interactions: State of the art")

POSTER PRESENTATIONS

"Synthesis and nuclease activity of novel bis(picolyl)amine Cu(II) complexes"
A. A. J. Sudarga Tjakraatmadja, N. Kulak
EUROBIC 11 in Granada, Spain, September 12-16, 2012.

BIBLIOGRAPHY

[1]   J. B. Reece et al., *Campbell Biology (10th Edition)*. Benjamin Cummings, **2013**.

[2]   J. D. Watson, F. H. C. Crick, *Nature* **1953,** *171*, 737-738.

[3]   L. A. Pray, *Nature Education* **2008,** *1 (1)*, 100.

[4]   F. Jacob, J. Monod, *Journal of Molecular Biology* **1961,** *3 (3)*, 318-356.

[5]   M. Whiteman, H. S. Hong, A. Jenner, B. Halliwell, *Biochemical and Biophysical Research Communications* **2002,** *296*, 883-889.

[6]   D. Branzei, M. Foiani, *Nature Reviews Molecular Cell Biology* **2008,** *9*, 297-308.

[7]   S. Nesnow et al., *Chemical Research in Toxicology* **2002,** *15 (12)*, 1627-1634.

[8]   J. B. Little, *Carcinogenesis* **2000,** *21 (3)*, 397-404.

[9]   N. F. Cariello, P. Keohavong, B. J. S. Sanderson, W. G. Thilly, *Nucleic Acids Research* **1988,** *16 (9)*, 4157.

[10]   J. A. Miller, *Cancer Research* **1970,** *30*, 559-576.

[11]   A. Roulston, R. C. Marcellus, P. E. Branton, *Annual Review of Microbiology* **1999,** *53*, 577-628.

[12]   U. Hübscher, G. Maga, S. Spadari, *Annual Review of Biochemistry* **2002,** *71*, 133-163.

[13]   A. Eastman, M. A. Barry, *Cancer Investigation* **1992,** *10 (3)*, 229-240.

[14]   C. A. Schmitt, *Nature Reviews Cancer* **2003,** *3*, 286-295.

[15]   R. L. Siegel, K. D. Miller, A. Jemal, *CA: A Cancer Journal for Clinicians* **2015,** *65 (1)*, 5-29.

[16]   C. Orvig, M. Abrams, *Chemical Reviews* **1999,** *99 (9)*, 2201-2203.

[17]   S. Neidle, D. E. Thurston, *Nature Reviews Cancer* **2005,** *5*, 285-296.

[18]   B. Rosenberg, L. V. Camp, T. Krigas, *Nature* **1965,** *205*, 698-699.

[19]   M. Kartalou, J. M. Essigmann, *Mutation Research* **2001,** *478*, 23-43.

[20]   B. W. Harper et al., *Chemistry - A European Journal* **2010,** *16 (24)*, 7064-7077.

[21]   C. N. Steinberg et al., *Journal of Clinical Oncology* **2009,** *27 (32)*, 5431-5438.

[22]   B. Rosenberg, L. VanCamp, J. E. Trosko, V. H. Mansour, *Nature* **1969,** *222*, 385-386.

[23]   E. Wong, C. M. Giandomenico, *Chemical Reviews* **1999,** *99*, 2451-2466.

[24]   L. H. Hurley, *Nature Reviews Cancer* **2002,** *2*, 188-200.

[25]   C. Santini et al., *Chemical Reviews* **2014,** *114 (1)*, 815-862.

[26]   F. Mancin, P. Scrimin, P. Tecilla, U. Tonellato, *Chemical Communications* **2005,** *(20)*, 2540-2548.

[27] V. Pinzani et al., *Cancer Chemotherapy and Pharmacology* **1994,** *35*, 1-9.

[28] C.-h. B. Chen et al., *ChemBioChem* **2001,** *2*, 735-740.

[29] L. J. Boerner, J. M. Zaleski, *Current Opinion in Chemical Biology* **2005,** *9*, 135-144.

[30] S. G. K. R., B. B. Mathew, D. N. Sudhamani, H. S. B. Naik, *Biomedicine and Biotechnology* **2014,** *2 (1)*, 1-9.

[31] W. Keller, R. Crouch, *PNAS* **1972,** *69 (11)*, 3360-3364.

[32] L. Hocharoen, J. A. Cowan, *Chemistry - A European Journal* **2009,** *15 (35)*, 8670-8676.

[33] J. A. Cowan, *Current Opinion in Chemical Biology* **2001,** *5*, 634-642.

[34] N. E. Dixon et al., *Chemical Communications* **1996,** *(11)*, 1287-1288.

[35] K. A. Deal, J. N. Burstyn, *Inorganic Chemistry* **1996,** *35 (10)*, 2792-2798.

[36] L. Tjioe et al., *Inorganic Chemistry* **2011,** *50 (2)*, 621-635.

[37] J. Bernadou et al., *Biochemistry* **1989,** *28*, 7268-7275.

[38] V. M. Manikandamathavan, B. U. Nair, *European Journal of Medicinal Chemistry* **2013,** *68*, 244-252.

[39] M. M. Meijler, O. Zelenko, D. S. Sigman, *Journal of the American Chemical Society* **1997,** *119 (5)*, 1135-1136.

[40] W. K. Pogozelski, T. D. Tullius, *Chemical Reviews* **1998,** *98 (3)*, 1089-1107.

[41] B. Selvakumar et al., *Journal of Inorganic Biochemistry* **2006,** *100 (3)*, 316-330.

[42] B.-E. Kim, T. Nevitt, D. J. Thiele, *Nature Chemical Biology* **2008,** *4 (3)*, 176-185.

[43] A. Gupte, R. J. Mumper, *Cancer Treatment Reviews* **2009,** *35*, 32-46.

[44] F. Tisato et al., *Medicinal Research Reviews* **2010,** *30 (4)*, 708-749.

[45] H. Krampe et al., *Alcoholism: Clinical and Experimental Research* **2006,** *30 (1)*, 86-95.

[46] C. W. Ritchie, A. I. Bush, C. L. Masters, *Expert Opinion on Investigational Drugs* **2004,** *13 (12)*, 1585-1592.

[47] T. Nguyen, A. Hamby, S. M. Massa, *PNAS* **2005,** *102 (33)*, 11840-11845.

[48] H. Pang, D. Chen, Q. C. Cui, Q. P. Dou, *International Journal of Molecular Medicine* **2007,** *19*, 809-816.

[49] D. Chen, Q. C. Cui, H. Yang, Q. P. Dou, *Cancer Research* **2006,** *66*, 10425-10433.

[50] D. Chen et al., *Cancer Research* **2007,** *67*, 1636-1644.

[51] C. Wende, C. Lüdtke, N. Kulak, *European Journal of Inorganic Chemistry* **2014,** *(16)*, 2597-2612.

[52] H. Sigel et al., *Journal of the American Chemical Society* **1984,** *106 (25)*, 7935-7946.

[53] K. J. Humphreys, K. D. Karlin, S. E. Rokita, *Journal of the American Chemical Society* **2002,** *124 (21)*, 6009-6019.

[54]   M. Tian, H. Ihmels, E. Brötz, *Dalton Transactions* **2010,** *39 (35)*, 8195-8202.

[55]   E. L. Hegg, J. N. Burstyn, *Coordination Chemistry Reviews* **1998,** *173*, 133-165.

[56]   N. H. Williams, B. Takasaki, M. Wall, J. Chin, *Accounts of Chemical Research* **1999,** *32*, 485-493.

[57]   M. J. Young, D. Wahnon, R. C. Hynes, J. Chin, *Journal of the American Chemical Society* **1995,** *117 (37)*, 9441-9447.

[58]   S. I. Kirin et al., *Dalton Transactions* **2004,** *(8)*, 1201-1207.

[59]   J. Katz, M. Levitz, S. S. Kadner, T. H. Finlay, *Journal of Steroid Biochemistry and Molecular Biology* **1991,** *38 (1)*, 17-26.

[60]   X.-B. Yang et al., *Bioorganic and Medicinal Chemistry* **2008,** *16 (7)*, 3871-3877.

[61]   G. Höfle, W. Steglich, H. Vorbrüggen, *Angewandte Chemie International Edition* **1978,** *17*, 569-583.

[62]   S. Ji et al., *Organic Letters* **2010,** *12 (12)*, 2876-2879.

[63]   J. Ettedgui, Y. Diskin-Posner, L. Weiner, R. Neumann, *Journal of the American Chemical Society* **2011,** *133*, 188-190.

[64]   S. Bodige, F. M. MacDonnell, *Tetrahedron Letters* **1997,** *38 (47)*, 8159-8160.

[65]   S. Huo-ming, L. Hua-ming, H. Chang-ri, W. Peng, *Chemical Research in Chinese Universities* **2004,** *20 (2)*, 149-151.

[66]   Z. Ahmad, A. Shah, M. Siddiq, H.-B. Kraatz, *RSC Advances* **2014,** *4*, 17028-17038.

[67]   B. Gruber et al., *Journal of the American Chemical Society* **2011,** *133 (51)*, 20704-20707.

[68]   Y. Mikata, T. Fujimoto, Y. Sugai, S. Yano, *European Journal of Inorganic Chemistry* **2007,** *(8)*, 1143-1149.

[69]   C.-M. Ting, C.-D. Wang, R. Chaudhuri, R.-S. Liu, *Organic Letters* **2011,** *13 (7)*, 1702-1705.

[70]   H. C. Brown, E. F. Knights, C. G. Scouten, *Journal of the American Chemical Society* **1974,** *96 (25)*, 7765-7770.

[71]   K. Jeong et al., *Journal of Industrial and Engineering Chemistry* **2009,** *15*, 342-347.

[72]   C. D. Cola et al., *Tetrahedron* **2012,** *68*, 499-506.

[73]   D. C. Beshore, C. J. Dinsmore, *Organic Letters* **2002,** *4 (7)*, 1201-1204.

[74]   M. Bertoldo et al., *Biomacromolecules* **2011,** *12 (2)*, 388-398.

[75]   G. W. Kalabka, K. A. R. Sastry, G. W. McCollum, H. Yoshioka, *Journal of Organic Chemistry* **1981,** *46*, 4296-4298.

[76]   A. S. B. Prasad, J. V. B. Kanth, M. Periasamy, *Tetrahedron* **1992,** *48 (22)*, 4623-4628.

[77]   N. Mizoshita, T. Tani, H. Shinokubo, S. Inagaki, *Angewandte Chemie International Edition* **2012,** *51*, 1156-1160.

[78]   M. Wyszogrodzka, R. Haag, *Langmuir* **2009,** *25 (10)*, 5703-5712.

[79]   J. Geschwind, H. Frey, *Macromolecular Rapid Communications* **2013,** *34*, 150-155.

[80]   D. Enders, A. Müller-Hüwen, *European Journal of Organic Chemistry* **2004,** *(8)*, 1732-1739.

[81]   S. I. Kirin et al., *Inorganic Chemistry* **2005,** *44 (15)*, 5405-5415.

[82]   B. J. Hathaway, P. G. Hodgson, *Journal of Inorganic and Nuclear Chemistry* **1973,** *35 (12)*, 4071-4081.

[83]   B. Murphy et al., *Dalton Transactions* **2006**, 357-367.

[84]   F. Bolivar et al., *Gene* **1977,** *2 (2)*, 95-113.

[85]   J. C. Dabrowiak, *Metals in Medicine*. John Wiley & Sons, New York, **2009**.

[86]   R. E. Weston, S. Ehrenson, K. Heinzinger, *Journal of the American Chemical Society* **1967,** *89 (3)*, 481-486.

[87]   E. M. Arnett, C. Y. Wu, *Journal of the American Chemical Society* **1962,** *84 (9)*, 1680-1684.

[88]   W. Wang et al., *Journal of Inorganic Biochemistry* **2015,** *153*, 143-149.

[89]   B. Halliwell, *The American Journal of Medicine* **1991,** *91 (3)*, S14-S22.

[90]   G. V. Buxton, C. L. Greenstock, W. P. Helman, A. B. Ross, *Journal of Physical and Chemical Reference Data* **1988,** *2 (17)*.

[91]   C. F. Babbs, J. A. Pham, R. C. Coolbaugh, *Plant Physiology* **1989,** *90 (4)*, 1267-1270.

[92]   M. Bancirova, *Luminescence* **2011,** *26 (6)*, 685-688.

[93]   I. Fridovich, *Annual Review of Biochemistry* **1975,** *44*, 147-159.

[94]   K. Böhme, H.-D. Brauer, *Inorganic Chemistry* **1992,** *31 (16)*, 3468-3471.

[95]   M. S. Melvin et al., *Journal of the American Chemical Society* **2000,** *122 (26)*, 6333-6334.

[96]   M. S. Melvin et al., *Journal of Inorganic Biochemistry* **2001,** *87 (3)*, 129-135.

[97]   P. U. Maheswari et al., *Chemistry - A European Journal* **2007,** *13 (18)*, 5213-5222.

[98]   N. J. Greenfield, *Nature Protocols* **2006,** *1 (6)*, 2891-2899.

[99]   S. Beychok, *Science* **1966,** *154 (3754)*, 1288-1299.

[100]   P.-x. Xi et al., *Journal of Inorganic Biochemistry* **2009,** *103 (2)*, 210-218.

[101]   R. Loganathan et al., *Inorganic Chemistry* **2012,** *51 (10)*, 5512-5532.

[102]   B. M. Weichman, A. C. Notides, *Endocrinology* **1980,** *106 (2)*, 434-439.

[103]   D. Dai et al., *Cancer Research* **2002,** *62*, 881-886.

[104]   D. M. Tannenbaum, Y. Wang, S. P. Williams, P. B. Sigler, in *PNAS,***1998**.

[105]   A. C. W. Pike et al., *The EMBO Journal* **1999,** *18 (17)*, 4608-4618.

[106]   K. Morito et al., *Biological and Pharmaceutical Bulletin* **2002,** *25 (1)*, 48-52.

[107]   J. Katz, T. H. Finlay, S. Banerjee, M. Levitz, *Journal of Steroid Biochemistry and Molecular Biology* **1987,** *26 (6)*, 687-692.

[108] K. R. Barnes, A. Kutikov, S. J. Lippard, *Chemistry & Biology* **2004,** *11 (4)*, 557-564.

[109] S. Wang, W. Fang, *Molecules* **2011,** *16*, 4748-4763.

[110] J. Liu, X. Zhang, M. Zhao, S. Peng, *European Journal of Medicinal Chemistry* **2009,** *44*, 1689-1704.

[111] T. O. Yellin, *Journal of Lipid Research* **1972,** *13*, 554-555.

[112] F. F. Wong et al., *Tetrahedron* **2010,** *66*, 4068-4072.

[113] A. P. Prakasham, K. Shanker, A. S. Negi, *Steroids* **2012,** *77 (5)*, 467-470.

[114] V. Boucheau et al., *Steroids* **1990,** *55*, 209-221.

[115] M. Di Antonio et al., *Angewandte Chemie International Edition* **2012,** *51 (44)*, 11073-11078.

[116] A. Sakakura et al., *Journal of the American Chemical Society* **2007,** *129 (7)*, 14775-14779.

[117] K. M. Amore, N. E. Leadbeater, *Macromolecular Rapid Communications* **2007,** *2007 (28)*, 473-477.

[118] P. Marwah, A. Marwah, H. A. Lardy, *Tetrahedron* **2003,** *59*, 2273-2287.

[119] P. S. Kiuru, K. Wähälä, *Steroids* **2006,** *71 (1)*, 54-60.

[120] R. Hrdina, C. E. Müller, P. R. Schreiner, *Chemical Communications* **2010,** *46 (15)*, 2689-2690.

[121] B. Neises, W. Steglich, *Angewandte Chemie International Edition* **1978,** *17 (7)*, 522-524.

[122] J. Guo, R. I. Duclos, V. K. Vemuri, A. Makriyannis, *Tetrahedron Letters* **2010,** *51 (27)*, 3465-3469.

[123] H. Wei et al., *Biochemistry* **1998,** *37 (18)*, 6485-6490.

[124] D. Roy, J. G. Liehr, *Mutation Research* **1999,** *424*, 107-115.

[125] L. M. Nutter et al., *Chemical Research in Toxicology* **1994,** *7*, 23-28.

[126] C. P. Martucci, J. Fishman, *Pharmacology & Therapeutics* **1993,** *57 (2-3)*, 237-257.

[127] Q. Felty et al., *Biochemistry* **2005,** *44 (18)*, 6900-6909.

[128] F. Lledias, P. Rangel, W. Hansberg, *Journal of Biological Chemistry* **1998,** *273 (17)*, 10630-10637.

[129] A. J. Davison, A. J. Kettle, D. J. Fatur, *1986* **1986,** *261 (3)*, 1193-1200.

[130] J. A. Escobar, M. A. Rubio, E. A. Lissi, *Free Radical Biology & Medicine* **1996,** *20 (3)*, 285-290.

[131] T. Mosmann, *Journal of Immunological Methods* **1983,** *65 (1-2)*, 55-63.

[132] J. C. Stockert et al., *Acta Histochemica* **2012,** *114 (8)*, 785-796.

[133] M. Ganeshpandian et al., *Journal of Inorganic Biochemistry* **2014,** *140*, 202-212.

[134] K.-L. Dao et al., *Bioconjugate Chemistry* **2012,** *23*, 785-795.

[135]   B. L. Vallee, J. A. Rupley, T. L. Coombs, H. Neurath, *Journal of the American Chemical Society* **1958,** *80 (17)*, 4750-4751.

[136]   B. L. Vallee, H. Neurath, *Journal of Biological Chemistry* **1955,** *217*, 253-262.

[137]   V. D'Aurora, A. M. Stern, D. S. Sigman, *Biochemical and Biophysical Research Communications* **1977,** *78 (1)*, 170-176.

[138]   T. B. Thederahn, M. D. Kuwabara, T. A. Larsen, D. S. Sigman, *Journal of the American Chemical Society* **1989,** *111*, 4941-4946.

[139]   D. S. Sigman, D. R. Graham, V. D'Aurora, A. M. Stern, *Journal of Biological Chemistry* **1979,** *254 (24)*, 12269-12272.

[140]   K. A. Reich, L. E. Marshall, D. R. Graham, D. S. Sigman, *Journal of the American Chemical Society* **1981,** *103*, 3582-3584.

[141]   X.-C. Su et al., *Polyhedron* **2001,** *20 (1-2)*, 91-95.

[142]   A. Barve et al., *Inorganic Chemistry* **2009,** *48 (19)*, 9120-9132.

[143]   Z.-Q. Bian, K.-Z. Wang, L.-P. Jin, L.-H. Gao, *Synthetic Communications* **2003,** *33 (20)*, 3477-3482.

[144]   S. Kraus, D. Mandler, *Langmuir* **2006,** *22*, 7462-7464.

[145]   H. Ding, X. Wang, S. Zhang, X. Liu, *Journal of Nanoparticle Research* **2012,** *14 (11)*.

[146]   K. Cho et al., *Clinical Cancer Research* **2008,** *14*, 1310-1316.

[147]   F. M. Menger, L. H. Gan, E. Johnson, D. H. Durst, *Journal of the American Chemical Society* **1987,** *109*, 2800-2803.

[148]   J. Zhang, X.-G. Meng, X.-C. Zeng, X.-Q. Yu, *Coordination Chemistry Reviews* **2009,** *253 (17-18)*, 2166-2177.

[149]   J. Etxebarria et al., *Journal of Organic Chemistry* **2009,** *74*, 8794-8797.

[150]   D. Plusquellec, F. Roulleau, M. Lefeuvre, *Tetrahedron* **1988,** *44 (9)*, 2471-2476.

[151]   J. Aguiar, P. Carpena, J. A. Molina-Bolívar, C. C. Ruiz, *Journal of Colloid and Interface Science* **2003,** *258*, 116-122.

[152]   S. Mahadevan, M. Palaniandavar, *Inorganic Chemistry* **1998,** *37*, 3927-3924.

[153]   C. Rajarajeswari et al., *Journal of Inorganic Biochemistry* **2014,** *140*, 255-268.

[154]   W.-J. Ma, E.-H. Cao, J.-F. Qin, *Redox Report: Communications in Free Radical Research* **1999,** *4 (6)*.

[155]   C. A. Price, *Annual Review of Plant Physiology* **1968,** *19*, 239-248.

[156]   H. Irving, D. H. Mellor, *Journal of the Chemical Society* **1962**, 5222-5237.

[157]   W. G. D. Santos et al., *Journal of Bacteriology* **2000,** *182 (3)*, 796-804.

[158]   J. H. Chang et al., *Analytical Biochemistry* **2010,** *405 (1)*, 135-137.

[159]   B. K. Paul, A. Samanta, N. Guchhait, *Journal of Physical Chemistry* **2010,** *114 (18)*, 6183-6196.

[160] V. Rajendiran, M. Palaniandavar, P. Swaminathan, L. Uma, *Inorganic Chemistry* **2007,** *46 (25)*, 10446-10448.

[161] H. Schägger, G. v. Jagow, *Analytical Biochemistry* **1987,** *166 (2)*, 368-379.

[162] T. P. Lo et al., *Protein Science* **1995,** *4 (2)*, 198-208.

[163] R. S. Kumar et al., *Collids and Surfaces B: Biointerfaces* **2011,** *86 (1)*, 35-44.

[164] Anvarbatcha Riyasdeen et al., *RSC Advances* **2014,** *4 (91)*, 49953-49959.

[165] S. Iglesias et al., *Journal of Inorganic Biochemistry* **2014,** *139*, 117-123.

[166] O. V. Dolomanov et al., *Journal of Applied Crystallography* **2008,** *42*, 339-441.

[167] G. M. Sheldrick, *Acta Crystallographica* **2007,** *A64*, 112-122.

[168] G. M. Sheldrick, *Acta Crystallographica* **2015,** *C71*, 3-8.

[169] R. P. Hertzberg, P. B. Dervan, *Biochemistry* **1984,** *23 (17)*, 3934-3945.

COMPOUND DIRECTORY
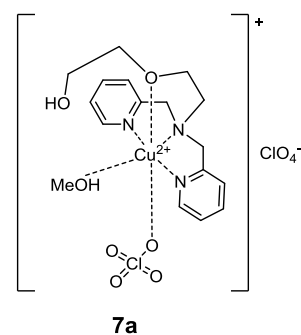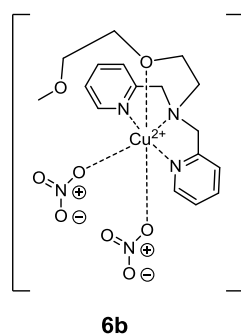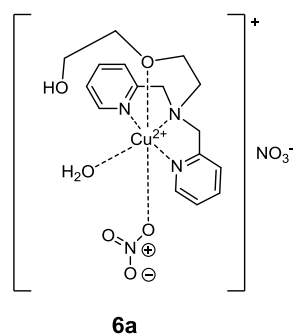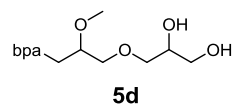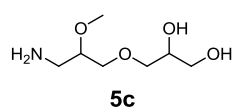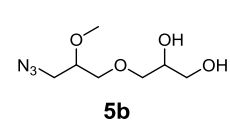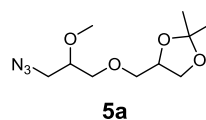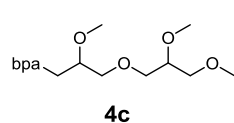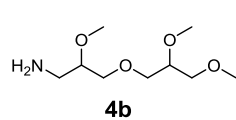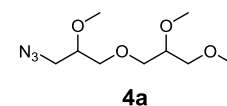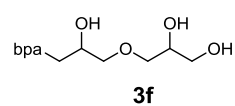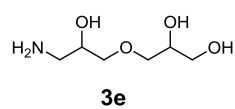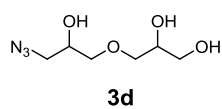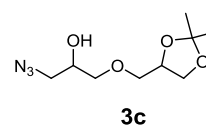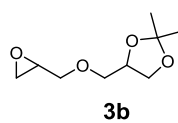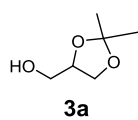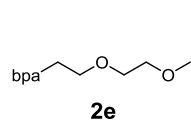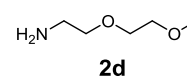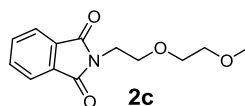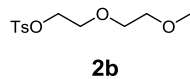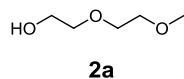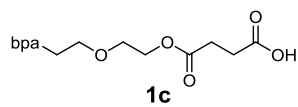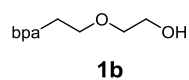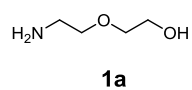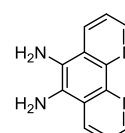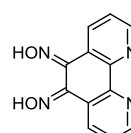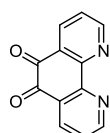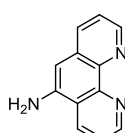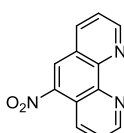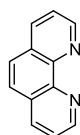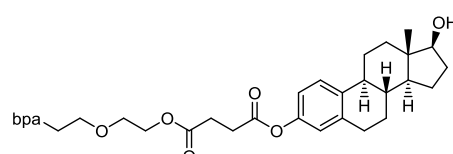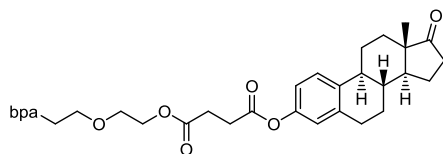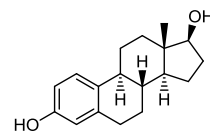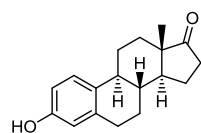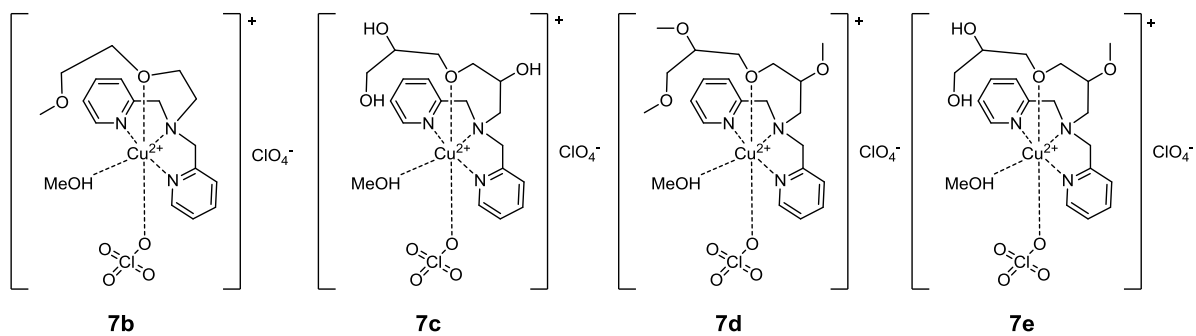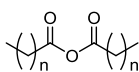
H₂N—O—OH
1a

bpa—O—OH
1b

bpa—O—O—O—OH
1c

HO—O—O
2a

TsO—O—O
2b

(phthalimide)—N—O—O
2c

H₂N—O—O
2d

bpa—O—O
2e

HO—(dioxolane)
3a

(epoxide)—O—(dioxolane)
3b

N₃—OH—O—(dioxolane)
3c

N₃—OH—O—OH—OH
3d

H₂N—OH—O—OH—OH
3e

bpa—OH—O—OH—OH
3f

N₃—O—O—O
4a

H₂N—O—O—O
4b

bpa—O—O—O
4c

N₃—O—O—(dioxolane)
5a

N₃—O—O—OH—OH
5b

H₂N—O—O—OH—OH
5c

bpa—O—O—OH—OH
5d

[Cu²⁺ complex] NO₃⁻
6a

[Cu²⁺ complex]
6b

[Cu²⁺ complex] ClO₄⁻
7a

7b **7c** **7d** **7e**

8a

9a

8b

9b

10a **10b** **10c**

11a **11b** **11c**

n = 6	**12a**	n = 6	**13a**
n = 7	**12b**	n = 7	**13b**
n = 8	**12c**	n = 8	**13c**
n = 10	**12d**	n = 10	**13d**
n = 14	**12e**	n = 14	**13e**
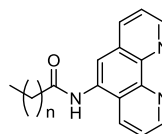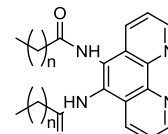
n = 6	**14a**	*n = 6*	*15a*
n = 7	**14b**	*n = 7*	*15b*
n = 8	**14c**	n = 8	**15c**
n = 10	**14d**	n = 10	**15d**
n = 14	**14e**	n = 14	**15e**

*List of commercially available (**1a**, **2a**, **3a**, **8a**, **9a**, **10a**, **12a-e**), literature-known (**1b**, **2b-d**, **3b-e**, **4a-b**, **5a-c**, **6a**, **7a**, **10b-c**, **11a-c**, **13e**, **14d**), novel (**1c**, **2e**, **3f**, **4c**, **5d**, **6b**, **7b-e**, **13a-d**, **14a-c**, **14e**, **15c-e**) and unsuccessfully (15a-b) synthesized compounds presented in this work.*